The Investigation of Transverse Joints and Grouts on Full Depth Concrete Bridge Deck Panels

Matthew K Swenty

Dissertation submitted to the faculty of the Virginia Polytechnic Institute and State University in partial fulfillment of the requirements for the degree of

Doctor of Philosophy
In
Civil and Environmental Engineering

Carin Roberts-Wollmann, Committee Co-Chair
Thomas Cousins, Committee Co-Chair
Jose Gomez
Elisa Sotelino
Linbing Wang

December 8, 2009
Blacksburg, Virginia

Keywords: Bridge Deck, Deck Panels, Grout, Post-Tensioning, Bridge Joints

The Investigation of Transverse Joints and Grouts on Full Depth Concrete Bridge Deck Panels

Matthew K Swenty

ABSTRACT

A set of experimental tests was performed at Virginia Tech to investigate transverse joints and blockouts on full depth concrete bridge deck panels. The joints were designed on a deck replacement project for a rural three span continuous steel girder bridge in Virginia. Two cast-in-place and four post-tensioned joints were designed and tested in cyclical loading. Each joint was tested on a full scale two girder setup in negative bending with a simulated HS-20 vehicle. The blockouts were built as hollow concrete rings filled with grout and left to shrink under ambient conditions. Thirteen combinations of different surface conditions and grouts were designed to test the bond strength between the materials. The strain profile, cracking patterns, and ponding results were measured for all specimens. A finite element analysis was performed and calibrated with the laboratory results.

The cast-in-place joints and the two post-tensioned joints with 1.15 MPa (167 psi) of initial stress experienced cracking and leaked water by the end of the tests. The two post-tensioned joints with 2.34 MPa (340 psi) initial stress kept the deck near a tensile stress of $1.5\sqrt{f'c}$ and performed the best. These transverse joints did not leak water, did not have full depth cracking, and maintained a nearly linear strain distribution throughout the design life. Full depth deck panel may be effectively used on continuous bridges if a sufficient amount of post-tensioning force is applied to the transverse joints. The finite element model provides a design tool to estimate the post-tensioning force needed to keep the tensile stresses below the cracking limit.

The blockouts with a roughened surface or an epoxy and a grout equivalent to Five Star Highway Patch grout had the highest bond stresses, did not leak water, and had smaller cracks at the grout-concrete interface than the control samples. A minimum bond strength of $2.5\sqrt{f'c}$ was maintained for all of the specimens with a grout equivalent to Five Star Highway Patch. A pea gravel additive in the grout reduced shrinkage and

reduced the bond strength. The finite element model provides a design tool to estimate cracking at the grout-surface interface.

TABLE OF CONTENTS

1 Introduction 1
1.1 Background 1
1.2 Objectives 3
2 Literature Review 5
2.1 Deck Panel History 5
2.2 Current Design Standards 6
2.3 Areas of Study 8
2.3.1 Economics 8
2.3.2 Construction Techniques 12
2.3.3 Composite Behavior and Shear Studs 20
2.3.4 Transverse Joints 24
2.3.5 Stiffness of Composite Deck Panels 32
2.3.6 Longitudinal Post-tensioning 37
2.3.7 Full Bridge Testing 42
2.4 Summary 44
2.5 Plan of Research 45
3 Experimental Research Methods 48
3.1 Transverse Joint Investigation 49
3.1.1 Transverse Joint Selection and Design 49
3.1.2 Transverse Joint Testing 54
3.1.3 Construction Study on the Transverse Joint Tests 57
3.1.4 Transverse Joint Instrumentation and Data Collection 64
3.2 Shear Stud Grout Pockets 67
3.2.1 Grout Investigation in the Transverse Joint Test Panels 68
3.2.2 Grout Testing for Deck Panel Pockets 72
3.3 Demonstration Bridge 79
3.3.1 Bridge Layout 79
3.3.2 Panel Design 83
3.3.3 Cost of the Project 85
3.3.4 Construction Monitoring 85
3.3.5 Instrumentation Plan 87
3.3.6 Joint Tests 89
4 Analysis of Data 91
4.1 Transverse Joint Results 91
4.1.1 Transverse Joint Design 92
4.1.2 Constructability Evaluation 96
4.1.3 Cracking in the Transverse Joints 118
4.1.4 Ponding on the Deck Panels 138
4.1.5 The Load-Strain Profile in the Transverse Joints 142
4.1.6 Strain Ranges in the Transverse Joints 151
4.1.7 Deflection of the Cantilevered Test 164
4.2 Grout Results 168

4.2.1 Transverse Joint Grouts 168
4.2.2 Grouted Ring Results 175
5 Finite Element Analysis 229
5.1 Finite Element Modeling 229
5.1.1 Transverse Joint Models 229
5.1.2 Grout Ring Models 236
6 Conclusion and Recommendation 250
6.1 Transverse Joint Tests 250
6.1.1 Construction 250
6.1.2 Performance 252
6.1.3 Finite Element Analysis 254
6.1.4 Transverse Joint Recommendations 254
6.2 Grout Ring Tests 255
6.2.1 Construction 255
6.2.2 Performance 256
6.2.3 Finite Element Analysis 259
6.2.4 Design Recommendations 259
6.3 Recommendations 260
6.4 Contributions of the Research 261
6.5 Future Research 262
References 263
Appendix A - VDOT Bridge Preliminary Design 267
A.1 Construction Drawings 268
A.2 Transverse Deck Design Calculations 276
A.2.1 Transverse Deck Analysis 276
A.2.2 Transverse Deck Design 285
A.3 Transverse Joint Design 295
A.3.1 Longitudinal Analysis 295
A.3.2 Longitudinal Strength Design 296
A.3.3 Horizontal Shear Design 300
A.4 Specifications 304
Appendix B - Documents for the Test Panels 309
B.1 Material Properties for the Panel Tests 310
B.2 Measured Stresses in the Deck Panels 312
B.3 Load Computations for the Transverse Joint Tests 313
B.4 Construction Drawings for the Test Panels 317
B.5 Cost Estimate of the Test Panels 324
B.6 Stresses in the Top of the Transverse Joints 326
B.7 Strain Levels in the Deck Panels 332
Appendix C - Grout Testing 335
C.1 Material Data Sheets 336
C.1.1 Five Star Grout 336
C.1.2 Five Star Grout with Fibers 338
C.1.3 Type K Concrete Mix 338

C.1.4 Set 45 Highway Grout 339
C.1.5 VDOT Post and Rail Bridge Deck Mix 342
C.2 Environmental Conditions During the Tests 343
C.3 Modified ASTM C157 Shrinkage Measurements 344
C.4 Deflection versus Time for the Rings 347
C.4.1 Five Star Control Specimens 347
C.4.2 Five Star Pea Gravel Control Specimens 348
C.4.3 Set 45 Control 349
C.4.4 Type K Control 350
C.4.5 Five Star Fiber Control 351
C.4.6 Five Star Exposed Aggregate 352
C.4.7 Five Star Pea Gravel Exposed Aggregate 353
C.4.8 Five Star Wire Brush 354
C.4.9 Star Pea Gravel Wire Brush 355
C.4.10 Five Star Epoxy 356
C.4.11 Five Star Pea Gravel Epoxy 357
C.4.12 Five Star Shear Key 358
C.4.13 Five Star Water Stop 359
C.5 Outlier Tests for the Ring Data 360
C.5.1 Dixon Outlier Test 360
C.5.2 ASTM E 178 T-test Outlier Analysis 361

List of Figures

FIGURE 1-1 CONSTRUCTING PRECAST PANELS AT A PRECAST PLANT 2
FIGURE 1-2 DECK PANEL LAYOUT 2
FIGURE 1-3 ELEVATION VIEW OF A DECK PANEL SYSTEM 3
FIGURE 2-1 FORMING TECHNIQUES FOR HAUNCHES AND TRANSVERSE JOINTS 13
FIGURE 2-2 ELEVATION VIEW OF ROUTE 7 DECK PANEL MECHANICAL SPLICE 17
FIGURE 2-3 NEW ENGLAND PRECAST/PRESTRESSED SPLICED REBAR DETAIL 18
FIGURE 2-4 SHEAR KEY AND BLOCKOUT FOR THE WISCONSIN BRIDGE 19
FIGURE 2-5 UNIFORM AND GROUPED SPACINGS OF SHEAR STUDS 20
FIGURE 2-6 SHEAR POCKET SHAPES 23
FIGURE 2-7 TYPICAL NON-POST-TENSIONED PANEL JOINT 25
FIGURE 2-8 EMBEDDED REINFORCING BAR JOINT 26
FIGURE 2-9 ELEVATION VIEW OF DIFFERENT JOINT TYPES BETWEEN PANELS 28
FIGURE 2-10 SIMPLE SPAN TEST OF EMBEDDED REINFORCING DECK PANEL JOINTS 34
FIGURE 2-11 ONE QUARTER SCALE TWO SPAN TEST SETUP 35
FIGURE 2-12 PROTOTYPE FULL SCALE BRIDGE 37
FIGURE 3-1 TRANSVERSE JOINTS 50
FIGURE 3-2 PROPOSED ELEVATION VIEW OF THE VIRGINIA BRIDGE 51
FIGURE 3-3 ORIGINAL VIRGINIA STEEL GIRDER BRIDGE 52
FIGURE 3-4 FULL DEPTH PRECAST PANEL PARTS (PLAN VIEW) 54
FIGURE 3-5 COMPOSITE CONNECTION BETWEEN THE PANELS AND GIRDERS (END ELEVATION VIEW) 55
FIGURE 3-6 TESTING SETUP (ELEVATION VIEW) 55
FIGURE 3-7 TRANSVERSE JOINT SETUP 56
FIGURE 3-8 INSTALLING THE VIBRATING WIRE GAUGES IN THE PANELS 57
FIGURE 3-9 BRIDGE HAUNCHES 59
FIGURE 3-10 FORMWORK AROUND THE TRANSVERSE JOINTS 60
FIGURE 3-11 TYPICAL GROUTING OF THE SHEAR POCKETS AND HAUNCH 61
FIGURE 3-12 GROUTING DOWN A GIRDER LINE 61
FIGURE 3-13 GROUT EXIT HOLE AT THE END OF A GIRDER LINE 61
FIGURE 3-14 GROUTING THE POST-TENSIONED DUCTS 62
FIGURE 3-15 POST-TENSIONING THE DECK PANELS 63
FIGURE 3-16 ELEVATION VIEW OF THE END OF THE TRANSVERSE JOINT TESTS 63
FIGURE 3-17 LOAD CELL ON THE DEAD END OF A STRAND DURING STRESSING 64
FIGURE 3-18 INSTRUMENTATION AT THE TRANSVERSE JOINTS 65
FIGURE 3-19 LOCATION OF THE DEMEC POINTS. 66
FIGURE 3-20 PONDING TEST 67
FIGURE 3-21 SHEAR POCKET SURFACES 70
FIGURE 3-22 SHEAR POCKET CONSTRUCTION DOCUMENTS 71
FIGURE 3-23 PONDING TEST ON THE SHEAR POCKETS 72
FIGURE 3-24 PLAN AND THREE DIMENSIONAL VIEW OF THE GROUT TESTING SETUP 74
FIGURE 3-25 GROUT RING FORMWORK A) TYPICAL B) WATER STOP C) SHEAR KEY 75
FIGURE 3-26 APPLYING THE BURLAP AND PLASTIC 76
FIGURE 3-27 DEMEC POINT LOCATIONS AND MEASUREMENTS 78
FIGURE 3-28 A) ORIGINAL BENT B) STAGED ONE CONSTRUCTION C) STAGED TWO CONSTRUCTION 81
FIGURE 3-29 PLAN VIEW OF THE PROPOSED FINAL BRIDGE DECK LAYOUT 82
FIGURE 3-30 ELEVATION VIEW OF A PANEL 87
FIGURE 3-31 INSTRUMENTATION PLAN 88
FIGURE 3-32 STRAIN GAUGE LOCATIONS 89
FIGURE 4-1 FORMING THE PANELS AT THE PRECAST PLANT 98
FIGURE 4-2 DIFFICULTIES FORMING PRECAST PARTS 99
FIGURE 4-3 CONSTRUCTION OF THE GIRDER ASSEMBLY 100

FIGURE 4-4 FIBER FORMWORK AND STEEL ANGLE FORMWORK 101
FIGURE 4-5 BLOCKOUTS AROUND THE LEVELING BOLT ASSEMBLIES. 102
FIGURE 4-6 REMOVING THE STYROFOAM FROM THE HSS ANCHORAGE ASSEMBLIES. 102
FIGURE 4-7 PLACING THE PANELS: POST-TENSIONING, LOOPED BARS, EMBEDDED BARS 104
FIGURE 4-8 JOINT FORMING METHODS: WITH STEEL ANGLES AND WITH WOOD 105
FIGURE 4-9 ELEVATION VIEW OF THE JOINT AND FORMWORK PRIOR TO POST-TENSIONING 106
FIGURE 4-10 FORMING FOR THE TRANSVERSE JOINTS INSIDE THE HAUNCHES. 106
FIGURE 4-11 LAYOUT OF SHEAR STUDS IN A POCKET 107
FIGURE 4-12 GROUTING THE DUCTS 109
FIGURE 4-13 GROUTING THE HAUNCH AND POCKETS 110
FIGURE 4-14 STRAND LAYOUTS IN THE FIRST AND SECOND POST-TENSIONED TESTS 112
FIGURE 4-15 STRESSING ASSEMBLY 113
FIGURE 4-16 LOAD CELLS ON THE DECK. 115
FIGURE 4-17 PANEL STRAIN PRIOR TO TESTING FOR THE 340 PSI POST-TENSIONED JOINT WITH EPOXY. 118
FIGURE 4-18 SHRINKAGE CRACKS IN THE 340 PSI POST-TENSIONED JOINTS: NORMAL AND EPOXIED 120
FIGURE 4-19 LOAD VERSUS DECK SURFACE STRAIN FROM DEMEC POINTS -LOOPED REINFORCED 122
FIGURE 4-20 LOAD VERSUS DECK SURFACE STRAIN FROM DEMEC POINTS -EMBEDDED REINFORCED JOINT - ONE SERVICE LOAD CYCLE 123
FIGURE 4-21 INITIAL CRACKS IN THE EMBEDDED BAR AND LOOPED BAR JOINTS 123
FIGURE 4-22 LOAD VERSUS DECK SURFACE STRAIN FROM DEMEC POINTS - POST-TENSIONED JOINTS AT 167 KSI STRESS – ONE SERVICE LOAD CYCLE 124
FIGURE 4-23 TYPICAL INITIAL CRACKING PATTERN FOR POST-TENSIONED JOINTS 124
FIGURE 4-24 LOAD VERSUS DECK SURFACE STRAIN FROM DEMEC POINTS - POST-TENSIONED JOINTS AT 340 KSI STRESS – ONE SERVICE LOAD CYCLES 125
FIGURE 4-25 LOAD VERSUS DECK SURFACE STRAIN FROM DEMEC POINTS - POST-TENSIONED JOINTS AT 340 KSI STRESS – 100,000 SERVICE LOAD CYCLES 126
FIGURE 4-26 CRACKS ALONG THE EMBEDDED BAR CAVITIES 129
FIGURE 4-27 LONGITUDINAL CRACKING ON THE BOTTOM OF THE LOOPED JOINT 130
FIGURE 4-28 SPALLING ALONG THE POST-TENSIONED PEA GRAVEL JOINT 131
FIGURE 4-29 SURFACE CRACKS IN THE NEAT GROUTED 340 PSI TRANSVERSE JOINT 132
FIGURE 4-30 CRACKS IN THE EPOXY GROUTED 340 PSI TRANSVERSE JOINT 132
FIGURE 4-31 SURFACE CRACKS IN THE NEAT GROUT AND EPOXY GROUT POST-TENSIONED POCKETS 133
FIGURE 4-32 ADHESIVE BARRIER ON THE SURFACE OF THE BRIDGE DECK 138
FIGURE 4-33 FINAL LEAKING - REINFORCED CONCRETE JOINTS: 141
FIGURE 4-34 FINAL LEAKING - POST-TENSIONED JOINTS WITH 167 PSI STRESS: 141
FIGURE 4-35 FINAL LEAKING – BOTH POST-TENSIONED JOINTS WITH 340 PSI STRESS 141
FIGURE 4-36 STRAIN PROFILE FOR THE EMBEDDED BAR JOINT AT 138,000 CYCLES 143
FIGURE 4-37 STRAIN PROFILE FOR THE LOOPED BAR JOINT AT 138,000 CYCLES 143
FIGURE 4-38 STRAIN PROFILE FOR THE EMBEDDED BAR JOINT AT 1,000,000 CYCLES 144
FIGURE 4-39 STRAIN PROFILE FOR THE LOOPED BAR JOINT AT 1,000,000 CYCLES 144
FIGURE 4-40 STRAIN PROFILE: NEAT GROUT POST-TENSIONED JOINTS WITH 167 PSI NORMAL STRESS AT 146
FIGURE 4-41 STRAIN PROFILE: EXTENDED GROUT POST-TENSIONED JOINTS WITH 167 PSI NORMAL STRESS AT 0 CYCLES .. 146
FIGURE 4-42 STRAIN PROFILE: NEAT GROUT POST-TENSIONED JOINTS WITH 167 PSI NORMAL STRESS AT 147
FIGURE 4-43 STRAIN PROFILE: EXTENDED GROUT POST-TENSIONED JOINTS WITH 167 PSI NORMAL STRESS AT 1 MILLION CYCLES 147
FIGURE 4-44 STRAIN PROFILE: NEAT GROUT POST-TENSIONED JOINTS WITH 340 PSI NORMAL STRESS AT 148
FIGURE 4-45 STRAIN PROFILE: EPOXIED GROUT POST-TENSIONED JOINTS WITH 340 PSI NORMAL STRESS AT 149
FIGURE 4-46 STRAIN PROFILE: NEAT GROUT POST-TENSIONED JOINTS WITH 340 PSI NORMAL STRESS AT 149
FIGURE 4-47 STRAIN PROFILE: EPOXIED GROUT POST-TENSIONED JOINTS WITH 340 PSI NORMAL STRESS AT 150
FIGURE 4-48 VWG LOCATION ON A PLAN VIEW OF THE EMBEDDED AND LOOPED BAR JOINTS 151
FIGURE 4-49 VWG LOCATIONS 152
FIGURE 4-50 PANEL STRAIN DURING STATIC LOAD TESTING FOR A LOOPED BAR JOINT 154
FIGURE 4-51 PANEL STRAIN DURING STATIC LOAD TESTING FOR THE EMBEDDED BAR JOINT 154

FIGURE 4-52 PANEL STRAIN DURING STATIC LOAD TESTING FOR THE 167 PSI POST-TENSIONED JOINT WITH PEA GRAVEL.. 156
FIGURE 4-53 PANEL STRAIN DURING STATIC LOAD TESTING FOR THE 167 PSI POST-TENSIONED JOINT WITH GROUT..... 157
FIGURE 4-54 PANEL STRAIN DURING STATIC LOAD TESTING FOR THE 340 PSI POST-TENSIONED JOINT. 159
FIGURE 4-55 PANEL STRAIN DURING STATIC LOAD TESTING FOR THE 340 PSI POST-TENSIONED JOINT WITH EPOXY..... 159
FIGURE 4-56 TYPICAL LOAD VERSUS STRAIN MEASURED BY THE DEMEC POINTS 162
FIGURE 4-57 MAXIMUM SURFACE STRAIN UNDER SERVICE LOADING (DEMEC READINGS) 163
FIGURE 4-58 MAXIMUM DEFLECTION OF THE GIRDERS VERSUS LOAD CYCLES – CAST-IN-PLACE JOINTS 164
FIGURE 4-59 MAXIMUM DEFLECTION OF THE GIRDERS VERSUS LOAD CYCLES – 167 KSI POST-TENSIONED JOINTS..... 165
FIGURE 4-60 MAXIMUM DEFLECTION OF THE GIRDERS VERSUS LOAD CYCLES – 340 KSI POST-TENSIONED JOINTS..... 166
FIGURE 4-61 POCKET LAYOUT ON THE TEST PANELS..... 169
FIGURE 4-62 CASTING FORMWORK AND FINAL BLOCKOUT CONDITION..... 170
FIGURE 4-63 TYPICAL SHRINKAGE CRACK PATTERNS IN THE SHEAR POCKETS PRIOR TO LOADING 170
FIGURE 4-64 COMPLETE LEAKING IN THE HAUNCH BENEATH A SHEAR POCKET JOINT..... 175
FIGURE 4-65 COMPRESSOMETER AND EXTENSOMETER ON A CONCRETE CYLINDER..... 180
FIGURE 4-66 TYPICAL MODULUS OF ELASTICITY GRAPH..... 181
FIGURE 4-67 TYPICAL POISSON'S RATIO GRAPH 181
FIGURE 4-68 ASTM C157 MODIFIED SHRINKAGE MOLD..... 187
FIGURE 4-69 SHRINKAGE IN THE FIRST 24 HOURS..... 189
FIGURE 4-70 VDOT POST AND RAIL CONCRETE SHRINKAGE..... 191
FIGURE 4-71 FIVE STAR HIGHWAY PATCH GROUT SHRINKAGE 192
FIGURE 4-72 FIVE STAR HIGHWAY PATCH GROUT WITH POLYPROPYLENE FIBERS SHRINKAGE..... 192
FIGURE 4-73 FIVE STAR HIGHWAY PATCH GROUT WITH PEA GRAVEL SHRINKAGE..... 193
FIGURE 4-74 TYPE K CONCRETE MIX SHRINKAGE 193
FIGURE 4-75 SET 45 GROUT SHRINKAGE 194
FIGURE 4-76 STRAIN VERSUS TIME FOR A FIVE STAR GROUT RING SAMPLE 197
FIGURE 4-77 STRAIN VERSUS TIME FOR A SET 45 RING SAMPLE 198
FIGURE 4-78 STRAIN VERSUS TIME FOR A TYPE K RING SAMPLE 199
FIGURE 4-79 COMPARISON OF GROUT RING AND ASTM C157 SHRINKAGE MEASUREMENTS 204
FIGURE 4-80 TIME TO FIRST INTERFACE CRACKS..... 214
FIGURE 4-81 AVERAGE SIZE OF THE FINAL INTERFACE CRACKS 216
FIGURE 4-82 DETERMINING THE DEFORMATION AT FIRST CRACK 218
FIGURE 4-83 AVERAGE STRESSES OF THE GROUT RINGS..... 222
FIGURE 5-1 SPRING STIFFNESS FOR THE POST-TENSIONED DECK CONNECTIONS..... 232
FIGURE 5-2 ABAQUS MODEL FOR THE DECK PANELS 233
FIGURE 5-3 FINITE ELEMENTS FOR THE DECK PANEL MODELS 233
FIGURE 5-4 TYPICAL STRESS DISTRIBUTION IN THE ABAQUS DECK PANEL MODELS 233
FIGURE 5-5 VERIFICATION OF THE ABAQUS MODEL WITH THICK WALLED CYLINDERS 238
FIGURE 5-6 FINITE ELEMENT LAYOUT FOR THE RINGS 239
FIGURE 5-7 ASTM C157 SHRINKAGE VERSUS TIME GRAPH 240
FIGURE 5-8 FIRST CRACKING PATTERN IN THE GROUT RINGS 244
FIGURE 5-9 DEFORMATIONS AT THE CONCRETE-GROUT INTERFACE 246
FIGURE 5-10 UNIFORM STRESS OUTPUT FROM ABAQUS FOR A RING SAMPLE 247
FIGURE 5-11 SAMPLE DESIGN OF A BLOCKOUT 249

List of Tables

TABLE 2-1 CONSTRUCTION TIMES FOR SULLIVAN'S TEST 11
TABLE 2-2 GROUT GUIDELINES 15
TABLE 2-3 STRESS LEVEL RECOMMENDATIONS FOR POST-TENSIONED DECK PANELS 30
TABLE 2-4 RECOMMENDED STRESS LEVELS IN PRECAST PANELS 31
TABLE 2-5 FINITE ELEMENT MODELS OF DECK PANELS 42
TABLE 2-6 RESEARCH NEEDS AND PLANS 47
TABLE 3-1 TRANSVERSE JOINT TESTING MATRIX 56
TABLE 3-2 STATIC LOAD AND PONDING TESTS DURING THE CYCLICAL TESTS 65
TABLE 3-3 TEST MATRIX OF TRANSVERSE JOINT 69
TABLE 3-4 PROPOSED SHEAR POCKET TESTING SPECIMENS 73
TABLE 3-5 DATA COLLECTION SCHEDULE FOR THE GROUT RINGS 78
TABLE 4-1 DECK STRESS LEVELS FOR A SIMPLE AND CONTINUOUS SPAN BRIDGE 95
TABLE 4-2 MATERIALS USED IN THE TRANSVERSE JOINT CONSTRUCTION 96
TABLE 4-3 MAN POWER TO BUILD THE POST-TENSIONED TEST BRIDGES 97
TABLE 4-4 GROUTING INFORMATION 111
TABLE 4-5 STRESS LEVELS IN THE PT1 SETUP 115
TABLE 4-6 STRESS LEVELS IN THE PT2 SETUP 116
TABLE 4-7 TIME AND LOAD OF THE FIRST CRACK 121
TABLE 4-8 STRESSES AT THE FIRST CRACK IN THE TRANSVERSE JOINTS 127
TABLE 4-9 FINAL SURFACE CRACK SIZES IN THE TRANSVERSE JOINTS 136
TABLE 4-10 FINAL CRACK OBSERVATIONS IN THE TRANSVERSE JOINTS 137
TABLE 4-11 PONDING TEST RESULTS: REINFORCING BAR CONNECTIONS 139
TABLE 4-12 PONDING TEST RESULTS: POST-TENSIONED CONNECTIONS 140
TABLE 4-13 STRAIN RANGE IN THE RC PANELS DURING THE CYCLICAL TESTS 153
TABLE 4-14 STRAIN RANGE IN THE PT1 (167 PSI) PANELS DURING THE CYCLICAL TESTS 155
TABLE 4-15 STRAIN RANGE IN THE PT2 (340 PSI) PANELS DURING THE CYCLICAL TESTS 158
TABLE 4-16 THE AVERAGE RANGE OF STRAIN IN EACH JOINT 163
TABLE 4-17 MAXIMUM DEFLECTIONS OF THE TRANSVERSE JOINT TESTS 164
TABLE 4-18 AVERAGE WEATHER CONDITIONS WHEN GROUTING THE SHEAR POCKETS 171
TABLE 4-19 AVERAGE CRACK WIDTHS IN THE SHEAR POCKETS OF THE SECOND PT PANELS 171
TABLE 4-20 AVERAGE CRACK WIDTHS IN THE GROUT POCKETS IN THE SECOND PT PANELS. 173
TABLE 4-21 PERCENT DIFFERENCE AMONG CRACK SIZES IN THE GROUT POCKETS 174
TABLE 4-22 PONDING RESULTS ON THE SHEAR POCKETS 174
TABLE 4-23 SHEAR POCKET CONSTRUCTION PROCESSES 176
TABLE 4-24 CONCRETE STRENGTH 178
TABLE 4-25 GROUT STRENGTHS 179
TABLE 4-26 MODULI AND POISSON'S RATIOS OF THE CONCRETE 182
TABLE 4-27 MODULI AND POISSON'S RATIOS OF THE FIVE STAR GROUT 183
TABLE 4-28 MODULI AND POISSON'S RATIOS OF THE FIVE STAR GROUT WITH PEA GRAVEL 183
TABLE 4-29 MODULI AND POISSON'S RATIOS OF THE SET 45 GROUT 184
TABLE 4-30 MODULI AND POISSON'S RATIOS OF THE TYPE K CONCRETE 185
TABLE 4-31 MODULI AND POISSON'S RATIOS OF THE FIVE STAR GROUT WITH FIBERS 185
TABLE 4-32 SHORT TERM SHRINKAGE 190
TABLE 4-33 STRAINS IN THE OUTER RING 201
TABLE 4-34 STRAINS IN THE INNER RING 202
TABLE 4-35 FINAL STRAINS IN THE INNER AND OUTER RING 205
TABLE 4-36 FIRST VISIBLE INTERFACE CRACKS IN THE RING SAMPLES 208
TABLE 4-37 FIRST INTERFACE CRACKS DETECTED BY DEMEC STRAIN READINGS 210
TABLE 4-38 TIME IN DAYS TO FIRST INTERFACE CRACKS 213
TABLE 4-39 FINAL CRACKS IN THE RINGS 217

TABLE 4-40 GROUT RING PROPERTIES AT FIRST CRACK 220
TABLE 4-41 BOND STRESS BETWEEN THE RINGS AT FIRST CRACK * 221
TABLE 4-42 BOND STRESS COMPARED TO FIRST CRACK IN THE TRANSVERSE JOINTS 224
TABLE 4-43 PONDING RESULTS IN THE RING TESTS 226
TABLE 4-44 SUMMARY OF RING TESTS 228
TABLE 5-1 VERIFICATION OF THE ABAQUS MODELS 231
TABLE 5-2 COMPARISON OF THE 340 PSI JOINT RESULTS 235
TABLE 5-3 COMPARISON OF THE 167 PSI JOINT RESULTS 235
TABLE 5-4 COMPARISON OF THE CAST-IN-PLACE JOINT RESULTS 235
TABLE 5-5 VERIFICATION OF THE ABAQUS RING MODELS 239
TABLE 5-6 RING MATERIAL PROPERTIES FOR THE FINITE ELEMENT MODEL 242
TABLE 5-7 COMPARISON OF LABORATORY AND ABAQUS DEFORMATIONS 245
TABLE 6-1 SUMMARY OF RESEARCH RESULTS 251

1 Introduction

1.1 Background

Each year, the average person spends almost a week waiting in traffic (US-News 2007). Reports have suggested this not only wastes a person's time but costs the United States billions of dollars (CBS-News 2005). A number of issues contribute to traffic congestion, but one of the most prominent is construction delays. Construction is a necessary, ongoing process that transportation officials continually orchestrate to upkeep, rehabilitate, and build highways. The key is to find a way to alleviate the inconveniences caused by construction. By improving the materials and methods used in constructing and rehabilitating bridges, the disruption to the traveling public can be reduced.

One of the largest and longest processes in construction is building the deck on a bridge. Bridge deck construction is labor intensive, places workers in dangerous situations, and costs a significant amount of money. Traditionally, bridge decks have been built of cast-in-place concrete. This type of construction requires extensive work forming the deck, placing the reinforcing steel, pouring the concrete, and waiting for the concrete to cure. If a method could be devised to eliminate or speed up these processes, construction delays could be limited and bridges would reopen more quickly.

Precast concrete bridge decks are one option to help speed up the construction of bridge decks at the bridge site. The deck is cast in pieces away from the construction site (Figure 1-1). This provides good quality control and more flexibility during construction. The curing process can be built into the precast process away from the bridge. In addition, there is minimal work done on the job site and large concrete pours are eliminated from the field. Panels may be lifted directly from a truck and placed on the girders. The panels are placed in their final positions and a minor amount of formwork is placed around the haunches and joints. The panels are then connected to the girders and to each other (Figure 1-2). Using precast deck panels should limit the amount of construction needed on the bridge site and reduce the disruption to the public.

Figure 1-1 Constructing Precast Panels at a Precast Plant

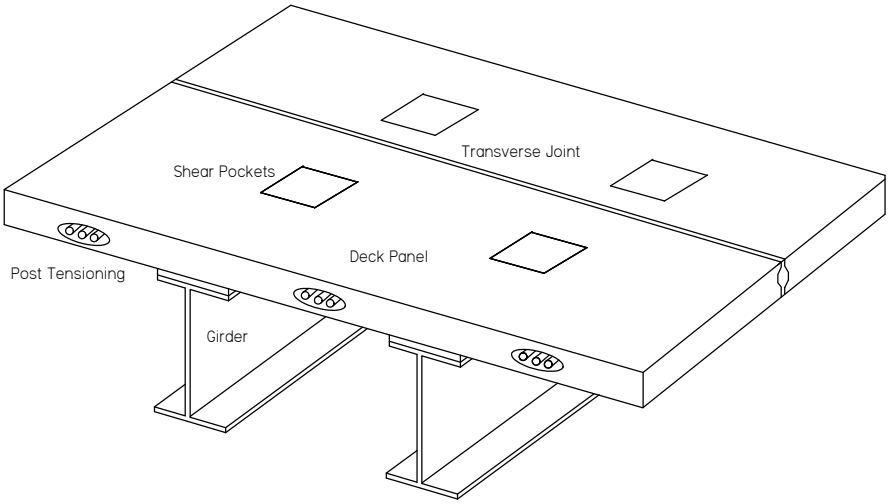

Figure 1-2 Deck Panel Layout

A hindrance to the widespread implementation of precast deck panels is the lack of guidance for designers. There are no standard design procedures for deck panels because the design of the panels has not been thoroughly investigated and implemented (Swartz 2008). When using precast parts, there are numerous new joints that must be designed on a bridge deck (Figure 1-3). As noted by Issa et al, "The joints are important because bridge deck performance is manifested in the behavior of its joints." (Issa et al. 1995a) Joints are a primary cause of deterioration on bridges, so this is a big concern for engineers. In addition, the traditional methods of attaching bridge girders to cast-in-place decks with shear studs must be

adjusted or changed. Past performance of bridges with deck panels has not been satisfactory in many cases because of faulty designs and bad detailing of the joints.

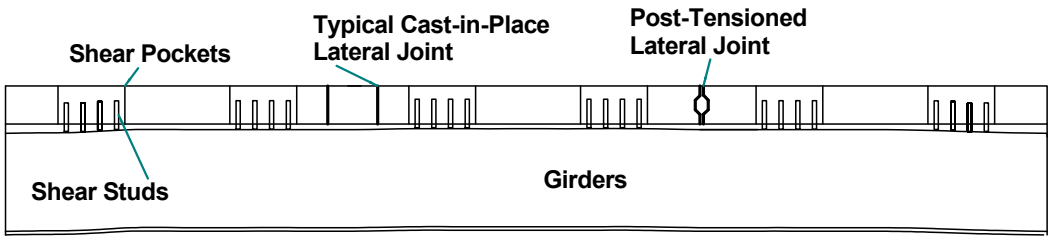

Figure 1-3 Elevation View of a Deck Panel System

1.2 Objectives

The purpose of this investigation was to systematically evaluate the serviceability response of various transverse connections and grouting methods in a precast concrete deck panel system through laboratory testing and finite element modeling and to devise construction and design procedures to implement the results. The final step of the research process was to prepare a bridge deck design for the implementation of precast deck panels with details based on the results of this research.

In particular, this study was designed to address the following questions:

1) Which transverse deck panel connection techniques will crack the least and be most durable under the worst case service load condition?
2) Do current recommendations for longitudinal post-tensioning stress in deck panels keep the deck and joints in compression during cyclical testing? Can a finite element model be built to simulate the results in the laboratory tests and be used for future post-tensioned, steel girder deck designs?
3) What types of surface treatments and grouts prevent cracking and water leakage in the shear stud pockets? Can a finite element model be built to simulate the laboratory results and be used on future deck designs?

4) How does the negative bending stiffness of different deck panel systems with transverse joints change over time?
5) Which construction techniques work best when building a full depth precast bridge deck? What are the material and labor estimates to build the bridge?

The first phase of the study tested post-tensioned and reinforcing bar transverse joints, shear stud pockets, and construction procedures for full depth precast concrete deck panels in a laboratory setting. Three separate specimens with two steel girders, three precast panels, two transverse joints, and twelve shear stud pockets were used. The transverse joint specimens were tested in negative bending under cyclical loading for the design life of the bridge deck. Both prestressed and non-prestressed joints were compared under the same testing scenario. All of the construction procedures, material quantities, and labor used to build the lab specimens were recorded to help develop standard construction procedures for the field.

The second phase was to test the grout materials used in the joints and pockets on the bridge for shrinkage. Thirty-eight concrete rings with grouts inside simulated the pockets on deck panels. The models were tested for shrinkage, bond stress, leakage, and crack dimensions. A comparison was made of the performance of 13 different grout and concrete surface combinations.

The final phase was to build finite element models of the transverse joints and the grout rings. The laboratory performance of each sample was simulated with finite element models. The final models provide a design tool for making finite element models to predict the stresses and deflections in post-tensioned transverse joints and blockouts.

Future research will include implementing design and construction procedures on a replacement bridge deck in Virginia. The designs and procedures associated with the testing were recorded for future use. The next phase of research is ready for implementation.

2 Literature Review

Full depth concrete deck panels offer a promising option for bridge decks. Precast products are efficiently fabricated in precast yards with better quality than similar items made in the field. Like other precast bridge parts, panels can be assembled quickly. However, universal design and construction methods are still needed to effectively implement deck panels on real bridges (Swartz 2008).

Full depth concrete deck panels are a technology that has been implemented in a variety of situations but have not yet been widely accepted. Many reasons have contributed to the slow pace of adopting this type of construction for bridge decks. Inconsistent construction and design techniques, particularly with the joints, add to the historical problems with deck panels. In addition, a lack of economic information prevents many designers from specifying this technology. A further look into the history of full depth concrete deck panels reveals the need to review past deck behavior, perform tests on deck panel joints and shear pockets, and develop standard design and construction methods.

2.1 Deck Panel History

Full depth precast concrete deck panels have been used on a variety of bridge applications since the 1970s with various levels of success. The history of deck panels started with the implementation of a variety of design and construction methodologies by design engineers. Research did not begin until many full depth bridge decks were built and had been in service for over a decade. "Because of the urgency and realities of bridge deck rehabilitation, the application of full depth precast decks had to go ahead of research. In effect, the bridge engineers ha[d] taken their experiments directly to the field" (Biswas 1986). The application of this technology resulted in uncertainties with the structural systems, components, and materials. Biswas noted that full depth deck panels were used before they were properly tested (1986).

Early studies recorded that bridge deck panels had no universally accepted designs or joining techniques. One of the first studies noted the wide variety of joints between the panels and girders on a relatively small number of bridges (Biswas 1986). Some systems were

acceptable in specific situations, but many others did not perform as expected. Another survey was sent to every state to find what entities used full depth deck panels and how they implemented the technology (Issa et al. 1995a). The results confirmed the earlier researchers' conclusions; No standard methods for design and construction existed and many decks had leaks and performance problems. Much of this was attributed to poor construction techniques. Engineers have continued to design deck panels on specific projects, but there are still no general conclusions or standards.

The previous surveys led to a more in-depth field investigation of various in-place bridge deck panels (Issa et al. 1995c). Problematic areas were identified on real bridges with deck panels. The conclusion was there was a need for laboratory research on connections types, construction procedures, materials, and post-tensioning. Nearly every state that tried implementing full depth deck panels used different joint types, materials, and layouts. The best performing decks typically had post-tensioning and were built with quality construction procedures and careful oversight. Bridge decks appeared to be a reasonable solution in specific situations, but no one had devised a standard method for design and construction.

2.2 Current Design Standards

The design and construction of full depth deck panels continues to remain fraught with questions for most engineers because of a lack of design standards (Swartz 2008). Badie et al. reported that current methods are not widely accepted, contradict one another, and have biases toward certain parties involved (2009). When designing a deck panel system there are several parts that require special attention. This includes designing the panels transversely with prestressed strands, attaching the girders to the panels for composite action, using high early strength grouts in the connections and haunches, and connecting the panels together transversely and longitudinally. Each of these procedures is in a different state of development.

The most recognized design standards in bridge engineering include little information on full depth deck panels. The American Association of State Highway and Transportation Officials (AASHTO) Load and Resistance Factored Design (LRFD) design specification briefly mentions the design of full depth concrete bridge deck panels in section 9.7.5: Precast Deck Slabs on

Girders (AASHTO 2007). The specification says the panels are permitted but gives no guidelines on the joints, shear connectors, or grouts. This leaves large gaps in the design procedures for the most challenging and problematic areas on a bridge deck panels. The most recent Precast Concrete Institute (PCI) Bridge Design Manual has a section in chapter 8 about deck slab designs. No specific design procedures are presented but caveats are mentioned for choosing transverse joints and non-shrink grouts (PCI 2003).

A working agenda item (WAI-139) is presently in the AASHTO bridge committee (T-10) for the Precast Deck Slabs on Girders, LRFD Article 9.7.5. The suggested additions to the LRFD code are based upon the research done by Badie and Tadros (2006b). The updates would include a basic guide for design and construction of deck panels. This includes a suggested shear key detail, grout design strength, shear stud pocket detail, and a post-tensioned minimum of 0.25 ksi for transverse joints. WAI-139 is presently being considered by committees T-14 (Steel) and T-4 (Construction).

A state of the art report from PCI is in a revision state but should be published in the near future. The draft copies of the report present a design example in Appendix E for full depth deck panels. The majority of the design procedures focus on shear connectors and transverse reinforcement. The recommendation is to use the current strip or strain compatibility methods in section 4.6.2 of the AASHTO LRFD specifications for transverse deck design. Section 2.4 suggests using post-tensioning for the longitudinal reinforcement but does not provide a recommendation on how to design continuous decks over interior supports. The suggestion is made to use the LRFD Specification Section 9.5.5.3 where a suggested minimum effective stress of 0.25 ksi is required on all components connected with post-tensioning. In the design example the AASHTO loss equations from Section 9.5.5 for elastic shortening, shrinkage, creep, and steel relaxation are used to find the final effective prestress force. The design does not take into account any interactions between the panels and the girders after making the system composite. There is also no guidance on shear stud pockets and grouts (PCI 2006).

The lack of standards implies that more research is needed on the design of deck panels. The technology will never be widely accepted without design guidelines for practicing

engineers. Design standards will be developed as new research confirms the soundness of full depth bridge deck panels.

2.3 Areas of Study

Past studies have shown the need for additional research on deck panels and the need for further development of standards. Some areas have been studied, such as shear stud spacing, but many items like panel joints, post-tensioning levels, construction techniques, grouting materials, and economics need further investigation. In addition, a better understanding of how these components perform as a unit would provide more confidence in deck panel systems. The techniques for constructing the systems need further development and documentation. Lastly, the economic advantages need documentation. It has always been assumed, but rarely documented, that full depth panels will save bridge owners money over time. A study on full depth deck panels is required to help promote the strengths of full depth deck panels and reveal any weaknesses.

Below is a list of full depth deck panel issues that need further attention. The goal of this research is to address these issues. Modeling will follow the laboratory investigations to further investigate the deck panel joints and blockouts. An eventual bridge replacement project that implements the best practice for each of these details will demonstrate and test the new developments.

2.3.1 Economics

Engineers are looking for economical ways to speed up construction times and reduce traffic disruption during construction. In theory, full depth deck panels should do both. They are placed as pieces on a bridge without requiring large forming processes or curing times. Joints and composite connectors are still needed but the overall construction process should be much faster. The assumption has been that deck panels are more economical when considering user costs but currently more expensive to construct. "Initial cost is still seen as a disadvantage for implementing innovative prefabricated systems because…the initial cost of prefabricated bridges is generally equal to or greater than those of alternative solutions"

(Shahawy 2003). The increase in material and labor costs could be offset by savings derived from fewer delays to motorists. Eventually, more widespread use may result in lower costs due to economics of scale and contractor's familiarity with the technology.

Little detailed quantitative data is available to show that full depth deck panels save money. In 1980, the first large scale bridge replacement project cost approximately the same price as a cast-in-place deck. The engineer suggested this price would go down as deck panels were widely adopted. These panels were not connected to one other, possibly contributing to the low cost (Knudsen 1980). In 2000, a set of deck replacements was completed in Connecticut. The engineers found the cost was slightly higher but that the savings to the public was substantial because of the quick construction time (Culmo 2000). A separate project in 1997 on the Jacques Cartier Bridge in Canada estimated the cost of deck panels was about the same as a cast-in-place deck (Zaki and Mailhot 2003). The cost breakdown and assumptions are not available for these projects.

In 2001 on Route 7 in Fairfax County Virginia, two bridge decks were replaced with full depth deck panels. An economic analysis was done on the replacement of both of these single span bridges. The price for a cast-in-place deck was $25 per square foot while deck panels cost $30 per square foot. Additionally, the cost for removal of the deck was $25 per square foot for the deck panels and $10 per square foot for the cast-in-place option. The additional cost was due to the construction sequence of removing only a small length of deck each night. The cast-in-place place option assumed removing the entire deck at one time. It must be realized that this additional cost would not be necessary if the deck was replaced during one construction sequence instead of during a nightly sequence.

The additional costs for night construction benefitted the public when the bridge was complete two and half months faster than scheduled. This savings was estimated at $2,000,000. The cast-in-place deck would have required a 4 month road closure while the deck panels only required lane reductions at night for 6 weeks. The deck panel option was chosen because of the total cost savings (Babaei et al. 2001).

A new approach to deck panels, the NUDECK system, is a partial depth, full width precast deck panel system. The details are slightly different than the full depth panels but the

processes to build and construct the deck are similar. The biggest difference is the requirement of placing a cast-in-place partial depth deck on top of the NUDECK panels. In 1998, a test bridge was built in Nebraska. The economic data showed that the cost was slightly higher than a cast-in-place system. The price to build and ship the panels (including material, overhead, profit, labor and shipping costs for the pre-caster) to a job was about $5.50 to $7.00 per square foot for the NUDECK system as opposed to $4.50-$6.00 per square foot for a traditional deck (Badie et al. 1998). Because this system was new and innovative, it required additional work in the field not typically done on a full depth panel system. The cost savings came from the reduced construction times and disruptions to motorists.

In Missouri, a 1,700 foot steel girder bridge spanning a lake was redecked. The price was $56 per square foot for redecking. At the time, the average cost to redeck a bridge ranged from $32 to $40 per square foot. However, when including staged construction and logistics over water, the actual price was estimated 9% higher than a cast-in-place deck. This did not include the user savings due to finishing the project over a year earlier than originally expected (Wenzlick 2005).

Other studies have given the cost estimates of different deck systems but provided even fewer details. A study on a 170 ft by 71 ft simple span steel plate girder bridge reported that the cost was approximately $200,000 more for the deck panels ($16.60 per square foot) but no base line price was reported (Harrison and LeBlanc 2005b). A cost assessment on a bridge in Connecticut estimated the re-decking cost at $71 per square foot for a cast-in-place deck versus $75 per square foot for a full depth panel deck (Issa et al. 1995c). In 1984 the cost was $41 per square foot to replace the deck on the Woodrow Wilson bridge while maintaining traffic (Lutz 1984). This cost included working on one lane each night and maintaining full serviceability during the day.

Sullivan built a 12 ft by 40 ft mockup of a simply supported two girder precast bridge (Sullivan 2007). His dissertation included a list of construction procedures along with a timeline for many of them. Additionally, an estimate of the work force needed for each major task was reported. Table 2-1 lists the procedures and man hours needed on the specimen built by Sullivan. A project with detailed information similar to this project could be extrapolated and

related to labor costs. A similar procedure was performed on the NUDECK system by Fallaha et al. (2004). Unit prices and quantities were included but labor requirements were left out on the NUDECK redecking project. A similar table with labor estimates would provide more information on deck panel construction. An overall cost and a cost per square foot of installing deck panels could then be extrapolated from local material and labor prices.

Table 2-1 Construction Times for Sullivan's Test

Process	Manpower	Time	Installation Rate	Notes
	(People)	*(Hours)*	*Units Installed/Hour*	
Placing Panels	3	1:40	3.0 Panel/Hour	Placing the panels (Does not Include Elevation Adjustments)
Haunch Formwork		4:10	19.2 ft/Hour	No Manpower was Given
Joint Grout	3	0:45	32.0 ft/Hour	2 – 12 ft Joints 4 Blockouts for Post-Tensioning were Included
Joint Epoxy	3	0:30	48.0 ft/Hour	2 – 12 ft Joints
Stressing Tendons	2	6:40	1.80 Tendons/hour	12 Tendons
Grouting Ducts	3	1:00	40.0 ft/Hour	A Hand Pump was Used
Grouting Haunches	8	1:30	53.3 ft/Hour	
Removing Leveling Bolts	1	1:00	16 Bolts/Hour	

All of these studies are limited and do not explain the increases in cost. A more detailed account of a bridge construction project is needed to clearly show the procedures. A direct comparison of full depth deck panel versus traditional deck construction could show the economic benefits and might lead to future uses for panels. This could lead to further reductions in the cost since it has been noted that "…precast concrete becomes increasingly economical with repetitive elements" (Biswas 1986).

2.3.2 Construction Techniques

Construction issues have been a primary concern for bridge deck performance. Many implemented projects may have started with good designs but the construction processes compromised the product. On early full depth panel projects in the 1970s through 1980s, such as those done by the New York State Thruway Authority, the construction techniques were of utmost concern. It was discovered that the performance of the panels over the first decade of their design life depended on the quality of construction (Biswas 1986). In order to properly implement good designs, solid construction techniques are necessary. One of the current goals is to find construction techniques that are cost effective but also promote long term durability. A number of issues should be investigated including forming techniques, grouting procedures, and staged construction.

2.3.2.1 Forming

There has been very little uniformity in forming methods with the exception of leveling bolts. Leveling bolts are a well documented option for placing the panels at the correct elevations (Figure 2-1). They have been used effectively on projects since the early deck panel trials (Biswas 1986).

The key to forming transverse joints is to have a method that minimizes protrusions and weaknesses in the joint. The methods of forming around the joints have varied but most use some form of wooden formwork on top and bottom. The formwork is then tied together with rods or wires protruding through the joints (Figure 2-1). The supports leave behind imperfections in the grout once the formwork is removed.

Multiple methods have been used to form around haunches but many did not provide flexibility for height adjustments (Biswas 1986). Today many contractors have used plywood, steel angles, welded shims, backer rods, and forming materials (Biswas 1986; Hanna 2008; Issa et al. 1995a). The forming materials are easiest to put in place and use with elevation changes. The only method that has not always worked effectively is backer rods (Badie 2009; Gulyas 1996; Nottingham 1996). The rods tend to move and leak grout (Figure 2-1). The other methods work effectively but can be labor intensive and not as adjustable.

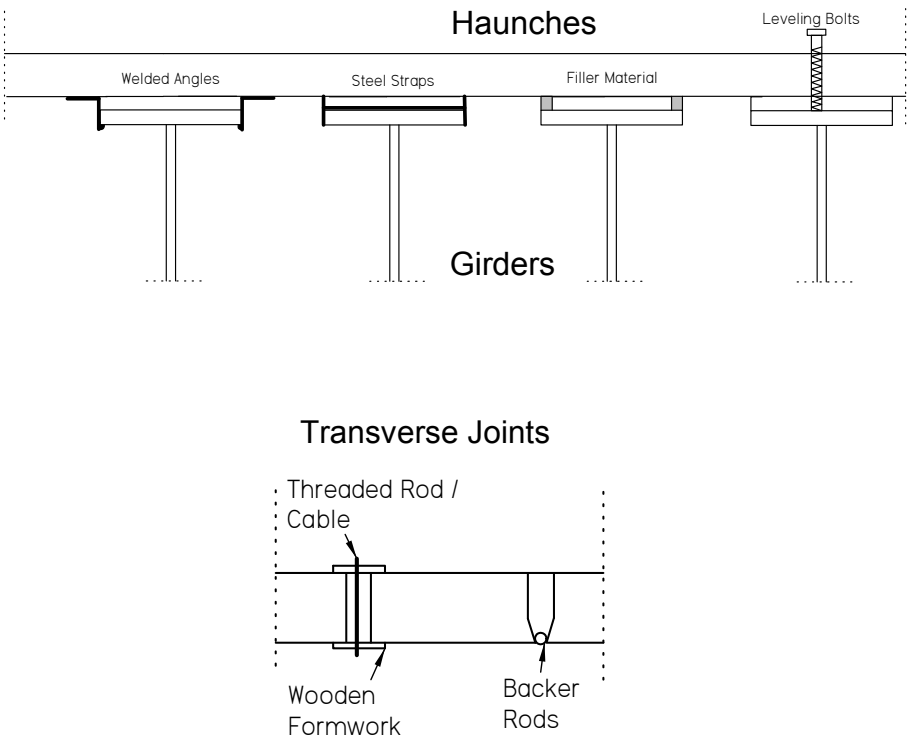

Figure 2-1 Forming Techniques for Haunches and Transverse Joints

2.3.2.2 Grouting

High strength, low shrinkage grout is essential for the joints, pockets, and haunches in a bridge deck. Joints without a grouted connection have performed poorly (Badie 2006b). Grout is "… critical for proper connection performance" (Badie 2009). Previous research shows that grout alone does not guarantee acceptable performance; the grout choice is also critical (Gulyas et al. 1995). Grout's high early strength and initial workability are desirable qualities. The tradeoff is the quick initial set and tendency to shrink and crack. When deck panel research began, it was questioned whether grout would provide the long term durability needed (Slavis 1983). Since then, it has been published that grout performs poorly when: 1) the grout does not reach its design strength 2) poor joint details are used 3) inconsistent grouting procedures are followed (Nottingham 1996). In theory, when grout is used properly it should provide the strength and durability needed in the joints.

Recent studies have shown the importance of choosing the correct type of grout. Master Builder's did research suggesting that not all non-shrink grouts are good for the joints (Culmo 2000; Gulyas et al. 1995). Some researchers believed that strength may be used to specify a good grout but the shrinkage and bond strength are equally as important (Badie 2009). Further research at Virginia Tech provided more precise material specifications for the grout. Scholz prepared a set of guidelines for choosing and installing grouts on bridge decks (Table 2-2). These results were found by doing standard ASTM tests on non-shrink grouts and extended grouts. Concurrently, ponding and cracking tests were done on 6 in. diameter pockets. The research focused on choosing the correct high strength, low shrinkage grout using standard ASTM tests. Problems arose with these tests when ponding and cohesive tests showed the best grouts were the ones with the most shrinkage. A solid correlation was not formed between the ASTM tests and best performing pocket tests (Scholz et al. 2007) .

A study on four grout materials was performed by Issa et al. in response to past deficiencies with grouts in transverse joints (2003). The focus of the study was the performance of grouts used in transverse joints. This included: polymer concrete, Set 45, Set 45 for hot weather, and set grout. A female-female shear key was tested in flexure, shear, and tension. The Set 45 grouts were cured for 24 hours with wet burlap and the set grout was cured for 6 hours with wet burlap. The polymer concrete was not cured with any special technique. In all of the tests the grouts and concrete failed before the bonds. In flexure the Set 45 grouts failed first followed by the set grout and polymer concrete. The polymer concrete had the highest shear strength and the lowest shrinkage followed by the Set 45 grouts. In these tests the polymer concrete performed well and the Set 45 grouts performed satisfactorily (Issa et al. 2003).

Gulyas and Champa reported that non-shrink grouts shrink too much and do not bond to concrete well (1997). They did tension and shear tests on female-female shear keys used between hollow box beams. All of their tests were finished within 7 days of pouring the grouts in the female-female specimens. Their conclusion was Magnesium-Ammonium-Phosphate grouts (Set 45) bond better to the concrete substrates. In addition, component testing, such as shear and flexure tests, should be done instead of materials tests (1997).

The past research has not included a distinct conclusion on the correct type of grout to use or the testing procedures to choose a grout. Much of the past research focused on short term behavior prior to the end of drying shrinkage. The grouts may continue to shrink and crack past the first week or month. Even on the best grouts, cracking has been observed, so better methods of applying the grout should be investigated. Size effects might also be considered since most tests are on small shear keys or scaled models.

Table 2-2 Grout Guidelines

Compressive Strength	ASTM C 109: 1 Hour = No Strength, 1 Day = Minimum 4000 psi 7 Day = Minimum 5000 psi
Splitting Tensile Strength	1 Day = 200 psi 7 Day = 400 psi 1 Day Compressive Strength/15 > 300 psi 7 Day Compressive Strength/15 > 400 psi
Shrinkage	ASTM C157 or ASTM C 596 28 Day microstrain less than 400
Sulfate Resistance	ASTM C 1012 28 Day microstrain less than 1000
Freeze-Thaw Resistance	ASTM C 666, Procedure A 300 Cycles: 80% Durability Factor
Scaling Resistance	ASTM C 672 25 Cycles: 0 Scaling Rating

The other facet of successful grout application is the condition of the connecting parts (Potter 2003). Research has shown that extensive cracking may occur between the grout and concrete surface. Markowski noticed large cracks surrounding the 13 in. by 13 in. shear pockets in his tests (Markowski 2005). The surfaces on the panels need proper preparation prior to grouting. Research has shown there is an interdependence between the bonding surface preparation and material choice in a key way joint (Gulyas 1996). However, there is no general consensus on the best surface preparation technique.

There has yet to be a uniform method of preparing panel surfaces for construction. The traditional method is to follow the manufacturer's recommendations and wet the substrate prior to applying the grout (Issa 2002). Another suggestion is to thoroughly clean and roughen the joints prior to pouring the grout (Culmo 2000). One idea suggests sandblasting a keyway and flushing it with water to remove the carbonation and laitance prior to grouting (Gulyas 1996; Issa et al. 2003). Laboratory testing has shown that this method is very promising (Yamane et al. 1998). However, other research showed that this did not significantly affect the bond strength (Scholz et al. 2007). Others have suggested sandblasting and pressure washing the joint surface, grouting in two lifts (or phases), or troweling the grout on the surface of the deck (Nottingham 1996). Another option to roughen the shear key is to use a retarding agent during construction. Hours after the panels are poured, the paste in the pockets is washed away leaving behind the course aggregate (Badie 2006b; Menkulasi and Roberts-Wollmann 2005). All of these methods are unique and take differing amounts of preparation. A direct comparison has never been done on surface preparation between grouted surfaces in deck panels.

2.3.2.3 Staging the Construction

For many deck replacement projects the bridge cannot be out of service. Staged construction is the typical method used to deal with this on cast-in-place bridge decks. With full depth concrete deck panels, staged construction will introduce additional joints in the longitudinal direction. Longitudinal joints must be designed and placed in a manner to ensure long term durability while still allowing portions of the bridge to stay in service during construction. By using the deck panel construction procedures, along with staged construction, the inconveniences of construction can be greatly reduced. This helps bridge owners, such as the Virginia Department of Transportation, meet many of their strategic goals of "maintain [ing] a transportation system that is safe, enables easy movement of people and goods, enhances the economy and improves the quality of life." (VDOT 2007a)

Past projects have demonstrated different methods of building with staged construction. On a project on Route 7 in Fairfax County, Virginia, the construction was done with a three stage process. Two lanes were always left open while a third lane was rebuilt.

Metal railings were attached through anchor bolts cast in the panels. Two longitudinal joints were placed over interior girders and contained a 3 ft section of spliced rebar (Babaei et al. 2001). The panels were only partial depth at these locations to allow room for the splicing (Figure 2-2). Concrete was placed over the splice during the third stage of construction after the panels were installed.

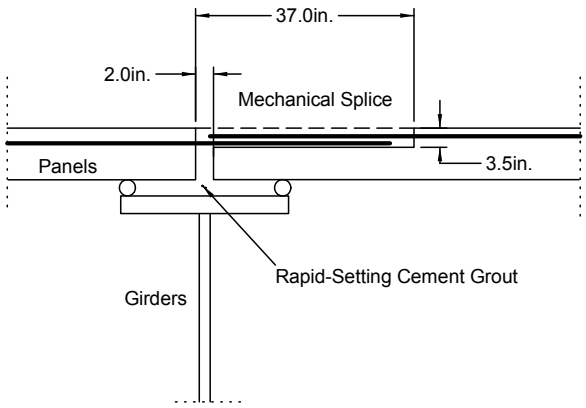

Figure 2-2 Elevation View of Route 7 Deck Panel Mechanical Splice

The initial results showed no cracking over the girders, however this method required numerous panel designs and large concrete pours over the deck surface. This joint option has not been thoroughly tested, so these issues may affect the long term viability. The placement and design of the joint are very important issues. There is little information on whether to place a joint between girders or over a girder. Longitudinal joints will be needed on many deck replacements, so the different joint options should be directly compared and tested under long term service conditions.

The New England Region of the Precast/Prestressed Concrete Institute (PCINER) published a set of guidelines and details for use with full depth deck panels (Precast/Prestressed 2002). Obtaining the correct crown can be a challenge with precast units (Issa et al. 1995b). The guidelines show a detail of a 2 ft wide cast-in-place concrete joint over the crown between two girders (Figure 2-3). The top and bottom rebar are spliced inside this

joint (Precast/Prestressed 2002). The detail provides load transfer in the transverse direction. A large quantity of concrete is needed for this pour in comparison to the size of the panels and the size of other joints. Research by Badie et al. confirms this method of construction. The caveat is to check any cantilevered deck sections for strength during the staged construction (Badie 2009).

A very similar detail was used on the Krum Krill bridge in New York in 1977 (Biswas 1986). This joint appeared to work satisfactorily after about twenty-one years of service, although there was evidence that water had leaked through the joint (Issa et al. 1998). A cast-in-place joint like this deserves further research on its design and implementation.

A recent failure study on Interstate 81 in Virginia, demonstrated that these longitudinal closure pours may create weak points in the bridge deck (Sprinkel et al. 2009). In the spring of 2009, a 2 ft – 2 in. wide closure pour failed in punching shear. The investigation revealed that cracks were created in the joint greater than 0.007 in. in width, the thresh hold that allows chlorides to penetrate. The entire closure pour was revealed to have corrosion problems and had to be replaced. The recommendations from this investigation were to use an expansive cement in closure pours, use MMFX or stainless steel rebar, and move the joint over a girder.

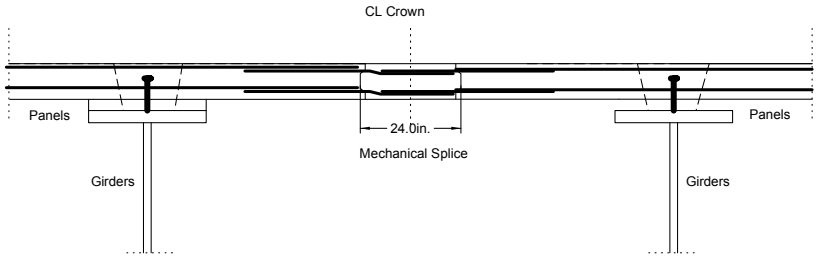

Figure 2-3 New England Precast/Prestressed Spliced Rebar Detail
(Precast/Prestressed 2002)

An upcoming bridge construction project is designed with a similar double looped, steel rebar joint at the crown. The difference between this detail and the New England standard is the 1 ft joint between the panels. This has the potential to cut down on the amount of cast-in-

place material in the joint and still meet the elevation requirements at the crown (Khalil 2008). The project is still in the planning stage and the joint has not been tested or implemented.

A study done in Wisconsin in 2007 investigated the option of using blockouts at the midpoint of the bridge. The prestressed strands from stage one panels were coupled with post-tensioned strands in the stage two panels and then stressed. A blockout measuring 14 in. by 8 in. was placed at the midpoint for the post-tensioning coupler (Carter III et al. 2007). A shear key was placed and grouted between the panels (Figure 2-4). The downside to this process was twofold: post-tensioning the bridge in the transverse direction took additional time and lining up the panels for orthogonal post-tensioning ducts required small tolerances. The benefit was that the blockouts were smaller than cast-in-place methods and needed less grout. Another benefit of this system was the placement of the joint at midspan between girders. The top surface of the panel should always remain in compression because of its location. A compression joint should not crack. In the event cracking did occur, a joint placed away from the girders would prevent water from depositing water and chemicals on the girders.

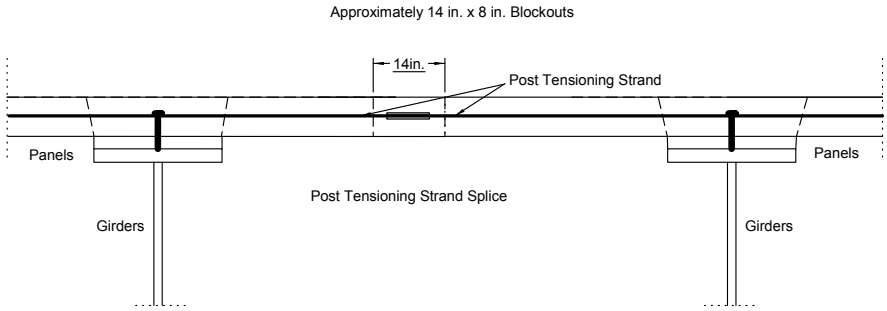

Figure 2-4 Shear Key and Blockout for the Wisconsin Bridge

Very little published literature addresses the problems with staged construction. A study on the different methods and service performances of longitudinal joints has not been completed. A joint at the centerline of the roadway has the potential to correct elevation problems at the crown. However, there are concerns about the long term durability of the closure pour. Joints between girders should primarily stay in compression when transferring

loads in the transverse direction. A future investigation into the staging process for deck panels would help make them a more viable option.

2.3.3 Composite Behavior and Shear Studs

The current standard for bridge construction is to connect the decks with a shear transfer mechanism, thereby making the deck composite with the rest of the superstructure (AASHTO 2007). Normally shear studs or reinforcing bars are attached to the girders at a uniform spacing and cast into the concrete deck during construction of cast-in-place decks. Full depth deck panels cannot easily be used with this system because of spacing limitations between the shear connectors. In the past, shear studs have been grouped together, placed in pockets, and welded to the girders (Figure 2-5). The pockets in full depth deck panels fit around the steel and are later filled with grout to create composite behavior.

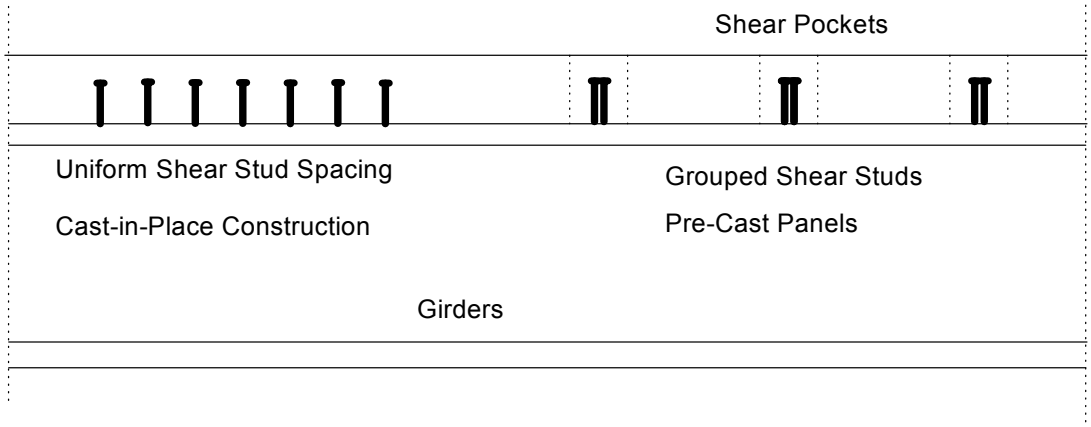

Figure 2-5 Uniform and Grouped Spacings of Shear Studs

The spacing of horizontal shear connectors is currently limited by design codes. The AASHTO LRFD guideline allows a maximum spacing of 24 in. between shear studs (AASHTO 2007). The most recent design details from the New England Region Precast/Prestressed Concrete Institute show 2 ft maximum spacing between shear pockets. Current published designs continue to use this spacing (Culmo 2000; Harrison and LeBlanc 2005b; Khalil 2008).

Using these design limitations result in a large number of pockets in the deck panels, potentially creating durability problems.

Recent tests on shear stud spacing and grouping showed that the current specifications may need clarifications (Menkulasi and Roberts-Wollmann 2005; Wallenfelsz 2006). Wallenfelsz recommended using the AASHTO LRFD (2004) guidelines for horizontal shear strength equation with cohesive and friction values stipulated for a smooth surface (Wallenfelsz 2006). However, there is still debate as to whether the shear stud testing methods correctly model bridge behavior. The methods test direct shear strength, but in bridge applications the stresses are not completely horizontal. Scaled bridge tests were recommended.

In 2006, Sullivan designed a test deck panel setup that was simply supported (Sullivan 2007). His designs of the shear connectors and transverse reinforcement parallel the procedures in the PCI state-of-the-art report (PCI 2006). A simple span full scale lab mockup of a deck panel system was tested with shear studs and looped reinforcing bars (Sullivan 2007). The results did confirm that the current AASHTO shear design equations are sufficient for shear pockets up to 4 ft spacings.

Sullivan's results were confirmed by other research projects. Badie et al. did a set of push off tests with 1 ¼ in. studs and found that the current LRFD specifications could be used for shear stud spacing up to 4 ft. (Badie 2006b). A NCHRP project demonstrated with fatigue and ultimate strength tests that 4 ft spacing should be sufficient (Badie 2006b). The LRFD specifications equation 6.10.10.4.3-1 accurately predicted the ultimate strength regardless of spacing or confinement type. Equation 5.8.4.1-1 of the LRFD guidelines gave an accurate estimate of ultimate capacity. The LRFD specification equation 6.10.10.2-1 accurately predicted the shear capacity up to 4 ft spacing (Badie 2006b).

The following year, a separate set of lab tests was done on 4 ft shear pocket spacing. Fatigue testing was run on girder line samples to ensure composite action was obtained. The researchers determined that full composite action was achieved and subsequently implemented this spacing on a bridge in Wisconsin (Carter III et al. 2007). More full scale testing of a bridge system has been recommended to compare results of different shear stud spacing and possibly change the design code (Badie 2006b). An additional study on a real bridge would help confirm the laboratory tests that have been done and the full scale bridge implemented in Wisconsin (Carter III et al. 2007). Issa tested a full scale two span continuous bridge in 2007. The results showed that the current AASHTO LRFD design codes are adequate for the design of precast slabs and shear connectors to achieve full composite behavior (Issa et al. 2007).

The shape of the shear pockets has been the focus of other investigations. Many different bridge projects used a top to bottom taper on the blockouts (Figure 2-6) (Biswas 1986). Push off tests were performed with good results on similar details (Chang and Shim 2000). Tapering was originally used to prevent uplift of the bridge deck (Babaei et al. 2001). Other bridges have used oval shaped and rectangular shaped blockouts without tapers (Issa et al. 1995c). Wallenfesz did a series of tests on shear pockets and concluded there was very little benefit to tapering the blockouts (Wallenfelsz 2006). There appears to be little difference in the performance of the various pocket configurations presented in current literature.

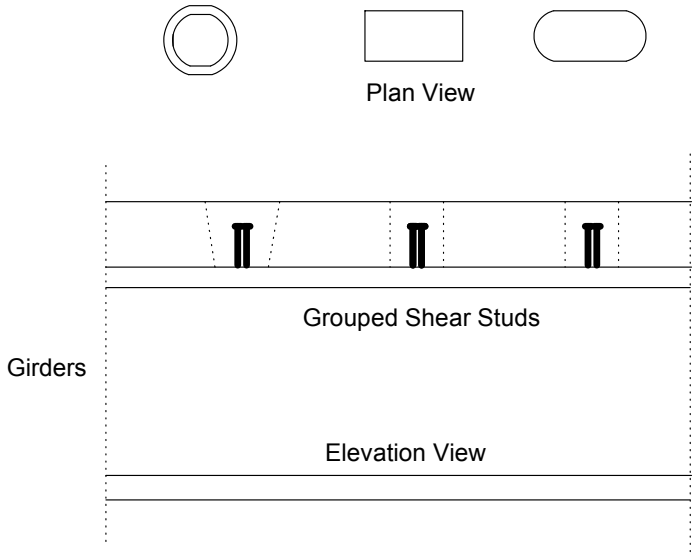

Figure 2-6 Shear Pocket Shapes

A rectangular shaped blockout without a taper could improve panel construction and still perform well. The tapers decrease the tolerances around the shear studs and make it harder to place the panels. Increasing tolerances is recommended by Nottingham when grouting in small, deep spaces like a shear pocket (Nottingham 1996). A non-tapered shape would also be easier for a precaster to form and subsequently less expensive. This was demonstrated by Badie with a rectangular non-tapered, hidden pocket and also Biswas et al. on a scaled test in Texas (Badie 2006b; Biswas et al. 1984). In the most recent tests by Badie et al., push off tests and fatigue tests were used to test the pocket design (Badie 2006a). Using pockets similar to these would provide easier installation without changing the amount of work or materials needed. Using a simpler shear pocket would reduce the time and cost to build the panels. The primary concern is that composite action is present throughout the design life of the panels.

When using shear studs in pockets, there are construction concerns. The spacing is very small for welding the studs to the girders and the crevices must be completely filled with grout. A solid bond bond between the grout and the surface on the panels is hard to obtain. The interface between two cementitious materials in a bridge deck tends to crack regardless of the

location. After two decades of service life, the panels on the Woodrow Wilson Bridge in Washington, D.C. showed evidence of corrosion from possible leaks around the pockets (Dinitz 2008; Kassner et al. 2007). Cracking around these pockets could result in long term deterioration and damage to the shear studs and girders. Recent studies have not focused on the surface preparation of the pockets (Badie 2006b; Markowski 2005; Sullivan 2007). More comprehensive research is needed on protecting the pockets. Using techniques similar to the joint preparation techniques previously mentioned (2.3.2.2 Grouting), could substantially reduce the durability problems. Using the same technique on both the joints and the pockets should ensure consistency in the precast plant and reduce the cost.

2.3.4 Transverse Joints

Since the inception of bridge deck panel testing, researchers have investigated the joints (Biswas et al. 1984). There have always been problems with the construction and long term performance of joints. Most studies have focused on an individual joint. There is a lack of data comparing the performance of different types of transverse joints, particularly cast-in-place versus post-tensioned. In addition, past tests were typically on joints in positive bending on simply supported bridges. Tests comparing multiple joints under the same worst case negative bending have not been reported.

2.3.4.1 Reinforcing Bar Joints

Reinforced joints do not provide active compression in the joint and will crack when loaded in a continuous composite deck. The transverse joints have become a concern because of observed durability problems. Most of the early projects in the 1970s had non-post-tensioned decks that did not perform well (Biswas 1974). In 1995, a study done on in service deck panels reported durability problems for non-prestressed joints (Issa et al. 1995c). These types of joints continue to be a problem for design engineers because the long term performance tends to be unpredictable.

Non-post-tensioned joints are typically easier to construct. The joints tend to have more space between the panels and involve traditional construction methods (Figure 2-7). This

is a benefit compared to post-tensioned joints which take specialized knowledge and additional construction experience on the job site.

The ministry of transportation in Ontario, Canada continues to pursue the use of cast-in-place longitudinal and transverse joints. They have used details similar to Figure 2-7 to connect the panels. A series of scaled tests with 7,000,000 cycles of the Canadian Highway Design Code truck produced minor cracks in the joints. A one and two span setup were both tested under the maximum service load. The results indicate cast-in-place joints may perform satisfactorily under some circumstances (Au et al. 2008).

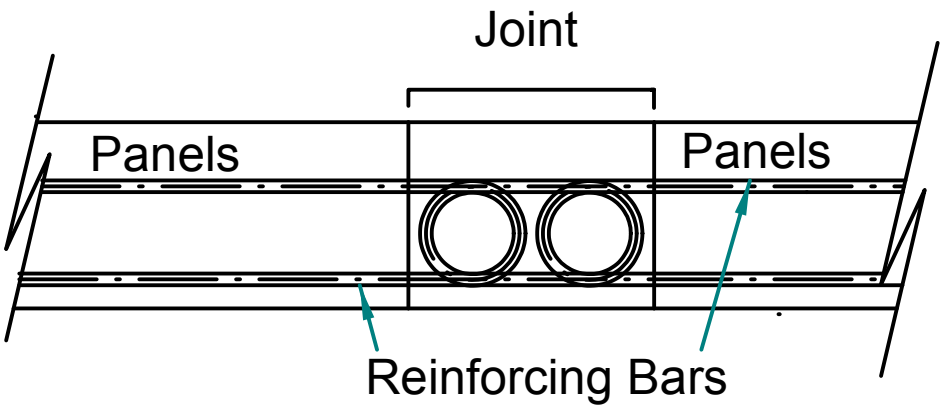

Figure 2-7 Typical Non-Post-Tensioned Panel Joint

Recent studies have focused on alternative cast-in-place joints. A study by Badie looked into a new method of connecting panels with normal reinforcing as shown in Figure 2-8. A series of cyclical tests were run with service loads. The joints did not crack or leak water after doing a 2,000,000 cycle test (Badie 2006b). The Fort Miller Company has devised a system of embedding hollow steel shapes in the panels that extend to the edge of the panel in a blockout. The steel shapes on adjacent panels are bolted together to connect the panels and the blockout that contains the connection is grouted. They have also experimented with using weldable rebar between panels and connecting the rebar with special welded connectors (The Fort Miller CO. 2002). Versace noted that these methods have been used effectively but they are proprietary and do not lend themselves to wide spread use (Versace 2004). Testing needs to be

done on newer joint types and compared with more traditional methods to find the best joint available.

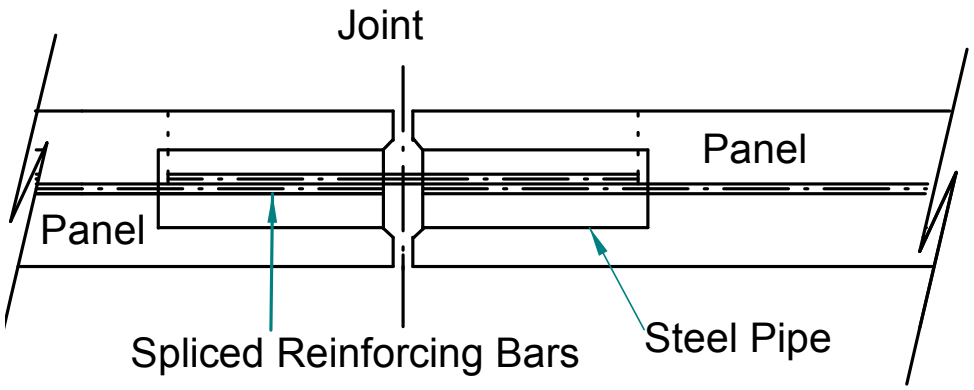

Figure 2-8 Embedded Reinforcing Bar Joint

2.3.4.2 Post-Tensioned Joints

Another option is to post-tension the deck and prevent the deck concrete from developing tensile stresses or cracking. Post-tensioning can keep a deck in a compressive state throughout its service life. If cracking does occur during loading, the post-tensioned force will close the cracks upon unloading. A post-tensioned deck should increase durability by preventing paths for chlorides to enter the deck (Swartz 2008).

In the early 1970's the first post-tensioned deck was built on a steel girder bridge in Dallas. The bridge was cast-in-place and therefore could not be made composite (Rawles 1973). Early designers realized post-tensioning works well for decks but making them composite prior to post-tensioning is very inefficient. This order of construction would transfer the force into the girders resulting in less force transfer to the deck.

The next phase of research focused on using precast decks and adding post-tensioning after installation. Precast decks with post-tensioning is a very promising option, however

relatively few bridges have been built this way (Issa et al. 1998). An observation has been made that "the biggest cause of any adverse effects (on bridge decks) was the lack of post-tensioning in the longitudinal direction of the structure to secure the tightness of the joints" (Issa et al. 2000). To date, the AASHTO specification does not provide any guidelines. Based on observations, using an appropriate level of stress and a good shear key design should provide a sound joint. Post-tensioning appears to improve the overall behavior of a deck panel system (Issa et al. 2000). The challenge is to correctly design the connection and implement a post-tensioned system with the correct amount of stress.

2.3.4.2.1 Post-tensioned Joint Shape

The shear key shape between the panels has been studied. Models were done in 1971 on the shape of match cast models. A flat rectangular joint was found superior to any circular shaped joints because of constructability (Figure 2-9), (Gutzwiller et al. 1971). This research led to early details used on many of the bridges in New York (Biswas 1974).

Subsequent research and projects focused on female-female shear keys (Biswas 1986; Biswas et al. 1984). Most joints are still designed and tested with dimensions similar to the joints used in the early stages of deck panel research. Today a typical female-female shear key has been shown to work well as long as backer rods are not used. The backer rods do not form a solid barrier because they move during construction (Figure 2-9), (Badie 2009; Gulyas 1996). Issa did a study on the grouting materials and strengths of the joints. He confirmed that female-female type joints work well (Issa et al. 2003). Many projects have used this type of key including the project on Route 7 in Virginia and bridges in Connecticut (Babaei et al. 2001; Culmo 2000).

Match cast joints have not been thoroughly designed and tested. Sullivan did a female-male joint but they were not built as match cast. He described construction difficulties when assembling the joint because the panels did not line up well (Sullivan 2007). More recently Badie reported that match cast joints are not the best choice (Badie 2009). Match cast joints do not have extensive testing and may work if the panel tolerances are very small. Precise casting with high quality forms would be necessary to avoid constructability issues.

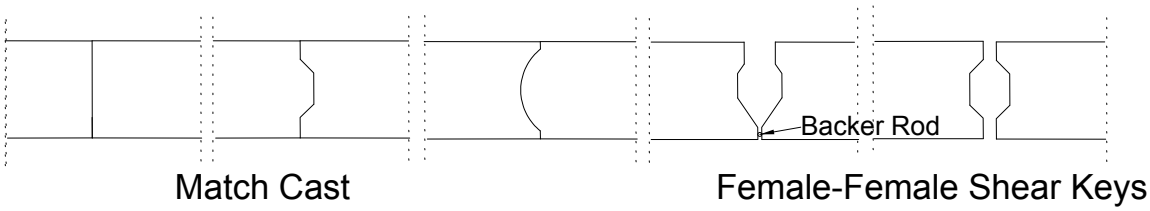

Figure 2-9 Elevation View of Different Joint Types Between Panels

2.3.4.2.2 Post-tensioned Joint Stress

The stress level applied to post-tensioned joints is critical. The stress values have varied greatly among different bridges and research projects. Many factors, including the number of spans and the material properties, will affect the ultimate force in the panels. Long term losses will also reduce the initial force in the panel. Determining the final force needed in the panels for each particular situation is a key to designing and constructing the deck panels.

Early tests and bridges designed with post-tensioned, non-composite decks did not perform well in the long term. A bridge in Indiana used a very small amount of prestressing (32 psi) to keep the panels from moving (Gutzwiller et al. 1971). The joints were match cast, rectangular shear keys. However, over the next three decades spalling and leaks occurred at the joints (Culmo 2000).

Some researchers have suggested that a finite element model is necessary to design a bridge with post-tensioning (Chang and Shim 2000). A recent simple span bridge project used a finite element model to look into the stress level needed for a bridge. The study looked at long term losses that would reduce the level of stress in the precast deck. The results were used to determine a sufficient stress level (Harrison and LeBlanc 2005a; Harrison and LeBlanc 2005b). This was the first reported study on the effects of long term losses on post-tensioning level. The stress level reduced from 435 psi to 405 psi by the end of the design life. The analysis was done during the design of a simply supported steel bridge and the methods were not published.

A number of studies suggest a level of stress for the deck panel system (Table 2-3). On one project, finite element modeling was done to determine what level of initial stress would be needed to keep simple and continuous spans in compression. Two specific bridges were

modeled for this study: a simple span bridge and a three span continuous bridge. The result was a recommendation of 200 psi compressive stress for the simple span and 450 compressive stress for the continuous span (Issa et al. 1998). Two other research reports suggest 150 psi and 250 psi as the minimum recommended compressive force in any deck (Potter 2003). In a separate study of two single span structures, 200 psi compression was chosen for the deck (Babaei et al. 2001).

The most comprehensive study to date on the level of prestressing was done by Bowers. She did a parametric study on different bridge types and post-tension levels (Bowers 2007). These values were all computed by using equilibrium, compatibility, and constitutive relationships. A force was added longitudinally to the composite deck panel and the effects on the girders and haunch were computed. Twelve equations were used to find the following unknowns: change in force in the strands, deck, girder, and haunch; change in strain in the strands, girder, deck, and haunch; moment induced in the girder, deck, and haunch; and curvature of the system. The 2006 Interim AASHTO LRFD Bridge Design Specification models for creep and shrinkage were used for the model. The age adjusted effective modulus was used in all constitutive equations. The data from this report suggested standard levels of prestressing in the longitudinal direction (Table 2-4). Two of the models were checked against a finite element model used by Sullivan but the CEB-FIP model code 1990 creep and shrinkage models were used instead (Bowers 2007). The results of the models were very close.

Table 2-3 Stress Level Recommendations for Post-tensioned Deck Panels

Bridge Type	Stress Level	Notes	Reference
Simple Span (138 ft, 110 ft)	200 psi	Lightweight concrete, Composite	(Babaei et al. 2001)
Three Bridges (34 spans)	250 psi	No cracks after 5 & 8 years respectively, Composite	(Culmo 2000)
Simple Span	32 psi	Non Composite	(Gutzwiller et al. 1971)
Simple Span*	435 psi initial (405 psi final)	Composite, 75 year design life	(Harrison and LeBlanc 2005b)
Two Span (9.5' modeled bridges)	208 psi, 380 psi	Composite	(Issa et al. 2000)
1 & 3 Span FEM Models*	200 psi & 450 psi	Losses not included in model	(Issa et al. 1998)
18 Simple Spans – Alaska Connecticut Simple/Continuous	149 psi 150 psi/300 psi		(Issa et al. 1995a)
All Spans	200 psi	After losses	(Precast/Prestressed 2002)
Two Span (modeled bridges)*	290 psi	Composite	(Shim and Chang 2002)
Simple Span Tested Continuous Span Studied	200 psi 200-800 psi Suggested		(Yamane et al. 1998)
Continuous	200 psi	NUDECK System, Partial Depth	(Tadros 1998)
Simple / Continuous*	150 psi / 300 psi Minimum	After all Losses	(Issa 2002)
Continuous – 2 Span*	500 psi	Prototype Bridge Test	(Issa et al. 2007)
Continuous, Simple	300-850 psi/250 psi	Not Tested	(PCI 2006)
Simple Span*	200 psi Concrete and Steel -Simple Spans 650 psi/500 psi Steel Two /Three or More Spans	Simple Span Prestressed Girder	(Bowers 2007), (Sullivan 2007)

*Modeled with a Finite Element Program

Table 2-4 Recommended Stress Levels in Precast Panels

Girder Type	Number of Spans	Initial Post-tensioning (psi)
Steel	1	200
	2	650
	3 or More	500
PCBT	1	200
	2	200
	3 or More	200
AASHTO	1	200
	2	200
	3 or More	200

One of the aspects of using post-tensioned panels is to keep the panels in compression during their design life (Swartz 2008). Chang and Shim suggested using a plastic analysis of the bending strength of a steel deck system. The caveat with using this procedure is keeping all transverse joints in compression throughout the design life. Cracking would affect these calculations (Chang and Shim 2000). The problem then arises as to how much compressive force must be kept in the panels to keep them in compression.

There are problems with suggesting a universal stress level for all situations because of the differences among bridge layouts. Simple and continuous spans; steel and concrete girders; girder spacing; and span length will all affect the level of stress needed. When comparing concrete and steel girders, the elastic moduli are different, causing differences in the long term stress distributions. Fewer problems have been seen with structures on concrete girders than on steel girders due to the differences in flexibility (Issa et al. 1995c). The stress level should be incorporated in a set of laboratory tests and a deck model. As previously referenced, Bowers did a design model of separate girder types but it was briefly tested with finite element models.

The model was tested with one single span prestressed concrete girder system. There were no tests done on continuous spans or steel girder bridges (Bowers 2007).

Most of the reports focused on the design and theory behind post-tensioning levels. Typically they were done on one specific structure (Table 2-3). A comprehensive design method, such as Bowers' recommendations, should be developed, tested in a laboratory, and modeled in a finite element program. This would provide further evidence for a universal recommendation or multiple recommendations.

2.3.5 Stiffness of Composite Deck Panels

Bridges and redecking projects can have design lives of fifty or more years. Many deck panel studies looked at the first year of the design life. Longer term, cyclical tests are needed to look at long term stiffness changes in the bridge system. If a post-tensioned deck stays in compression throughout its design life then the system should maintain its stiffness (Swartz 2008). However, joints that lose their post-tensioned force may crack and begin to act more like reinforced joints. The study of long term behavior is a key component in the implementation of deck panels.

2.3.5.1 Simply Supported Cyclical Tests

One of the first tests on deck panel systems was done in the early 1970's at Purdue University. Two non-composite simply supported systems were tested: a set with two steel girders spaced at 8 ft and a set of three steel girders spaced at 4.5 ft. Four panels were used on the systems and deflections were measured beneath the center of the two 20 ft spans. The service load was applied at the edge of the center panel joint, near the midspan. Compressive strains were measured on the top surface of the concrete panels. The longitudinal post-tensioning force was maintained at 32 psi throughout (Gutzwiller et al. 1971).

Initially, the decks with girders at 8 ft spacing had spalling problems around the joints. A second set of tests with better quality control during construction did not exhibit problems after 10,000,000 cycles. The tests done on the three girder setup had similar results. There was no loss in the post-tensioning stresses throughout the tests and the maximum concrete

strains did not increase over time (Gutzwiller et al. 1971). There were no problems observed with the joints and no significant changes in the system.

Bridges are primarily built composite and therefore depend on the structural behavior of the deck panels. A one third scale, steel girder model was built in the early 1980s to test the composite behavior of a deck panel system. Strain gauges were applied to the girders and the top surface of the deck panels. Strains were measured in three loading situations. First the strains were measured in a non-composite system. Then the strains were measured with only two of the ten panels composite. The last test was a fully composite system. The results showed that a composite system could be built successfully. The deflections of the third-point loaded system matched the theoretical deflection calculations very closely. The strain distributions measured on the beam and deck system closely mimicted the theoretical predications. All testing was done in the elastic zone of the steel stringers (Biswas et al. 1984). The primary purpose of these tests was to show that composite action could be obtained. These tests only looked at the immediate strains and deflections and did not test long term behavior.

A recent study on embedded reinforcing bar joints looked at the fatigue life of the joints. A 24 ft, simple span test was used on full size deck panels. Three different panels were used with two different embedded joints between the panels (Figure 2-10). None of the joints were post-tensioned. The panels were 20 ft wide and 8 in. thick throughout. An HS-20 center axle load was used at each edge of the joint to simulate a fatigue load for 2,000,000 cycles. Displacements were measured beneath the joints and strains were measured on both sides of the panel joints (Badie 2006b).

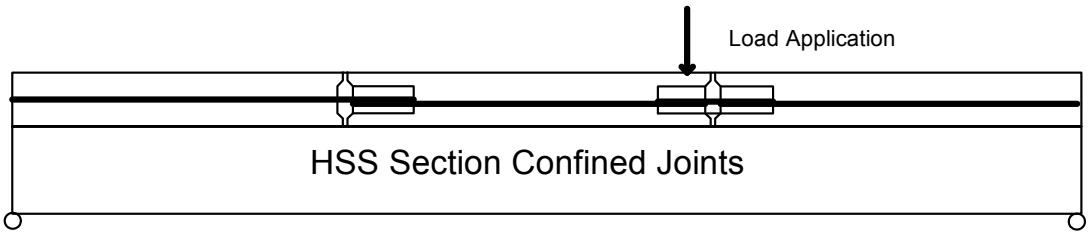

Figure 2-10 Simple Span Test of Embedded Reinforcing Deck Panel Joints

The joints performed very well on all measures during the test. The results indicated no cracking, no leaks during ponding tests, and no evidence of rebar slippage. There was also no concrete crushing or any separation of grout in the shear keys. The strain gauges had comparable strain on each side of the joint throughout the tests. Displacements measurements beneath the joints showed no signs of change after the fatigue loading (Badie 2006b). The primary objective was to check that the bridge remained composite over time with 4 ft shear stud spacing and that the joints were durable.

2.3.5.2 Continuous Span Cyclical Tests

In 2000, Issa et al. performed a one quarter scaled two span test on three sets of deck panels (Figure 2-11). The spans were 9 ½ ft long and consisted of two girders spaced at 18 in. The first model had no longitudinal reinforcement connecting the panels but did have shear connectors in pockets. The second two models had shear pockets and post-tensioned joints to connect the panels. Loading was applied simulating a HS-20 truck with the worst case negative stresses on the setup. A static test was performed and then followed by a two million cycle fatigue test (Issa et al. 2000).

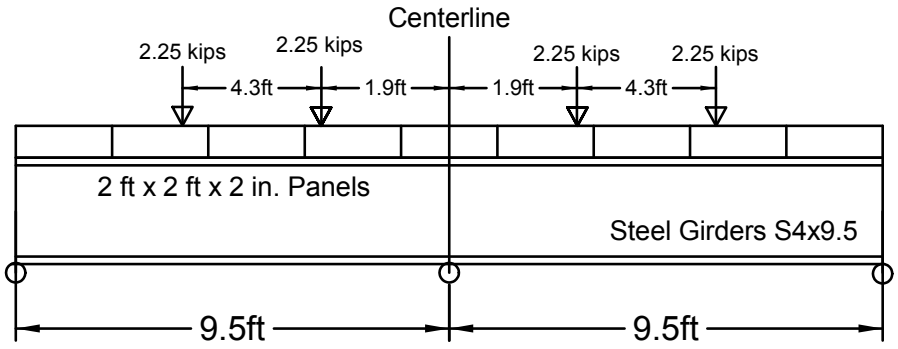

Figure 2-11 One Quarter Scale Two Span Test Setup

Data was taken throughout the process. Vibrating wire gauges were placed inside the panels near the joints. Crack displacement transducers monitored the cracks around the joints and LVDTs were used to measure deflections at the critical locations. All deterioration measurements were done visually as cracks opened in the panels.

The non-post-tensioned bridge showed deterioration. There was a small amount of permanent deformation observed. The largest problems occurred at the panel centered over the bent. The first two cracks appeared in each of the two joints on each side of the panel during the first static load. Once these cracks opened, the center panel ceased to take more load and the deck system failed. There was little change in the deflection measurements from the initial static test until the end of the load cycles from the HS-20 scaled truck.

The next two tests were post-tensioned panels. The size of the girders was reduced by a stiffness factor of 0.4 in order to reduce the bridge stiffness and result in more cracks. Neither of the bridges (208 psi and 380 psi post-tensioning) cracked at the first static load.

The load for first crack in the bridge with 208 psi stress was measured at three times the value for the non-post-tensioned bridge. The amount of deterioration in this bridge was more pronounced at every static load taken throughout the cyclical tests. The deterioration was in the panel over the bent and not in the joints. The cracks continued to propagate but never appeared in the transverse joint.

In the 380 psi post-tensioned bridge, no initial cracking occurred. A larger load was applied in order to induce cracks. No significant deterioration occurred in the first 1,700,000

million cycles so the stress range was increased. Eventually the stress range was raised enough to produce a fatigue crack in the beam but the panels never had anything more than hairline cracks.

These tests demonstrated the importance of having the correct level of post-tensioning force in the panel system. The post-tensioned panels performed significantly better but still cracked upon overcoming the stress level in the panels. One of the most important observations was the cracks in the highly stressed panels closed upon unloading the system. There was never any major deterioration in the deck.

A separate set of scaled tests were done by Shim and Chang in 2002. These tests looked at a two girder, two span setup, 40 in wide and 19.7 ft long. A post-tensioned force of 290 psi was used longitudinally through the panels. The tests were very similar to the one done by Issa et al in 2000. Loads were applied and deflections were measured at the midpoint in each span. Strains were measured on the girder and slab beneath the loading points. One panel was centered over the interior bent, so the worst stresses were at the midpoint of the center panel.

The initial cracks all occurred over the bent. Under service loading the joints did not crack but cracking did occur during an ultimate load test. However, when the load was released the cracks closed. The conclusion was that if enough force was placed in the panels the entire concrete section could be used to design for service loads (Chang and Shim 2000) .

Following the scaled tests, Issa et al. built a prototype full size two span bridge for testing purposes (Issa et al. 2007). The bridge had 11 full size 8 in. thick panels with one centered over the interior bent. Three girders were used on the 18 ft wide by 82 ft long bridge (Figure 2-12). A 500 psi effective stress was applied to the strands over the negative moment region. Strain gauges were applied to the stressed rods and strands and strains were measured for one year. The strands, haunches, and shear studs were not grouted until the end of the year. At this point there were no recorded losses in the prestressing strands.

Maximum negative and positive moments were applied using an HS-20 truck load. Strain gauges and embedded vibrating wire gauges were placed at the midspan of each girder line and next to two joints: one interior joint near the bent and one joint near the middle off the spans. Strain gauges were also placed on the middle steel girder over the bent and at the

maximum positive moment locations. LVDTs were used to measure the deflection at two points in each span.

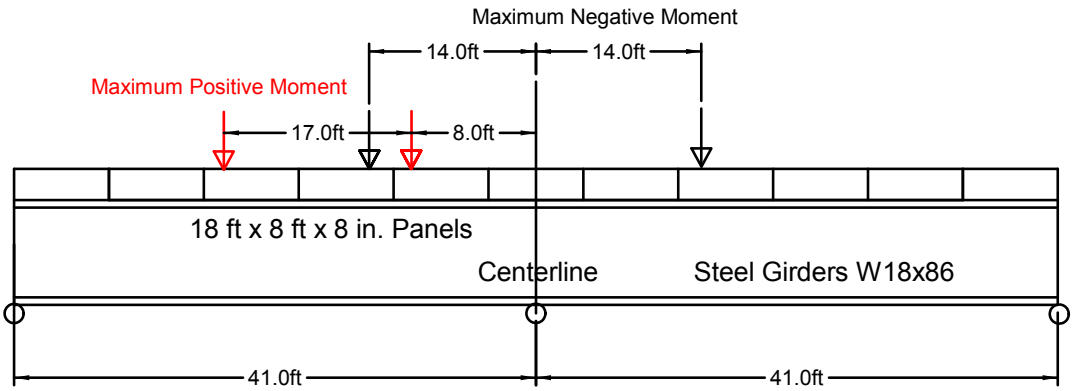

Figure 2-12 Prototype Full Scale Bridge

Load versus deflection graphs were produced for each loading case. No cracks were observed in the panels under the maximum service load. A maximum overload case (two times the HS-20 truck load) was placed on the bridge. The joints performed well and did not crack. Lastly, a pseudo ultimate load that yielded the flanges of the girders was applied. Strain versus load graphs were made of the entire system for the various tests. No fatigue loading was done on this setup. The system maintained its integrity after loading the bridge to approximately eight times a HS20 truck.

There is a lack of data on the change in stiffness of continuous full scale deck panel systems. A more comprehensive study is needed to look at the effects of cyclical loading on joints over time, particularly in negative moment regions. Prestress losses and durability issues due to cyclical loading may affect the long term performance of a deck panel system.

2.3.6 Longitudinal Post-tensioning

2.3.6.1 Past Experience

A wide variety of initial prestress has been used on past projects (Table 2-3). Most of the values were developed for and used on a single bridge. Only a few studies looked at a wide number of bridges to suggest universal guidelines (Bowers 2007; Issa et al. 1998). Of these

studies, they were primarily analytical. There is a need to test these design recommendations with modeling and full scale bridges.

2.3.6.2 Analysis Modeling

Bowers did a parametric study to determine the minimum amount of stress needed in the longitudinal direction to keep the panels from cracking (Bowers 2007). The models looked at the effects of long term creep, shrinkage, and steel relaxation. The AASHTO LRFD 2006 creep and shrinkage models were used for the long term losses. Simply supported and continuous bridge configurations were considered with steel and concrete girders. The basics of equilibrium, compatibility, and constitutive relationships were analyzed from casting through 10,000 days after installation. Span lengths varied from 40 ft to 160 ft with girder spacings between 6 ft and 9 ft. Two sample bridges were checked with a finite element model as explained in the next section. For this verification, the CEB-FIP model code 1990 was used for creep and shrinkage. The results provided evidence for the validity of the models in Mathcad (Bowers 2007).

The results of the study suggested generic levels of initial prestressing in the longitudinal direction (Table 2-4). These values were compared to design recommendations from previous studies and one ongoing project by Sullivan (Sullivan 2007). However, the models have not been investigated on steel girders or continuous designs. A recent report suggests that the affects of creep and shrinkage on a steel girder/deck panel system is very small. A design guide was published with an example that ignores the long term effects (Swartz 2008). This discrepancy warrants further testing.

2.3.6.3 Finite Element Analysis Studies

A study looked at six different steel girder bridges. They were all modeled with three dimensional finite element models to predict the longitudinal behavior of two and three span continuous bridges. The program *Diana-7* was used for the modeling. Plate elements were used for the concrete deck and plate girder and three dimensional truss elements were used for the transverse beam. The longitudinal tensile stresses were computed by placing a standard design truck at numerous points along the bridge (Chang and Shim 2000).

A phase analysis was done to simulate the construction procedures in deck panels. The MC-90 creep and shrinkage models were used. The relative humidity was 70 percent and the time from casting of the panels to stressing was 90 days. The results showed that creep and shrinkage reduced the prestressing force by about 50 percent over the life of these six bridges (Chang and Shim 2000). These bridges were not built and there was no lab testing to verify the models.

Another finite element model was made using the program *ALGOR*. One and three span bridges were modeled to investigate the longitudinal post-tensioning forces. Ten different component models were built and combined for the bridge model: beams and diaphragms, precast panels, grout material in pockets, transverse joints, closure pours, parapets, shear connecting studs, mild steel in panels, mild steel in closure pours, and post-tensioning strands. Beam, brick, plate, and truss elements were used to model the different parts of the bridge. The analysis was to determine what stress level was needed to keep the bridge in compression (Issa et al. 1998). No modeling was done on losses.

The loads were estimated using *PCBRIDGE* and various levels of post-tensioning forces were applied to the bridge model. A graph was produced of the stresses on the surface of the panels. The minimum level of post-tensioning needed for simply supported and continuous bridges was found to be 200 psi and 450 psi, respectively (Issa et al. 1998).

2.3.6.4 Finite Element Analysis on Bridge Models

One of the few full scale tests was modeled with finite elements prior to construction. A two span full scale deck panel system tested at University of Illinois-Chicago was modeled in *ABAQUS*. The model was done using three dimensional nonlinear finite elements. Service loads, overloads, and ultimate loads were applied to the bridge in the positive and negative moment regions. A time step function was used to incrementally apply the self weight, prestress, and imposed live loads to the model (Issa 2002).

The predicted strength and deflections of the model were very close to the test results. For this particular bridge, a stress level of 500 psi would keep the deck in compression up to a load equivalent to the AASHTO service truck load including the 30 percent impact factor (Issa et

al. 2007). The bridge was tested one year after construction. The long term losses were not investigated in this model.

Bowers used finite element models created in DIANA to compare finite element results to her Mathcad analysis models. The CEB-FIP Model Code 1990 equations were used to model the creep and shrinkage in both models. Two sample Mathcad models were checked using the finite element models. The differences in curvature, strain, and longitudinal force in the deck were all compared and came within 15% of the values in the Mathcad models. As the initial level of prestressing force was increased in the finite element models, the losses predicted by the analytical model increased. This provided evidence that the Mathcad models were valid and conservative for levels of high stress (Bowers 2007).

The finite element models used in Bowers research were taken from research done by Sullivan on a lab test of a simply supported deck panel system (Sullivan 2007). The model was designed to parallel the process of building the slab specimen in the lab. The model was made in *DIANA* using the CEB-FIP Model Code 1990. Two months of data were taken in a deck panels system on AASHTO prestressed girders. The data was then compared with the finite element model and extrapolated over twenty five years. This provided an estimate of the amount of stress loss in the longitudinal direction. The initial stress level of 298 psi was adequate to keep the simply supported system in compression throughout its design life. It was noted that a lower value closer to 200 psi may have been adequate. Using a finite element model or a simplified model with effective modulus values was suggested for future designs (Sullivan 2007).

2.3.6.5 Finite Element Analysis on Constructed Bridges

A two span continuous composite bridge was modeled, built and tested. The initial model was made and the strains at the critical locations in the panels were predicted. A two span continuous bridge with shear keys was modeled with the finite element program *ABAQUS* to investigate its performance under loading (Badwan and Liang 2007). The bridge consisted of bridge deck beams with full depth shear keys between the deck beams. Solid and link elements were used to make the mesh. Separate meshes were made for the beams, shear keys, post-tensioning cables, sidewalks, and barrier curbs. Solid elements with 8 nodes and 3

degrees of freedom were used for the deck and shear keys. Link elements with three degrees of freedom and uniaxial tension and compression capabilities were used for the post-tensioning tendons.

After building the bridge, a single axle dump truck was used on the constructed bridge with strain gauges on the surface of the concrete beams. The truck was placed at three different places across the width of the bridge. Strain gauges were placed at the locations of maximum strain as predicted by the finite element model. The results of the tests followed the same trends as the computer model, however some variations in quantity did exist. The researchers attributed this to the difficulty in modeling concrete, differences in material properties, and incorrect modeling of the boundary conditions. The percent differences in strains ranged from 18 to 30 percent (Badwan and Liang 2007). All of the predictions were made for the short term without accounting for losses due to creep and shrinkage.

In 2005 a single span steel girder bridge with deck panels was built in Ohio. The designers developed a finite element model of the bridge in *SAP2000* to determine the stress levels needed in the longitudinal direction. The entire model consisted of 80 plate elements for the deck and 72 beam elements for the girders. A level of 400 psi was determined necessary. The shrinkage of the concrete was the limiting load case.

A second time dependent model was made using *Bridge Designer II*. The model uses matrix analysis and time dependent properties to determine force effects in the structural steel. The compressive stress in the deck reduced from 435 psi to 405 psi over the life of the bridge (75 years) in the model (Harrison and LeBlanc 2005b). No testing on the bridge was reported after it was completed.

2.3.6.6 Summary of Finite Element Models

The finite element models have been limited to three different circumstances: parametric studies of bridges with no test data, models of a particular test bridge with test data, and models used in the design of a specific bridge. Table 2-5 shows a comparison of previous modeling cases. A more comprehensive comparison among models would help summarize the research. A study would be useful comparing the parametric study results with more comprehensive finite element testing, actual testing data, and full scale modeling.

Table 2-5 Finite Element Models of Deck Panels

Software	Bridges Modeled	Model Tested	Reference
Structural Analysis Principles, DIANA	Parametric Study – Multiple Spans, Spacings, and Materials	One Simply Supported Lab Test & two Finite Element Models, CEB-FIP Model Code 1990	(Bowers 2007)
FEM Diana-7	Six Unique Bridges – 2 and 3 Spans	CEB-FIP, MC-90 creep and shrinkage, No comparisons	(Chang and Shim 2000)
ALGOR	Multiple Bridges - 1 and 3 spans	No long term effects, No comparisons	(Issa et al. 1998)
ABAQUS	One 2 Span Bridge	Full size model tested, No long term effects	(Issa 2002)
DIANA	1 Simply Supported Lab Specimen	CEB-FIP, MC-90	(Sullivan 2007)
ABAQUS	2 Span continuous	Bridge Modeled, No long term effects	(Badwan and Liang 2007)
SAP2000, Bridge Designer II	1 Simply Supported Bridge	Bridge Modeled, Separate Model for long term effects	(Harrison and LeBlanc 2005b)

2.3.7 Full Bridge Testing

Most tests have been performed on bridge deck components or models and not on complete bridges. The system behavior of a full depth precast panel bridge may be different than the behavior of each component. Tests have been done on single girder lines by researchers to see how a segment of the bridge will work. These tests have shown that the bridge deck panels can act compositely and support their design strength (Chang and Shim 2000). Similar tests were done on simple span models with reinforcing bar connections (Badie 2006b). Other tests were done on a one span full scale model in the laboratory (Sullivan 2007). All of this testing has been useful, but needs to be carried to a full bridge.

There are two recent projects that looked into full scale bridge systems. In Wisconsin, a two staged process was used with a two phase transverse and longitudinal staged construction process. This process is new and follows different construction processes than what has been

previously proposed (Carter III et al. 2007). The longitudinal post-tensioning force used to hold the panels together has performed well to date. The results were very good and the full system initially has performed similarly to what was predicted by lab studies. However, no data has been taken on the full scale bridge. The bulk of the research was done on scaled models prior to building the bridge.

Another study looked at innovative post-tensioning processes in a full scale test for high traffic volume routes. The bridge was a two span continuous system with eleven full size deck panels placed on three girders (Issa 2002). The researchers developed a method with a secondary post-tensioning system with Dywidag rods to increase the stress level over the bents (Issa et al. 2007). As described previously, this system performed very well, stayed composite throughout the testing, and did not crack under service loads. However, no long term loading was placed on the bridge.

Both of these tests were done on very unique systems. The first system applies a very unique staged construction technique and the second system used additional post-tensioning rods to increase the stress level over the bents. These tests are very useful to examine alternative methods for constructing deck panels. However, many bridge deck replacement projects are not as large or complicated as both of these large scale tests. Innovative systems are an important part of research, but research is also needed on standard designs and construction procedures that can be implemented on a wide number of bridges very quickly. More research data is needed on typical systems.

To date, there is no deck panel system that has been built and monitored for long term effects. Studies such as the one done by Issa in 1995, demonstrate how systems have performed over time (Issa et al. 1995c). The problem is that these systems were not built for research purposes. There is no historical traffic data, no long term monitoring, and no construction details on most of the bridges. All of these factors can contribute to the condition and performance of the bridges.

2.4 Summary

The literature has a variety of information on full depth deck panels. There are documented cases of precast deck panel use throughout the past thirty years, but the results have been mixed. Very little research has been done on the panels prior to their initial implementation in the 1970s and 1980s.

There are still limited guidelines in design codes and specifications. The few recommendations that do exist on post-tensioning stress have not worked well on previous projects. A gap exists between field performance, lab testing, and designer recommendations.

The construction processes and materials in deck panels need to be documented and tested. Previous projects have not focused on a list of materials and processes needed to build deck panels. A better understanding of the processes and materials would assist in estimating the costs of the deck panels and comparing it to other design methods.

In recent years, there has been an increase in testing of deck panel parts. Tests have been done on the shear connectors, pocket spacing and joint types. Numerous studies have shown that shear pocket spacing up to 4 ft is acceptable. Grouped shear studs and looped reinforcing bars have both been shown to be effective. Post-tensioned joints tend to perform better in laboratory tests than on real bridges. There has been renewed interest in cast-in-place joints because of their simplicity, although past performance has been mixed. Most of the joint tests have been on a single bridge application and on simple spans.

To date, there has been no comprehensive study on deck panel transverse joints. A comparison of post-tensioned and cast-in-place joints is needed. In addition, joint tests are needed for negative moment bending. There have been very limited tests on continuous deck panel bridges and no tests on the effects of joints over interior bents. Joints should be analyzed and tested. A comparison is needed between the behavior and stiffness of the deck panel system with the varying joints over time.

A comprehensive study is needed to compare the analysis techniques used to determine post-tensioning forces in deck panels. Most successful deck panel systems have been post-tensioned but the analysis techniques are varied and most are isolated to an individual project. The few techniques that have been developed should be compared to actual deck panel tests.

Finite element modeling would assist in comparing the analysis methods and the behavior on real joints.

The grouting materials and techniques used for the joints between deck panels have had varied results. Many times shrinkage and durability problems plague the long term behavior of the panels. Specifications have been suggested, but tests on real deck panel systems have not been performed. The grouts need to be compared head to head on actual deck panel situations in a controlled environment. This includes looking at the grouts used in shear pockets. In addition, a modeling technique for the selection of a grouted system would help in design. Recommendations could then be made for construction processes, material preparation, and design.

Finally, deck panel systems need to be constructed and tested. There is very limited information on the behavior of a designed and tested deck panel system. The recommendations that are being developed should be tested on a full scale bridge. Interactions among the parts could then be observed and long term effects could be better quantified. The final step in deck research is to summarize the results of this technology and determine its overall viability as an alternate method of building concrete bridge decks.

2.5 Plan of Research

In order to accomplish the goal of implementing deck panels on a wider scale, the literature review was undertaken to examine the previous research on deck panels and to determine areas that need further investigation. This research project is designed to address many of these problems (Table 2-6). This includes:

1) There is a lack of construction data to support the use of deck panels. Previous uses of deck panels have assumed that deck panels are economical but actual data on a project would help provide a comparison. A detailed list of the processes and materials will help quantify the construction of a deck panel system.
2) Shear stud pockets are widely accepted but the grouts have not been widely studied. One set of specifications has been formulated but they should be further

tested. The preparation, construction, and design procedures should also be monitored for these pockets. A modeling technique in finite elements would help in the selection in quality materials for the blockouts.

3) Transverse joints have always been a problematic area on deck panels. A number of different post-tensioned and reinforcing bar transverse joints have been implemented. Direct tests of the different joint types, including post-tensioned and reinforced, will provide data as to which method works the best. The tests should look at the worst case tensile stresses that the joints will experience.

4) Post-tensioned joints have been stressed to different levels based on analysis models. There is limited information on the best method to use for the design of post-tensioning stress in bridge decks. A study on post-tensioning design stress and actual behavior would help engineers design deck panels. This will include testing a previous reported design model, comparing the results with laboratory tests, and building a finite element model.

5) Many tests have focused on the initial stiffness and deflections of deck panel systems under short-term loads. Few tests have investigated the loss in stiffness and deflections after cyclical loading. The joint tests will analyze the change in strain distribution during the life cycle of transverse joints.

6) The long term goal is to bring together past research and laboratory research and implement the best practices on a full scale bridge. Implementing a state of the art full-scale bridge will provide real world data to compare with the research models. The finite element modeling of a real bridge's response to loading will help determine what types of joints and what post-tensioning levels are necessary for a fully composite and durable bridge. The culmination of this research project will be the design of deck panels for a bridge redecking project. Design and construction recommendations will be made for the next phase of research. The actual implementation is beyond the scope of this project.

Table 2-6 Research Needs and Plans

Research Need	Research Plan
1. Construction Methods for Joints and Haunches	Document all Construction Procedures and Compare Techniques
2. Performance of Grouts Used in the Shear Pockets	Compare Multiple Grouts in Circular Shear Pockets along with Multiple Surface Preparation Techniques; Model the Results
3. Compare Post-Tensioned and Cast-In-Place Transverse Joints	Direct Comparison on Full Scale Models
4. Negative Moment (Tensile) Tests on Transverse Joints	Negative Moment Full Scale Modeling
5. Post-Tensioning Level in Transverse Joints	Test two Post-Tensioned Joints with two Different Stress Levels – Compare the results to Analysis Methods and Model in Finite Elements
6. Stiffness Loss in Transverse Joints Over the Design Life	Perform Cyclical Tests on all Transverse Joints for the Full Design Life
7. Implement the Results on a Real Bridge	Design and Analyze the Design of a Real Bridge. Help Prepare the Construction Documents
8. Monitor the Behavior of a Real Bridge Designed With Deck Panels	Prepare an Instrumentation Plan for Testing of the Real Bridge

3 Experimental Research Methods

The objectives of this research project were to address the design, construction, and performance issues with transverse joints placed in continuous composite full depth precast bridge deck panels and to investigate the grouts and grouting techniques used on the panels. Two laboratory testing programs located at the Virginia Tech structures laboratory were used: one testing transverse joints and one testing grouting materials. The results of the joint tests produced a recommendation for the selection and construction of transverse joints. The results of the grout tests produced guidelines for selecting, constructing, and designing the grouted shear pockets. Finite element methods were used to model the transverse joint tests. Once compared with the laboratory results, the model was used to compare previous joint design methods with the laboratory tests. The results were used to design a bridge deck for a composite, three span continuous steel girder bridge. Lastly, an instrumentation plan was developed for future analysis of the bridge's response to load tests.

The research needs developed based on the literature review (Table 2-6) were addressed in this research project. Each of the eight research objectives was addressed in the following four phases of research. The completion of the last two objectives will be a continuation of this research project.

1. Transverse Joints Tests

(1) Construction methods for joints and haunches

(3) Transverse joint comparison

(4) Negative moment tests on transverse joints

(5) Post-tensioning level in transverse joints.

(6) Stiffness loss in transverse joints over their design life

2. Grout Ring Tests

(2) The performance of grouts in shear pockets and joints

3. Finite Element Modeling

(2) The performance of grouts in shear pockets and joints

(5) Post-tensioning level in transverse joints.

4. Implementation on the Virginia Bridge

(7) Implement the results on a real bridge

(8) Monitor the behavior of a real bridge designed with deck panels

3.1 Transverse Joint Investigation

3.1.1 Transverse Joint Selection and Design

Three transverse joints for full depth deck panels were chosen for direct comparison. The joints were chosen based on their use in previous construction and research projects. Two of the joints incorporated mild reinforcing bars and four included post-tensioned strand (Figure 3-1). The embedded bar joint is similar to the cast-in-place joint tested on a simply supported bridge in the NCHRP 584 report (Badie and Tadros 2008). The looped reinforcing bar joint is similar to numerous cast-in-place joints used on previous bridges (Precast/Prestressed 2002). The post-tensioned joints were designed with a shear key and post-tensioned strands. The post-tensioned joints had the same geometry, however two had neat grout, one had a pea gravel grout and one had an epoxy between the grout and concrete interface. In addition, the first neat grouted joint and pea gravel grouted joint had a different level of post-tensioning stress applied than the second neat grout joint and epoxied joint. Every joint was designed to carry the same, worst case negative bending moment over an interior support. A plan view of all the joints is in Appendix B.4 Construction Drawings for the Test Panels. The tests provided information to directly compare the performance of the joints. The six joints were named as follows:

1. **Embedded Reinforcing Bar Joint**
2. **Looped Reinforcing Bar Joint**
3. **Post-Tensioned Joint – 167 psi**
4. **Post-Tensioned Pea Gravel Joint -167 psi**
5. **Post-Tensioned Joint – 340 psi**
6. **Post-Tensioned Epoxy Joint – 340 psi**

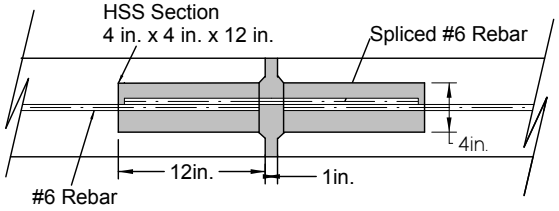

A) Embedded Reinforcing Bar

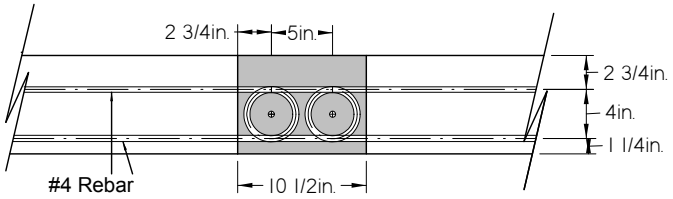

B) Looped Reinforcing Bar

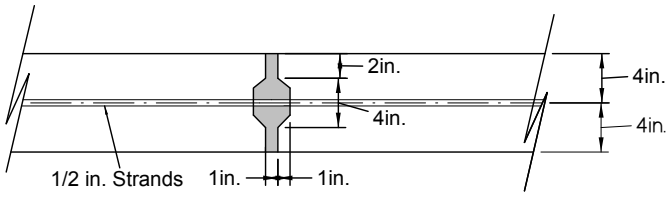

C) Post-Tensioned

Grouted regions are shaded

Figure 3-1 Transverse Joints

A continuous three span bridge in Southwest Virginia provided guidance for the design of the test setup and transverse joint specimens (Figure 3-2, Figure 3-3). The requirements for

the bridge were that it was continuous, had steel girders, and could be redecked with deck panels from the research. The steel girders were required because steel provides a larger constraining force that causes more losses in the post-tensioned panels. Past research has shown that steel is the worst case situation (Bowers 2007). The chosen bridge represented a typical layout for a steel girder bridge in need of a new deck. The owner was The Virginia Department of Transportation (VDOT). The layout for the project included W21x83 girders spaced at 4.8 ft, a deck width of 30.3 ft, and a composite three span design (31 ft - 32.5 ft - 31 ft).

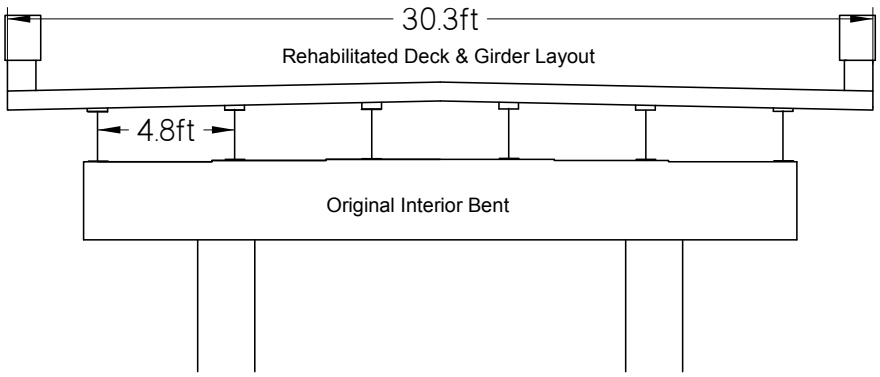

Figure 3-2 Proposed Elevation View of the Virginia Bridge

Aftering choosing the transverse joints and bridge for redecking, the design of the six panels began. The focus was on the continuous, composite region over the interior bent where the joints would experience the highest tensile stresses (Figure 3-3). The panels were designed following the procedures in the Standard Specifications for Highway Bridges because VDOT planned to design the real bridge with this method (2002). The steel girder size was provided by VDOT and not designed as part of this project.

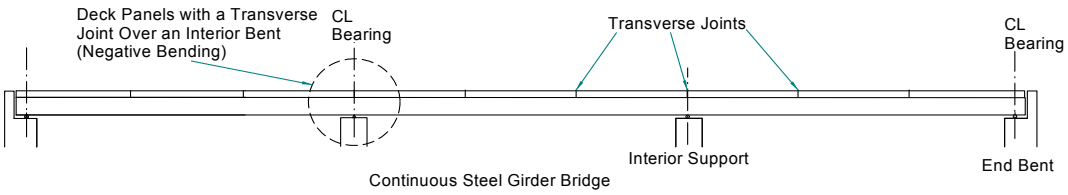

Figure 3-3 Original Virginia Steel Girder Bridge

The bridge was first analyzed to determine the maximum stresses the superstructure would see in the transverse and longitudinal direction with a standard HS-20 design truck. The HL-93 truck was not chosen because the bridge was to be designed by VDOT with the Standard Specification (AASHTO 2002). The HL-93 load is a lane load combined with the HS-20 design vehicle, therefore the stresses would be higher. The deck was then designed using a combination of standard and new methods unique to deck panels. The only deviations from the standard design methods were on the aspects unique to full depth bridge deck panels.

Three main differences exist between the design of deck panels and conventional cast-in-place decks: transverse prestressing, transverse joints, and shear pockets (Figure 3-4). These design methods are not explicitly addressed in the Standard Specifications as discussed in the literature review.

The first step was to design the panels with prestressed tendons in the transverse direction. A continuous analysis was done across the bridge deck in the transverse direction using an HS-20 design vehicle (Appendix A.2.1). The supports over each girder were analyzed as pin supports. The panels were designed using a 1 foot strip of concrete and two concentric, transverse prestressing strands. The stress levels were checked to ensure the panels met the Standard Specification (Standard Specification 9.15.2), (Appendix A.2.2). This provided a compressive force in the panels during production, transportation, and placement that prevented cracking and provided transverse strength.

Next, the panels were designed with transverse joints to transfer stresses in longitudinal bending. An analysis of the bridge was done in the longitudinal direction. The end bents and interior supports were modeled as pin supports. The analysis was done with an unfactored HS-20 vehicle using the computer analysis program Q-CON. The moment envelope was recorded

from the HS-20 vehicular live loads and then it was factored using the load factors from the Standard Specification (Appendix A.3.1). The transverse connections were designed to withstand the factored design moments though service loads were applied during testing. The post-tensioned joints were designed with a stress analysis. The stresses were checked throughout the post-tensioned deck panels to ensure they stayed within the compression and tension limits. The limits from the AASHTO Standard Specification were used. All of the joints were designed for strength. A strength analysis was performed on the post-tensioned and reinforced joints to carry the factored design moments (Appendix A.3.2).

Lastly, the panels were designed as composite with the steel girder system. The horizontal shear forces were computed, then the steel needed to transfer the force was determined (Standard Specification 10.38.5). The horizontal shear connections were shear studs placed in pockets spaced at 3 ft throughout. The shear pocket dimensions were chosen based on the minimum spacing allowed between the shear studs in the Standard Specification 10.38.2.4. The spacing of the shear pockets was chosen based on the 4 ft maximum from previous research and on geometric limitations within the panels (Appendix A.3.3). As discussed in the Section 2.3.3, there has been little reported difference in the performance of different blockout shapes. Rectangular was chosen because it has been used in previous projects as shown in the literature review. The final panel drawings are included in Appendix A.1.

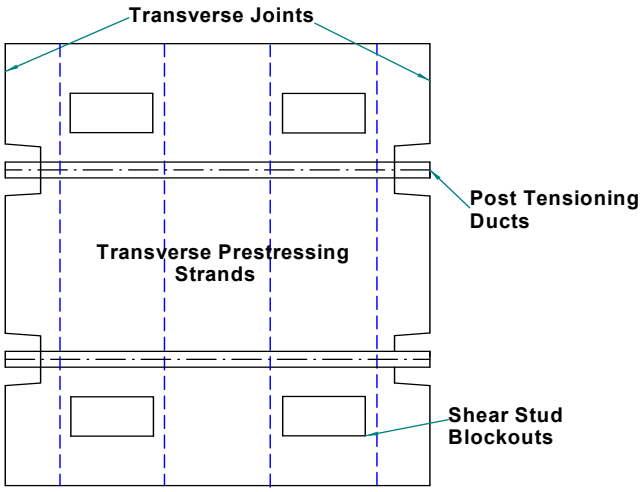

Figure 3-4 Full Depth Precast Panel Parts (Plan View)

3.1.2 Transverse Joint Testing

Following the design of the complete deck system, the negative bending test was devised. The test was modeled after the interior supports on the Virginia Bridge (Figure 3-3). The goal was to test full size transverse joints under cyclical, service loads. All testing was performed at the Virginia Tech Thomas M. Murray Structures Laboratory.

In order to use resources efficiently, the testing only focused on a section of the bridge with transverse joints. A full scale, two girder portion of the interior support was chosen for testing (Figure 3-4, Figure 3-5). Everything on the models was kept similar to the bridge deck design to limit the number of variables among the tests (Section 3.1.1). Shear studs were welded at the same uniform pocket spacing of 3 ft, the bridge deck depth remained at 8 in., and the girder spacing was 4.8 ft. A haunch height of 1.5 in. was used throughout to simulate a typical situation. The design compressive strength of the concrete used in the panels was 5,000 psi. The girders used in the test were W21x101, instead of W21x83, because of local availability.

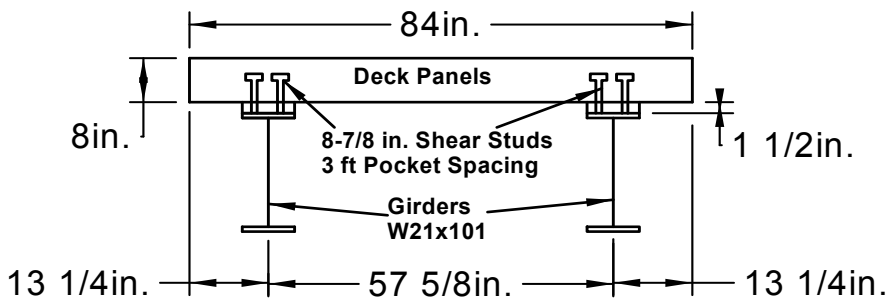

Figure 3-5 Composite Connection between the Panels and Girders (End Elevation View)

The laboratory test setup was a double cantilevered system symmetric about the center support (Figure 3-6). A load was applied at one end with a servo hydraulic controlled actuator. The load frame was built using two W12x58 shaped columns bolted to the strong floor and a double channel C15x50 beam connecting the columns. The other end was tied down with 8 – 1 in. threaded tension rods (Figure 3-7). The midpoint of the bridge had a steel roller under each girder simulating a frictionless support. Because of the symmetry of the loads in the system, two joints were tested simultaneously. The model had joints spaced at an equal distance from the center support.

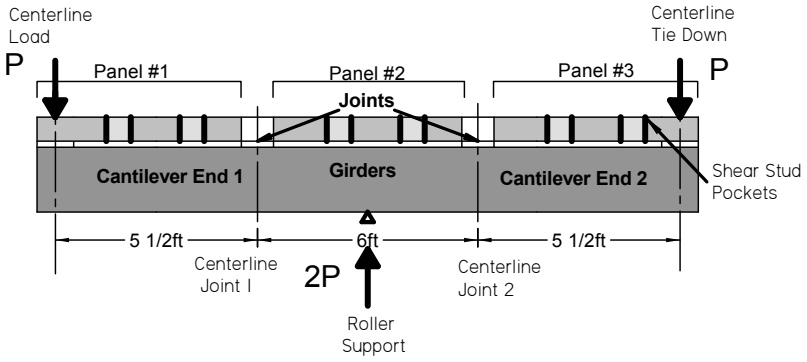

Figure 3-6 Testing Setup (Elevation View)

The model was designed to test the full scale transverse joints under the maximum stress caused by an HS-20 vehicle. As mentioned previously, the HL-93 vehicle in the LRFD code uses a lane load with the HS-20 and would produce slightly higher stresses. Using the

maximum moments computed from the joint design (Section 3.1.1), a stress level in the panels over the interior bents was computed. The stress levels in the joints during testing were designed to be the same as the stress level produced by the design loads on the real bridge (Appendix A.3). The stress range for the joint was created by applying a 75.5 kip force to each cantilever at 5.5 ft from the centerline of the transverse joints. Because the stress range for each transverse joint was the worst case on the Virginia bridge, the stress at the midpoint of the test setup was greater than the stress level created by an HS-20 truck. A sinusoidal load was applied at a rate of 1 Hertz throughout the cyclical tests. The load range for the cycles was 75.5 kips but the actual loads varied between 2.5 kips and 78 kips. The testing matrix is shown in Table (Table 3-1).

Table 3-1 Transverse Joint Testing Matrix

Test Performed	Joints Tested
1) Cast-in-Place Joints	Embedded Reinforcing Bar Joint Looped Reinforcing Bar Joint
2) Post-Tensioned Joints	Post-Tensioned Joint – 167 psi Post-Tensioned Pea Gravel Joint -167 psi
3) Post-Tensioned Joints	Post-Tensioned Joint – 340 psi Post-Tensioned Epoxy Joint – 340 psi

Figure 3-7 Transverse Joint Setup

3.1.3 Construction Study on the Transverse Joint Tests

Many of the steps used in the construction processes contribute to the performance of the deck panels as documented in the literature review. In the tests presented here, the construction of the precast panels and the transverse joint tests was carefully documented. The observations started in the precast panel plant and continued through the end of testing in the laboratory. By the end of the testing, there was a basic outline of the processes used to build full depth deck panel systems.

The first part of the construction process was done in a precast plant at The Shockey Precast Group in Winchester, Virginia. This precast plant was chosen because of its relative proximity to the testing lab and their employees' experience at making precast parts. The panels were built in on outdoor stressing beds with an awning covering the construction area. The locations of different panel components, including the post-tensioning duct, the leveling bolt anchor, and the prestressing strands, were monitored. Vibrating Wire Gauges (VWGs) were installed at the joint edges inside the panels during this process (Figure 3-8). These were used during testing to determine the strains in the top of the panels at midspan (Section 3.1.4). Four inch by eight inch concrete cylinders were made for strength and modulus tests.

Figure 3-8 Installing the Vibrating Wire Gauges in the Panels

After the panels were made and delivered by truck, construction began on the test specimens. The construction process in the laboratory had a number of unique steps that are normally performed differently on standard cast-in-place concrete decks. Particular attention was paid to processes that have no widely accepted method as demonstrated in past literature. This included:

1) Forming the haunches
2) Leveling the panels
3) Forming the joints
4) Grouting the deck
5) Post-tensioning the panels.

The haunches were formed between the panels and steel girders to keep the grout in place during placement. In the first test setup, two methods were used to form the haunches; fiber forming board and cold formed steel angles (Figure 3-9). The fiber forming board was made of recycled paper fiber produced by the Homasote Company. The board was purchased in ½ in. sheets, cut to size, and glued with liquid nails. A 1½ in. think haunch was used throughout. The boards were then glued to the outer edge of the top flange of the girders. The second material used was a cold formed steel angle with leg dimensions of 1½ in. A ¼ in. tie rod was used at approximately 4 ft spacing along the girder to provide transverse support. The bottom leg of the angle was glued to the top flange of the girder to ensure stability during construction. Prior to putting the panels in place a small strip of weather seal was placed on the top edge of the flange of the angles. The fiber board was glued to the girder and panels with construction adhesive while the cold formed steel was held together by tie rods and glued to the girders. Observations were made of the ease of construction and effectiveness at containing the grout. In the last two setups, the fiber forming board was used throughout.

After forming the haunches, leveling bolts were installed in the panels and the panels were lifted into place using a crane. The leveling bolts were used to adjust the height of the panels (Figure 3-9). This is a method that has been previously reported for deck panel construction. The bolts were installed with a protrusion of approximately 4 in. from the bottom of the deck panels. The bolts rested on the girders while the panels were put into place with

cranes. The bolts were then adjusted with a hand wrench to lower the panels to the final elevation. Care was taken to ensure the panels touched the haunch formwork but did not damage it.

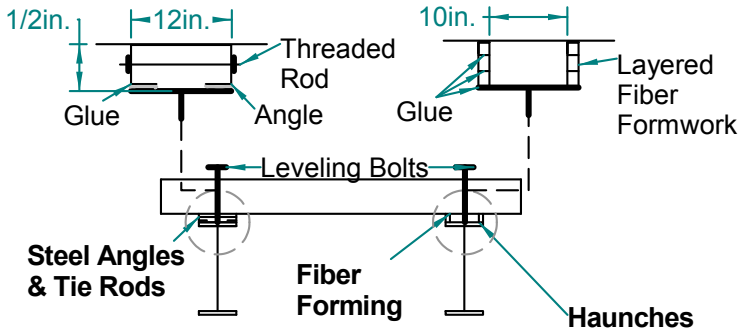

Figure 3-9 Bridge Haunches

Wooden formwork with threaded tie rods was used for all of the transverse joints. A liquid adhesive was applied around the joints between the wood and concrete to ensure the grout would not leak. The time and ease of construction was monitored. After the grout cured, the wooden formwork was removed but the tie rods were left in place. In five of the six joints, the tie rods left weak spots that extended through the entire depth of the joint. In the looped reinforcing bar joint the reinforcing within the joint was used as support for the bottom formwork. This method was devised to prevent protrusions in the top surface of the grout (Figure 3-10).

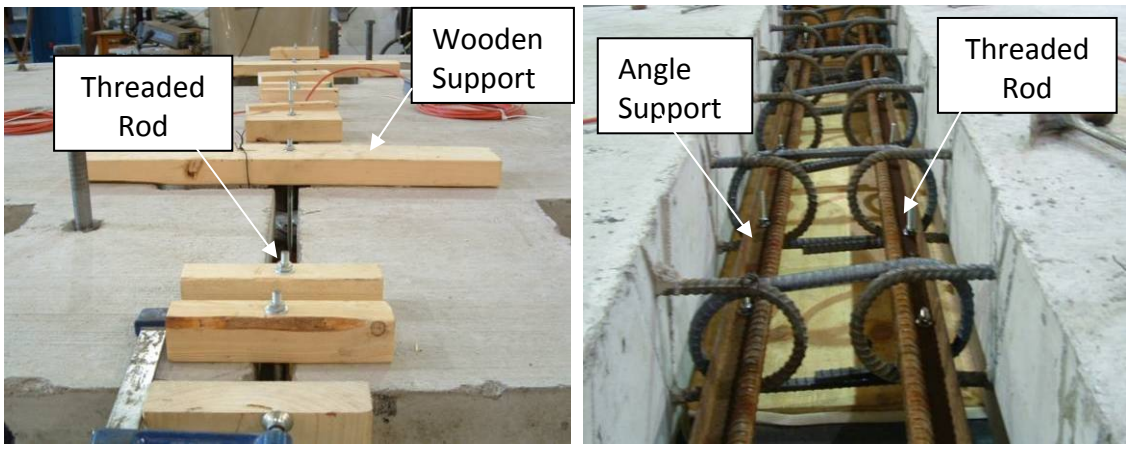

Figure 3-10 Formwork around the Transverse Joints

Standard Five Star highway patch grout was used on all joints, haunches, and shear pockets. The grout is typically used in bridge deck rehabilitation projects for patching deck surfaces. Previous research by Scholz showed that this type of grout was one of the best choices for deck panels (Scholz 2004). All mixing procedures followed the recommendations of the manufacturer (Appendix C.1.1). On one transverse joint the grout had an additional $^{3}/_{8}$ in. nominal maximum size pea gravel extension as allowed by the manufacturer. Differences between the construction of the grout with and without the extension were monitored. Workability and strength considerations were documented for each batch of grout.

The cast-in-place joint required one continuous grout pour. The transverse joints, haunches, and shear pockets were all connected and poured down the girder lines. The pour started in the first shear pocket and continued in this pocket until grout exited through the haunch in the next shear pocket along the girder line (Figure 3-11). This process continued in each pocket along the girder line (Figure 3-12). When a joint was encountered it was filled in the same manner as the shear pockets. At the end of the girder line a 1 in. exit hole was left open until the grout flowed out (Figure 3-13). The hole was then capped.

Figure 3-11 Typical Grouting of the Shear Pockets and Haunch

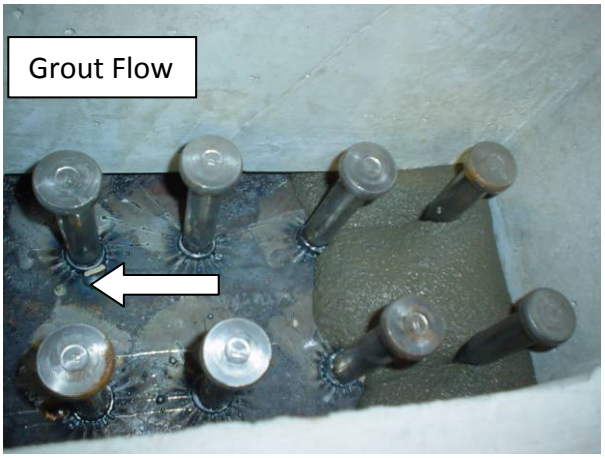

Figure 3-12 Grouting Down a Girder Line

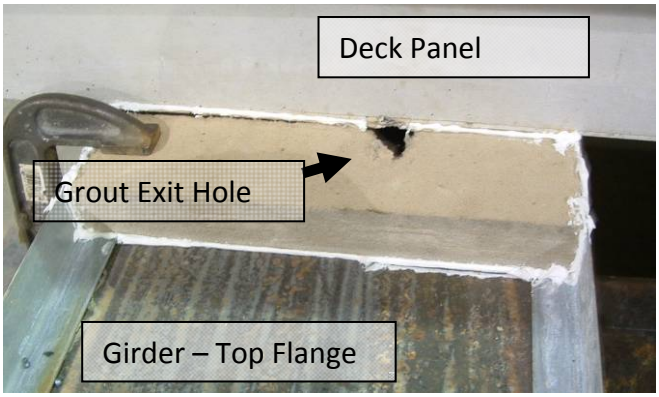

Figure 3-13 Grout Exit Hole at the End of a Girder Line

The post-tensioned joints required three separate grout pours. First, the grout was poured in the transverse joints. A special forming technique was used to form beneath the joints inside the haunches. A piece of plywood was held in place with wedges placed in the shear pockets on each side of the joint. Once the grout was cured, the wedges were removed and the plywood was pulled out through the haunch. After the joints were poured, the post-tensioning was added to the deck panels. Once the post-tensioning was stressed, the strands were encased with grout using a grout pump (Figure 3-14). The grout was pumped through a grouting tube at one end of the post-tensioning duct. Grout was pumped until it came out of the grouting tube at the other end of the post-tensioning duct. The final grouting procedure was to fill the shear pockets and haunch with grout using the same procedure followed in the cast-in-place joints.

Figure 3-14 Grouting the Post-Tensioned Ducts

On two of the specimens, post-tensioning was applied to the deck in the longitudinal direction (Figure 3-15). The force due to the post-tensioning compressed the panels and transverse joints in the longitudinal direction. This involved an additional procedure that took extra time. Extra care was taken to safely stress the strands to the correct level without injuring anyone or damaging the laboratory equipment.

Figure 3-15 Post-Tensioning the Deck Panels

In both tests, there were two ducts centered at mid-depth in the panels. The ducts were situated 24 in. from the outer edge of the panels (Figure 3-16). In the first set of post-tensioned panels, there were two strands in each duct. In the second set of post-tensioned panels, there were four strands in the ducts.

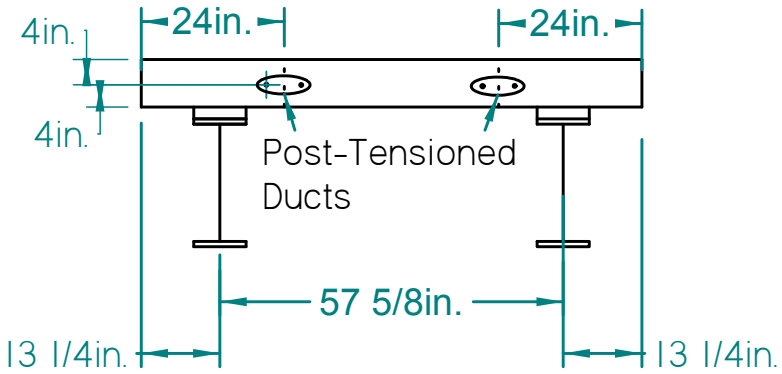

Figure 3-16 Elevation View of the End of the Transverse Joint Tests

One load cell was added to the dead end of one strand in each duct (Figure 3-17). The load cells ensured that the load in the strands was correct and provided data to back calculate friction losses. The strand with the load cell was stressed first so that elastic shortening losses

from subsequent stressing could be monitored. After post-tensioning, the ducts were grouted as described above. The additional time and labor needed to add post-tensioned strands was measured.

Figure 3-17 Load Cell on the Dead End of a Strand During Stressing

3.1.4 Transverse Joint Instrumentation and Data Collection

The transverse joint testing consisted of applying an HS-20 vehicle 1,000,000 times, the design life of the Virginia bridge. The design life was provided by the bridge owner, VDOT. The stress range was 0.56 ksi and 0.10 ksi at the top and bottom of the deck, respectively. At predetermined points in the test, the cycles were stopped and data was taken during a static test (Table 3-2). Strains were monitored at the bottom and top flange, midpoint of the girder, and top of the slab. Any cracks were recorded and measured and ponding was performed at intervals on the surface of the decks. Good joint behavior was defined as little cracking, no water leaking through the deck, and a linear strain distribution through the depth of the composite section.

Table 3-2 Static Load and Ponding Tests During the Cyclical Tests

HS-20 Vehicle Load Cycles	Static Load Tests	Ponding Tests
0	x	X
1	X	X
1,000	X	
5,000	X	
10,000	X	X
20,000	X	
30,000	X	
40,000	X	
50,000	X	X
100,000	X	X
200,000	X	
300,000	X	
400,000	X	
500,000	X	X
600,000	X	
700,000	X	
800,000	X	
900,000	X	
1,000,000	X	X

Strains were collected during the laboratory tests on a number of parts in the deck system. Vibrating wire gauges (VWG) were cast in the panels on each side of the joints at the precast plant in order to monitor the strain levels in the deck. Strain gauges were applied on the steel girders beneath each joint at the top flange, bottom flange, and mid height of the web. DEMEC gauges were used to measure any opening of the joints on top of the slab, the point of highest stress (Figure 3-18, Figure 3-19).

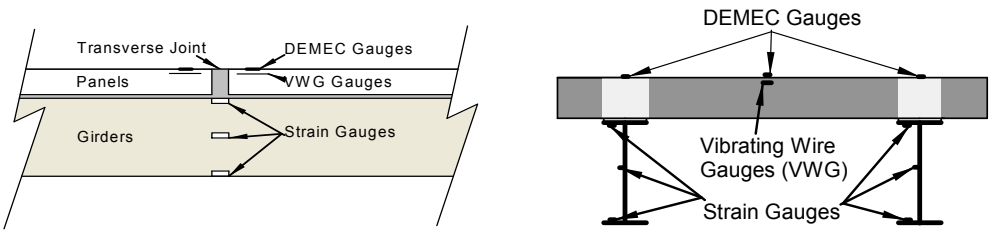

A) Side Elevation View B) End Elevation View

Figure 3-18 Instrumentation at the Transverse Joints

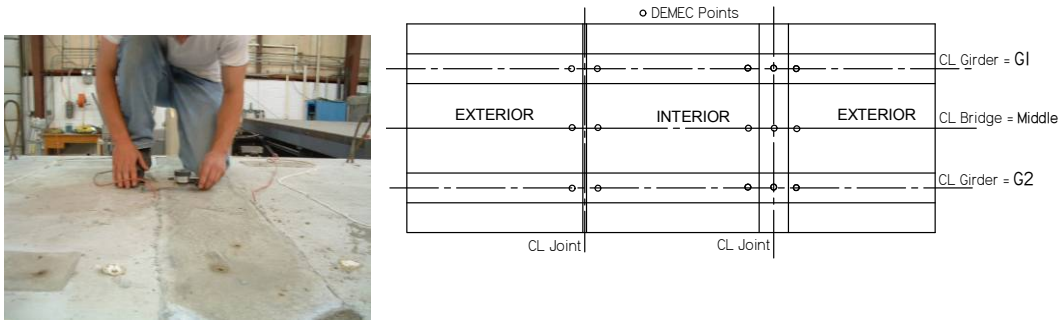

Figure 3-19 Location of the DEMEC points.

A ponding test was performed at particular points during the load cycles (Table 3-2, Figure 3-20). A 1 in. high layer of construction adhesive was applied around the edge of the surface of the panels. Water was then placed on the bridge deck. The ponding test determined the point when the cracks in the deck were big enough to allow water to flow through the deck in a two hour time period. No load was applied during these tests except at the final ponding. After the one millionth cycle, a ponding test was performed while applying ten service load cycles and then while applying one hundred service load cycles. The bottom and side of the deck panels were observed for leaks.

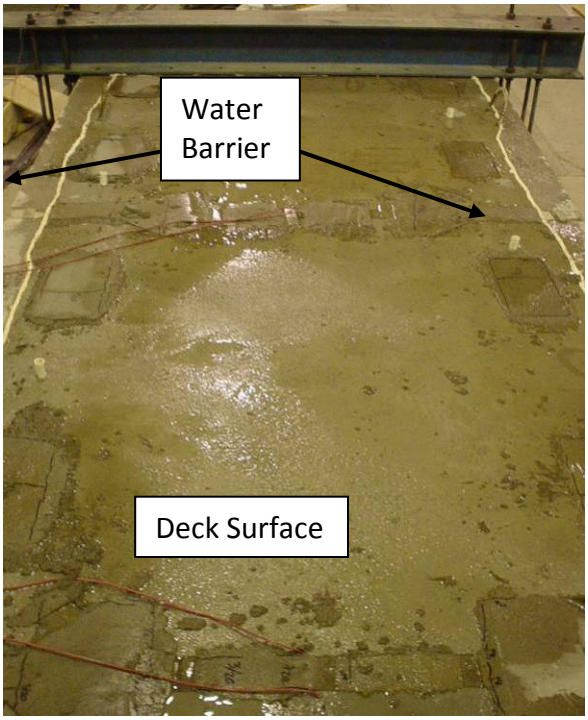

Figure 3-20 Ponding Test

As cracks occurred, they were marked on the deck surface. Shrinkage cracks were marked after construction and prior to applying the service loads. They were marked and documented as non-load induced cracks. The crack widths, with and without the service load, were measured with a crack gauge at the conclusion of the cyclical loading.

3.2 Shear Stud Grout Pockets

The next investigation focused on the grouts and grouting procedures used on the shear pockets in full depth deck panels. The high early strength, non-shrinking highway patch grouts used in deck panels have a tendency to crack over time. This phase of the research tested different shear pocket conditions and compared the results to standard ASTM material tests. The objective was to find a grout and shear pocket surface that effectively prevents cracks and leakage in the joints.

The first tests were on the panels used in the transverse joint tests and the second tests were on ring samples created to test shear pockets. Five Star Highway patch grout was chosen for the transverse joints, haunches, and pockets for the first two full scale deck panel tests

(Section 3.1), because of previous research (Scholz 2004). On the last transverse joint test, six different surface preparation techniques were tested with the Five Star Highway patch grout. The ring sample tests investigated four different types of cementitious materials and six surface preparation techniques on circular shear pockets. The ring tests included measuring material characteristics of the grouts in order to relate them to the performance of the shear pockets.

3.2.1 Grout Investigation in the Transverse Joint Test Panels

Each of the three transverse joint tests had twelve shear stud pockets. Shear studs were applied in pockets spaced at 3 ft throughout the deck panels. All of the shear pockets were filled with Five Star Highway Patch grout mixed per the manufacturer's recommendation (Appendix C.1.1). The pockets measured 14.5 in. long by 7.5 in. wide by 8 in. thick. The amount of highway patch grout in these pockets was substantially more than the amount used in most transverse joints or in typical bridge patching applications. The larger volumes of grout placed in the shear pockets created a higher probability of cracking.

The shear pockets of the first two specimens of the transverse joint tests were filled with standard highway patch grout. The processes to place the grout remained consistent, but the techniques used on the shear stud pockets varied. Water was applied to the pocket surfaces to maintain a moist condition and grout was poured per the manufacturer's guidelines. After the grout was placed, as mentioned in Section 3.1.3, the pockets were monitored for shrinkage. Monitoring continued on the panels while the transverse joint loading tests were performed. Cracking was labeled on the deck panel top surface and the widths were measured by comparing them to crack gauges (0.005 in. or greater). The time from pouring the grout to the end of testing for the first and second tests was 42 days and 52 days, respectively.

Section 4.2.1 describes the performance of the Five Star grout in the first two transverse joint tests. In response to the results, six new surface preparation techniques were chosen for the final transverse joint test specimen. In addition, the pockets were ponded with water and monitored for leaks. The goal was to find a better preparation method for the shear pockets that prevented cracking and leaking.

Two pockets with each surface preparation technique were built for a total of 12 shear pockets. The methods for pouring the grout did not change (Section 3.1.3). Two control pockets were built following the manufacturer's guidelines by moistening the surface prior to applying the grout (Appendix C.5). Two pockets were built with each of the following surface treatments: epoxy coated, sand blasted, exposed aggregate, and grouted surface (Figure 3-21). The last set of two pockets had water stops placed in the joint to prevent water from penetrating the deck. The test matrix for the shear pockets is shown in Table 3-3.

Table 3-3 Test Matrix of Transverse Joint

	Transverse Joint Test #1 (Number of Samples)	Transverse Joint Test #2 (Number of Samples)	Transverse Joint Test #3 (Number of Samples)
Moist (Control)	12	12	2
Epoxy Coated	0	0	2
Sand Blasted	0	0	2
Exposed Aggregate	0	0	2
Grouted Surface	0	0	2
Water Stop	0	0	2

a) Grouted Surface

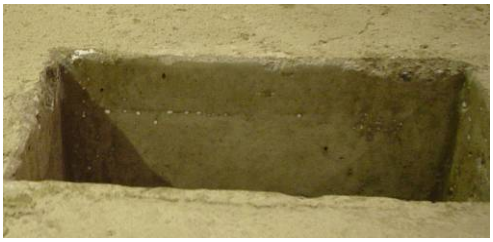

b) Epoxy Coated

c) Water Stop

d) Exposed Aggregate

e) Sand Blasted

f) Moist Surface

Figure 3-21 Shear Pocket Surfaces

Three of the techniques required additional work from the precast manufacturer. The exposed aggregate pockets were treated with BASF MBT-HeatCote prior to pouring the concrete. When removing the forms, the pockets were sprayed with water to remove the paste. Sand blasting was performed on two pockets immediately after removing the formwork. It is noted that the sand blasting took place 49 days before the grout was poured in the shear pocket. The water stops were placed inside the pocket formwork and cast into two shear pockets. The construction diagrams are shown in Figure 3-22.

Three of the surface conditions required additional work prior to pouring the grout. The epoxy coating was added approximately 30 minutes before the grout was poured as required by Dap, the maker of the bonding liquid epoxy. The epoxy had a “tacky” feel when pouring the grout. The grout paste was applied approximately 15 minutes before grouting two pockets. An approximately ¼ in. layer of Five Star grout was placed on the inner surface of two pockets. The

mix proportions of the grout were the same as the manufacturer's guideline. The surface grout was still moist when the pocket grouting began. The wetting of the surface on the last two pockets took place approximately 10 minutes before pouring the grout. This method was the same one used on the first two sets of panel tests.

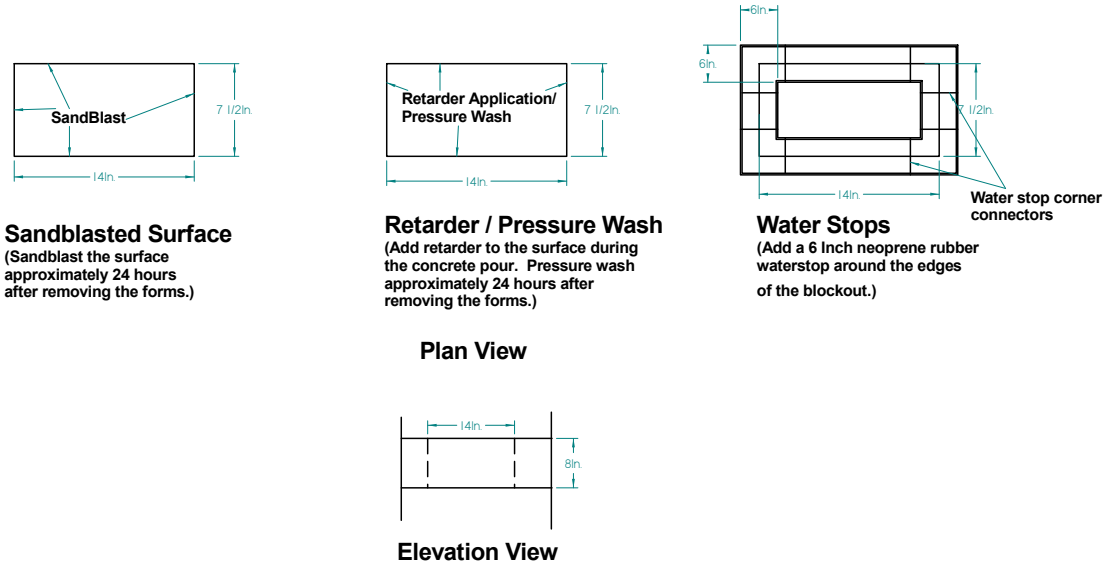

Figure 3-22 Shear Pocket Construction Documents

The pockets were monitored for cracking in and around the grout. Cracks were marked on the panel and grout surface starting at construction and continuing through the end of the cyclical loading. The crack widths were recorded if they were large enough to measure with a crack gauge (0.005 in. or greater). The time from grout construction through the end of testing was 67 days.

Ponding tests were also performed on each shear stud pocket. First a barrier was formed around the deck with a 1 in. tall layer of construction adhesive. After the adhesive dried, a layer of water was applied inside the barrier to a depth of about one quarter of an inch. Only the exterior edge of the shear pockets was exposed on the bottom of the panels near the edge of the haunch (Figure 3-23). Leaks were observed only on this outer edge since the other edges were not visible. Any other cracks that appeared and leaked were also noted.

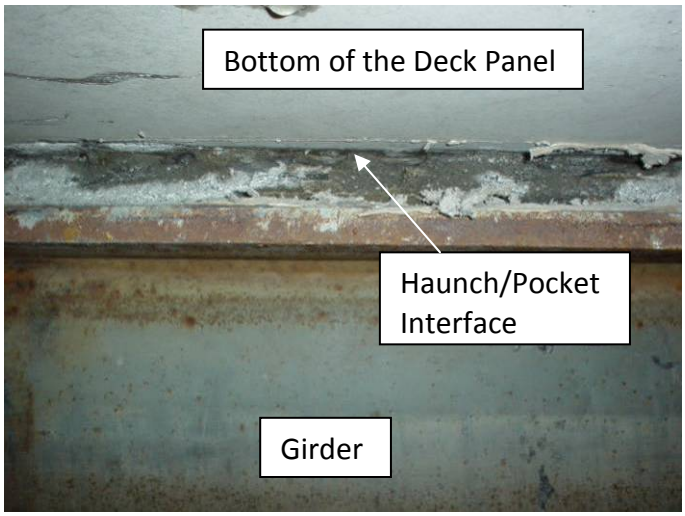

Figure 3-23 Ponding Test on the Shear Pockets

3.2.2 Grout Testing for Deck Panel Pockets

The second phase of the grout testing focused on the materials and processes used to make the shear stud pockets. Previous research showed inconsistent behavior of shear pockets. The grouts tended to crack between the concrete and grout during the transverse joint tests in the first phase of this research. The objective of this phase of research was to find a surface preparation technique that forms a solid bond and cracks the least. A variety of specimens were built and the material properties and construction processes were recorded. An analysis was performed on the different cementitious materials, their performance, and the stresses that formed between them.

3.2.2.1 Grout Testing Design

The grout tests investigated numerous types of grout and surface preparation techniques. The grouts included: Five Star Highway Patch Grout, Five Star Highway Patch Grout with a $^{3}/_{8}$ in. pea gravel extension, Five Star Highway Patch Grout with a 1- ½ in. polypropylene fiber, Set 45 Grout, and Type K concrete. A control specimen was created for each type of grout with a standard wetted pocket surface. Because the Five Star grout had been used previously, it was used as the control variable when testing surface conditions. Five surface conditions were tested with the Five Star grouts: Exposed Aggregate, Wire Brushed,

Epoxy Coated, Water Stop, and Shear Key. Table 3-4 lists the 13 specimen types and the number of specimens per test.

Table 3-4 Proposed Shear Pocket Testing Specimens

Surface Condition	Grout Type	Label	Number of Specimens
Wet Surface (Control)	Five Star	FC	3
	Five Star/Pea Gravel	FPC	3
	Five Star/Fibers	FF	3
	Set 45	SC	3
	Type K Cement	KC	2
Exposed Aggregate	Five Star	FA	3
	Five Star/Pea Gravel	FPA	3
Epoxy	Five Star	FE	3
	Five Star/Pea Gravel	FPE	3
Wire Brush	Five Star	FB	3
	Five Star/Pea Gravel	FPB	3
Shear Key	Five Star	FS	3
Water Stop	Five Star	FW	3
Total			38

Circular specimens were built to simulate the conditions experienced by the shear pockets in the deck and to compute the stresses formed between the materials (Figure 3-24). As described in Section 2.3.3, multiple rectangular and circular layouts have been attempted. The 8 in. diameter of the grout blockout was similar to the dimensions used on the laboratory test panels (14 in. by 7.5 in. by 8 in. deep). Additionally, the interface on the rectangular specimens had stress concentrations at the corners that were not present in the circular specimens. In order to use a basic thick walled cylinder stress equation (Eq 1 (Riley 1999)), the specimens were all designed as 18 in. concrete cylinders with an 8 in. inner ring of grout (Figure 3-24). The depth was 4 in., the same as tests done by Scholz et al. (Scholz et al. 2007; Wallenfelsz 2006). The outer ring was made of a typical deck concrete and made with cardboard forms. A piece of plywood was attached to the bottom of the forms to contain the concrete. The inner ring was poured inside the concrete ring with grouting materials.

Thick Walled Cylinder Stress Equation

$$\sigma_r = \frac{\Delta(c^2-b^2)E_g E_c}{2b(E_g(1-v_c)b^2+E_g(1+v_c)c^2+E_c(1-v_g)(c^2-b^2))} \quad \text{Eq. 1}$$

where

Δ	=	Change in diameter of the grout ring (Grout)
v_c	=	Poisson ratio of the outer material (Concrete)
v_g	=	Poisson ratio of the inner material (Grout)
E_g	=	Modulus of elasticity of the inner material (Grout)
E_c	=	Modulus of elasticity of the outer material (Concrete)
c	=	Outer radius (Concrete)
b	=	Inner radius (Concrete-Grout Interface)

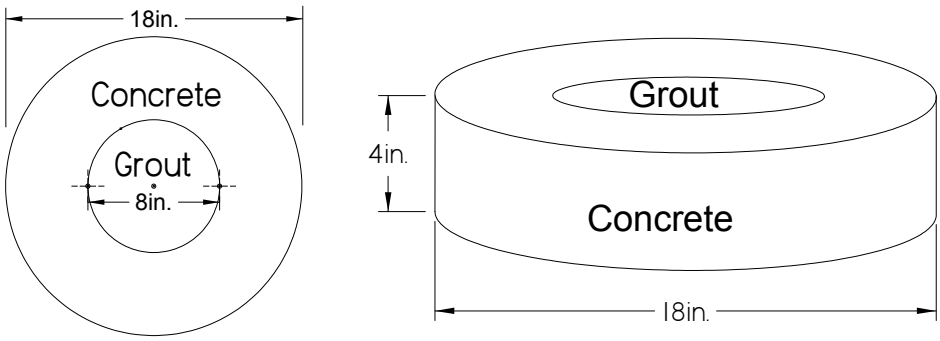

Figure 3-24 Plan and Three Dimensional View of the Grout Testing Setup

3.2.2.2 Grout Testing Construction

All of the grout rings were created and stored under the same conditions. The base of the rings were formed with a ½ in. plywood covered in plastic in order to obtain a uniform base and aid in form removal. The sides were formed with wax coated, paper-fiber forming tubes made by The Construction Materials Group and CarauStar. The exterior of the 8 in. tubes were used for the inner rings and the inside of the 18 in. tubes were used for the outer ring (Figure 3-25). The rings were glued to the base with Liquid Nails construction adhesive. The formwork

for the shear keyed specimens was adjusted to install a 1-1/2 in. deep by 1-1/2 in. wide ledge. The formwork for the water stopped specimens was adjusted to install a 3 in. wide water stop, 1 in. below the surface of the ring. All of the formwork and specimens were placed on two wooden shelves in the Virginia Tech Thomas M Murray Structures Laboratory for the duration of the tests.

Figure 3-25 Grout Ring Formwork A) Typical B) Water Stop C) Shear Key

The outer ring was poured with a 4000 psi VDOT Post and Rail Concrete Mix (Appendix C.1.5). The concrete was ordered from a local ready mix plant, ConRock, and the same batch was used for all of the rings. The rings were filled with shovels and then vibrated with pencil vibrators in two lifts. The rings were cured with wet burlap covered in plastic for 7 days following the concrete pour (Figure 3-26). The rings then cured in ambient conditions for an additional 35 days prior to filling them with grout.

The ring formwork was removed after 35 days and the specimens were cleaned. All residue from the cardboard was removed. The only rings uncovered prior to 7 days were the exposed aggregate specimens. They were uncovered after 24 hours for approximately 1 hour. The formwork on the inner ring was removed and the specimen was hosed down to remove the paste.

Figure 3-26 Applying the Burlap and Plastic

The inner surfaces of the grout rings were all prepared prior to pouring the grout. The wire brushed surfaces were prepared and cleaned the day before pouring the grout. The water stops, shear keys, and exposed aggregate surfaces were cleaned with a damp rag the day before the grout pour. The epoxy coating was applied once 30 minutes prior to pouring the grout, and then a second time approximately 10 minutes before pouring the grout. Elmer's ProBond Concrete Bonder was used. All rings except the epoxy coated ones were moistened approximately 15 minutes before commencing with each grout pour.

The five grout mixes were all poured within 6 hours of one another, 42 days after pouring the concrete. Forty-Two days (6 weeks) was chosen because the concrete shrinkage began to slow and the duration was similar to a deck panel construction schedule. No curing techniques were used on the grouts in order to simulate an accelerated construction project. The grout mixes were based on the manufacturer's recommendations and workability concerns. Everything was mixed, poured, and cured inside the laboratory. The environmental conditions and mix designs are listed in Appendix C.2. The specimens were left in the same location on the shelves with the bottom formwork for 2 days. The bottom formwork was removed at 2 days and the bottoms of the rings were left exposed.

3.2.2.3 Grout Ring Data Collection

Strength, elastic modulus, poisson's ratio, and shrinkage were measured for the grouts and concrete. Concrete compressive strength was obtained using ASTM C31 and C39 with 4 in. by 8 in. cylinders at 1, 7, 28, 56, and 84 days. Grout compressive strength was obtained using ASTM C109 with 2 in. by 2 in. cubes at 1, 7, and 28 days. The elastic modulus and poisson's ratio was measured for each material using ASTM C 469 at 1,7, 28, 42, and 56 days. Shrinkage was measured daily for the first 7 days and weekly for the next 10 weeks using ASTM C157. The bars were 1 in. by 1 in. for the grouts and 3 in. by 3 in. for the concrete and pea gravel grouts. The samples were kept next to the ring samples inside the structures laboratory for the duration of the test.

Cracking in the rings was monitored visually starting the day after the grout was poured. The rings were viewed daily for the first 7 days and every 3 days for the next 35 days. From day 42 to day 84 the samples were checked weekly. Cracks were marked and the size was measured using crack gauge cards (0.005 in. minimum size).

Ponding was performed on the surface of the specimens two days after the grout was poured. It continued on a weekly basis for the next 84 days. Water was ponded to a minimum depth of 0.25 in. on top of the pocket at all times. A 0.50 in. layer of liquid nails construction adhesive was placed around the edge of each ring to act as a barrier. At each measuring cycle, the bottom surface of the pocket was checked for signs of leaking water. The ponding was done for a minimum of 2 hours. The procedures were the same as those used on the transverse joint tests (Section 3.1.4).

Surface strain was measured across the concrete-grout interface in six locations and inside the grout ring in three locations. DEMEC points were placed in two concentric rings in six directions on top of the rings (Figure 3-27). A point was also placed at the center of the ring. The spacing between the DEMEC points was 7.875 in. (200 mm). The measurements were numbered 1-9; the first three were inside the grout ring and the last six were across the grout/concrete bond. Measurements were taken every two days for the first week and then weekly for the next 11 weeks. Table 3-5 explains the data collection schedule for the grout rings.

Table 3-5 Data Collection Schedule for the Grout Rings

Data Collection (Days from Pour)															
Samples	**1**	**2**	**3**	**4**	**5**	**6**	**7**	**14**	**21**	**28**	**35**	**42**	**49**	**56**	**84**
Shrinkage	x	x	x	x	x	x	x	x	x	x	x	x	x	x	x
Concrete Strength	x						x			x				x	x
Grout Strength	x						x			x					
Elastic Modulus	x						x	x		x		x		x	
Poisson's Ratio	x						x	x		x		x		x	
DEMEC	x						x	x	x	x	x	x	x	x	x
Ponding		x					x	x	x	x	x	x	x	x	x
Cracking	x	x	x	x	x	x	x	x	x	x	x	x	x	x	x

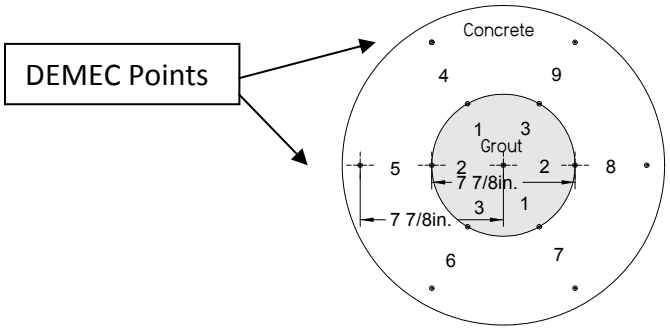

Figure 3-27 DEMEC Point Locations and Measurements

3.3 Demonstration Bridge

A demonstration bridge is scheduled to be built and tested based on the results from the laboratory tests. The bridge is the one the transverse joint test design was based upon (Section 3.1.1). The objectives of this phase of research are to implement a full scale deck panel system on a real bridge and monitor its behavior under loading. This will include measuring deflections, panel strain, girder strain, and cracking in the deck surface. The design vehicle (HS-20) will be used to load the bridge and monitor its response. Upon completion of the tests, a comparison will be made with past research results.

The field test was designed based on the results of the laboratory testing. The design of the deck panel system, the documents for construction, and an instrumentation plan were created. The best performing joint, grout, and shear stud pocket were chosen for the bridge. Past research at Virginia Tech was used to choose the shear stud pocket spacing and composite design. The construction and testing of the bridge will be a future phase of the research.

3.3.1 Bridge Layout

A series of meetings with VDOT engineers laid out the parameters for the design. The original bridge plans were provided at the onset of the research. The agreement was that the researchers would provide recommendations and a suggested design. The final design decisions and preparation of construction documents would be the responsibility of the VDOT engineers. All changes to the girders or substructure were also the responsibility of the VDOT. The bridge was originally a three span, continuous, steel girder bridge located in Scott County Virginia on Route 65 (Figure 3-3). The VDOT engineers decided to redesign the girders for a composite six girder system (W21x83) spaced at 4.8 ft with a deck width of 30 ft 4 in. (Figure 3-2). The barrier curbs, slope on the deck, and crown followed the guidelines provided by VDOT (VDOT 2007b). The joint configurations were tested during the transverse joint investigation presented in Section 3.1.

The biggest difference between the laboratory and the final design of the test panels was the staged construction plan. Due to the importance of the bridge, it could not be completely taken out of service at any time. In order to keep one lane open, VDOT helped

produce a staged construction plan. The plan was devised to replace half of the bridge, while leaving the other half of the deck in service. Once the first half of the deck is replaced, it will be opened to traffic. Next, the second half of the deck would be closed to traffic and replaced. A longitudinal joint will exist between the two lanes that will need to be connected at the end of the staged construction (Figure 3-28).

The first step was to decide on the dimensions for the panels. The VDOT standard 8 in. deck thickness was used throughout. During construction, the optimum driving lane width per VDOT is 12 ft. However, with an available deck width of 30 ft 4 in. and the need for a two stage process, there was very limited space on the bridge. The barrier curbs and longitudinal joints reduced the available driving width. The maximum available driving width for the stage 1 deck was reduced to 10 ft. During stage 2 construction, the maximum available driving width was limited to 11 ft 9 in. The difference was due to the slightly wider replacement deck. The final panel widths were designed as 15 ft 2 in. for stage one and 14 ft 3 in. for stage two. As is shown in Figure 3-28, the bents will need to be widened to handle the larger spacing between girders. The staged construction layout is show in Figure 3-28. The final construction documents are in the Appendix A.1.

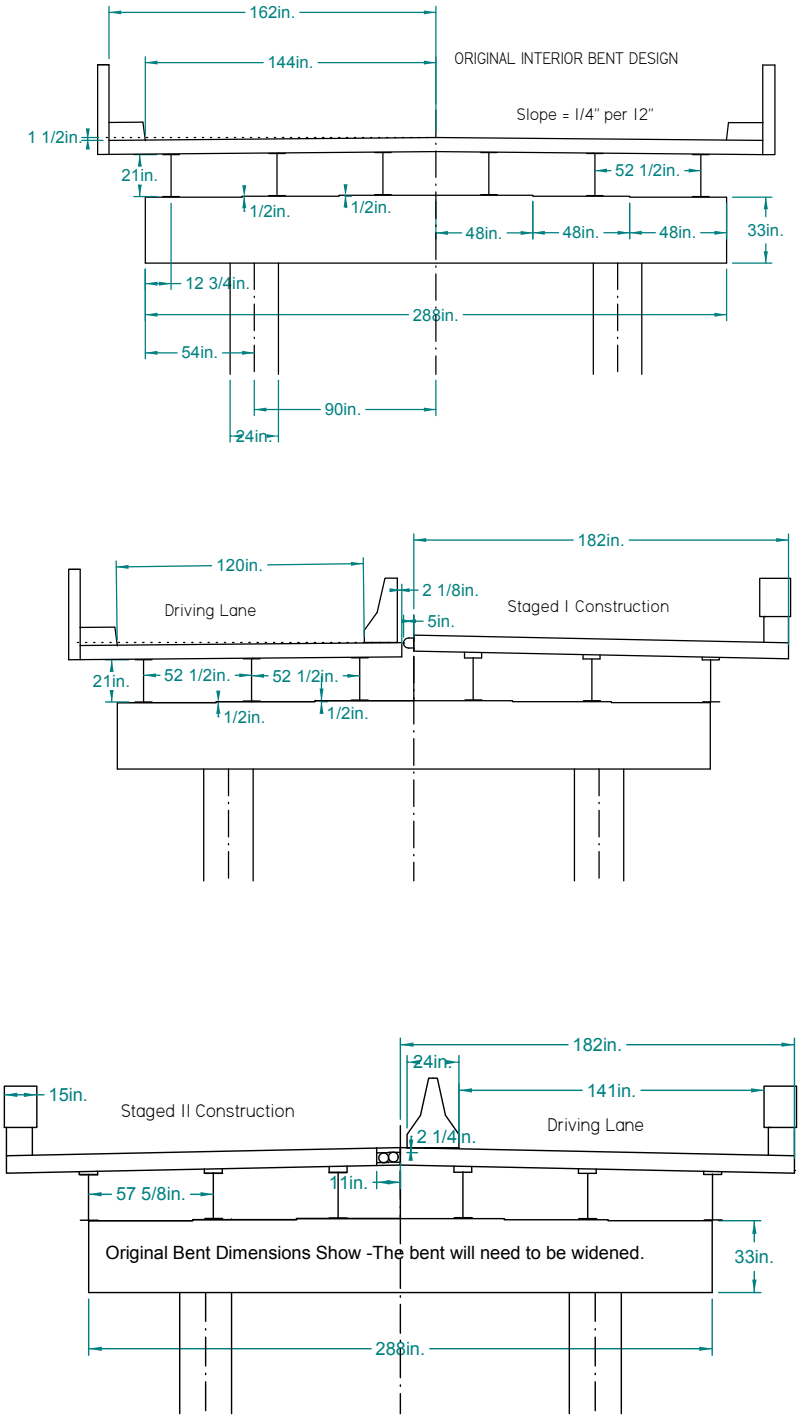

Figure 3-28 A) Original Bent B) Staged One Construction C) Staged Two Construction

The deck segments were designed so that when connected, they fit the desired bridge dimensions (Figure 3-28). Four unique panels were designed because of the geometry and staging on the bridge: Interior Stage one, Exterior Stage one, Interior Stage two, and Exterior Stage two (Figure 3-29). In addition an 11 in. looped bar longitudinal joint was used for the longitudinal construction joint (Figure 3-1). This decision was based on the results from the transverse joint tests and past research. The longitudinal joint will be placed between girders three and four in a region of positive moment. Traffic should create compressive forces in the top surface of the deck thereby preventing cracks from forming on the surface of the deck (Precast/Prestressed 2002). This joint will be built at the conclusion of stage two construction (Appendix A.10).

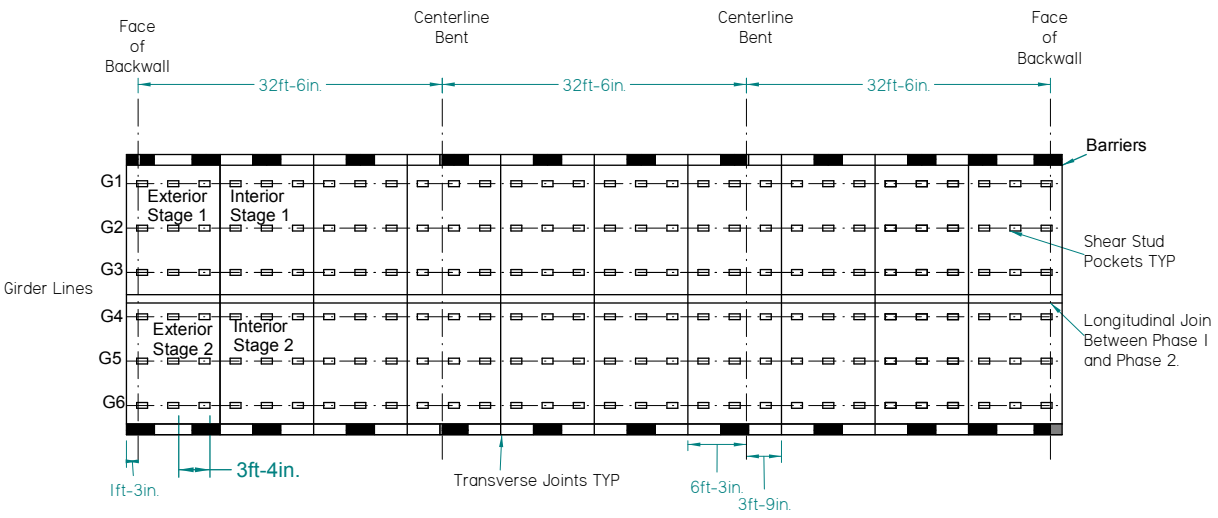

Figure 3-29 Plan View of the Proposed Final Bridge Deck Layout

The final step in the deck panel construction will be the application of an overlay. The joints and blockouts on the deck have a tendency to crack. An additional layer of protection provided by an overlay will help prevent surface water and chlorides from entering the joints. A number of possible materials should be considered including: asphalt, epoxy, and latex

modified concrete. The final decision for the surface treatment will be made by the VDOT engineers.

3.3.2 Panel Design

Once the layout was configured, the preliminary design of a post-tensioned connection was started based on the current VDOT Bridge Standards and the test results (VDOT 2007b). The transverse joint tests were designed based on the test bridge, as mentioned in Section 3.1. A final design was performed for the bridge system with the same methodologies. The decision to use post-tensioned joints was based on the superior performance of the panels stressed to 340 psi in the transverse joint tests. The preliminary drawings for each panel are included in Appendix A.1. The detailed calculations were included in Appendix A.2.

The basic steps for the panel design are outlined below.

1) Continuous deck analyses were performed in the transverse direction based on the girder spacing and design vehicle (HS-20). Three deck analyses were performed: Stage 1 panels, Stage 2 panels, and the full deck width. The worst case truck loading was applied to each geometry.
2) The maximum loads were factored and the slab was designed in the transverse direction using concentric prestressing strands. The stress limits in the Standard Specification were used in the design (AASHTO 2002). Additional mild steel was added in the cantilevered sections for the staged construction and final overhang.
3) The longitudinal joint was designed for the maximum factored load. The procedures for a cast-in-place concrete deck design were used from the Standard Specification. Steel was added on the top and bottom of the slab and spliced in the joint.
4) A continuous analysis of the superstructure in the longitudinal direction was performed based on the bent spacing. The worst case factored vehicle loads were used to design the deck in the critical locations.
5) The transverse joints over the bents were designed by doing a stress analysis of the deck for the post-tensioned joints. The maximum tensile stresses were kept less

than or equal to $6\sqrt{f'c}$ for the post-tensioned joints. Bowers model was used to check the losses in this deck (Bowers 2007).

The next phase of design was to make the system composite. A pocket spacing between 2 ft and 4 ft was preferred to speed up construction and replicate the lab tests. Past research showed that the limit could be extended from 2 ft to 4 ft (Section 2.3.3). The final shear pocket spacing of 3 ft – 4 in. was decided upon based on the results of the laboratory tests and the geometry of the bridge. The spacing was made as large as possible in order to test a spacing larger than 2 ft while keeping the spacing uniform throughout.

The shear studs were designed with the following procedure :

1) The moment and shear envelope was computed based on the longitudinal analysis along the bridge. The horizontal shear was computed along the bridge at tenth points based on the moment diagram.
2) The number of standard shear studs (7/8 in.) was determined along each girder line. The strength and fatigue design procedures in the AASHTO standard specification were followed (AASHTO 2002). The spacings allowed in the standard specifications were used as a guide to place the shear studs in the horizontal and transverse directions.
3) The shear studs were regrouped into standard pockets evenly spaced along the bridge deck. The shear studs were spaced as close together inside the pockets as allowed in the standard specification.

The shear stud pockets details and grout were chosen based on the results from the laboratory tests and placed in the construction documents. A Five Star Highway Patch grout used under the manufacturer's guidelines was specified because it performed satisfactorily in the laboratory tests. In order to test two surface preparation techniques, the stage one pockets were specified as epoxied and the stage two were specified exposed aggregate. A standard concrete epoxy will be applied to the pockets approximely 30 minutes prior to placing the grout

on stage one panels. In stage two panels, a retarder will be placed on the formwork around the shear pockets when creating the panels. Upon removal of the formwork (approximately 12-24 hours later), the concrete paste will be washed away to expose aggregates in the panels. A total of 90 pockets with each surface preparation technique will be built.

3.3.3 Cost of the Project

The initial information on cost and labor estimates needed for deck panels will be based on the laboratory tests. The cost and man hours for the test setup were recorded and provided to VDOT for their cost estimating (Appendix B.5). This information will also be used to compare the cost of the final VDOT bridge to the costs of the laboratory tests at Virginia Tech.

Projects are awarded through a competitive bid process for the state of Virginia. The researchers at Virginia Tech will be available to provide advice to VDOT and any contractors bidding on the project. Pre-bid meetings are an option, at the discretion of VDOT, to educate any contractors on the processes needed to build deck panels. The objective is to get the most competitive bid based on a thorough understanding of the deck panel system.

A comparison will be part of the future research project. The state of Virginia keeps detailed records of the public money spent on bridges. The future goal is to document and compare the price of a full depth bridge replacement with a traditional cast-in-place deck. The breakdown of the cost for this bridge will be recorded. In addition, typical costs for similar bridge replacement projects will be requested from VDOT. The information from these bridges should provide data for a cost comparison.

The last step will be to compare time savings on the project. The entire construction process will be carefully monitored and the construction times will be recorded. These values will be compared to typical construction times for cast-in-place bridge decks. A reduction in time may be used to show a reduction in delays to the users of the bridge.

3.3.4 Construction Monitoring

In order to gain a better understanding of how a real deck panel bridge is constructed, the processes will be carefully monitored. Many procedures currently used by researchers may

be less efficient than methods used by the construction industry. A comparison will be made to learn from contractors and further expedite deck panel construction.

The first phase will be to construct the panels. The contractor selected by VDOT will be responsible for acquiring the panels. Included in the contract documents will be provisions for the research team to instrument the panels and monitor construction. Approximately twenty panels will be constructed according to the construction documents provided to VDOT. The process of the making the panels will be closely monitored and the price will be recorded.

After making the panels they will be transported to the field. Field work will include placing the panels on the girders to the correct height, forming the joints and haunch, pouring the grout in the transverse joints and shear pockets, and post-tensioning the panels. Placing the panels in the field is the job of the contractor. The researchers will be available to make suggestions based on experience and to document methods used by the contractors. While the final result is the primary concern of this research, new construction methods are still of interest.

Particular attention will be paid to the materials used for formwork and the time needed to complete the task. Most formwork consists of pieces of plywood, tie rods, and steel angles. The method selected by the contractor will be documented and photographed.

Another area of interest will be the techniques used to grout the haunches. The material properties will be carefully analyzed and tested for strength and shrinkage. Additionally, the time needed to pour the grout, the difficulty preparing the shear stud pockets, the number of pours, time of each pour, and type of grout will be documented.

Any changes from the processes used in the testing procedure may be important deviations. Change orders or procedures that the contractor alters will be recorded. The decision to change the construction processes will not be made by the researchers, however comparisons will be made between any differences.

The transverse joints between the panels will be post-tensioned. The bridge is short enough to use strands the length of the deck. The procedures used to thread the strands through the panels, connect the ducts, and tension the strands will be observed. The list of the

elongations used by the contractor will be requested. The elongations will then be used to make comparisons between the design and real stress in the bridge.

3.3.5 Instrumentation Plan

The transverse edges of the panels over the bents and at the midpoint of the spans will have vibrating wire gauges. They will be inserted at the midpoint of the panel approximately 1 in. from the top surface (Figure 3-30). This will provide strain data at the maximum positive and negative moment regions. The location of the VWGs will be as shown in Figure 3-30. Any changes in strain between the panels will be recorded. Care will be taken to attach the wires to the gauges and protect the instruments during construction of the panels, transportation, and final assembly. This will be the responsibility of the researchers on the job site.

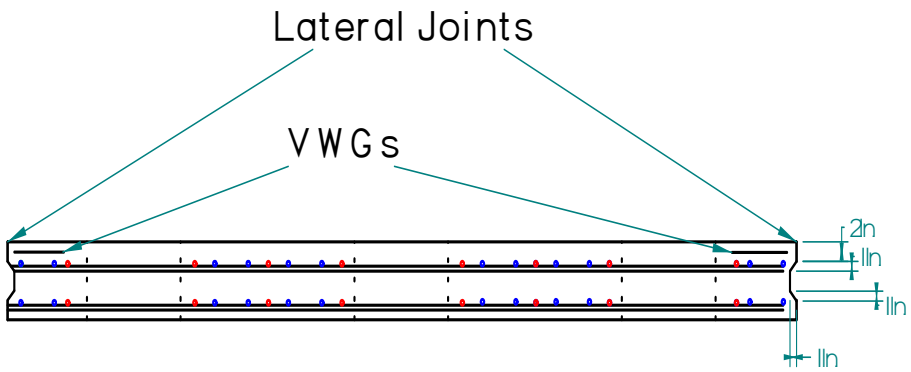

Figure 3-30 Elevation View of a Panel

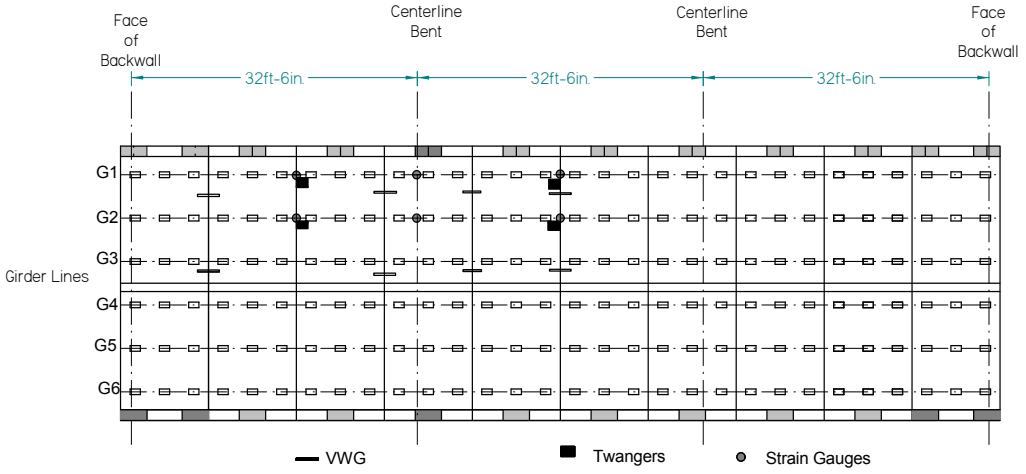

Figure 3-31 Instrumentation Plan

Strain gauges will be placed on the girders at the point of maximum positive moment and over the interior bents (Figure 3-31). At each point a gauge will be placed on at least one exterior and one interior girder on the top flange, bottom flange, and the middle of the web (Figure 3-32). These gauges will be located at an interior bent, at the middle of the center span, and at approximately 60% of the length of the exterior spans measured from the outer support. These are all critical locations for maximum moments in the bridge deck panels.

The gauges will be attached prior to placing the girders on the bridge. This will allow data to be taken from the very beginning of construction through the live load tests. Of particular interest will be any changes in strain during the post-tensioning of the panels and grouting of the haunches. A prediction of the losses in the post-tensioning system is very important. Any stress that is transferred between the deck and girders is of concern. This will also help determine if the finite element and analysis models are correctly predicting the stress levels in the system over time.

Deflections at midspan of the center girder and at the sixth point in the first and third girders will be measured with deflectometers (Twangers). Deflectometers will not measure long term deflections because they are fragile and would impede traffic. However, these

devices will measure the deflection of the superstructure at critical locations during the final live load tests.

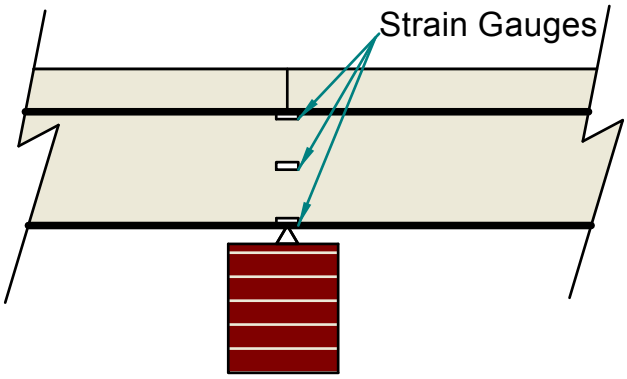

Figure 3-32 Strain Gauge Locations

3.3.6 Joint Tests

After constructing the bridge and prior to opening the bridge to traffic, a live load test will be performed on the bridge deck. Service load trucks will be driven across the bridge to test it under typical loading conditions. The test will consist of using a standard 25 ton dump truck, fully loaded, provided by VDOT. Parallel and tandem loading configurations will be used to put the bridge under a worst case load.

Data will be collected from all the instruments except the VWGs at a constant rate (approximately 1 per second) as the trucks move across the bridge. The VWGs will collect data once every 30 seconds or less depending on the physical limitations of the gauges. The VWGs and strain gauges on the girders will provide information on strains in the superstructure. In addition, the twangers will provide deflection measurements that can be compared to deflection estimates.

Cracking may occur in the deck, particularly in the transverse joints, longitudinal joint, or around the shear pockets. The best methods from the laboratory testing will be used for the design and construction, however cracking may still occur. Cracks should be very minimal but the area will be closely monitored after construction and during load tests. The first cracks in

the joints are most likely to occur during the first load test. Cracking in the shear stud pockets are most likely to occur during the first week after placement. If cracking does occur, then the location and size of the cracks will be measured. Crack gauges will be used if the cracks are at least 0.005 in. in width.

4 Analysis of Data

The results from the research program are broken down into two segments:

4.1 Transverse Joint Results

4.2 Grout Results

The results from the laboratory tests on the transverse joints are discussed first. The second discussion is on the results from the shear pockets in the transverse joint tests and the grouted ring tests. After reporting the physical modeling results, they are compared to the results from the finite element models (5 Finite Element Analysis).

4.1 Transverse Joint Results

Three test setups were built in sequence and improvements were made as needed during the construction process. The names of the three test setups were as follows:

1. **Reinforcing Joints (RC) – Embedded Reinforcing Bar**
   Looped Reinforcing Bar
2. **Post-tensioned Joints 1 (PT1) – Post-tensioned 167 psi**
   Post-tensioned Pea Gravel 167 psi
3. **Post-tensioned Joints 2 (PT2) – Post-tensioned 340 psi**
   Post-tensioned Epoxy 340 psi

The results of the transverse joint tests were four fold. First, the final designs are reported. The designs included the final effective stress level after short term losses for post-tensioning and the reinforcing bar layout for cast-in-place joints. Second, a list of recommended construction techniques was created. All of the main steps used to build the setup were documented along with the amount of time and human resources needed. The effectiveness of the various techniques was also observed. Third, the durability of the joints was measured through cracking and ponding observations. Lastly, the joints ability to provide continuity

between panels was documented. Strain profiles were computed at the transverse joints and deflections were measured.

4.1.1 Transverse Joint Design

Six unique transverse joints were designed as explained in Section 3.1.1. The final layout for the cast-in-place looped reinforcing bar joint and embedded reinforcing bar joint are shown in Appendix B.4. The joint girder composite section was designed for a factored moment of 587 k-ft, the moment over an interior bent on the Virginia bridge (Appendix B.3). The looped reinforcing bar joint, composite section had a design strength of 754 k-ft with looped #4 reinforcing bars spaced at 10 in. The embedded bar joint had a similar design strength of 735 k-ft with #6 reinforcing bars spaced at 18 in. The strengths were higher than expected due to the use of larger W shape than the design required. The strength calculations were done using the standard specification to meet the requirements of the VDOT. The details are provided in Appendix B.

A parametric study was done on the level of prestressing in a full depth precast panel system by Bowers (Bowers 2007). The result was a list of recommendations for stress levels in the panels. For a post-tensioned three span continuous girder system, a design value of 500 psi was recommended (Table 2-3).

In order to test the design method used for this stress recommendation, two stress levels were used on the two post-tensioned tests. The same stress design methods were used in the design of each panel. The goal was to design the first set of panels with the absolute minimum amount of stress needed. The panels were designed with the same maximum design service moment used for the cast-in-place joints (266 k-ft). The maximum allowable tensile stress permitted in the top of the concrete deck under the service load was 0.42 ksi. This was based on a tensile limit of $6\sqrt{f'c}$ (f'c in psi) using a design f'c value of 6000 psi. The estimate was conservative compared to the $7.5\sqrt{f'c}$ (f'c in psi) stress allowed in the ACI 318-08 design code ((ACI-318 2008) Section 18.3.3). The estimate was also conservative compared to the $0.24\sqrt{f'c}$ (f'c in ksi) stress allowed in the AASHTO LRFD design code ((AASHTO 2007) Section 5.4.2.6). The

assumption was that if enough prestressing force was placed in the panels, then the tensile stresses would remain low and cracking would be prevented.

The designed stress levels using Bower's model are shown in Table 4-1 for the Virginia demonstration bridge and the transverse joint panels. The columns in the tables are as follows:

1) Steel girder type analyzed
2) Girder spacing
3) Span length (center of support to center of support)
4) # of strands in the deck per girder line
5) Initial compression in the deck (negative is compression)

6- 8) Final deck compression from self equilibration over the design life (negative is compression)

9) Stress at the top of the deck due to restoring forces caused by interior bents
10) Stress at the top of the deck due to the HS-20 truck
11) Distribution factors computed from the AASHTO Standard Specification
12) Stress at the top of the deck due for one girder line (Column 10 * Column 11)
13) Final Stress in the top of the deck
    i) For the laboratory specimen (Column 5 + Column 12)
    ii) For the Demonstration Bridge (Column 6 + Column 9 + Column 12)
14) Tensile stress limit, $f_r = 6\sqrt{f'c}$

The first five columns compare the girder types, girder spacing, and number of strands per girder line for different deck designs on the demonstration and test bridges. Columns 6 - 8 in Table 4-1 show the anticipated final compressive stress in a simply supported span with no load. The losses in stress are due to the self equilibrating stresses that occur over time. These are due to the creep and shrinkage using the AASHTO LRFD loss methods over a 10,000 day design life (AASHTO 2007).

Column 9 is the stress due to the restoring force over an interior bent resulting from continuity in the bridge. For the demonstration bridge, an analysis was performed on the three span continuous bridge (Appendix A.3). The longitudinal analysis considered three supports as

rollers and one end support as a pin. A longitudinal analysis was done with the laboratory bridge but with the two girder system (7 ft. wide) and 18.2 ft cantilever test setup. A restoring force was only computed for the demonstration bridge because it was continuous. It would be created by the reaction on an interior bent. The restoring force was not included for the test setup because it was not continuous. The final value was computed for one girder line based on the distribution factor from the Standard Specification (column 12).

The final stress expected, column 13, is the sum of the initial effective stress, the stress induced by the restoring force, and the stress due to a live load (HS-20 vehicle). The final stress levels in the deck are compared with column 14, the maximum permissible tensile stress. The highlighted values are the two values tested in the laboratory specimens and the suggested design for the Virginia demonstration bridge.

The goal was to use a similar effective stress level in the laboratory setup and the final demonstration bridge design. All of these stress values for the continuous bridge were computed at the top surface of the deck. The first stress level selected in the laboratory bridge was for 2 strands per girder line. The final tensile stress with live loads was expected to be 0.42 ksi, the same value as the absolute limit. The second stress level selected in the laboratory bridge was for 4 strands per girderline. The final stress with live loads was expected to be 0.26 ksi, a value lower than the 0.42 ksi maximum tensile limit.

These values used in the laboratory bridges are highlighted. The lower stress level is a test of the absolute minimum amount suggested for the panels. The higher stress is similar to a system with 4 strands per girder line in the demonstration bridge.

It is noted that both values are less than Bower's parametric study recommendation (500 psi) because an exact analysis was performed for the test panels and the real bridge.

Table 4-1 Deck Stress Levels for a Simple and Continuous Span Bridge

					Simply Supported Bridge Analysis				Continuous Bridge Analysis – Interior Support					
					Initial Comp. in Deck (ksi)	Final Compression in the Deck			Tension in the Top of the Deck					
	Girder Type	Girder Spacing (ft)	Span Length (ft)	# Strands in Deck		Top (ksi)	Middle (ksi)	Bottom (ksi)	Stress Redistribution (ksi)	Live Load Stress (ksi)	Distribution Factor (DF)	LL Stress * DF	Final Stress (ksi)	Stress Limit 6√f'c (ksi)
Column #	1	2	3	4	5	6	7	8	9	10	11	12	13	14
Laboratory Bridge	W21x101	4.8	18.2	2	-0.164	-0.129	-0.066	-0.003		0.588	1.00	0.588	0.42	0.42
	W21x101	4.8	18.2	4	-0.328	-0.281	-0.207	-0.133		0.588	1.00	0.588	0.26	0.42
Demonstration (Virginia) Bridge	W21x83	4.8	32/32.5/32	2	-0.133	-0.138	-0.071	-0.003	0.169	0.862	0.437	0.301	0.33	0.42
	W21x83	4.8	32/32.5/32	4	-0.266	-0.268	-0.190	-0.112	0.194	0.865	0.437	0.302	0.23	0.42
	W21x83	4.8	32/32.5/32	6	-0.399	-0.394	-0.306	-0.219	0.218	0.863	0.437	0.301	0.13	0.42

4.1.2 Constructability Evaluation

The construction processes performed in the laboratory are listed at the beginning of this section in Table 4-2 and Table 4-3. A summary of all of the materials, man power, and time needed to perform each task is included. Following is more detailed information on unique processes used for precast panels. This includes the precast panel construction, forming, grouting, post-tensioning, and joint connections.

Each process performed in the laboratory is broken down into a quantity for the test bridge based on the model's dimensions and layout. The information in Table 4-2 and Table 4-3 was provided to the research sponsor, VDOT, for use in estimating the cost for the demonstration bridge project. The information may also be used by contractors who may bid on the future project. Given that the demonstration bridge will have a similar layout on a much larger scale, the quantity per square foot and installation rates per hour were included.

Table 4-2 Materials Used in the Transverse Joint Construction

Test Bridges ***7 ft wide by 18.2 ft long by 8 in. deep*** ***2 – W21x101 Girder Lines***			
Lab Materials	**Quantities**	**Description**	**Quantity/ft^2**
Grout (5 Star Hwy Patch)		50 lb Bags	0.32 (Post-Tensioned Option)
Post Tensioned Joint	**6**		
Pea Gravel Extended Post Tensioned Joint	**3**		
Looped Joint	**10**		
Embedded bar Joint	**7**		
Ducts	**4**		
Haunches	**23**		
Strands (Oversized)	**8**	½" x 32' Grade 270	0.06
Formwork	**1**	½" x 8' x 4' Sheet of Plywood	0.01
	3	2" x 2" x 8' sawn lumber	0.02
	72	¼" washer/nut sets	0.57
	36	Feet - ¼" threaded rod	0.29
B-14 Coil Leveling Bolts	**9**	¾" x 14"	0.07
Haunch Material	**72**	Feet - ½" x 3 ½" fiber formwork	0.57
Shear Studs	**96**	7/8" x 5 ½"	0.76
Ferrules	**96**	7/8"	0.76

Table 4-3 Man Power to Build the Post-Tensioned Test Bridges

	Procedures				
Construction Process	Details	Manpower *(People)*	Time *(Hours)*	Installation Rate *Units*	
Girder Installation	Installing Haunch Fiberboard	1	3	12.00	ft/hour
Transverse Joint	Making Joint Formwork	2	4	3.50	ft/hour
	Placing Panels	3	3	1.00	Panel/Hour
	Placing Joint Formwork	3	2	7.00	ft/hour
	Making Haunch Formwork	1	3	1.33	Form/Hour
	Installing Haunch Formwork	1	1	0.25	Form/Hour
	Joint Grout	6	1	14.00	ft/hour
	Formwork Removal	1	1	---	
Post-Tensioning (4 Strands/Girder Line Option)	Installing Tendons or Rebar	2	1	144.00	ft/hour
	Stressing Tendons	3	6	1.33	Tendons/hour
	Grouting Ducts	5	1	36.00	ft/hour
Composite Action	Shear Studs	2	3	32.00	studs/hour
	Cleaning Haunches	2	1	36.00	ft/hour
	Grouting Haunches	7	2	18.00	ft/hour
Panel Support Release	Removing Leveling Bolts	1	1	9.00	bolts/hour

The materials came from a variety of distributors. The formwork and fiber forming material were acquired from a local lumber yard. The strands came from the precast panel manufacturer. The grout, leveling bolts, shear studs, and ferrules required special order because of their limited availability in southwest Virginia. The grout was the hardest material to acquire and required very careful storage to prevent contact with water.

The only additional materials required for the post-tensioning joint versus the cast-in-place joints were the strands and grout inside the strand duct. The ducts required an additional 4 bags of grout. In comparison the embedded bar and looped joints required an additional 1 and 4 bags of grout, respectively, above the amount required for post-tensioned joints.

The most time consuming processes were making and installing the formwork and stressing the tendons. The formwork was installed on all types of joints and took approximately the same amount of time for all types of joints. Post-tensioning (4 strands per girder line) took approximately 11 additional hours to stress the tendons, form and grout the joints, and grout the ducts. The cast-in-place joints only required one continuous pour thereby saving time. The installation of the reinforcing bars did not take any significant additional time over installing the post-tensioned strands (not including stressing).

4.1.2.1 Observations when Constructing the Panels

The precast panels were built by The Shockey Precast Group in Winchester, Virginia. They were selected because of their close proximity to the testing lab and experience making prestressed panels. The panels were fabricated on two different days: the first two sets of panels (RC and PT1) were built in April 2007 and the second set was built (PT2) in December 2007. The list of materials and drawings are shown in B.4 B.4 Construction Drawings for the Test Panels. The material data is provided in Appendix B.1. The precaster followed the drawings on everything except the anchoring steel in the post-tensioned panels (Figure 4-1).

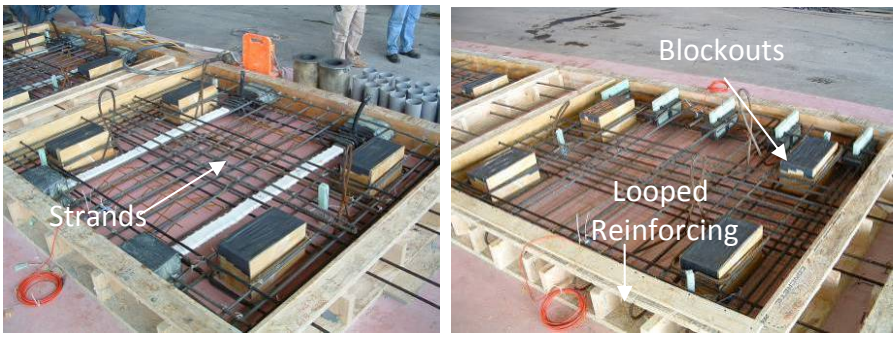

Figure 4-1 Forming the Panels at the Precast Plant

Observations at the precast plant were documented to help with future projects. The employees at Shockey mentioned that the formwork, pre-stressing strands and reinforcing bars were not hard to install. The difficulties started with the post-

tensioning anchor assembly. Instead of using looped reinforcing anchorage reinforcing as designed, hairpin bars were preferred and substituted in the post-tensioned panels.

There were also comments by the precasters on the difficulty of placing the HSS sections and post-tensioning ducts at the right location in the panels. The HSS sections were 4 in. by 4 in. x 12 in. long and spaced at 18 in. throughout. The weight of the steel made the sections hard to stabilize in the formwork. The ductwork was very flexible and was hard to keep at the correct elevation.

The leveling bolt assemblies and HSS sections needed a blockout above the assembly to install the bolts on the job site. Styrofoam was initially used on the first set of panels. The Styrofoam above the HSS sections and leveling bolts was very difficult to remove. On the last set of panels, PT2, a 1 in. diameter PVC pipe was used for the leveling bolt blockouts. The pipe provided a better quality product, kept the blockouts vertical and the same dimension, and was easier to install.

The water stops for the last set of panels, PT2, were built by the researchers and given to Shockey to install. Shockey had no problems installing the blockouts but the workers did comment on the complexity and challenge to build a large number of these assemblies. In general, when pieces had to be suspended in the formwork (ductwork, water stops, HSS Assembly), the complexity increased and created problems (Figure 4-2).

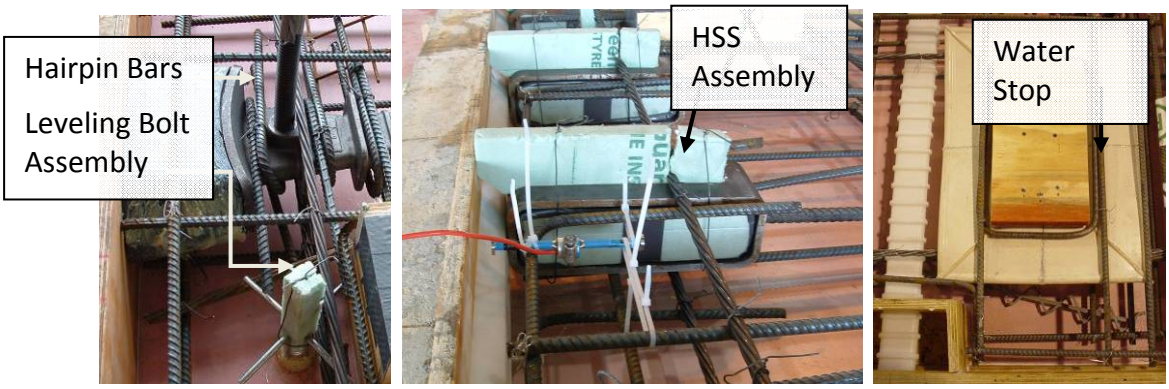

Figure 4-2 Difficulties Forming Precast Parts

Additional observations were made on the efficiency of the operation. It was clear that a lot of strand and additional bed space was wasted on these panels. About 40 ft of bed length was used on the first pour and about half of that on the second pour. The beds were hundreds of feet long. The Shockey engineers commented that on a real project the cost and efficiency could clearly be improved.

4.1.2.2 Setting the Girders and Forming the Haunches

Each girder was placed on three support points: the roller in the middle and the temporary support beams on each end. Temporary steel angles were clamped to the flanges of each girder for stability during construction. The top surfaces of the girders were cleaned with a grinder and washed prior to placing the haunch formwork (Figure 4-3).

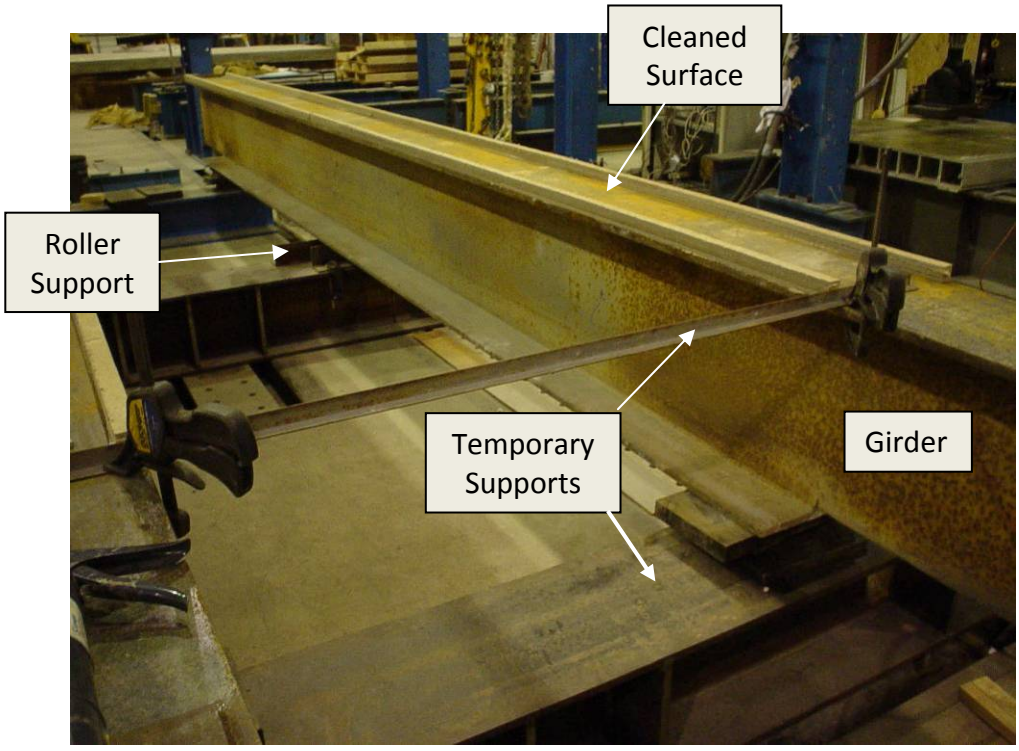

Figure 4-3 Construction of the Girder Assembly

Two types of haunch formwork were used on the initial setup. The first was a fiber forming board made of recycled paper fiber produced by the Homasote Company. The second was the 1.5 in. cold formed steel angles tied transversely together with 0.25 in. threaded rods. A 1½ in. think haunch was used throughout (Figure 4-4).

Figure 4-4 Fiber Formwork and Steel Angle Formwork

The fiber board worked best for the haunch formwork. Cutting, gluing, and placing the fiber formwork was easy and quick. In addition, the material could be cut to height and it was advertised as biodegradable. The cold-formed steel angles provided a good seal, however they were hard to align. Placing the tie rods between the angles took additional time and the angles were difficult to align. The angles did not provide much flexibility with haunch heights unless the angles were cut or bent. In general, this process was harder to construct but took about the same amount of time to setup as the fiber formwork.

4.1.2.3 Setting Panels and Forming Transverse Joints

Upon arrival at the lab, the first problem was observed on the panels. The Styrofoam used as blockouts for the HSS sections and the leveling bolts did not work well. In every location, the Styrofoam was extremely difficult to remove and the tolerances for the leveling bolts were significantly off. Many of the leveling bolt locations had to be adjusted with a hand held concrete hammer drill (Figure 4-5). The HSS sections did not have any concrete inside, however the Styrofoam and duct tape

were hard to remove. A chisel and a propane torch were used to remove the Styrofoam (Figure 4-6). In the future, the leveling bolt assembly should be used with pvc pipe at the blockouts. The HSS sections should be blocked out with a different material that is easier to remove. A possible option would be to tape around the exterior of the assembly.

Figure 4-5 Blockouts Around the Leveling Bolt Assemblies.

Figure 4-6 Removing the Styrofoam from the HSS Anchorage Assemblies.

Placing the panels was not difficult with the looped reinforcing bar or post-tensioned joints but was challenging on the embedded bar joints. The embedded bar assemblies were difficult to line up. On the test panel only two of the five embedded holes lined up directly across from one another. The other pieces of rebar were forced in the joints and were not perpendicular to the joint after placement (Figure 4-7). From

a construction standpoint, this joint needs bigger tolerances between the rebar and the embedment.

The post-tensioning joints lined up well and the panels were easy to set into place. A few extra minutes were needed to tape each duct together in the blockout regions. Typically, the duct had to be lined up by hand and then taped but the process worked effectively (Figure 4-7).

The looped reinforcing bars with the looped connecting bar were easy to place. This joint took a little more time because the bars had to be tied together at a 6 in. spacing throughout. However, there was ample space to place the rebar and tie it by hand (Figure 4-7).

The leveling bolts were used effectively to obtain the correct panel elevation. A problem arose with the panels twisting as the bolts were adjusted. Movement would likely be reduced if the panels were full size and had more dead weight to hold them in place. Regardless, the movements were only about ½ in. in any direction and could be alleviated by placing shims between the panels.

Figure 4-7 Placing the Panels: Post-Tensioning, Looped Bars, Embedded Bars

All of the transverse joints except the looped bar joint were formed with ½ in. plywood and ¼ in. threaded rods. Typically, the formwork was held in place with 2 in. by 2 in. pieces of wood on top of the joint and threaded rods (Figure 4-8). On the looped bar joint, a 1 in. by 1 in. steel angle was used to hold the bottom formwork. The

angles were used to form the joint without leaving holes in the top surface of the transverse joint. The angle was placed through the looped bars on each side of the joint (Figure 4-8). All of these forming techniques worked as expected and kept the grout from leaking out of the formwork. The angles worked especially well because they left no holes in the surface of the panels.

After grout was placed in the haunches, the leveling bolts were removed from the panels. Typically this was done twenty-four hours after finishing the grout. The bolts came out easily by hand with a crescent wrench. The holes that remained were not filled with grout after removing the bolts, although this would be done in the field.

Figure 4-8 Joint Forming Methods: with Steel Angles and with Wood

During the first pour in post-tensioned transverse joints, a barrier was added between the joint and the haunches. This was required to prevent the grout from entering the haunch space (Figure 4-9). Two different methods were used to form the haunches. Both methods required the removal of the barrier after the grout cured and prior to post-tensioning the panels.

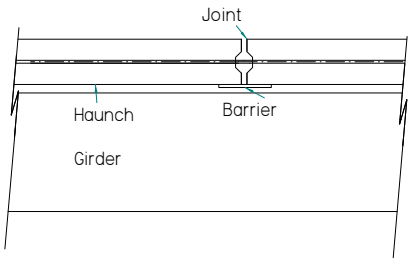

Figure 4-9 Elevation View of the Joint and Formwork Prior to Post-tensioning

The first barrier was built by placing a piece of plywood in the haunch on top of a layer of fiber forming material. The second method was designed with the same type of plywood with wedges inside the haunches to hold the plywood in place (Figure 4-10). Both methods worked and limited grout from flowing into the haunch. The second method had a tighter bond around the edges of the joint but the performance was not greatly improved. However, the second method was easier to remove. The wedges were pried out of the shear pocket and the formwork was slid out of the haunch. The first method also required pulling the plywood out of the haunch but the force and time required both increased.

Figure 4-10 Forming for the Transverse Joints Inside the Haunches.

In this test setup, the haunch formwork was already in place so the formwork for the joints had to be removed through the haunch. An alternative idea would be to place the haunch formwork after this process; however, this seemed less efficient in the field.

Placing the haunch formwork later would require access beneath the panels and might increase the work and cost.

4.1.2.4 Placing Shear Studs and Grouting

Grout was placed in the shear stud pockets after the shear studs were welded in the pockets. The pockets had been designed to be as small as allowed by the design code and only provided a couple inches of space between the shear studs and the walls of the pocket (Figure 4-11). The process of welding 96 shear studs took approximately one hour for one experienced welder. The welder commented that the process was not overly difficult. Cleaning the ferrules out of the pockets was the most difficult part after welding the studs. A hand pick was used to break the ferrules off of the studs and a vacuum was used to remove the pieces. The entire process appeared similar to standard bridge welding operations.

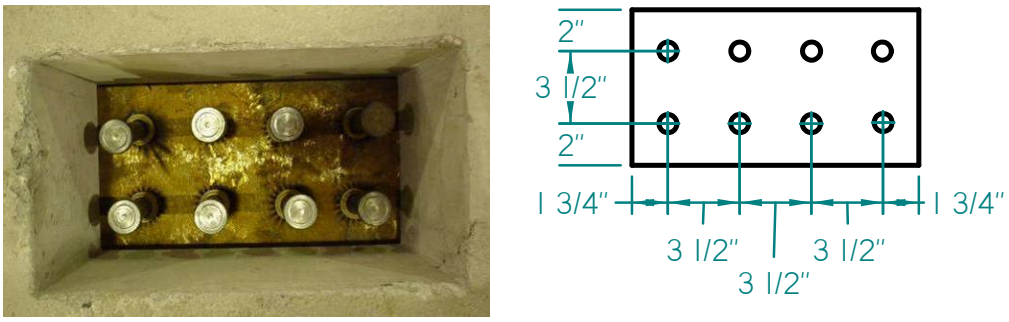

Figure 4-11 Layout of Shear Studs in a Pocket

The first grouting procedure was on the specimen with the reinforced joints. The joints, haunches, and shear stud pockets were all grouted together due to the lack of post-tensioning. This grouting on the cast-in-place joints was the largest grout pour of the test program because it encompassed the entire bridge. The Five-Star Highway grout was very workable for approximately ten minutes. Twenty minutes after mixing, the grout reached an initial set. The maximum amount of water recommended by the manufacturer (3 quarts per 50 pounds of grout) was used for the desired flow characteristics. Forty bags of grout were used within 75 minutes to fill all of the spaces.

The embedded reinforcing bar joint was a problem because of the tight space inside the HSS section. A pencil vibrator was used extensively to force grout into the crevices of the HSS section.

Grouting the second and third sets of test panels, Post Tensioned Joints 1 & 2, required more time because of multiple grout pours. The joints between the panels were filled with grout first. The grout was mixed with the maximum amount of allowable water (3 quarts per 50 pounds of grout) and then poured into one end of the joint. Once the end of the joint began to fill, the adjacent section of the joint was filled. This continued until the joint was completely full. Filling the joints was very easy and less messy because they were easy to access and required a small amount of grout.

One of the four post-tensioned joints had pea gravel added to the grout (extended grout). Thirty-Five pounds of a $^{3}/_{8}$ in. maximum size river pea gravel was added per the instructions of the grout manufacturer. This almost doubled the output of grout per bag. About $3\text{-}^{1}/_{3}$ quarts of water were added to each mix instead of the recommended maximum 3 quarts. This decision was made because workability suffered from the dry aggregate. The aggregate tended to segregate in the wheel barrow. Care was taken to mix the grout in the wheel barrow to solve the segregation problem. Overall, using pea gravel was not significantly more difficult.

One of the four post-tensioned joints had an epoxy placed on the panel joints prior to pouring the grout in the transverse joint. The epoxy was mixed and placed on the face of the concrete joint with a paint brush approximately 30 minutes prior to pouring the grout. The epoxy was slightly “tacky” to the touch once the grout was poured, as instructed by the manufacturer DAP. This took careful coordination because the epoxy could not set up prior to pouring the grout.

The second grouting for the post-tensioned decks occurred after the joints were poured, the formwork was removed, and the tendons were stressed. The same grout mix was used in the post-tensioning ducts. This would not be done on a real bridge because special grout formulations are made for filling ducts. Using the same grout was convenient and effective for creating a bond in the duct. The 5-Star Highway Patch

grout was mixed with 3 quarts of water, the maximum amount allowed. The process started slow but became much easier with experience. The pump used for these ducts is shown in Figure 4-12. A small hand pump like this one worked effectively to create a bond between the grout and duct. In a real deck panel project industrial grade, electric pumps would be used.

On the first duct, the grout would not flow into the tube. This was attributed to using too little water in the mix and not properly prepping the mixer with water. Grout was pumped into the tube until it flowed out the exit tube on the opposite end. A very liquid grout was observed coming out of the dead end of the strand assembly while pumping the grout. Expanding insulation foam was added around the ends of the duct to keep grout from leaking out around the strands and anchors (Figure 4-12). Once the grout and water started to come out of the anchor assembly, pumping ceased. Typically, grout sprayed out of the tube after removing the pump because the system was under pressure. Experience taught the team to plug the hole after removing the tube.

A) Expansion Foam at the End of the Post-Tensioned Ducts B) Pump Used for the Grout in the Ducts.

Figure 4-12 Grouting the Ducts

The objective of the last pour on the post-tensioned decks was to fill the haunches and shear pockets. This process went very smoothly, mainly due to the experience of the workers. First, the shear studs were welded to the top of the girder

through the shear pockets. This was done the same way as for the cast-in-place jointed deck panels. Like the previous haunch grout pour, grout was placed along each girder line starting at one end. After a pocket was full, the next pocket in line was filled. Grout flowed out of the pockets into the haunch. The flow of the grout was monitored through the shear pockets (Figure 4-13). Generally, a vibrator was not required to consolidate the grout, however on a couple dry mixes a pencil vibrator was temporarily used.

A) Filling the Shear Pockets

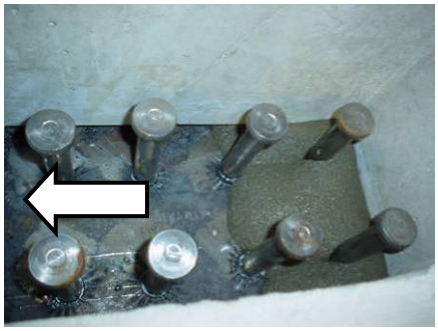

B) Grout Flowing Through the Haunch

Figure 4-13 Grouting the Haunch and Pockets

Overall, the grouting process was not difficult if the crew had experience. The biggest problem was the set time of the grout. Having a sufficiently large crew to mix, pour, finish, vibrate and make cubes was essential. Table 4-4 shows the standard mix proportions used in each grout pour, the respective strengths of the grout, and the conditions at the time of the pour. More information is available in Appendix B.

Table 4-4 Grouting Information

Grout Pour*	Ambient Conditions	Mix Proportions**	Grout Strengths – First Day of Testing
Embedded and Looped Reinforcing Bar Panels	Afternoon - Clear, Low 60's,	2 1/3 Quarts / 50 lb Bag	4640 psi
PT Joint – 167 psi	Afternoon – Partly Cloudy, Low 80's, Low humidity	2 1/3 Quarts / 50 lb Bag	3970 psi
PT Pea Gravel Joint – 167 psi	Afternoon – Partly Cloudy, Low 80's, Low humidity	3 1/3 Quarts / 50 lb Bag	4700 psi
PT Joint – 167 psi – Ducts	Noon – Sunny, Low 70's, Low humidity	3 Quarts / 50 lb Bag	4230 psi
PT Joint – 167 psi – Haunches /Pockets	Late Morning – Cloudy, 70's	3 Quarts / 50 lb Bag	6550 psi
PT Joint – 340 psi – Joints***	Mid-afternoon – Sunny 45 Outside, 65 Inside	3 Quarts / 50 lb Bag	5360 psi
PT Joint – 340 psi – Ducts***	Early-Afternoon – 50 Outside, 71 Inside	3 Quarts / 50 lb Bag	5170 psi
PT Joint – 340 psi Haunches /Pockets***	Afternoon – Low 60s Outside – Rain, Low 70s Inside	3 Quarts / 50 lb Bag	4800 psi

*PT = Post-Tensioned Panels
**The maximum recommended dosage was 3 Quarts / 50 lb Bag
***Same Brand of Grout but a different order from the supplier

No special curing process was used for the grout. A tarp was draped over the panels for the first twenty-four hours but no additional moisture was added to the system. The heat of hydration was very high for first few hours after the grout was placed and the strength gain was fast. By the second day there was no apparent difference in temperature between the surface of the grout and the adjoining panels. The biggest difference between the grout pours was the ambient temperature. As seen

in Table 4-4, the temperature varied greatly from the summer pours to the winter pours.

The strengths varied among the grouts even though the mix proportions and brand remained relatively constant. Some of the variation may have been due to two different batches (from two different orders) of patch grout. The grout was the same brand, Five Star Highway Patch, however minor deviations within a brand could have caused some variation. The supplier, brand, and storage conditions all remained constant for the test bridges.

Grout strength was the primary concern during the joint construction. The strength of 4000 psi was desired for the joint grout before stressing the tendons. The first post-tensioned neat grout was a few psi low, but the remainder of the joint grouts met the requirement. The strengths all reached 4000 psi prior to testing the system.

4.1.2.5 Post Tensioning

4.1.2.5.1 Post Tensioning Construction

The last four transverse joints were longitudinally post-tensioned. In the first post-tensioned deck, two strands were used per duct. This amounted to a total of four strands in the seven foot wide bridge deck or two per girder line. The second post-tensioned deck was the same width but four strands were placed in each duct. Oversized (super) ½ in. strands were used throughout (Figure 4-14). Threading the strands through the ducts was very easy and only took one person a few minutes per strand.

Figure 4-14 Strand Layouts in the First and Second Post-Tensioned Tests

The steel strands were stressed by placing an actuator against a stressing chair. The stressing chair was placed around the anchor assembly and against the end of the panels. The anchor assembly was then accessible for aligning and anchoring the strands (Figure 4-15). The assembly was easy to use, especially after gaining experience. Two people were needed: one to hold the assembly in place and another to apply the load and monitor the gauges. The hardest part was properly seating the chucks in the anchor. A hammer was used to push them into the anchor as far as possible to reduce seating losses. Stressing alternated between strands in each duct. This required more work to move the stressing chair and actuator to a different duct for each strand.

Figure 4-15 Stressing Assembly

Once stressing began, the elongation and load applied to the strands were carefully monitored. A load cell was placed on the live end of each strand when the load was applied. Measurements were made of the strand elongation at 5 kips intervals up to the maximum jacking force of 32 kips. This corresponded to 70% of the ultimate strength of the strand ($0.70*f_{pu}$).

One load cell was on the dead end of the first strand placed in each duct. The load cells on the dead ends of the strands provided an estimate of any elastic shortening

losses in the system. The biggest problem was preventing damage to the dead end load cells. This occurred twice during stressing and data was lost each time.

Measurements were kept on the movement of the chucks on the live end after release. This provided a good estimate of the seating losses after the live load cell was released. No data was taken on the chucks on the dead end. They were assumed seated prior to release.

For comparison during stressing, elongation measurements were estimated for the loads applied to the strand based on elastic deformation equations (Appendix B). Seating losses, elastic shortening losses, and friction losses were included in the estimate. Long term creep, shrinkage, and relaxation losses were considered but not measured. They made a negligible difference because testing was scheduled to begin immediately after construction.

4.1.2.5.2 Post Tensioning Force Applied

Calculations were made of the expected losses in the strands during the stressing process and then compared to the actual values (Appendix B.2). The strands were straight and 19 ft long, so friction and wobble losses were very small. On the first two strands in each setup, a load cell was used on the dead and live ends (Figure 4-16). The ultimate jacking force of 32 kips was measured on both the dead and live end of the strands indicating little friction and wobble losses.

Seating losses were the largest losses because of the short length of the deck (18.2 ft). The first strand had a seating loss of 6 kips because the chucks did not seat well in the anchoring device. As the workers gained experience, the seating losses on future strands were limited to 2-3 kips.

Elastic shortening losses were computed based on the stressing sequence of the strands. The losses averaged about 1 kip per strand. The biggest losses were measured on the stressing of the first two stands. Subsequent strands had smaller elastic shortening losses.

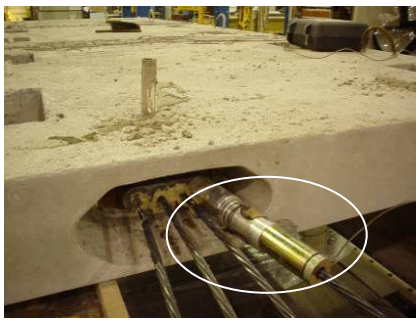

Figure 4-16 Load Cells on the Deck.

Table 4-5 shows the average stress level in each strand at the end of the stressing process in the assembly with two strands per girder (PT1). The measured losses are in Appendix B. Each of these joints was initially stressed to approximately 32 kips with four ½ in. diameter oversized strands (A_s = 0.167 in^2). Seating, elastic shortening, and wobble losses were taken into consideration during the stressing process. The average seating loss was about 1.94 kips or 0.11 in. of movement based on measured movement of the anchors. Elastic shortening values were estimated based on the change in force in the load cells on the dead end of the strand. The friction and wobble losses were estimated based on the difference in force in the live and dead end load cells of the first two stressed strands. The final stress level computed in the panels was 167 psi at the end of the stressing process. The values in Table 4-5 were all computed based on the values recorded from the load cells and chucks during stressing.

Table 4-5 Stress Levels in the PT1 Setup

	Final Force (kips)	Stress (ksi)	Percent f_{pu}
Strand 1	25.3	152	56.2
Strand 2	28.0	168	62.2
Strand 3	29.6	178	65.8
Strand 4	28.8	173	64.0
Slab	111.9	0.167	

Table 4-6 shows the average stress level in each strand at the end of the stressing process for the assembly with four strands per girder line (PT2). The measured losses are in Appendix B. Each of the eight ½ in. diameter oversized strands was stressed to 32 kips (A_s = 0.167 in^2). Seating, elastic shortening, and wobble losses were taken into consideration during the stressing process. The seating loss on average was about 3.0 kips or 0.17 in. of movement. Elastic shortening values were estimated based on the change in force in the load cells on the dead end of the strand. The friction and wobble losses were estimated based on the difference in force in the live and dead end load cells of the first two stressed strands. The final stress level in the panels was 340 psi at the end of the stressing process. The values in Table 4-6 were all computed based on the values recorded from the load cells and chucks during stressing.

Table 4-6 Stress Levels in the PT2 Setup

	Final Force	Stress (ksi)	% f_{pu}
Strand 1	27.4	164	60.7
Strand 2	27.1	162	60.1
Strand 3	27.0	161	59.8
Strand 4	31.3	187	69.3
Strand 5	29.0	174	64.3
Strand 6	28.9	173	64.1
Strand 7	29.8	179	66.2
Strand 8	28.2	169	62.5
Slab	229	0.340	

The final effective stresses on each joint were very close to the design values. The initial design value for the two strand per girder line system was 0.164 ksi and the measured value after immediate losses was 0.167 ksi. The initial value for the four strand per girder line system was designed as 0.328 ksi and built with 0.340 ksi. The actual values were slightly higher but reasonably close. In comparing the design values to the actual values, the seating losses were slightly higher than expected but the elastic shortening losses were smaller. The friction and wobble losses were very small as expected. Obtaining the design level was much easier on the second bridge once the construction team had experience.

The VWGs in the second set of post-tensioned joints were monitored during construction and prior to the load tests. The strain ranges in the 0.340 ksi stressed panels across all four VWGS were measured to observe what happens in the early stages of the panels prior to the service life of the deck. This included 53 days, the time between making the deck composite and applying the first load test. Figure 4-17 shows the change in strain of the VWG on the exterior side of the post-tensioned joint. The other VWGs displayed similar trends.

Construction of the panels took place from January 18th to February 5th. The strain increased after the grout was placed in the two transverse joints by about 70 microstrain on average. The panels were not connected to the girders, however friction between the girder and panels may have created some of this compression stress. When the grout was initially poured, it has a tendency to expand. This expansion along with friction may have created the compressive force.

After 10 days of setting the strands were stressed over a 2 day period. The increase in strain over this two day period was 82.3 με. Based on the measured force applied and the strength of the panels, the expected strain was 70.5 με. The difference between measured and predicted strain was 14%. The strands were then grouted the last day of stressing, January 28th.

By the end of grouting the strands, VWG 1 read about 130 microstrain in compression. This continued to increase to about 150 microstrain in compression for the next eight days. On February 5th the haunches and pockets were grouted. At this point the system was composite. After the last grouting procedure the system sat in the laboratory for 53 days. Over this period the strain increased by about 50 microstrain at all VWGs. The final value in VWG1 was about 200 microstrain.

The continued increase in strain in the panels was not expected after the bridge was made composite. In particular, the 50-70 microstrain of compression that occurred during the 53 days prior to testing was unusual. Initially, the assumption was made that the tests would commence prior to significant shrinkage and creep effects. According to the design model, the top of the deck panels should have lost approximately 5% of the

effective compressive stress (340 psi to 312 psi) during the 53 days of waiting. Instead, a net gain of 25% strain was recorded by the VWGs. It should be noted that the load strain was being recorded and compared here. The actual strain, which included temperature effects, was about 9% different during the 53 days prior to testing.

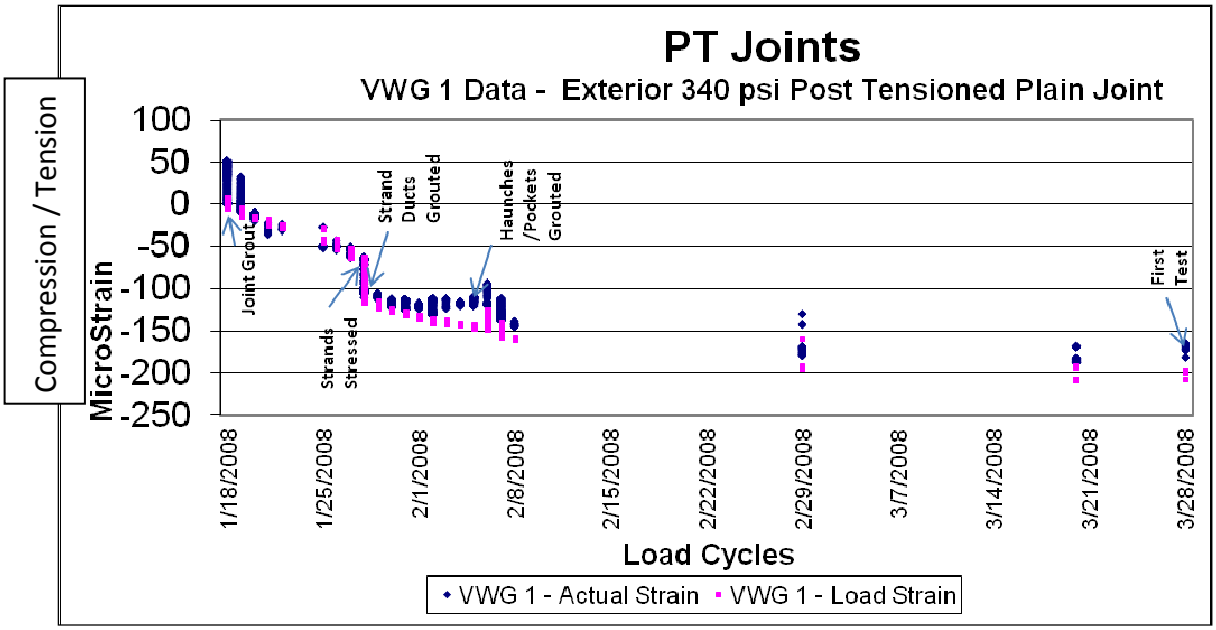

Figure 4-17 Panel Strain Prior to Testing for the 340 psi Post-tensioned Joint with Epoxy.

4.1.3 Cracking in the Transverse Joints

The cracks in the deck were measured from the day after pouring the grout to the end of the cyclical tests. The size and location of cracks were measured at key points in the test. This included cracks that appeared prior to loading, during the first load cycle, and at the end of the cyclical tests. A comparison was made among the different types and sizes of cracks that appeared during the transverse joint tests.

4.1.3.1 First Cracking

4.1.3.1.1 Shrinkage Cracks

The cyclical loading was started shortly after placing the grout in the deck panels. The time between the first loading and the grouting of the transverse joints was 7 days

for the cast-in-place joints, 28 days for the 167 psi post-tensioned joint, and 71 days for the 340 psi post-tensioned joint. These times were not predetermined but were used because of construction timing and lab accessibility. During these interim periods, the joints were visually monitored for cracking on the exterior surfaces.

The longer the joints set before testing, the more they shrank. The first test with cast-in-place joints did not exhibit any visible cracks during the period before testing. They only set for one week before testing began.

The first set of post-tensioned joints set for 28 days and had a few minor hairline cracks in the grout only joint. The cracking occurred on the top surface of two of the post-tensioning blockout corners and on the overhang of the joint at the concrete-grout interface. The joint with a pea gravel extension did not exhibit any initial cracking.

The last set of post-tensioned joints sat for over 2 months and cracked the most. The epoxied joint had a crack longitudinally through both of the post-tensioned blockouts on the top and bottom surface. There were also cracks on the bottom of the joint near the threaded rods used on the formwork. The normal grout had shrinkage cracks throughout the joint at the concrete-grout interface (Figure 4-18).

Shrinkage cracking was a problem in the transverse joints in these tests. The joints that cracked the most were the ones that sat the longest. The lack or presence of post-tensioning stress in the deck did not alleviate the problem. The joint with the highest stress, sat the longest and cracked the most.

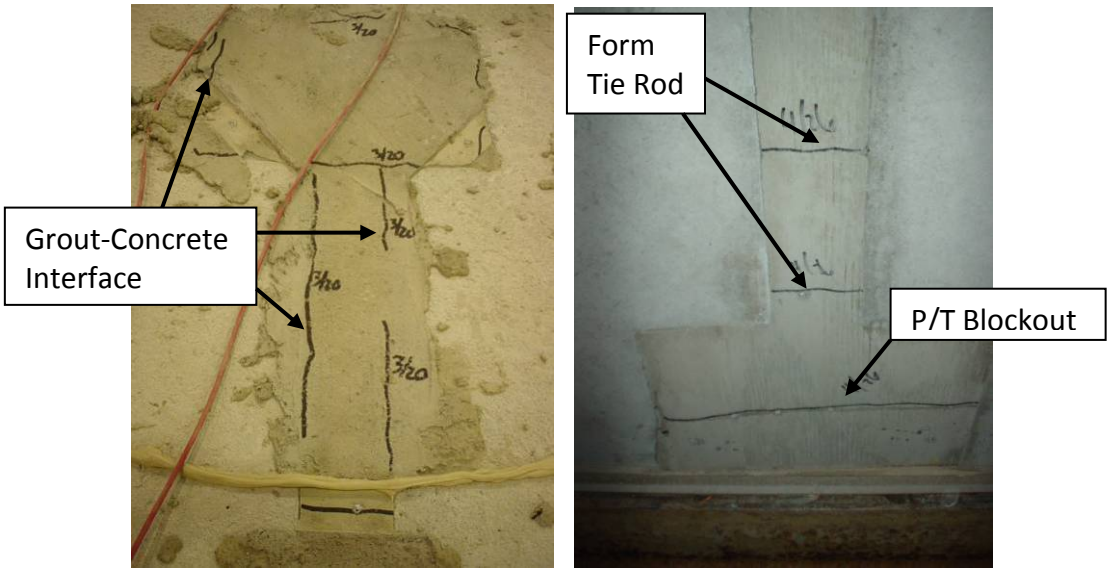

Figure 4-18 Shrinkage Cracks in the 340 psi Post-Tensioned Joints: Normal and Epoxied

4.1.3.1.2 The First Load Induced Cracks

During the first static load test, the transverse joints were carefully monitored for cracking. Visual data and DEMEC readings were used to find the first crack. Graphs were made of the load versus strain recorded on the top surface of the panels with the DEMEC points. Table 4-7 displays the number of load cycles and load that caused the first crack in each joint.

Table 4-7 Time and Load of the First Crack

Sample Name	First Cracking Load	Service Load Cycles at the First Crack
Looped Reinforcing Bars	40 kips	1
Embedded Reinforcing Bars	60 kips	1
Post-Tensioned 0.167 ksi Neat Grout	40 kips	1
Post-Tensioned 0.167 ksi Extended Grout	60 kips	1
Post-Tensioned 0.340 ksi Neat Grout	70 kips	5000
Post-Tensioned 0.340 ksi Epoxied Grout	70 kips	5000

The DEMEC data for the first load cycle for the looped bar joint is shown in Figure 4-19. Three measurements were made across this joint; one above each girder line and one at the midpoint between the girders. The exterior and interior lines on the graph demonstrate the two sides of the joint. The load versus strain diagram shows a large decrease in slope at the point of first crack. A clear change in slope is seen on the interior side of the joint at a load between 35 and 40 kips and on the exterior side at a load between 55 and 60 kips. The looped bar joint cracked at both concrete-grout interfaces during the first static load.

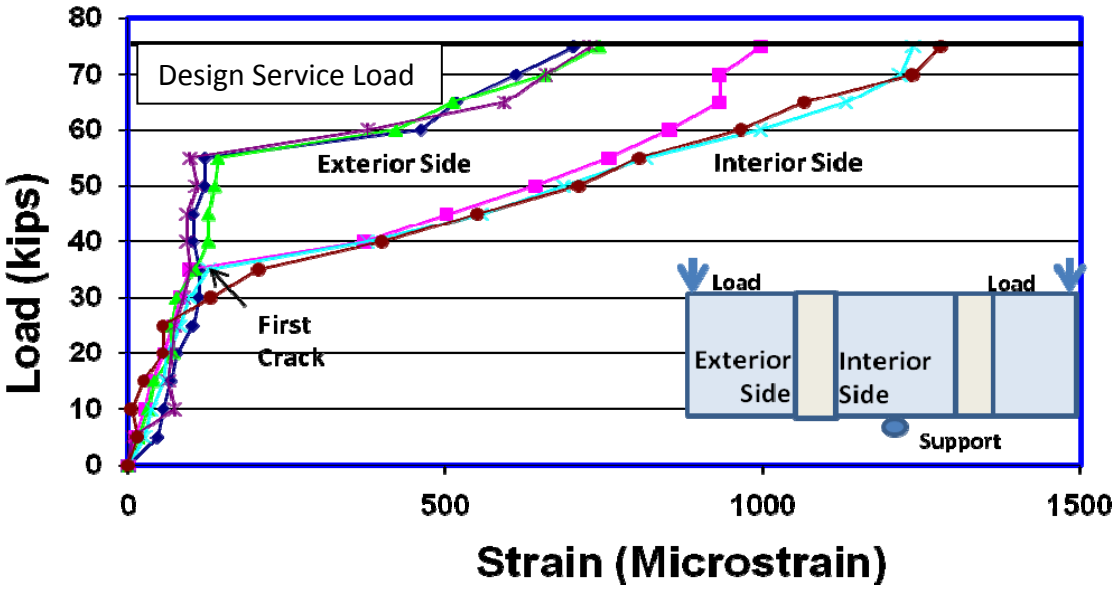

Figure 4-19 Load versus Deck Surface Strain from DEMEC Points -Looped Reinforced Joint - One Service Load Cycle

The embedded reinforcing bar joint cracked at approximately 60 kips on the first cycle (Figure 4-20). A large increase in microstrain from about 100 to 1200 demonstrates the appearance of the first crack. In addition the crack was visible during the initial load cycle. Both reinforced joints cracked prior to starting the cyclical load tests (Figure 4-21).

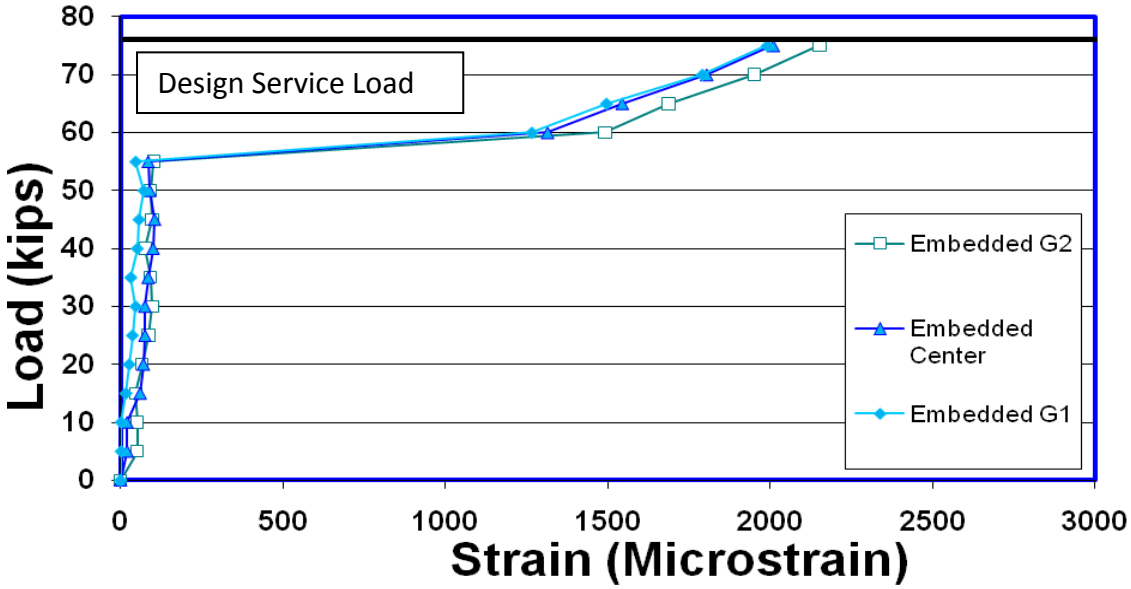

Figure 4-20 Load versus Deck Surface Strain from DEMEC Points -Embedded Reinforced Joint - One Service Load Cycle

Figure 4-21 Initial Cracks in the Embedded Bar and Looped Bar Joints

The four post-tensioned joints cracked at different loads and points in the cyclical loading. The initial cracks in the neat and extended joints with a 0.167 ksi level of stress, occurred during the first static load (Figure 4-22). The neat grout joint cracked

at 40 kips whereas the extended grout cracked at 60 kips. In both joints, one transverse crack appeared throughout the entire grouted joint (Figure 4-23).

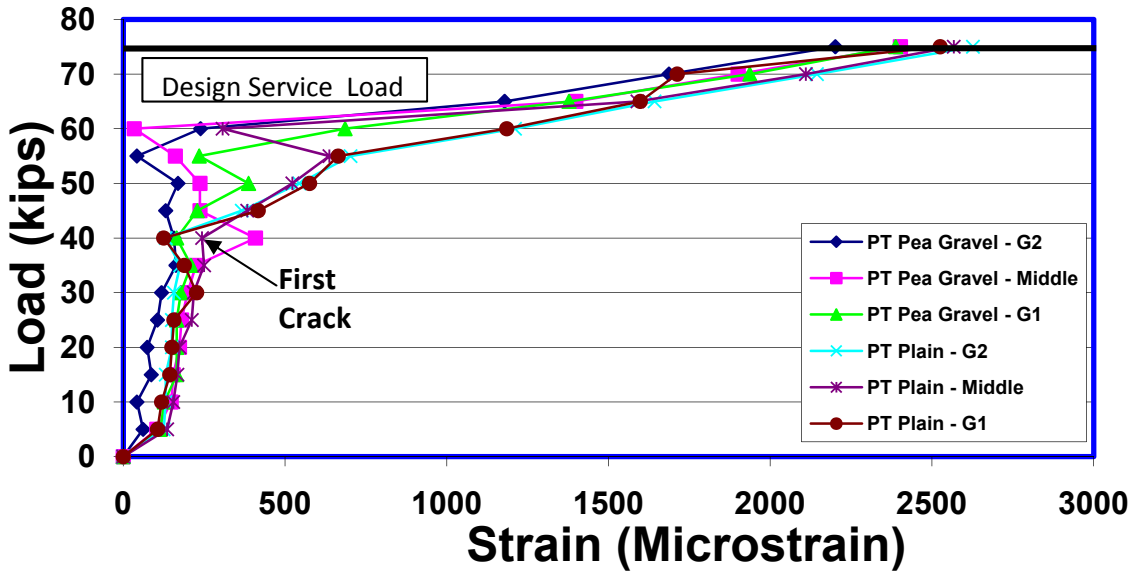

Figure 4-22 Load versus Deck Surface Strain from DEMEC Points - Post-Tensioned Joints at 167 ksi Stress – One Service Load Cycle

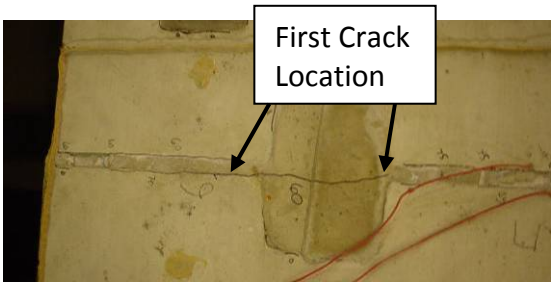

Figure 4-23 Typical Initial Cracking Pattern for Post-Tensioned Joints

In the post-tensioned joints with the prestress level of 0.340 ksi, the joints did not experience large cracking. While no cracking was predicted, small shrinkage cracks occurred at the concrete-grout interface in the joints prior to service loading. The first crack due to service loads was seen at 5000 cycles for both joints; however the DEMEC measurements on top of the deck were not conclusive (Figure 4-24). Figure 4-25 shows

the load versus strain at 100,000 cycles with a slight nonlinearity. This nonlinearity in the graph never grew during the cyclical tests. The joint with the higher level of prestress did not see the large strains during any of the loadings that were seen in the previous four joints. Maximum surface strains in this joint peaked at about 800 microstrain, almost one fourth the size of the maximum values in the other two post-tensioned joints. The cracks that did appear were extensions of the shrinkage cracks at the grout/concrete interface.

The first crack depended on the level of prestressing force. With little or no post-tensioning stress, the crack occurred on the first load cycle. When about twice the minimum prestressing force was applied, the first cracking occurred after a larger number of service load cycles and with a very minimal change in surface strain. A sufficient prestressing level postponed the first crack in the transverse joints and greatly reduced the strain gain after cracking.

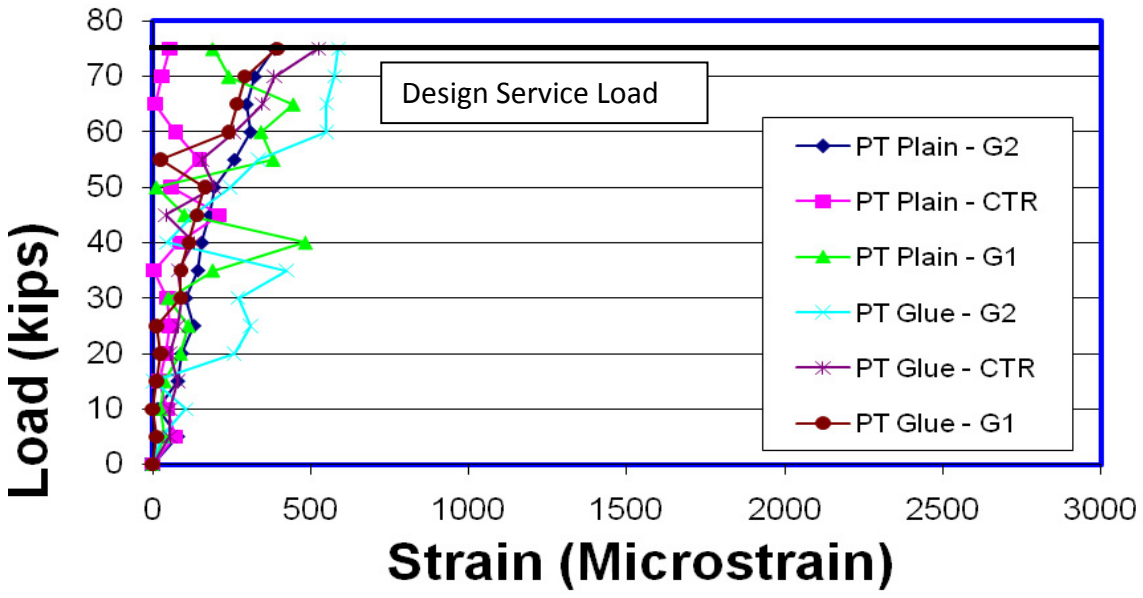

Figure 4-24 Load versus Deck Surface Strain from DEMEC Points - Post-Tensioned joints at 340 ksi Stress – One Service Load Cycles

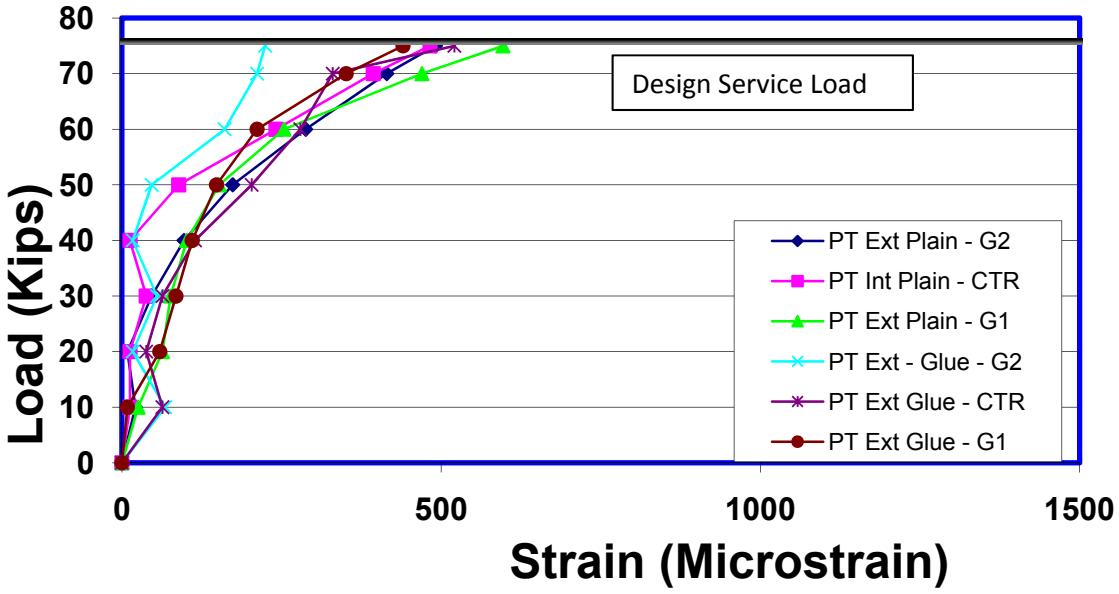

Figure 4-25 Load versus Deck Surface Strain from DEMEC Points - Post-Tensioned joints at 340 ksi Stress – 100,000 Service Load Cycles

4.1.3.1.3 Stress Level at the First Crack

A stress analysis was performed on the vertical cross section of the transverse joint to determine the stress in the top of the joint at the first crack. The material properties tested on the day of the first test were used to determine the stress profile. In the first analysis, the creep and shrinkage losses were not considered in these stress analyses. This final stress value was compared to the modulus of rupture of the grouts and concretes used in the respective joints. The detailed calculations are included in Appendix B.6. Table 4-8 summarizes the results of the three transverse joints.

The second set of post-tensioned joints (0.340 ksi stress) sat in the lab for 53 days, a much longer period than expected. An analysis showed that creep and shrinkage affects could have reduced the effective stress by as much as 5%. Originally, the panels were expected to be tested right after building the joints prior to significant long term

losses. The long term effects were minor but could have created small discrepancies in the test results.

Table 4-8 Stresses at the First Crack in the Transverse Joints

	Looped Bar Joint	**Embedded Bar Joint**	**Grout Only Post-Tensioned Joint 167 ksi**	**Pea Gravel Grout Post-Tensioned Joint 167 ksi**	**Grout Only Post-Tensioned Joint 340 ksi**	**Epoxied Grout Post-Tensioned Joint 340 ksi**
Stress at First Crack (Applied Stress – Prestress) (Top Surface)	0.30 ksi	0.44 ksi	0.13 ksi	0.28 ksi	0.17 ksi	0.17 ksi
Design Service Stress in the Joint (Top Surface)	0.56 ksi	0.56 ksi	0.39 ksi	0.39 ksi	0.21 ksi	0.21 ksi
Concrete Rupture Strength (Frc)*	0.55 ksi	0.55 ksi	0.55 ksi	0.55 ksi	0.54 ksi	0.54 ksi
Ratio (Applied Stress/Frc*)	0.55	0.73	0.24	0.51	0.31	0.31
Grout Rupture Strength (Frg)*	0.41 ksi	0.41 ksi	0.38 ksi	0.41 ksi	0.41 ksi	0.41 ksi
Ratio (Applied Stress/Frg*)	0.73	0.98	0.34	0.68	0.41	0.41
$1.5\sqrt{f'c}$	0.14 ksi	0.14 ksi	0.14 ksi	0.14 ksi	0.14 ksi	0.14 ksi
$1.5\sqrt{f'g}$	0.10 ksi	0.10 ksi	0.095 ksi	0.10 ksi	0.10 ksi	0.10 ksi
First Crack Location	Interface	Interface	Interface	Interface	Interface	Interface

*Rupture strengths determined based on $f_r = 6\sqrt{f'c}$ on the day of the first test.

The grout and concrete rupture strengths were consistent throughout all the tests. The concrete was expected to crack with a tensile stress around 0.54-0.55 ksi and the grout should have cracked between 0.38-0.41 ksi. The post-tensioned joints were designed to keep the tensile stress at the top surface of the panels lower than the

rupture strength of the concrete. The cast-in-place joints were designed for strength and not stress.

All of the joints cracked at tensile stresses less than the rupture strength of both the grout and concrete except the embedded bar joint. The looped bar joint cracked at about 75% off the tensile modulus strength of the grout. The embedded bar joint cracked at about 107% of the tensile strength of the grout. The design service loading of both cast-in-place joints was 137% higher than the tensile moduli of the grout strengths. Some level of cracking was expected.

The post-tensioned joints were all designed to have applied tensile strengths lower than the rupture strength. The as built values all followed this trend, however the joints cracked prior to reaching the tensile capacity. The post-tensioned joints with the 167 psi of effective stress cracked on the first load cycle. The grout only joint cracked at a stress level of approximately one third of the design value. The extended grout cracked at a stress level of approximately two thirds of the design value. The tensile rupture strength of the grouts in these joints was approximately the same as the maximum tensile stress applied.

The post-tensioned joints with 340 psi of effective stress cracked at approximately 81% of the design tensile strength. The grout rupture strength was about 2.4 times higher than the tensile cracking load. However, it must be noted that the first crack was much more inconclusive on these tests. The first crack load and number of cycles were hard to detect as noted in the previous section.

The results were compared to previous research at Virginia Tech by Scholz et al. (2007). In that research, neat Five Star grout cast against a wetted surface cracked at 46% of its rupture strength. The Five Star extended grout cast against a wetted surface cracked at 32% of its rupture strength. This research confirmed that the bond strength is significantly less than the rupture strength for Five Star neat and extended grouts.

The joints cracked at levels of stress less than expected in the design. As noted previously, the cracks in the joints all started at the concrete-grout interface. The cracks did not go through the middle of the concrete or grout. The tensile strength of the

transverse joints was based on a typical relationship to the measured compressive strength. The strength of the bond between the materials was assumed as strong or stronger than the material tensile strength. This was shown to be incorrect and warrants future investigation. The results of these tests show that the interface is the weakest part of the joint and the location of the first crack.

4.1.3.2 Crack Expansion

The cyclical tests simulated the design life of the Virginia bridge. The cracking in the joints was carefully monitored every 100,000 cycles (10% of the design life) for crack propogation.

At the initial loading, the embedded bar joint cracked across the entire top and bottom surfaces of the joint at the exterior side of the grout/concrete joint. The vertical edge on each side of the transverse joint cracked at both the exterior and interior grout/concrete interface. The only major additional cracks occurred along the length of the embedded bar cavities. Both exterior embedded bar cavities cracked between 600,000 and 700,000 cycles (Figure 4-26). The cracks were formed primarily along the interface and not within the grout itself. Complete cracking was displayed.

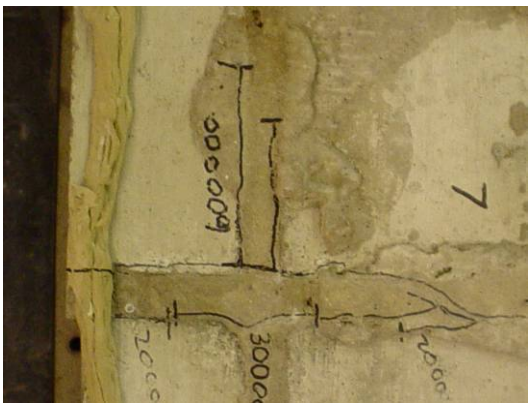

Figure 4-26 Cracks Along the Embedded Bar Cavities

The looped bar joint had minor cracking throughout the joint. The cracking at the initial loading on both sides of the joint was not visible but did exist according to the

strain measurements. Cracks became visible across the top of the joint on both sides of the grout/concrete interface around 20,000 cycles. There were no cracks visible on the bottom of the joint until 300,000 cycles. By 600,000 cycles there were cracks on the top and bottom surfaces of both sides of the joint. The cracks slowly became more visible along the entire joint. Additional cracking did occur longitudinally at 300,000 cycles along the joint were the tie rods were left in the grout (Figure 4-27). Otherwise, the cracks concentrated at the material interface. By the end of the cycles there was complete cracking along both interfaces.

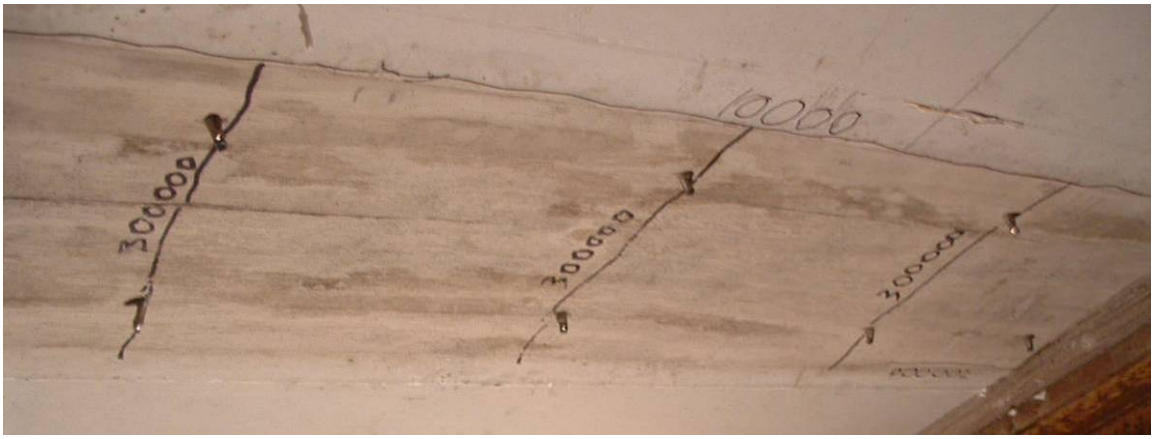

Figure 4-27 Longitudinal Cracking on the Bottom of the Looped Joint

The post-tensioned joint with 167 psi stress and pea gravel grout had one complete crack on the interior side of the joint/concrete interface at first loading. Over the course of the loading, the cracks did not change but the area around the cracks developed spalling problems (Figure 4-28). The main crack went completely through the joint to the bottom of the panels and was visible on the vertical edges. It also went through the center of the post-tensioned blockout on the top and bottom. Additional, cracking appeared around the PT pocket corners on the top and bottom throughout the tests. Most of the cracks occurred from the first static load cycle.

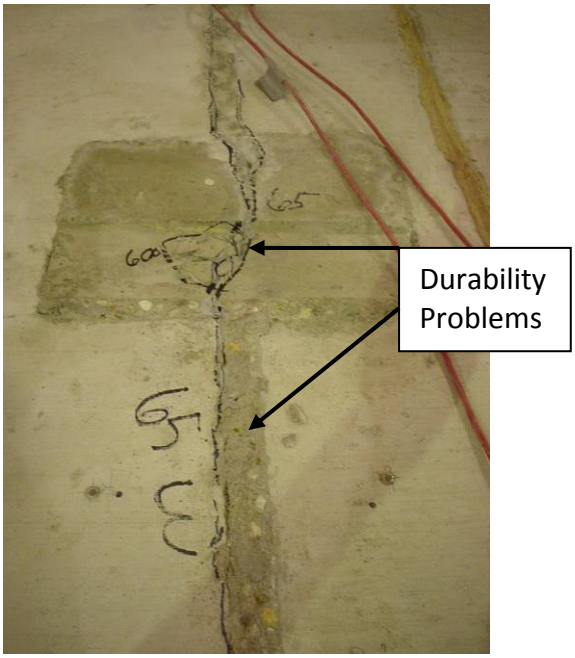

Figure 4-28 Spalling along the Post-Tensioned Pea Gravel Joint

The 167 psi plain grout joint had one complete crack on the exterior side of the joint and an additional crack along one half of the interior side of the joint. This crack on the interior extended to two thirds of the grout/concrete interface by 200,000 cycles. The cracking extended to the bottom of the panels on the interior side of the joint. Cracking also appeared around the PT pocket corners throughout the tests. More cracking appeared on the plain grouted joint than the pea gravel joint.

The 340 psi post-tensioned joint with grout showed shrinkage cracking along most of the entire grout/concrete interface prior to testing. These cracks expanded throughout the load application (Figure 4-29, Figure 4-31). Vertical cracking on the edges of the panels and cracking on the bottom of the panels were never visible.

The 340 psi post-tensioned joint with epoxy in the concrete-grout interface cracked in the middle of the post-tensioned blockouts prior to testing (Figure 4-30, Figure 4-31). During the first static tests a complete crack appeared along the interior side of the joint. Cracks occurred across the bottom of the joints at the threaded rod locations. Shrinkage cracking expanded significantly around the corners and in the

interior of the post-tensioned blockouts throughout the tests. There were never any visible cracks on the vertical sides or bottom of the panels.

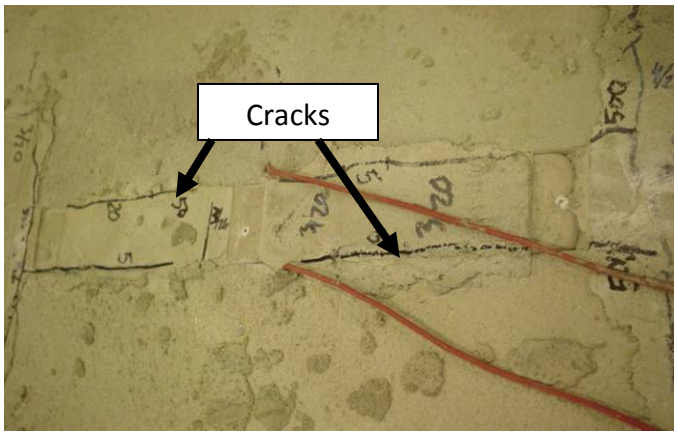

Figure 4-29 Surface Cracks in the Neat Grouted 340 psi Transverse Joint

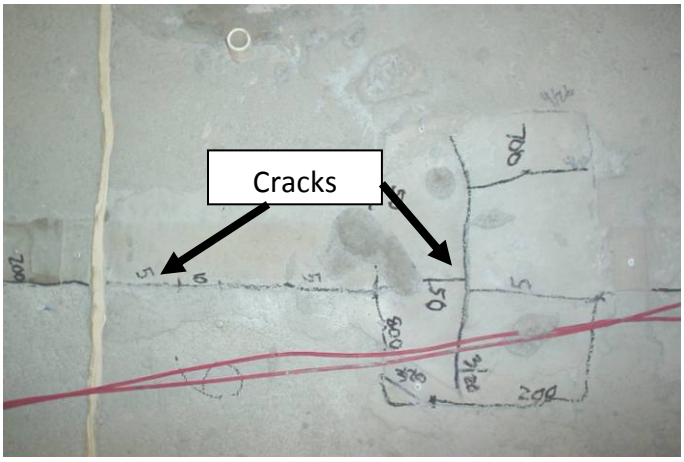

Figure 4-30 Cracks in the Epoxy Grouted 340 psi Transverse Joint

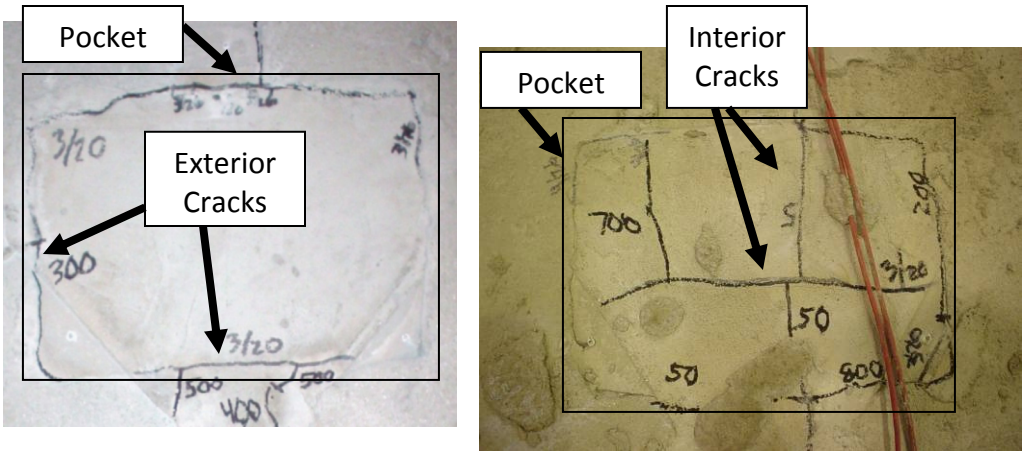

Figure 4-31 Surface Cracks in the Neat Grout and Epoxy Grout Post-Tensioned Pockets

In summary, the majority of the cracks occurred at the grout/concrete interface. The grouts did not crack except when epoxy was added to the material interface. With epoxy the cracking tended to occur in the middle of the pockets. Pea gravel caused spalling problems but otherwise had similar crack patterns. Most of the cracks due to loading occurred during the first few thousand load cycles. Some extensions appeared after the initial loading but very few new cracks appeared later in the tests with the post-tensioned joints. The cracking in the cast-in-place joints continued to widen until the end of the test.

4.1.3.3 Final Crack Sizes

The location and size of the cracks were recorded at the end of the cyclical tests. The size of these cracks was measured with crack gauges (0.005 in. accuracy) on the top, side, and bottom surfaces of the transverse joints (Table 4-9). The crack distributions along the boundary interface and within the grout were recorded (Table 4-10). All of these values were measured with the service truck load applied (HS-20).

The looped reinforcing bar joint had complete cracking along all the visible grout and concrete interfaces. This included the top, bottom, and elevation view of the deck at the cantilevers. All of the crack sizes were less than or equal to 0.01 in. except for one crack above girder G1 that had a width of 0.015 in. The crack sizes did not vary

significantly from the top to the bottom of the slab. On average, the crack sizes were 0.0085 in. throughout.

The embedded bar joint had the largest cracks on all surfaces of the joint. On the top surface one side of the grout/concrete interface cracked across the entire joint. The other side cracked along approximately half of the joint. The bottom of the joint had one complete crack down the outer edge of the joint. The elevation views on the end of the joint were cracked on both sides. The top had a crack width of 0.025 in. while the bottom had crack widths of 0.02 in. The average crack width was 0.0225 in. throughout.

The post-tensioned joints with 167 psi of compressive force performed similar to one another. The grout only joint had an average crack size of 0.012 in. while the pea gravel extended grout had an average crack size of 0.009 in. The cracking on top of the joints primarily occurred on one side of the interface. The grout only joint had cracking on both sides of the interface above girder one but otherwise performed the same as the extended joint. Both had an average crack size of 0.015 in. on top. The cracks on the bottom of the extended grout were 0.005 in. while the cracks on the grout only were 0.01 in. The performances were similar but the extended grout cracked a little less and had smaller crack sizes on the bottom of the joint.

The post-tensioned joints with 340 psi performed very similarly. They had an average crack width of 0.008 in. on top. The bottom of both joints had little or no visible cracks. A few visible ones did exist around the edge of the post-tensioned pockets on the bottom but they were all 0.005 in. or less in size. The vertical edge of the deck at the transverse joint had no visible vertical cracks. A few horizontal cracks did appear across the shear keys.

Three different types of grout material were used in the post-tensioned joints: Five Star Highway Patch Grout, Extended (3/8 in. Pea Gravel) Five Star Highway Patch Grout, and Epoxied Five Star Highway Patch Grout. The extended grout cracked slightly less than the plain grout, however there were additional pop-out cracks on the top surface of the deck. The durability may have suffered due to the extended grout. The

epoxied grout initially prevented shrinkage cracks in the joints between the concrete-grout interface. Once loading started the epoxied joint cracked along the interface but had fewer cracks in the post-tensioned blockouts edges. By the end of the tests the epoxy did not significantly alleviate cracking in the joints. Adding a pea gravel extension and epoxy did not significantly change the cracking size or patterns in the transverse joints.

The embedded bar joint had the largest crack sizes on both the top and bottom of the joint and the largest average crack size. The joints with 167 psi of post-tensioning stress had the second largest average crack sizes on the top. Adding an extension to the grout did not significantly affect the results. The looped bar joint cracks on the top were slightly larger than the average crack sizes in the 340 psi post-tensioning joint. The joints with 340 psi of stress had the smallest cracks on the bottom of all the joints. On all accounts the post-tensioned joint with 340 psi of stress performed the best, however, the looped bar joint performed as well or better than the joints with 167 psi of stress. An epoxied transverse joint initially reduced shrinkage cracking but it did not significantly alleviate cracking during the load tests. The benefit of the looped bar joint over the 167 psi stressed joints is that the cracks occurred over both interfaces whereas the cracks in the post-tensioned joint occurred primarily on one side of the joint.

Table 4-9 Final Surface Crack Sizes in the Transverse Joints

Crack Sizes in the Transverse Joints (Inches)						
	Reinforcing Bar Connections		Post Tensioned Connections			
(All values Measured at Service Load)	**Looped Bars**	**Embedded Bars**	**Pea Gravel Grout (167 psi)**	**Grout Only (167 psi)**	**Grout Only (340 psi)**	**Epoxied Surface (340 psi)**
G2 Elevation	0.01	0.025	0.01	0.015	0	0
G2 Overhang Bottom	0	0.015	0	0.01	0	0
G1 Elevation	0.01	0.03	0.015	0.015	0	0
G1 Overhang Bottom	0.005	0.02	0.005	0.005	0	0
Top G1	0.015	0.025	0.015	0.015	0.01	0.01
Top Middle	0.01	0.025	0.015	0.015	0.01	0.01
Top G2	0.005	0.025	0.015	0.015	0.005	0.005
Bottom G1/PT Pocket	0.01	0.02	0.005	0.01	0	0.005
Bottom Middle	0.01	0.02	0.005	0.005	0	0
Bottom G2/PT Pocket	0.01	0.02	0.005	0.015	0.005	0.005
Average	**0.0085**	**0.0225**	**0.009**	**0.012**	**0.003**	**0.0035**

Table 4-10 Final Crack Observations in the Transverse Joints

Final Cracking Observations						
	Reinforcing Bar Connections		Post Tensioned Connections			
	Looped Bars	Embedded Bar	Pea Gravel Grout (167 psi)	Grout Only (167 psi)	Grout Only (340 psi)	Epoxied Surface (340 psi)
Top	Both Sides of the joint cracked.	One Side Completely Cracked. The other was almost Completely Cracked	Almost all cracks on one side.	Almost all cracks on one side.	1 Main Crack in Middle, Cracks Surround Edge of PT Pocket	1 Main Crack in Middle, Cracks Surround Edge of PT Pocket
G1 Side (Elevation)	Both Sides Cracked.	Both Sides Cracked.	Inner Side Cracked.	Outer side cracked. Half of the Inner side cracked.	Horizontal Cracks Near Shear Keys	Horizontal Cracks Near Shear Keys
G2 Side (Elevation)	Both Sides Cracked.	Both Sides Cracked.	Inner Side Cracked.	Outer Side Cracked.	Horizontal Cracks Near Shear Keys	Horizontal Cracks Near Shear Keys
Bottom	Both Sides Cracked.	Outer Side Cracked.	One Crack in the Middle, Cracks on the Corner of the PT Joints. Crack between PT Joints-Inside Only.	One Crack in the Middle, Cracks on the Corner of the PT Joints. Crack between PT Joints-Inside Only.	A few slight cracks around PT pocket, perpendicular cracks to tie rods for formwork	Slight cracks around PT pocket, Large longitudinal crack down middle of PT Pocket, perpendicular cracks to tie rods for formwork

4.1.4 Ponding on the Deck Panels

The ponding test was performed on the surface of the bridge decks to determine if cracking was large enough to allow water to flow through the bridge deck. The test was done on the panels and joints while they had no service load applied. To perform the test, the deck was left in the unloaded condition for two hours with a layer of approximately ¼ in. of water (Figure 4-32). Tap water from the Virginia Tech structures lab was placed within the contained area on the bridge deck. The sides and bottom of the deck were monitored for water leaking through the joints.

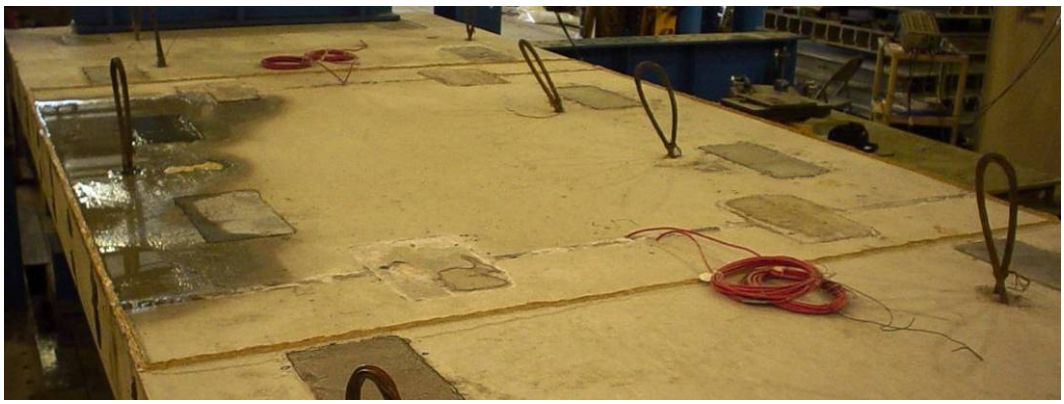

Figure 4-32 Adhesive Barrier on the Surface of the Bridge Deck

The reinforcing joints were tested first. Neither joint leaked for the first five hundred thousand cycles (Table 4-11). At the five hundred thousand cycle point, or half the design life, the embedded bar joint began to leak throughout its entire length. The leaks started within 15 minutes of applying the water and continued for the duration of the test. The looped bar joint did not have any leaking at the same point in the test.

By the end of the test, the leakage patterns followed the same trends. The looped bar joint did not leak and the embedded bar joint leaked profusely. After the final static ponding test was performed, the test was repeated with 10 load cycles and with 100 load cycles. The cycles consisted of applying the equivalent HS-20 service load at 1 Hz. While under the cyclical ponding load, the embedded bar joint leaked profusely. Water continuously flowed through the cracks in the middle of the joint.

Approximately 25% of the looped bar joint began to leak under the 10 cycle load. By the end of 100 cycles, about 75% of the looped bar joint showed signs of leaks (Figure 4-33). Most of the water beaded up along the crack between the grout and concrete but did not drip to the ground.

Table 4-11 Ponding Test Results: Reinforcing Bar Connections

Ponding	Reinforcing Bar Connections	
(All Values Measured by Visual Detection)	**Looped Bars**	**Embedded Bar**
500,000 Cycles	No Leaks	Leaks throughout
1,000,000 Cycles	No Leaks	Leaks throughout
10 Cycles with Water	25% of Joint Leaked	100% of Joint Leaked
100 Cycles with Water	75% of Joint Leaked	100% of Joint Leaked
Notes:	A small amount of water wetted most of the area beneath the looped bar joint.	The embedded bar joint streamed water during the final ponding with load cycles.

The first post-tensioned test had two joints with 167 psi initial compressive strength: One joint with neat grout and one with a pea gravel extended grout. Neither joint leaked until the end of its design life or one million cycles.

At the conclusion of the cycles, the pea gravel joint had three small leaks between the grout and panels that were 1 – 2 in. long (Table 4-12). There was no significant change in the pea gravel joint until ponding with 100 cycles of service load. By the conclusion of the ponding, approximately two thirds of the joint leaked (Figure 4-34). Water beaded up on the cracks between the grout and panels but very little water leaked to the ground.

The grout only joint had one minor crack on the corner of one of the post-tensioning pockets that leaked water. The leak was approximately 1 in. long. This joint leaked very little and did not have water beading up around it until the conclusion of the test. After the 100 cycles with the water, about twenty percent of the joint between the panels leaked water. The water beaded up in a few spots and did not drip to the

ground. There was less water moving through this joint as compared to the pea gravel joint.

The last test was on two post-tensioned joints with 340 psi compressive force. Both joints were identical except for an epoxy bonding agent between the grout and panel interface on one joint. Neither leaked water at any of the interface cracks during the static ponding tests or the ponding tests with cyclical loads. The joint with the epoxy formed a crack in the middle of the post tensioned grout pocket that showed signs of leaks around 100,000 cycles. However, the water never appeared again in the tests.

The post-tensioned joints with the highest level of post-tensioning exhibited the best behavior in the ponding tests. These joints had the smallest cracks and showed little evidence of durability problems on the external surfaces (Figure 4-35). Joints with average crack sizes of 0.0035 in. or less never leaked. The looped reinforcing bar joint also exhibited satisfactory results, although it did leak a minor amount at the end of the testing. Joints with average crack sizes of 0.0085 in. or greater leaked by the end of their service life. The joints with the lower level of prestressing and the embedded bar joints performed the worst. They would not be recommended based on the ponding results.

Table 4-12 Ponding Test Results: Post-Tensioned Connections

Ponding	**Post-Tensioned Connections**			
(All Values Measured by Visual Detection)	**Pea Gravel Grout (167 psi)**	**Grout Only (167 psi)**	**Grout Only (340 psi)**	**Epoxied Surface (340 psi)**
500,000 Cycles	No Leaks	No Leaks	No Leaks	No Leaks
1,000,000 Cycles	3 Leaks – 1-2” long	1 Leak – PT Pocket 1” long	No Leaks	No Leaks
10 Cycles with Water	3 Leaks – 1-2” long	1 Leak – PT Pocket 1” long	No Leaks	No Leaks
100 Cycles with Water	~66% of Joint Leaked	~20% of Joint Leaked	No Leaks	No Leaks
Notes:	Very little water dripped through in both PT joints.		There were only a few signs of leaks (< 100,000 Cycles) = middle of the PT pockets with Epoxy.	

Figure 4-33 Final Leaking - Reinforced Concrete Joints:
Looped Bars & Embedded Bars

Figure 4-34 Final Leaking - Post-tensioned Joints with 167 psi Stress:
Pea Gravel Extended and Grout Only

Figure 4-35 Final Leaking – Both Post-tensioned Joints with 340 psi Stress

4.1.5 The Load-Strain Profile in the Transverse Joints

During the tests, a record was made of the vertical strain profile at each transverse joint. The strain profiles were measured with the strain gauges on the girders, the VWGs in the top of the deck, and DEMEC points on the surface of the deck (See Figure 3-18). The change in strain distribution at the joints indicated changes in joint stiffness.

In each joint, the theoretical strain distribution was computed. The measured material properties were used for the concrete (f'c and Ec) along with the assumed properties for steel (Es). In both post-tensioned joints, an uncracked strain profile was computed based on the design assumption that the concrete would not crack because of the post-tensioning force. In the reinforced joints, the uncracked profile was computed along with the profile in a completely cracked deck. Full composite action between the deck and girder was assumed for all models. The detailed calculations are included in Appendix B.7 - Strain Levels in the Deck Panels.

The strain distribution in the reinforced joints differed from the post-tensioned joints. Data prior to 138,000 cycles was not available for the cast-in-place joints because of data acquisition problems during the initial tests. Figure 4-36 and Figure 4-37 show the typical strain distributions for the embedded bar and looped bar tests at 138,000 cycles, respectively. The strain in the concrete panels remained very similar to these values for the duration of the tests. The distribution in the girders remained linear but the strain in the deck was very small throughout (Figure 4-38, Figure 4-39). The panels cracked at the initial loading and ceased to take on significant load at the joint. This was shown by the lack of strain change in the panels during service loading.

The neutral axes moved lower than the theoretical value by the end of the tests. The theoretical value based on no cracking in the decks was 21 in. By the end of the tests, the neutral axis had moved to approximately 13 in for the embedded bar joint and 15 in for the looped bar joint. The strain distribution was not linear in these joints and the panels had very small amounts of strain under the service load.

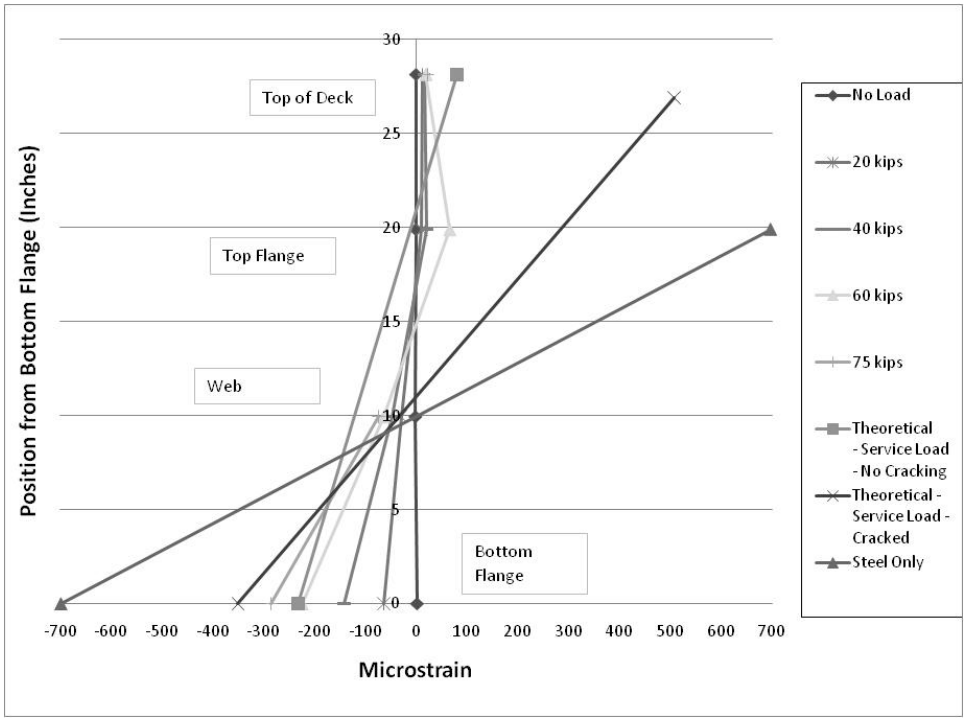

Figure 4-36 Strain Profile for the Embedded Bar Joint at 138,000 Cycles

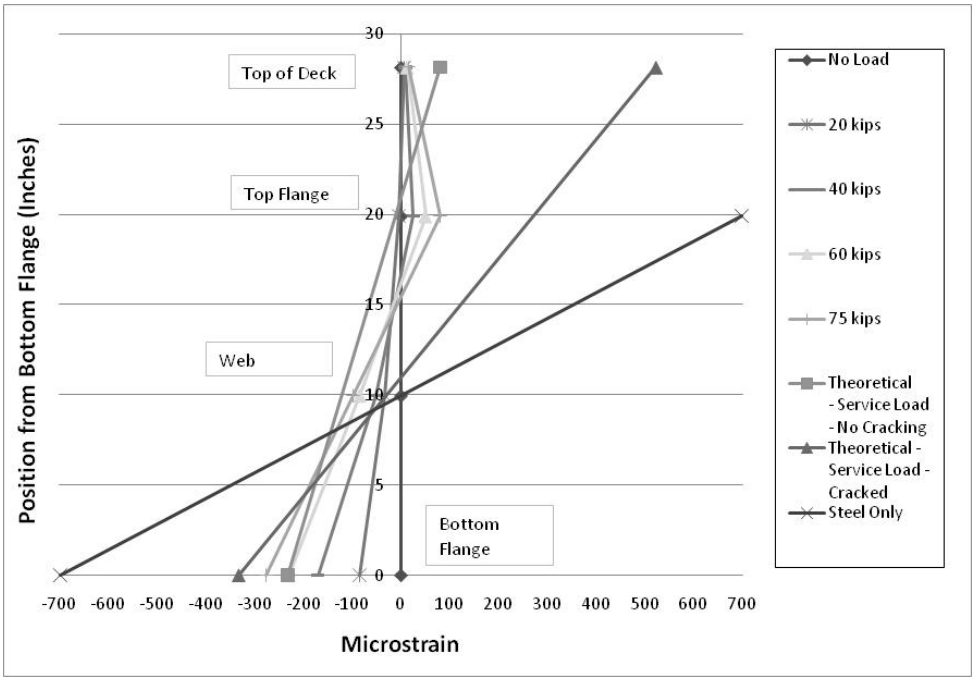

Figure 4-37 Strain Profile for the Looped Bar Joint at 138,000 Cycles

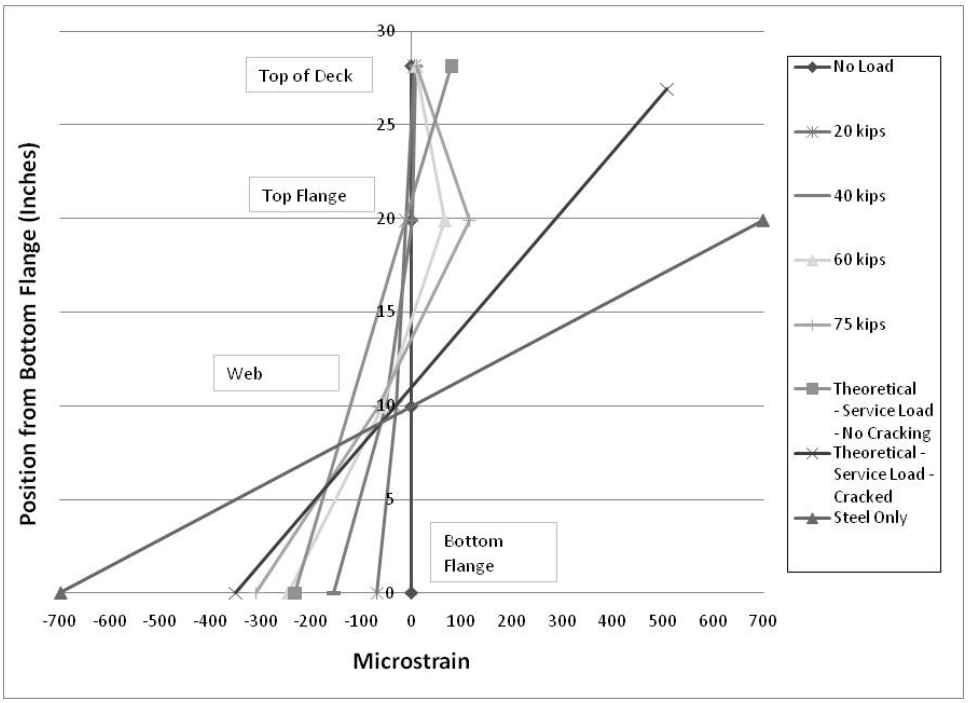

Figure 4-38 Strain Profile for the Embedded Bar Joint at 1,000,000 Cycles

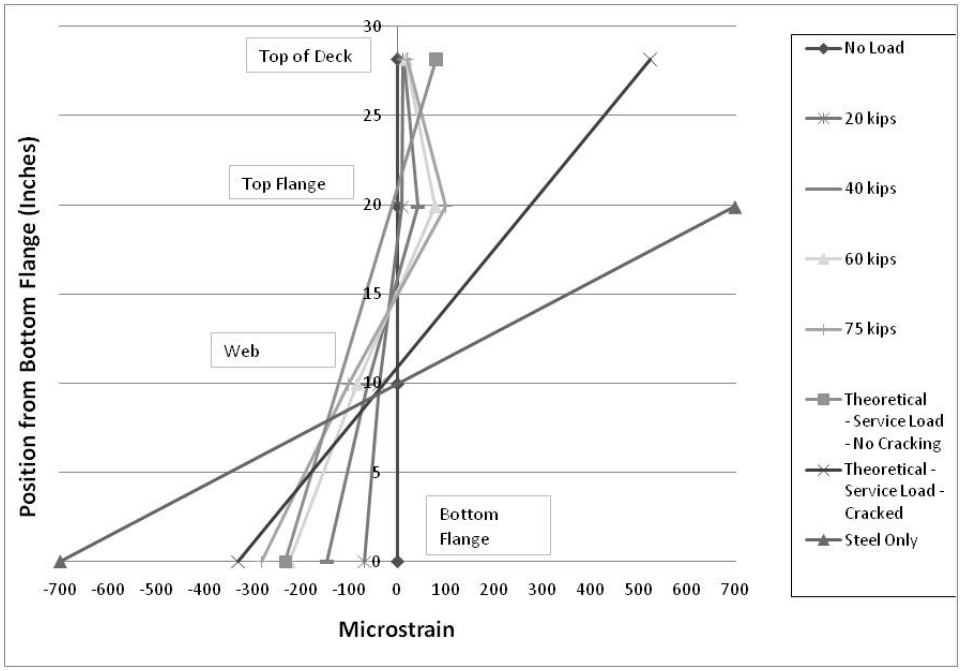

Figure 4-39 Strain Profile for the Looped Bar Joint at 1,000,000 Cycles

The neat and pea gravel joints with a 167 psi of post tensioning started with a linear strain distribution then abruptly deviated (Figure 4-40, Figure 4-41). This continued throughout the test as shown in Figure 4-42 and Figure 4-43. As the load was slowly increased, the strain in the composite joint profile reached a linear distribution under approximately two-thirds of the service stress level. At this point the panels cracked and the strain in the concrete panels stopped increasing even though the load continued to slowly increase. The steel girder continued to take additional strain under the full service load. This pattern continued throughout the life of both joints. The maximum strain level in the concrete did not increase once the panels reached cracking.

The neutral axis moved under service loads for both joints. For the first 50 kips of applied load, or two-thirds of the service load, the neutral axis was very close to the 21 in theoretical value. After cracking, the neutral axis dropped to about 16-17 in. in the extended grout joint. The neutral axis dropped to approximately 14-15 in. in the neat grout joint. The strain distributions started in a linear manner but deviated around 60 kips throughout. This value corresponds to the first cracking load.

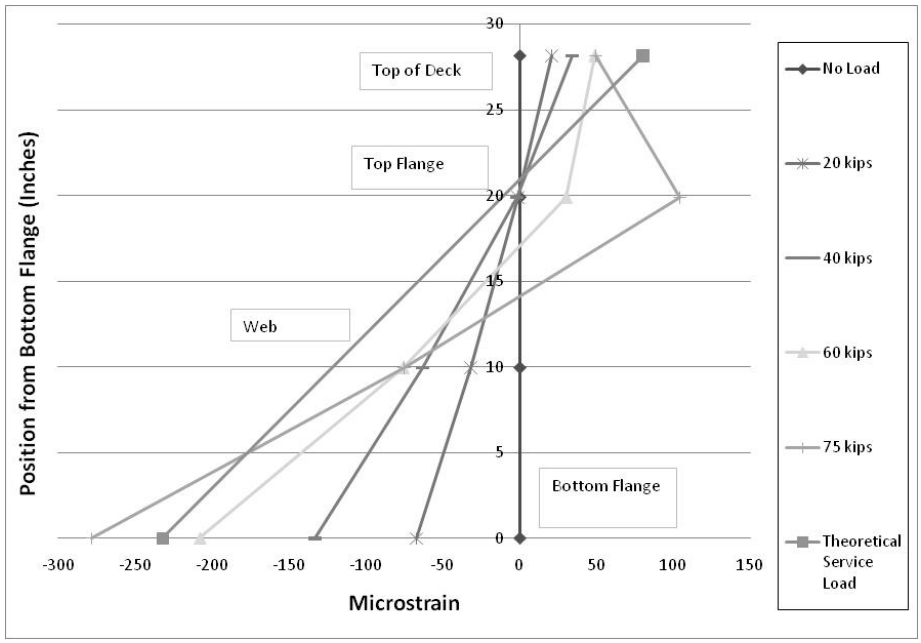

Figure 4-40 Strain Profile: Neat Grout Post-Tensioned Joints with 167 psi Normal Stress at 0 Cycles

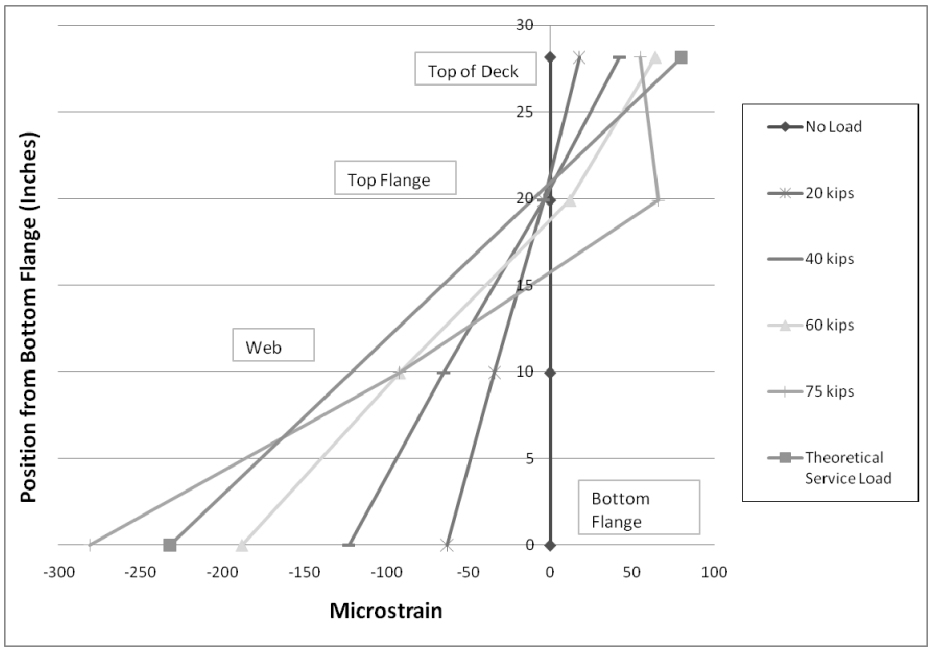

Figure 4-41 Strain Profile: Extended Grout Post-Tensioned Joints with 167 psi Normal Stress at 0 Cycles

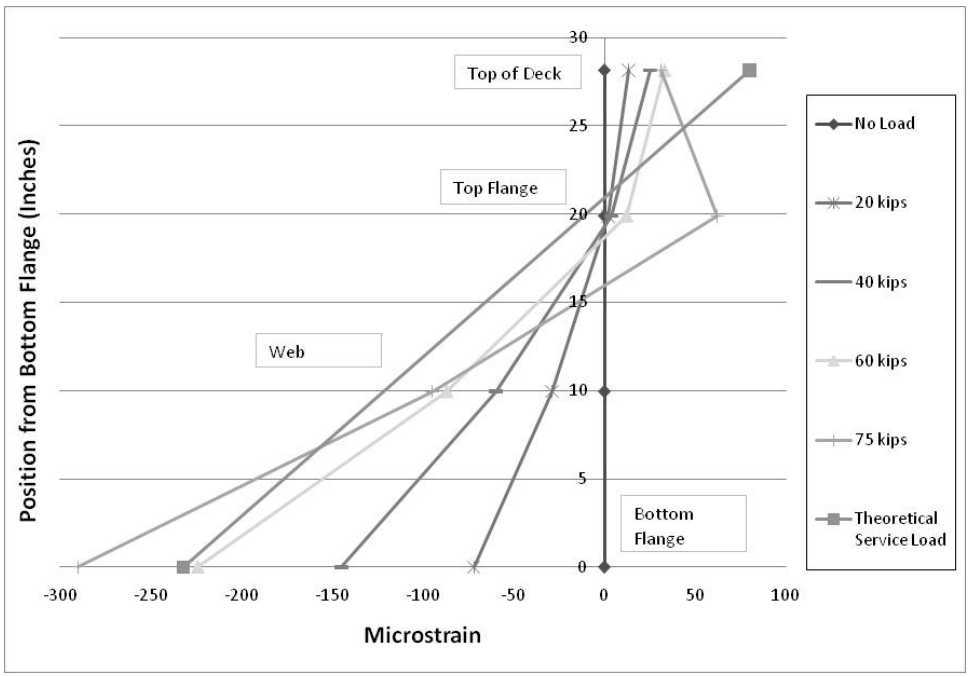

Figure 4-42 Strain Profile: Neat Grout Post-Tensioned Joints with 167 psi Normal Stress at 1 Million Cycles

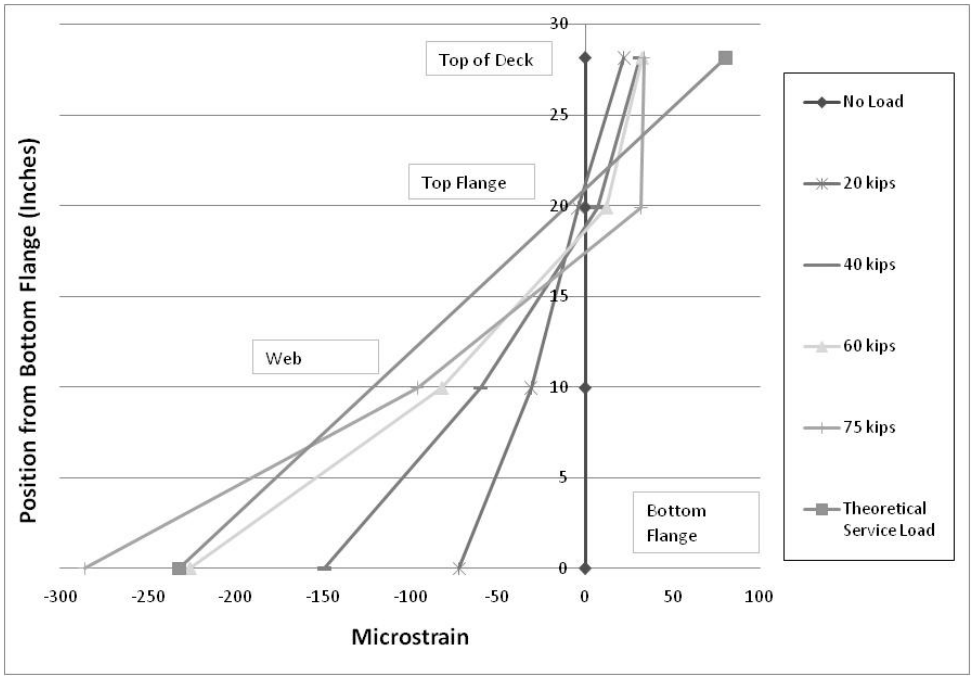

Figure 4-43 Strain Profile: Extended Grout Post-Tensioned Joints with 167 psi Normal Stress at 1 Million Cycles

The strain profiles for the neat and epoxied post-tensioned joints with 340 psi initial compressive stress were almost linear (Figure 4-44, Figure 4-45). The neat grout joint was nearly linear through the 75 kip service load. The neutral axis was approximately 19 in., a value close to the 21 in. uncracked theoretical answer. The epoxy grout joint was linear until a 30 kips service load. At this point the neutral axis moved down to about 17 in. and the strain distribution showed a slight increase in slope.

Throughout the remainder of the tests, these joints maintained a nearly linear stress distribution (Figure 4-46, Figure 4-47). There was a slight deviation in the linear distribution in the deck, however the deviation remained constant throughout the cyclical tests. The neutral axis in both joints stayed around 17 in., lower in the cross-section than the 21 in. theoretical value. Surface cracking was apparent throughout the joints and may have contributed to the slight increase in the strain distribution in both joints. Overall, these two joints were closest to the uncracked strain distribution expected in the joints.

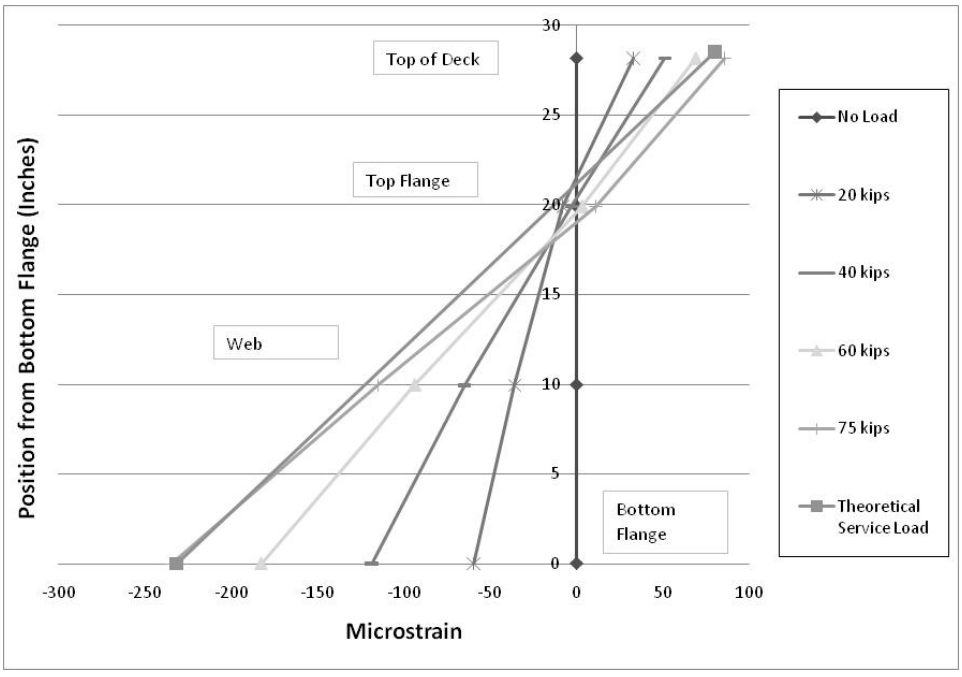

Figure 4-44 Strain Profile: Neat Grout Post-Tensioned Joints with 340 psi Normal Stress at 0 Cycles

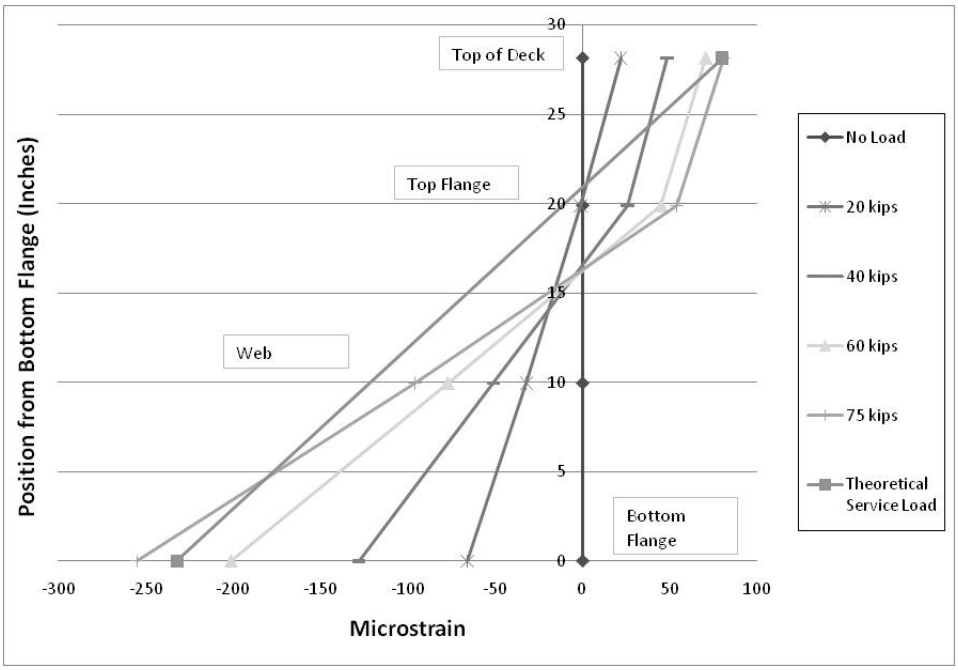

Figure 4-45 Strain Profile: Epoxied Grout Post-Tensioned Joints with 340 psi Normal Stress at 0 Cycles

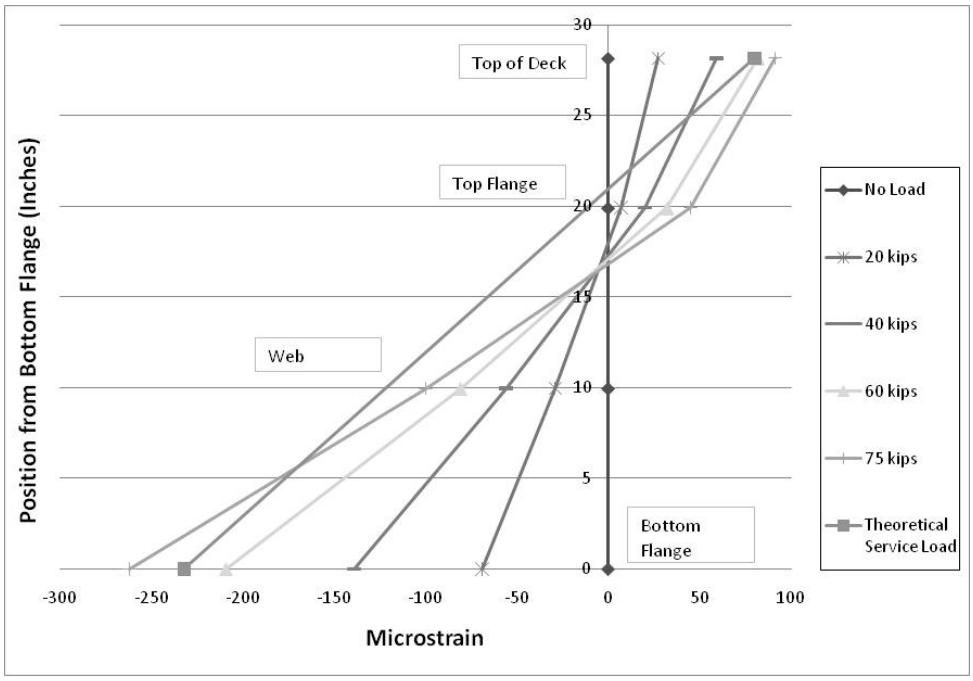

Figure 4-46 Strain Profile: Neat Grout Post-Tensioned Joints with 340 psi Normal Stress at 1 Million Cycles

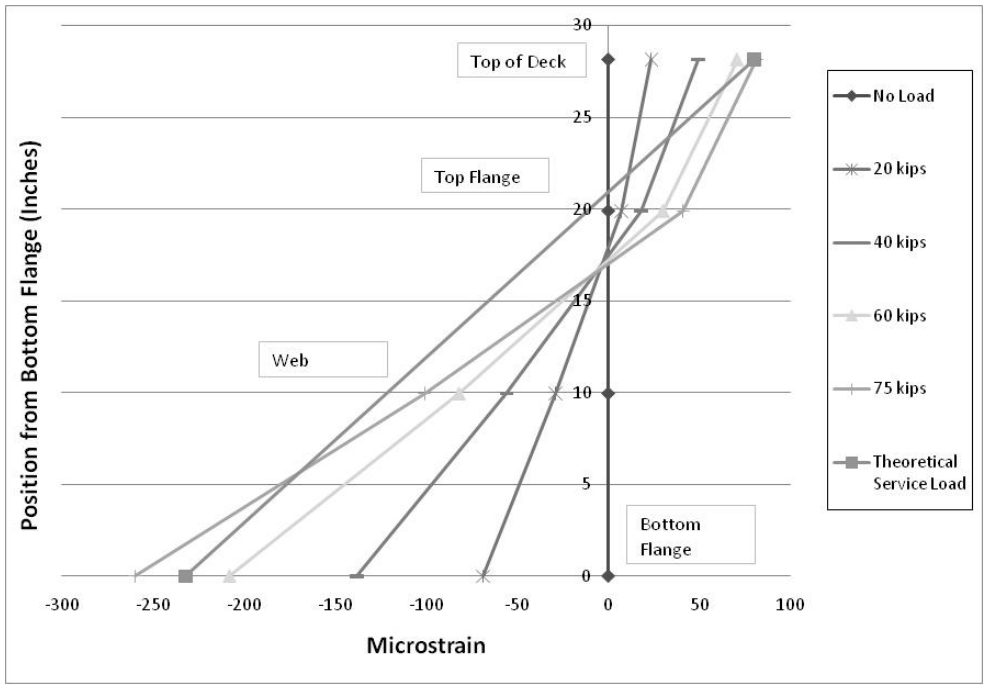

Figure 4-47 Strain Profile: Epoxied Grout Post-Tensioned Joints with 340 psi Normal Stress at 1 Million Cycles

The maximum strain values in the top flange and web varied among the three tests. The neutral axis moved down towards the mid-height of the steel girder (10.7 in.) as the joints redistributed strain to the girders. For the joints with 340 psi stress, the neutral axis consistently stayed around 17 to 18 in. from the bottom flange in the girder web. In the 167 psi stressed joints, the neutral axis moved to about 16 to 17 in. from the bottom flange. In the looped reinforced joint, the neutral axis dropped to about 15 in. from the bottom flange. The embedded bar joint's neutral axis dropped to about 14 in. from the bottom flange. The 340 psi post-tensioned joints had the highest neutral axis of all the joint types.

Cracking was observed in all of the transverse joints to some degree. The cracks were primarily parallel and inside the joint. These cracks indicated that there was a loss in compression in the concrete deck panels. The smaller neutral axes were likely due to the effects of cracking.

Composite action was not tested and the bridges were assumed to remain composite throughout testing. This was a reasonable assumption based on past research.

4.1.6 Strain Ranges in the Transverse Joints

The strains in the transverse joints were measured using VWGs in the concrete panels. One VWG was placed on each side of the joint. The VWGs were centered across the joint in the post-tensioned joints. The VWGs were positioned approximately midway between the reinforcing bars in the embedded and looped bar joints (Figure 4-48). Additionally, the surface strain across the joints was measured using DEMEC points (Figure 4-49). The readings from these devices provided an indication of how much strain the top surface of the panels underwent during service loading over time.

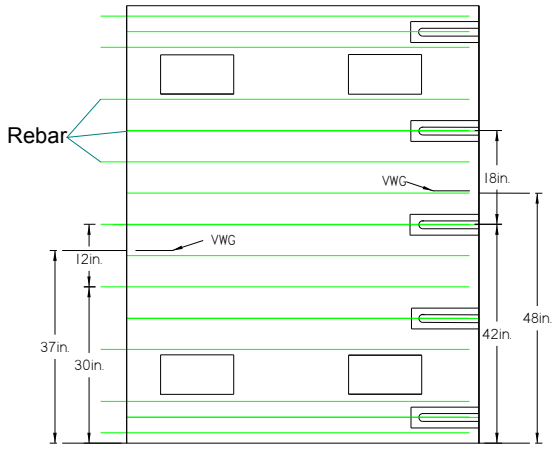

Figure 4-48 VWG Location on a Plan View of the Embedded and Looped Bar Joints

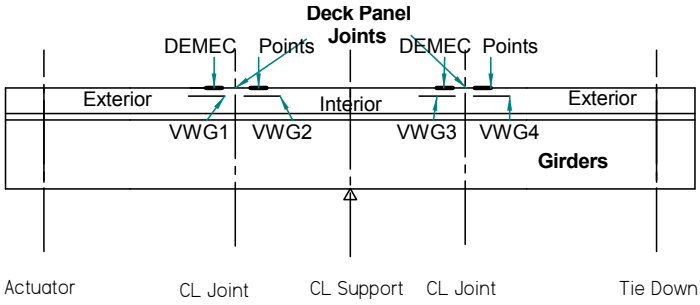

Figure 4-49 VWG Locations

The strain ranges for the reinforced joints are given in Table 4-13. The range was found by monitoring the strain values recorded by the VWGs inside the concrete panels on each side of the transverse joints. The values were found by taking the initial strain value unloaded and subtracting the final strain while the service load was applied. Initially, both joints had high strain values, but these dropped after the first static load test. This drop corresponded to the first cracking load. The looped bar joint had average strain values near 30 microstrain at the beginning of the test but these values decreased to around 20 microstrain by the end of the test. The interior panel of the embedded bar joint was also in this range until after 700,000 cycles when it began to drop below 20 microstrain. The exterior embedded bar joint readings were all less than 10 microstrain after 100,000 cycles. In general, the looped bar panels lost some of its ability to strain under loading as evidenced by the strain range. The embedded bar joint appears to have lost most of its ability to strain under loading by the end of this test.

Table 4-13 Strain Range in the RC Panels During the Cyclical Tests

	Looped Bar Joint			Embedded Bar Joint		
	Exterior	Interior		Interior	Exterior	
Service Load Cycles	**Range VWG1 Load Strain**	**Range VWG 2 Load Strain**	**Average Across Joint**	**Range VWG 3 Load Strain**	**Range VWG 4 Load Strain**	**Average Across Joint**
1	48.0	51.7	49.8	48.3	39.7	44.0
1,000	29.1	26.3	27.7	29.1	10.9	20.0
5,000	29.9	26.1	28.0	26.8	9.6	18.2
10,000	30.0	28.0	29.0	31.9	13.0	22.4
20,000	27.7	24.8	26.3	29.6	10.4	20.0
30,000	29.9	25.1	27.5	30.9	9.1	20.0
40,000	27.2	23.4	25.3	27.2	8.9	18.1
50,000	27.0	25.0	26.0	28.9	10.7	19.8
100,000	29.0	25.9	27.5	28.8	9.6	19.2
200,000	24.9	22.1	23.5	24.0	8.6	16.3
300,000	23.1	20.3	21.7	24.9	7.8	16.3
400,000	22.1	20.2	21.1	24.1	7.9	16.0
500,000	24.2	20.2	22.2	21.3	6.0	13.7
600,000	26.4	24.5	25.4	22.4	9.9	16.2
700,000	26.0	23.1	24.6	19.3	7.7	13.5
800,000	24.3	22.4	23.3	20.0	6.0	13.0
900,000	22.2	20.2	21.2	17.4	5.8	11.6
1,000,000	21.2	18.4	19.8	17.3	4.9	11.1

A graphical representation of the inability of the panels to strain under loading is given for the embedded bar and looped bar joints in Figure 4-50 and Figure 4-51 . For the first 20 kips applied to the looped bar, the strain increased at a linear rate with respect to the load increase. By 30 kips the strain increased much more slowly and almost ceased to increase in strain as load was applied. This indicates the panels are not straining as much even though load is still increasing. The pattern remains almost constant throughout the design life.

On the first static load, the embedded bar panels increased in strain linearly for the first 30 kips applied. After that the strain increase abruptly stopped even though more load was applied. From that point, the strain in the joint did not change significantly. This indicates that the panels were not straining much after the first load cycle.

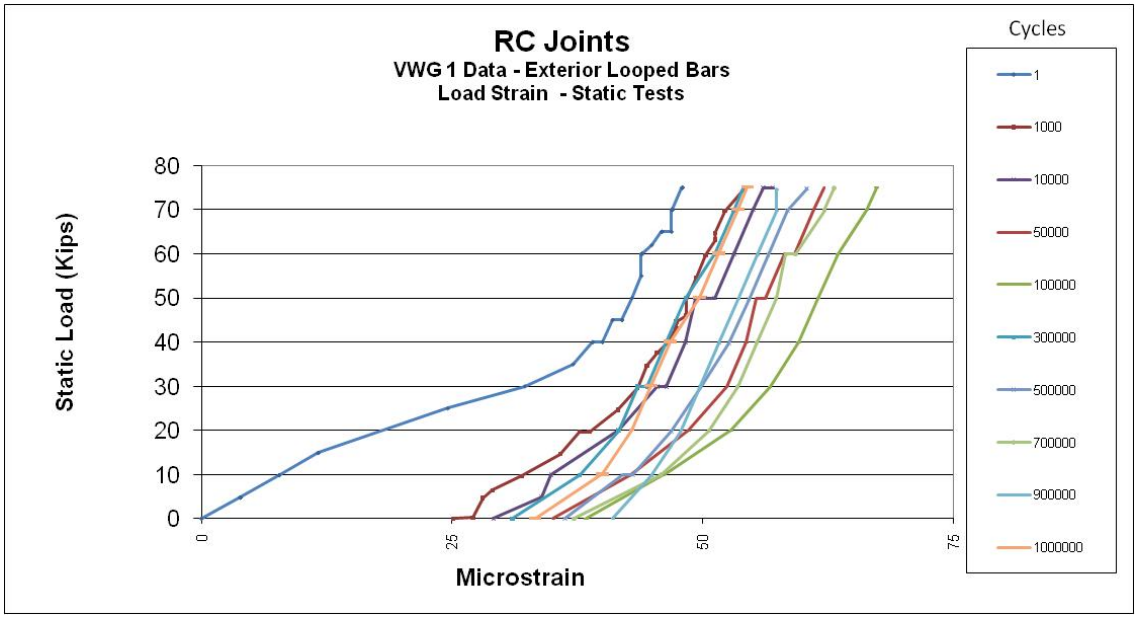

Figure 4-50 Panel Strain During Static Load Testing for a Looped Bar Joint

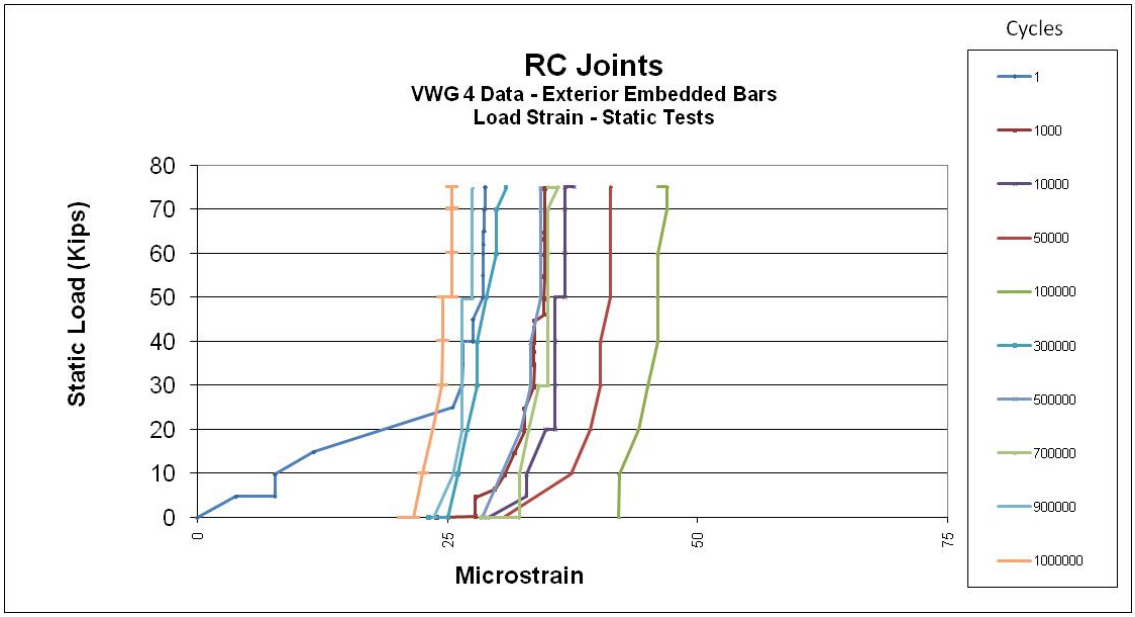

Figure 4-51 Panel Strain During Static Load Testing for the Embedded Bar Joint

Data acquisition began the day of the first test for the two post-tensioned joints with 167 psi of effective stress. The tests were started 20 days after stressing the strands. The average strain in both joints was consistent after the first 1000 cycles

(Table 4-14). After an initial peak in strain during the first static load, the average value began to level off around 40 microstrain during the first 50,000 cycles. The neat grout joint remained in the low 40 microstrain level until 500,000 cycles while the pea gravel grout joint moved toward the mid 30 microstrain level. After 500,000 cycles, the neat grout joint moved toward the mid 30 microstrain level too. Both joints slowly lost their ability to strain under service loads over time. The biggest loss was during the first 1000 cycles when the first crack occurred.

Table 4-14 Strain Range in the PT1 (167 psi) Panels During the Cyclical Tests

	Pea Gravel Grout			Neat Grout Only		
	Exterior	Interior		Exterior	Interior	
Cycles	**Range VWG1 Load Strain**	**Range VWG 2 Load Strain**	**Average Across Joint**	**Range VWG 3 Load Strain**	**Range VWG 4 Load Strain**	**Average Across Joint**
0	0.1	0.0	0.1	0.1	0.0	0.0
1	66.2	68.1	67.2	56.9	48.0	52.4
1000	51.4	50.3	50.9	50.6	42.0	46.3
5000	46.8	38.1	42.5	42.7	40.0	41.3
10000	45.5	35.9	40.7	41.3	38.9	40.1
20000	46.7	36.3	41.5	41.3	40.2	40.7
30000	44.3	36.6	40.4	41.3	40.4	40.9
40000	45.5	38.8	42.1	43.6	43.6	43.6
50000	46.3	40.5	43.4	45.2	42.5	43.8
100000	46.2	36.6	41.4	47.1	49.0	48.0
200000	40.8	34.1	37.5	41.8	44.7	43.2
300000	39.7	31.1	35.4	41.6	45.4	43.5
400000	40.4	31.8	36.1	43.1	46.1	44.6
500000	41.3	34.5	37.9	43.5	47.7	45.6
600000	32.8	28.0	30.4	30.9	28.0	29.4
700000	31.8	26.9	29.3	31.7	28.8	30.3
800000	33.5	28.7	31.1	33.5	30.6	32.1
900000	31.8	27.9	29.9	33.7	30.8	32.2
1000000	36.4	32.3	34.4	37.2	33.4	35.3

Figure 4-52 and Figure 4-53 show the strain progression in each of the post-tensioned joints with 167 psi of effective stress. For the extended grout joint, the strain exhibited a linear relationship with the load until 50 kips was applied. At this point the panel ceased to show an increase in strain. The same pattern was exhibited with the neat grout joint when 60 kips was applied. Both of these loads correspond to the first

cracking load. What separates these joints from the cast-in-place joints is the ability of the joints to restore strain after cracking. This linear strain range is constant because of the post-tensioned force. Only a small amount of strain increase was lost throughout the design life of the joint.

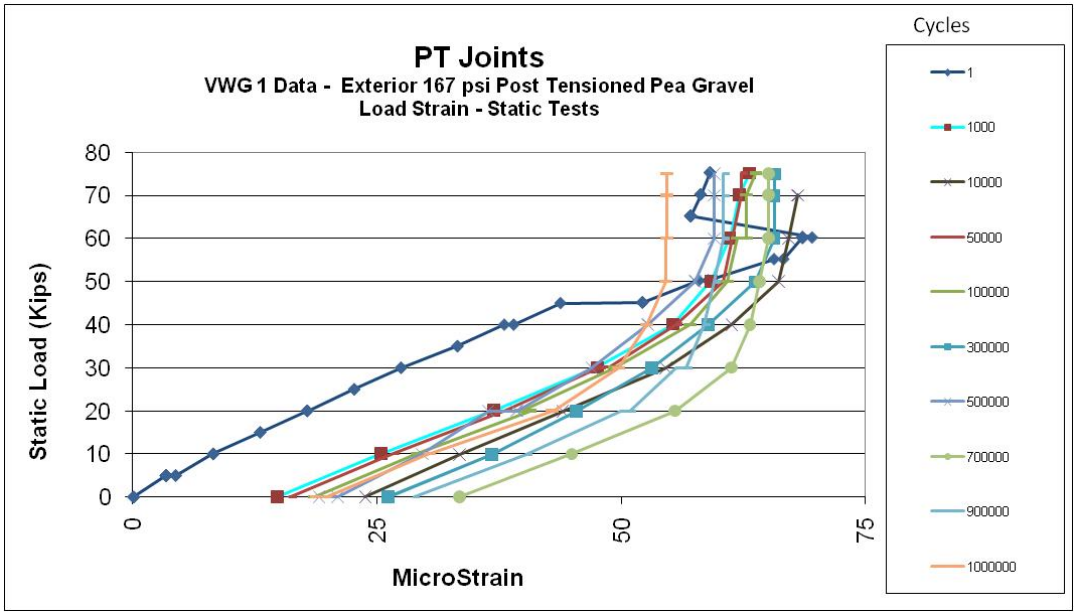

Figure 4-52 Panel Strain During Static Load Testing for the 167 psi Post-tensioned Joint with Pea Gravel.

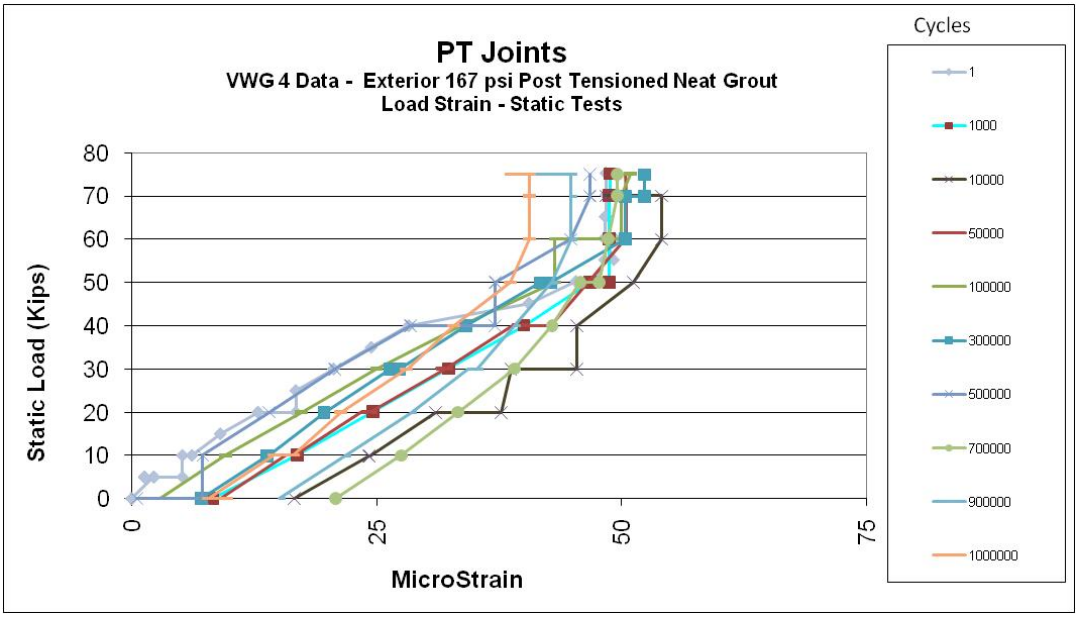

Figure 4-53 Panel Strain During Static Load Testing for the 167 psi Post-tensioned Joint with Grout

Data acquisition began the day of the first grout pour for the two post-tensioned joints with 340 psi of effective stress. The load tests were started 61 days after stressing the strands. The average strain in both joints did not drop a significant amount over the life of the joints (Table 4-15). After the first cycle, all four VWGs saw a small reduction in the amount of compressive strain in the panels. The average drop was 7 microstrain. In the neat grout joint, the strain increased to the initial values (more compression) within 50,000 cycles. Over the course of testing the neat grout joint did not see any permamant loss in strain. The epoxied joint saw approximately a 5 microstrain drop over the course of the testing. Overall, these joints had very consistent strain distributions throughout.

Table 4-15 Strain Range in the PT2 (340 psi) Panels During the Cyclical Tests

	Grout Only			Epoxied Grout		
	Exterior	Interior		Interior	Exterior	
Cycles	**Range VWG1 Load Strain**	**Range VWG 2 Load Strain**	**Average Across Joint**	**Range VWG 3 Load Strain**	**Range VWG 4 Load Strain**	**Average Across Joint**
0	0.7	1.8	1.2	1.4	2.0	1.7
1	67.5	107.8	87.6	92.4	72.3	82.4
1000	63.5	98.0	80.8	83.7	67.5	75.6
5000	65.4	98.1	81.8	86.6	69.3	78.0
10000	64.5	97.2	80.8	87.5	69.3	78.4
20000	69.3	103.8	86.6	81.7	62.9	72.3
30000	71.1	104.7	87.9	85.5	66.4	76.0
40000	71.1	105.6	88.4	88.3	67.3	77.8
50000	71.2	106.7	88.9	88.5	67.4	77.9
100000	73.0	108.6	90.8	90.2	68.3	79.2
200000	75.1	109.6	92.3	91.4	69.3	80.3
300000	75.0	109.5	92.2	91.3	68.2	79.7
400000	76.9	109.6	93.2	91.4	68.3	79.8
500000	77.1	110.7	93.9	93.4	69.3	81.4
600000	76.9	109.5	93.2	93.2	69.2	81.2
700000	77.9	112.4	95.2	94.2	70.2	82.2
800000	80.0	112.4	96.2	93.4	69.4	81.4
900000	77.8	109.5	93.7	91.3	68.2	79.7
1000000	75.9	107.6	91.8	88.4	66.3	77.4

Figure 4-54 and Figure 4-55 show the strain progression in each of the post-tensioned joints with 340 psi of effective stress. For the neat grout joint, the strain increased at a linear rate with little variation during the static load tests. The first static load was linear but had a slightly steeper slope, possibly due to a stiffer joint. The behavior was very consistent and predictable. The same pattern is exhibited with the epoxied grout joint. There is a very slight change in slope around 60 kips but it is barely detectable. This corresponds to the small cracking seen in the top of the joints under the full service load. The joints exhibit linear strain versus load behavior throughout. The linear strain range is constant because of the high initial post-tensioned force. Overall, these joints maintained their ability to strain elastically under loading throughout their design life.

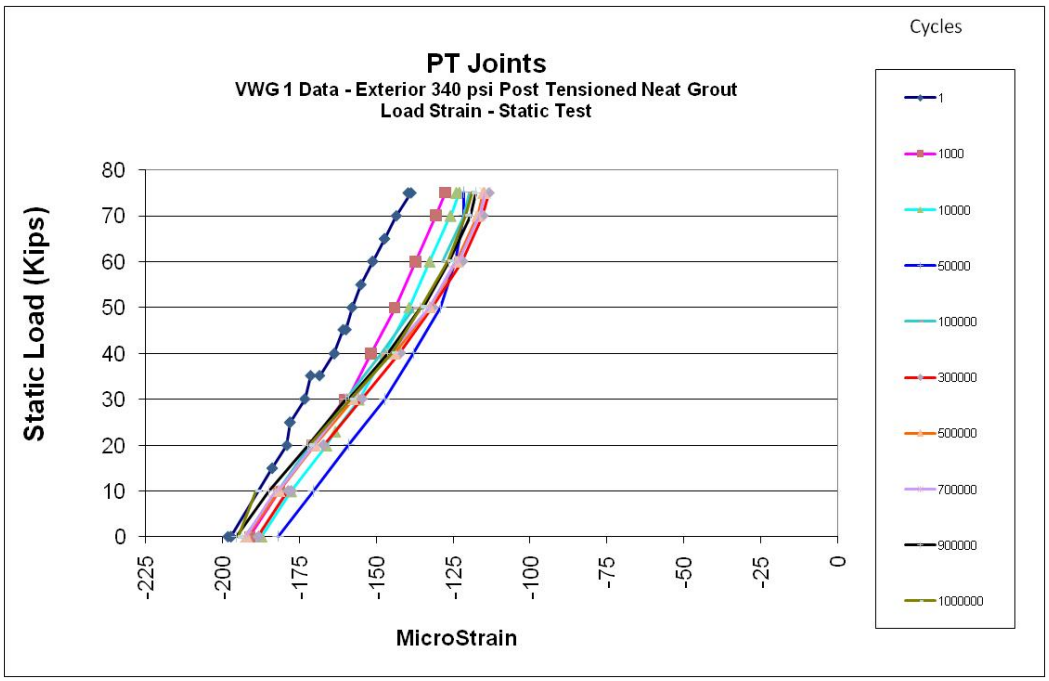

Figure 4-54 Panel Strain During Static Load Testing for the 340 psi Post-tensioned Joint.

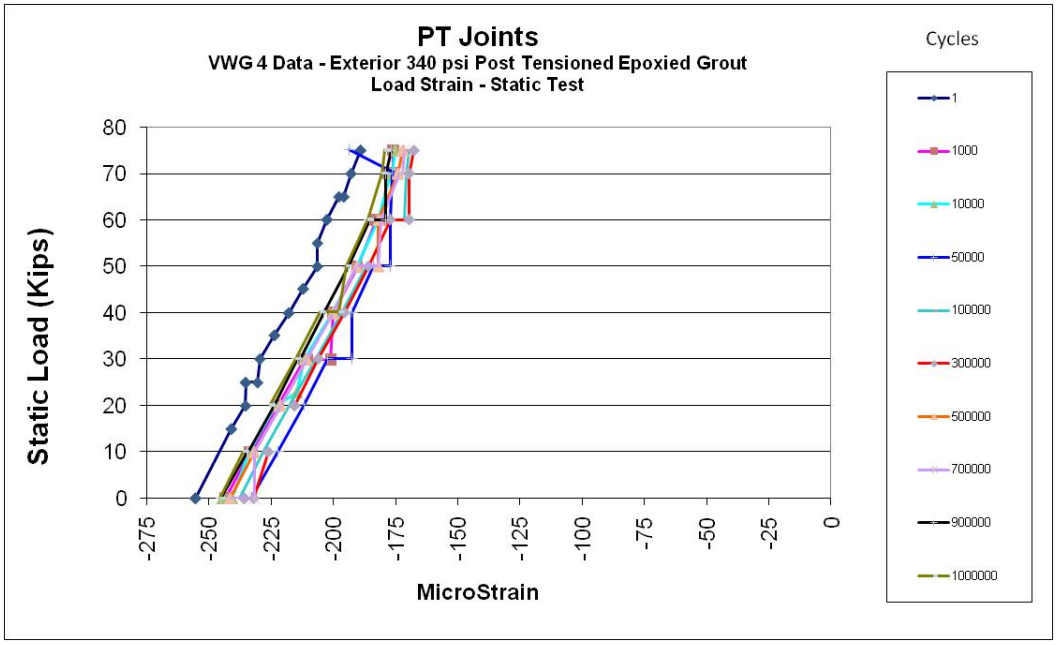

Figure 4-55 Panel Strain During Static Load Testing for the 340 psi Post-tensioned Joint with Epoxy.

The typical strain values measured by the DEMEC points after cracking are shown in Figure 4-56. Graphs A and B are of the cast-in-place joints and the 167 psi

post-tensioned joints. These graphs were both taken during the first 50,000 cycles and represent the shape of the load versus strain on the top surface of the joint. In these graphs there are pronounced changes in slope. Between 20-40 kips in each joint the graphs begin to increase in strain. Both of the reinforced joints and the 167 psi stressed joints looked similar and increased in strain. Among this group the looped bar joint had the smallest increase in strain.

In Figure 4-56, a typical graph of the strain increase is shown for the 340 psi stressed joints. This set of load versus strain data was taken at 1,000,000 cycles. These joints never significantly increased in strain. The strain gain was relatively linear throughout the testing. There is a slight bend around 50 kips but not a pronounced change in slope.

Figure 4-57 shows the maximum surface strains at different points in the cyclical loading. The joints with the 340 psi of effective stress had maximum strains around 500 microstrain. The looped reinforcing bar had the third smallest maximum strains around 1500 microstrain. These three joints had consistent strains that did not significantly deviate throughout the tests.

The joints with 167 psi of effective stress and the embedded bar joint had maximum strains between 2000 and 2500 microstrain. Their values continued to rise, particularly after 500,000 load cycles. These joints continued to lose stiffness as demonstrated by the increase in strain.

The patterns in the DEMEC readings confirm the conclusions seen in the strain profiles of the joints. Table 4-16 presents the strain during the first load and the maximum strain measured by the DEMEC points across each transverse joint. The highly stressed joints perform the best and have the lowest level of surface strain. The joints with the high surface strain did not have linear strain profiles throughout the profile (depth) of the transverse joint. The joints with low surface strains acted linearly throughout the strain profile.

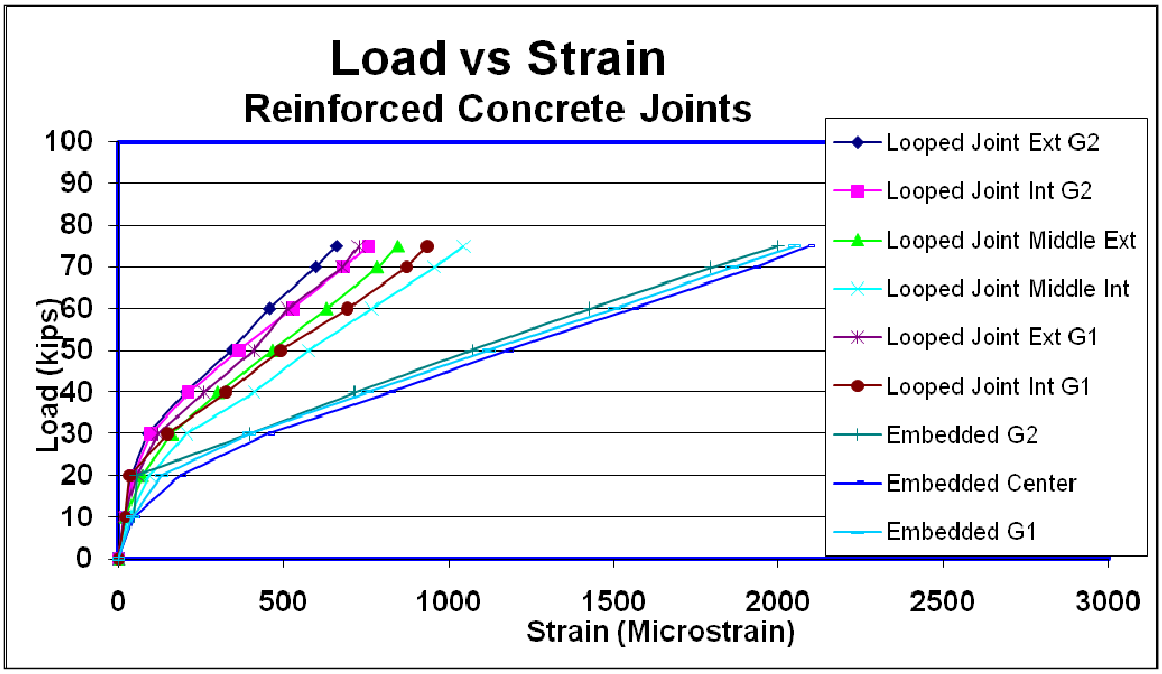

A) Reinforced Concrete Joints (40,000 Cycles)

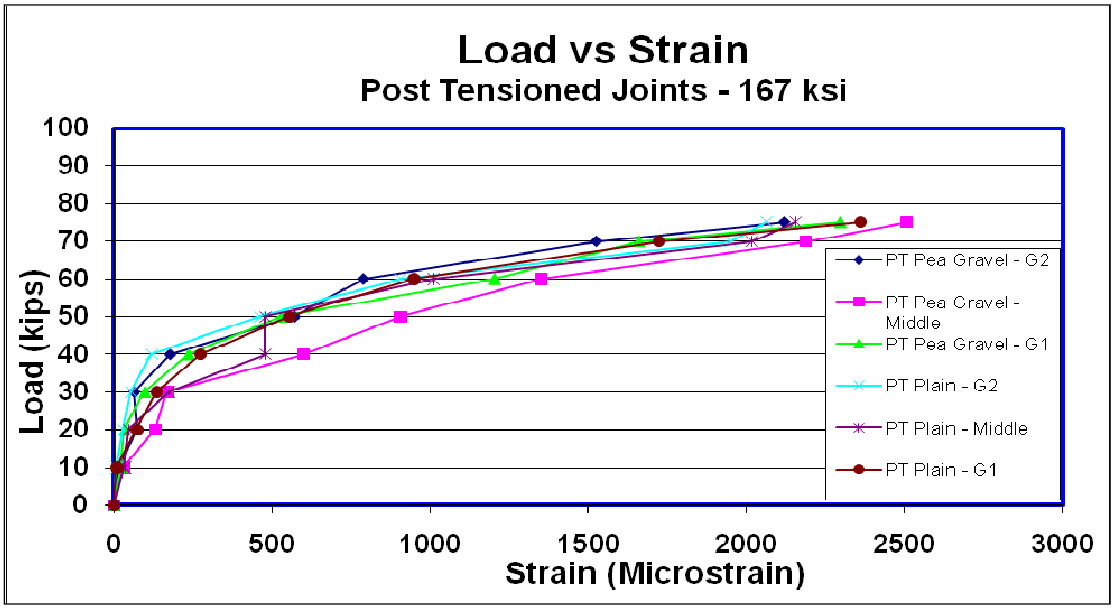

B) Post-tensioned Joint 167 ksi (20,000 Cycles)

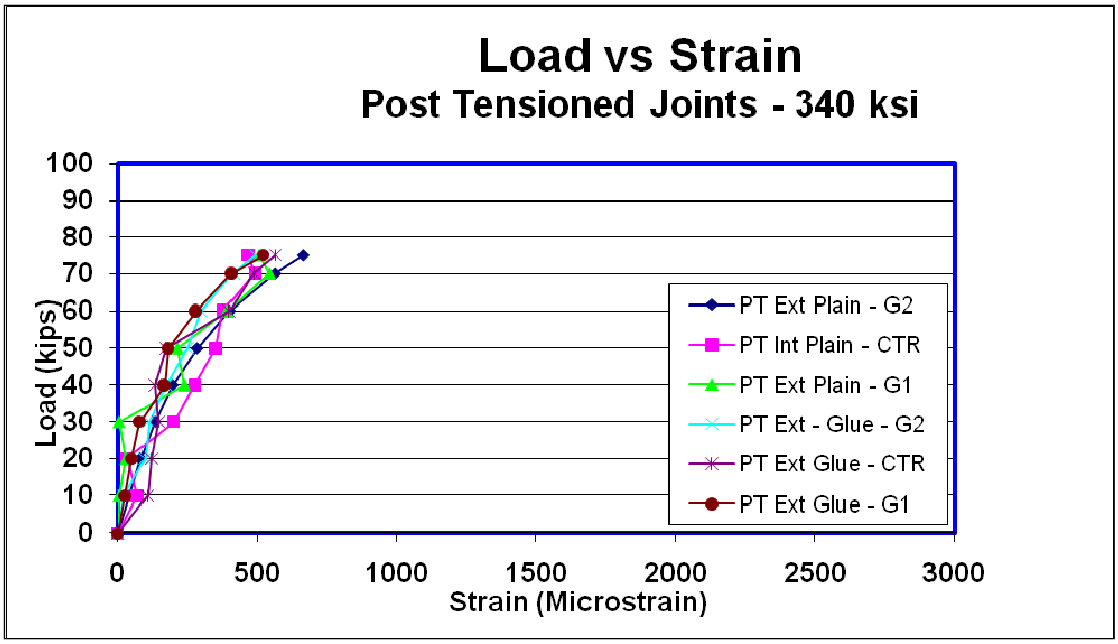

C) Post-tensioned Joint 340 ksi (1,000,000 Cycles)

Figure 4-56 Typical Load Versus Strain Measured by the DEMEC Points

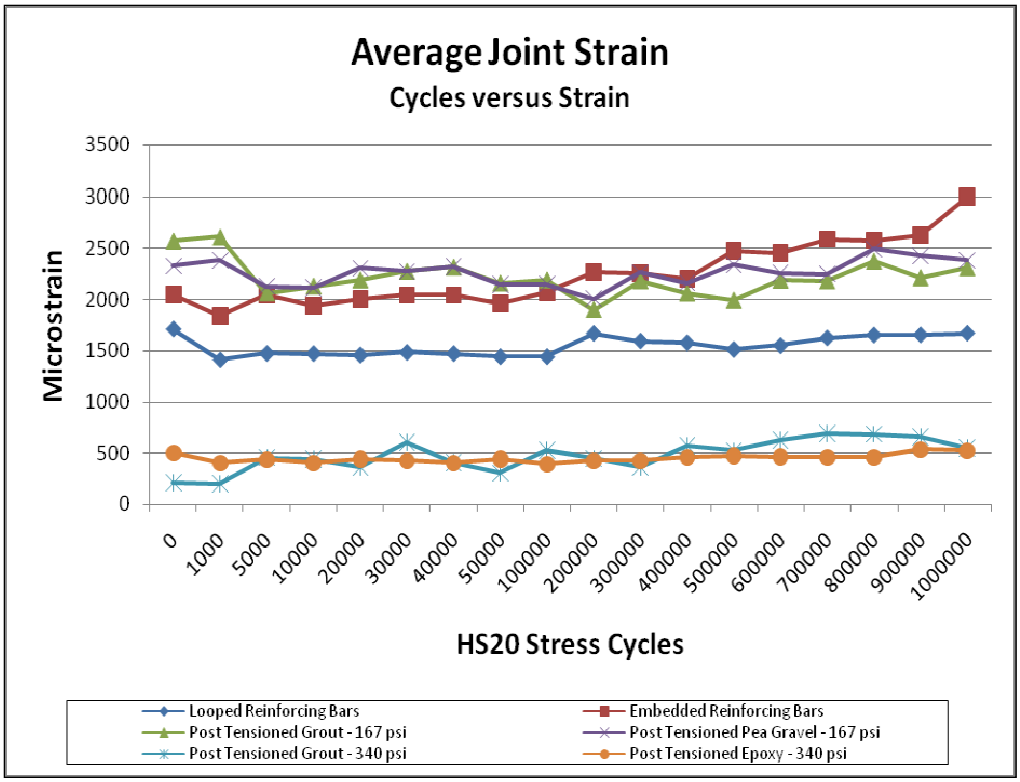

Figure 4-57 Maximum Surface Strain Under Service Loading (DEMEC Readings)

Table 4-16 The Average Range of Strain in Each Joint

Joint	First Cycle Maximum Strain (Microstrain)	Largest Maximum Strain (Microstrain)	Number of Cycles at the Maximum Strain
Large Looped Reinforcing Bars	1714	1714	0
Embedded Reinforcing Bars	2051	3004	1,000,000
Post-tensioned Grout – 167 psi	2573	2612	1000
Post-tensioned Pea Gravel Grout – 167 psi	2330	2491	800,000
Post-tensioned Grout – 340 psi	210	690	700,000
Post-tensioned Epoxy – 340 psi	502	533	900,000

4.1.7 Deflection of the Cantilevered Test

During each static load test, the maximum vertical deflection of the girders was measured directly beneath the loaded end of the cantilever test. A comparison was made of the maximum deflections versus the number of load cycles for each test setup. Figure 4-58 through Figure 4-60 show the progression of deflections during the tests. Table 4-17 shows the deflection at key points throughout the tests.

Table 4-17 Maximum Deflections of the Transverse Joint Tests

	Maximum Deflections (inches)		
Cycles	**Cast-in-Place**	**Post-Tensioned 167 psi**	**Post-Tensioned 340 psi**
1	0.464	0.420	0.386
10,000	0.425	0.394	0.384
20,000	0.397	0.394	0.399
100,000	0.419	0.394	0.399
500,000	0.417	0.405	0.409
1,000,000	0.433	0.398	0.412

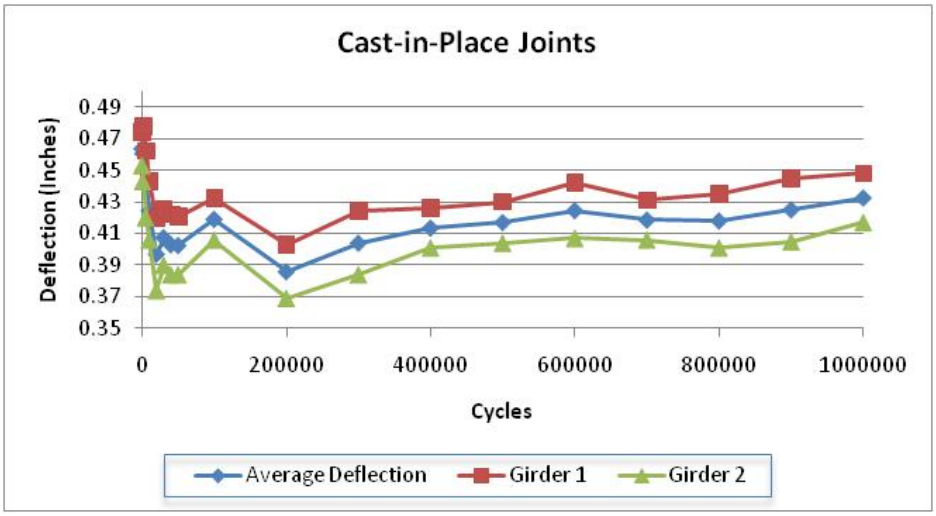

Figure 4-58 Maximum Deflection of the Girders versus Load Cycles – Cast-in-Place Joints

The cast-in-place deflections dropped during the first 10,000 cycles. These reductions were due to tightening the tie down points in the system. From 20,000

cycles through the end of the test the deflections slowly increased. The average maximum deflection of the girders at 20,000 cycles was 0.397 inches. The deflection slowly increased and peaked at 0.433 inches at the end of the test. The deflection increased 9.0% from 20,000 through 1,000,000 cycles.

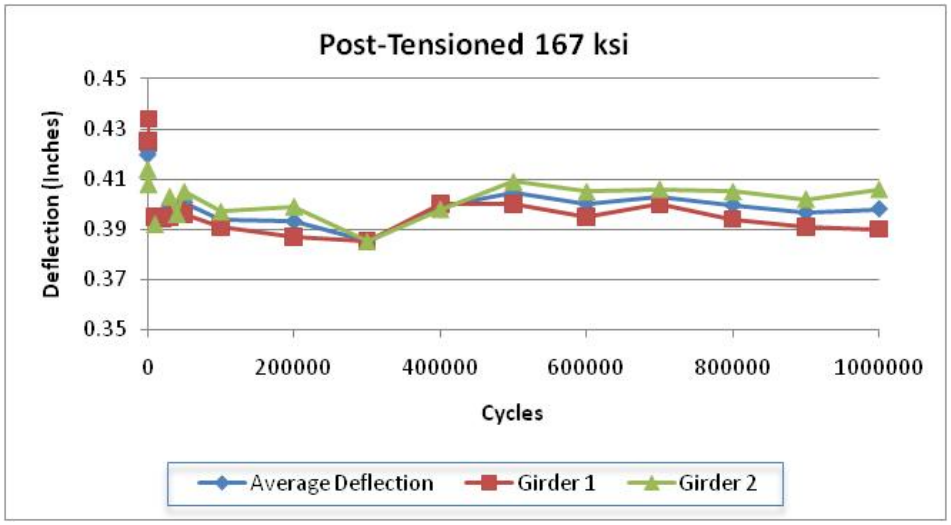

Figure 4-59 Maximum Deflection of the Girders versus Load Cycles – 167 ksi Post-Tensioned Joints

The post-tensioned joints with 167 ksi of effective stress dropped in deflection initially. This was due to tightening the tie down points during the first 10,000 cycles. By 10,000 cycles the system stabilized at a maximum deflection of 0.394 inches. The values increase to 0.405 inches at 500,000 cycles before finishing at a value of 0.398 inches. The maximum percent increase in deflection was 2.8%, however the final percent difference was 1.0%.

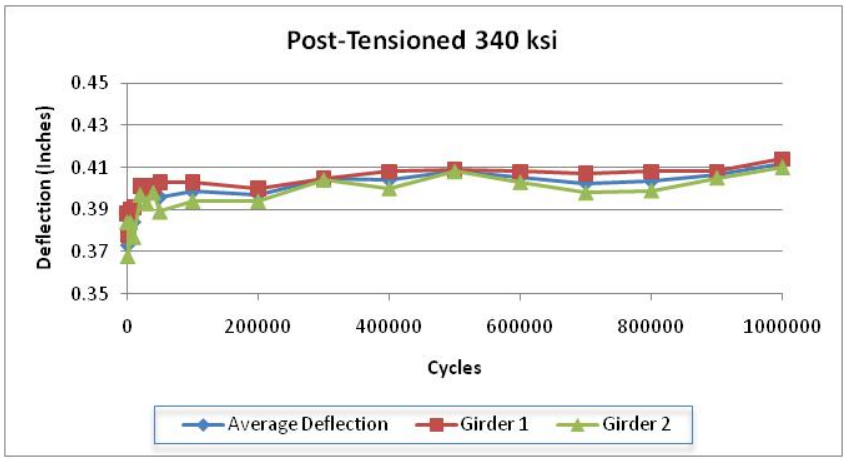

Figure 4-60 Maximum Deflection of the Girders versus Load Cycles – 340 ksi Post-Tensioned Joints

The post-tensioned joints with 340 ksi of effective stress increased in deflection initially. Unlike the previous two tests, the tie down was not tightened during the first 10,000 cycles. The previous two systems began with abrupt changes in deflection because the systems settled in place; therefore, the deflections from 10,000 cycles on were used for comparison in this system. By 20,000 cycles the system stabilized at a maximum deflection of 0.399 inches. The values increase to 0.412 inches by the end of the test. This corresponded to a maximum percent increase in deflection of 3.3%.

The post-tensioned systems increased in deflection the least throughout the tests. The 167 ksi system increased in deflection 2.8% while the 340 ksi system increased in deflection by 3.3%. When looking at the graphs in Figure 4-59 and Figure 4-60, the change in deflection over time is barely detectable.

The cast-in-place joints increased in deflection by a larger percent over their design life. The final value was 9.0% more than the value after 20,000 cycles. However, unlike the post-tensioned joint pairs in the previous tests, these two cast-in-place joints were very different from one another. It must be noted that the deflection accounts for loss in stiffness in both joints.

The initial deflections in all three tests for the first 10,000 cycles were not used. This was due to constructability problems in the first two tests. The tie down rods would lose initial stiffness and need to be retightened early in the tests. The last post-

tensioned test was not retightened. It exhibited an early increase of deflection of 3.4% not accounted for in the comparison above.

4.2 Grout Results

Transverse joints, shear pockets, and post-tensioned blockouts are filled with grout on precast full depth deck panels. In the first two sets of transverse joint tests extensive cracking was observed around the shear pockets. In the second post-tensioned transverse joint test, additional grouting procedures were used to prevent cracking. The results led to the final laboratory tests on grouts in circular shear pockets. Thirty-Eight grouted rings were made with different grouts, concretes, and surface preparations. Cracking, ponding, and strains were measured on each sample. A list of the best grouts and surface conditions for precast panel blockouts was produced.

4.2.1 Transverse Joint Grouts

4.2.1.1 Grout Observations on the First Two Transverse Joint Tests

On the first two transverse joint tests, Five Star Highway Patch grout was used on all the haunches, shear pockets, and haunches. This grout was chosen because the producer sells it as a low shrinkage, high early strength grout and it had performed satisfactorily in previous tests. During the tests, observations were made of all cracking that occurred on the surfaces of the panels. This included close inspection of the shear pockets.

On each transverse joint test there were twelve shear pockets. The panels were all doubly symmetric and had four pockets (Figure 4-61). Inside each pocket, eight shear studs were welded to the steel girder beneath the panels. The pockets were then filled with high early strength, low shrinkage grout to make the system composite. The grout was cured and ready for use within twenty-four hours.

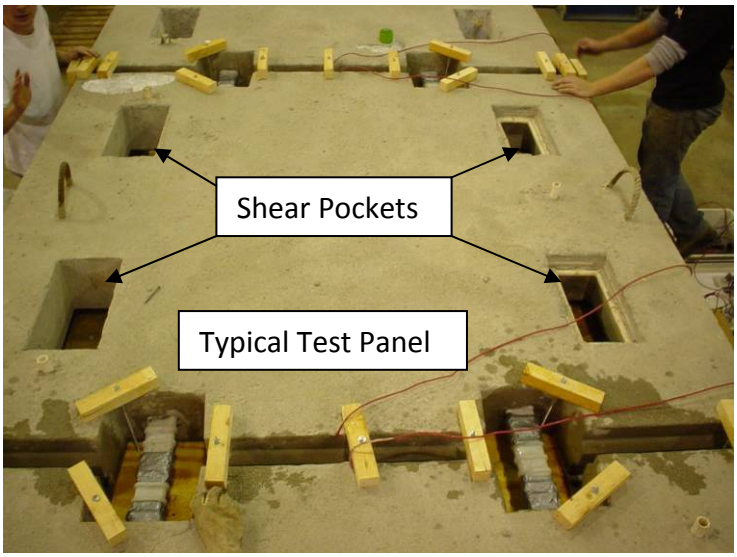

Figure 4-61 Pocket Layout on the Test Panels.

The first setup was built with two cast-in-place joints. Both joints were cast along with the shear pockets and haunch. This was done with one continuous pour on a spring afternoon in early May with temperatures in the mid 60's and 50-60% humidity (Table 4-18). The panels were then tested one week later in a controlled environment. The grout remained in the laboratory conditions; low humidity and temperatures between 60-70˚F. Throughout the tests there were no shrinkage cracks observed in the shear pockets. The grouts were observed from the day of their pour through the end of the testing or approximately 42 days. The performance was considered satisfactory.

The second test setup was built after the first one in the same laboratory with the same type of grout. The procedures were exactly the same. The blockouts had been formed against a smooth piece of plywood in the precast plant and were extremely smooth (Figure 4-62). The blockouts were prepared by wetting them down to a moist surface condition prior to grouting. The only difference in this pour was the grout was placed in the shear pockets and haunches at the same time. The pour was done at the end of July with highs around 70˚F and 100% humidity (thunderstorms all afternoon) (Table 4-18).

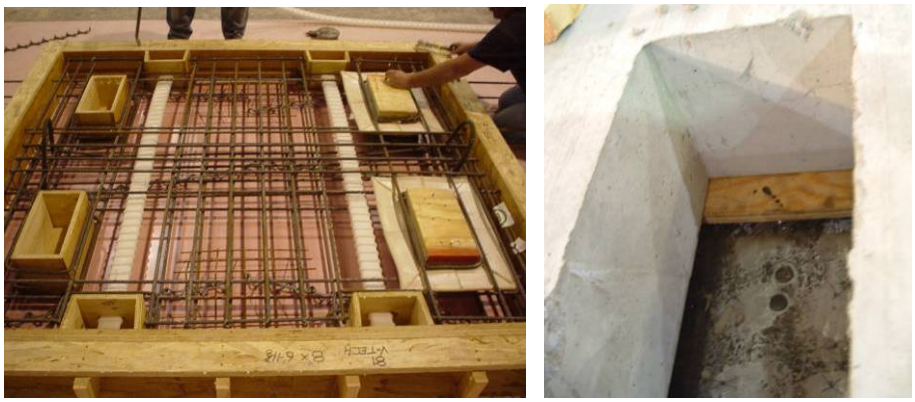

Figure 4-62 Casting Formwork and Final Blockout Condition.

The grouts in the second test began to shrink right after the pour. In this specimen, cracks appeared the day after grouting around the edge of half of the blockouts. At the beginning and end of the load test, the average widths were measured using a crack card (0.005 in. accuracy). Average widths were computed by taking the width measurements around the entire perimeter of the blockout. The average widths of each pocket are listed in Table 4-19. A typical crack pattern is shown in Figure 4-63. The number of cycles was written next to the crack as it became visible in the test. The cracks were nearly ubiquitous between the panels and grout in the second test. The extensive cracking warranted further investigation.

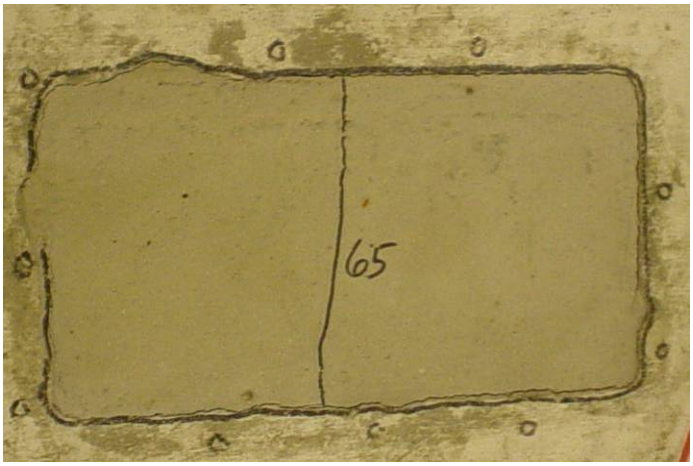

Figure 4-63 Typical Shrinkage Crack Patterns in the Shear Pockets Prior to Loading

Table 4-18 Average Weather Conditions When Grouting the Shear Pockets

Panel Test	**Temperatures – Day of the Grout Pour**	**Humidity – Day of the Grout Pour**
#1 – Reinforced Joints	64 Degrees Inside/Outside	50-60% Humidity
#2 Post-tensioned – 180 psi	70 Degrees Outside/Inside	100% Humidity – Thunderstorms
#3 Post-tensioned – 340 psi	70 Inside, Low 60's Outside	100% Humidity – Rainy Day

Table 4-19 Average Crack Widths in the Shear Pockets of the Second PT panels

Pocket Number	Initial Average Width (14 Days)	Final Average Width (53 Days)	Percent Difference
	(Inches)	(Inches)	(%)
1	0.012	0.008	-28.6
2	0.016	0.022	34.6
3	0.018	0.019	3.4
4	0.014	0.013	-8.7
5	0.016	0.019	19.2
6	0.017	0.015	-10.0
7	0.005	0.005	0.0
8	0.008	0.006	-16.7
9	0.013	0.021	65.0
10	0.019	0.023	23.3
11	0.009	0.012	26.7
12	0.005	0.005	0.0
Average	**0.013**	**0.014**	**11.1**

4.2.1.2 Grout Testing in the Shear Pockets on the Third Transverse Joint Test

On the third test specimen, new bonding techniques between the concrete panels and the grouts in the pockets were investigated. Six different types of joining methods were used. The first method was a control specimen built with the original smooth, moistened concrete. The second method had a roughened surface. It was constructed by placing a retarder on the pocket surface prior to casting at the precast plant. The paste was then sprayed off with water when removing the forms approximately 18 hours later. The third method employed sand blasting the surface of

the pocket after removing the formwork at the precast plant. The fourth method was to apply a concrete epoxy to the pocket approximately thirty minutes (per the manufacturer's recommendation) prior to placing the grout in order to bond the surfaces. The fifth method was to place a water stop in the panel during casting that fit across the joint between the concrete and grout. The six and last method was to place a grout paste on the surface of the pocket approximately one hour before pouring the grout. The six methods are as follows:

1. Control (Wetted Surface)
2. Epoxy Coated
3. Sand Blasted
4. Exposed Aggregate
5. Water Stop
6. Grout Paste

Each method was monitored throughout the cyclical loading of the last post-tensioned specimen. Crack widths were measured from the day of the first test until the conclusion of the cyclical loading. Observations were made from February 5, 2008 to April 19, 2008 or 74 days.

Table 4-20 shows the difference between the pockets in the first post-tensioned test and the new pockets. There is also a comparison between the two control pockets and each test pocket in this table. The first post-tensioned pockets were all built the same way as the control pockets in the second post-tensioned test. Average crack widths closer to the control pocket crack widths have a smaller percent difference in the table. The larger percent different (bigger negative values) are the pockets that had the smallest average crack widths. The larger percent difference is desirable because these pockets cracked less.

The control and epoxy coated pockets consistently had the largest cracks among all of the tests. The water stop and sandblasted joints consistently performed well. The exposed aggregate and grouted pockets exhibited average crack sizes. The average widths of all the cracks are shown in Table 4-20. This table compares the average values for each sample with the average crack widths in the control pockets. The control pockets had the largest average widths at 0.009 in. The average control pocket crack sizes are from the first and second post-tensioned tests. In Table 4-21 the overall average crack sizes are compared with the average crack size in the control pockets. The larger negative values represent smaller average crack sizes for the respective surface condition.

Table 4-20 Average Crack Widths in the Grout Pockets in the Second PT Panels.

Shear Stud Pocket Type	Final Average Width	Percent Difference from **Control Average P/T Test #1**	Percent Difference from **Control Average P/T Test #2**
	(Inches)	(%)	(%)
1 – Sand Blasted	0.003	-77.7	-64.3
2 – Exposed Aggregate	0.006	-59.8	-35.7
3 – Control	0.008	-46.4	-14.3
4 – Control	0.010	-28.6	14.3
5 – Epoxy	0.006	-59.8	-35.7
6 – Epoxy	0.009	-37.5	0.0
7 – Sand Blasted	0.001	-91.1	-85.7
8 – Exposed Aggregate	0.002	-86.6	-78.6
9 – Water Stop Melted Joint	0.003	-82.1	-71.4
10 – Water Stop Epoxied Joint	0.002	-86.6	-78.6
11 – Grout	0.005	-64.3	-42.9
12 – Grout	0.001	-91.1	-85.7
Average	0.005	-67.6	-48.2

Table 4-21 Percent Difference among Crack Sizes in the Grout Pockets

	Percent Difference from **Control Average PT Test #2**
Material	(%)
Control	0.0
Sand Blasted	-75.0
Exposed Aggregate	-57.1
Water Stop	-75.0
Grout	-64.3
Epoxy	-17.9

A ponding test was performed on the shear pockets during the cyclical testing. This was accomplished with same procedures used in the ponding tests for the joints. At set intervals, the surface was ponded with water for two hours. The bottom outer edges of the pockets were monitored for leaks. The pockets did not have a clearly identifiable interface on the bottom of the panels because they intersected the haunch (Figure 4-64). In these tests, the haunch forming material was removed so that any water that filtered through the pocket and the haunch could be observed. Table 4-22 shows qualitative results observed during the tests.

Table 4-22 Ponding Results on the Shear Pockets

Cycles	Control	Grouted Surface	Water Stops	Epoxy	Exposed Aggregate	Sand Blasted
0	None	None	None	None	None	None
1	None	1-Complete Leak	None	None	None	None
10000	None	1-Complete Leak	None	None	None	None
50000	2-Partial Leaks	1-Complete, 1 Partial	None	None	1-Partial Leak	None
100000	2-Partial Leaks	1-Complete	None	None	2-Partial Leaks	None
500000	2-Partial Leaks	1-Complete, 1 Partial	None	None	1-Partial Leak	1 Very Slight
1000000	1-Partial Leak	2-Complete	1 Slight Vertical Leak	2 Slight	1-Partial Leak	1 Slight

The joints that leaked the least were the epoxied joints, the joints with water stops, and the sand blasted joints. The exposed aggregate was satisfactory but the control and grouted surface both performed poorly (Figure 4-64). The control joints consistently leaked the most. One of the grouted surface joints had a small imperfection that caused the leaking to appear severe, however the other grouted surface joint also leaked considerably. The one leak in the water stop joint was in a vertical crack that appeared to extend beyond the width of the water stop in the center of the joint.

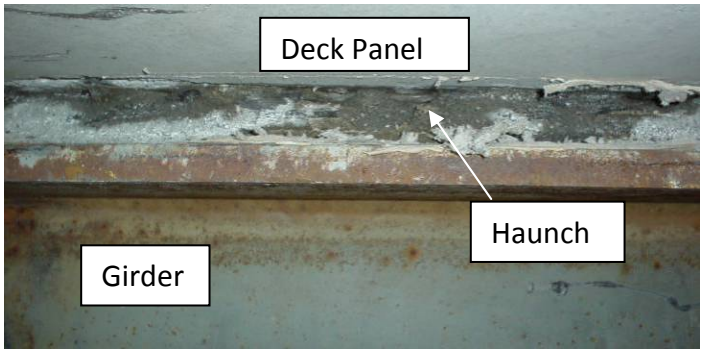

Figure 4-64 Complete Leaking in the Haunch beneath a Shear Pocket Joint

The sand blasted and water stopped joints performed the best in both tests. They consistently cracked the least and leaked water infrequently. The exposed aggregate was satisfactory in both cases. The grouted surface was satisfactory in terms of crack width but leaked too much. The epoxied blockouts cracked significantly but did not exhibit many leaks. The control was the worst in both cases and showed that some form of treatment is needed to alleviate some of the cracking problem.

4.2.2 Grouted Ring Results

The results from the transverse joint shear pocket tests demonstrated the need for further investigation of the grouts. The grouted ring tests were built to test a wider number of grouts and surface characteristics. Thirteen different unique pockets were tested. The material properties were recorded along with the performance of the shear

pocket rings. A correlation was made between the materials and performance of the tests.

4.2.2.1 Constructability

The amount of work and time required to build each pocket varied. On a bridge deck such as the demonstration bridge in Virginia there will be dozens of shear pockets. The amount of extra time and work needed to build the deck may increase the overall cost. Table 4-23 lists the 13 unique samples and the additional construction processes for the respective methods.

Table 4-23 Shear Pocket Construction Processes

Surface Condition	Grout Type	Unique Construction Processes
Wet Surface (Control)	Five Star	
	Five Star/Pea Gravel	-Add Pea Gravel to the Grout
	Five Star/Fibers	-Add Fibers to the Grout
	Set 45	-Install Grout within 5 Minute Work Time
	Type K Cement	-Mix a Complete Concrete -Cures in 24 hours
Exposed Aggregate	Five Star	-Retard Concrete Pockets/Spray with Water 24 hours after pouring
	Five Star/Pea Gravel	-Retard Concrete Pockets/Spray with Water 24 hours after pouring -Add Pea Gravel to the Grout
Epoxy	Five Star	-Apply Epoxy Coating ~30 Minutes Prior to Grouting
	Five Star/Pea Gravel	-Apply Epoxy Coating ~30 Minutes Prior to Grouting -Add Pea Gravel Grout
Wire Brush	Five Star	-Wire Brush the Concrete Pocket Prior to Grouting
	Five Star/Pea Gravel	-Wire Brush the Concrete Pocket Prior to Grouting -Add Pea Gravel Grout
Shear Key	Five Star	-Cut and Install a Shear Key when Casting the Panels
Water Stop	Five Star	-Cut, Shape, and Install a Water Stop when Casting the Panels

The processes listed were performed in addition to the typical procedures used on a control specimen (i.e. a wetted surface with neat grout). The four pea gravel grout

pockets required a negligible amount of additional work. The pea gravel was added while mixing and required care when placing the grout in the pockets. Segregation could occur between mixing and pouring. The addition of polypropylene fibers was difficult. The fibers tended to bunch together in the mixer and stick to the blades and sides of the mixer. After a failed attempt using the mixer, the fibers were added to the mix by hand after mixing. This took an extra 2-3 minutes per batch. The Type K cement required additional time to measure out the materials. A mix design with water, course aggregate, cement, and sand was used. The actual mixing did not take any additional time. The Set 45 grout left no room for error or flexibility. The grout reached an initial set within 5 minutes from the point water was added. While the fast set time could be desirable for quicker construction, it was very difficult to use. All of the grouts except the Set 45 were easy to use and had a sufficient workability. The pea gravel Five Star and polypropylene fiber mixes required care to prevent segregation of the materials.

The surface preparation techniques required different levels of effort. The exposed aggregate surface required brushing a retarder on the formwork for each pocket prior to pouring the concrete. Once the formwork was removed, each pocket had to be hosed down with high pressure water. This process took about an hour for six specimens. It was performed within 12-24 hours after placing the concrete. In a precast yard, the process would likely be quicker.

The epoxy coating and wire brushed surfaces took a small amount of time. Each pocket could be wire brushed in less than a minute. The wire brushing was not time dependent and could be accomplished days ahead of time. The epoxy coating was added between 15 and 30 minutes before pouring the grout. The epoxy coating would require careful application on a large project were grout is added over a long period of time.

The shear keys and water stops require coordination with the precaster who makes the panels. The shear keys require an additional forming process inside each shear pocket. This process took an additional hour of work to cut and install the formwork for the 3 test pockets. The water stops also required significant additional

work. The water stops had to be cut and glued into the formwork. Once both the shear key and water stops were cast, the formwork was harder to remove and took extra time. These two methods required the most additional work.

All of the grouts took approximately the same amount of time to install except for Set 45. It required less time but left a very limited workable range. The control surface condition was easiest to build followed by the wire brushed surface. The exposed aggregate and epoxy coating were not difficult but required careful time management. The shear key and water stops took a significant amount of additional time and required coordination with the precaster.

4.2.2.2 Material Properties of the Grout Tests

Material properties were recorded for the concrete rings and the five cementitious materials used in the blockouts. The recordings began the day after pouring the material and continued through the end of testing. This included: compressive strength, Poisson's ratio, elastic modulus, and shrinkage.

4.2.2.2.1 Compressive Strengths

The concrete was designed as a VDOT 4000 psi post and rail bridge deck mix. The strength gain was rapid for the first 7 days and then tapered by 28 days. The grout was poured on day 42 of the concrete life. The goal of having an approximate concrete strength of 5000 psi was met (Table 4-24).

Table 4-24 Concrete Strength

Days	Average Concrete Strength (psi)
1	2090
7	3820
28	5010
42	4960
56	4970

The grouts were mixed with the proportions recommended by their respective manufacturers. The Type K mix was designed from the manufacturer's published mix for bridge decks. The mixes were all designed for bridge deck rehabilitation and repair. The tested strengths are in Table 4-25.

Table 4-25 Grout Strengths

	Average Grout Strengths (psi)				
Days	Five Star	Five Star with Pea Gravel	Five Star with Polypropylene Fibers (1 in.)	Type K Concrete	Set 45*
1	3113	2508	2663	3538	2167
7	3733	3100	3208	4517	2542
28	3525	3050	3088	5308	2875

*The cubes were damaged during removal and resulted in low strengths

The neat Five Star Highway Patch Grout had a 28 day strength stronger than the Five Star mixes with additives. All of the Five Star mixes gained strength in the first 7 days and dropped slightly in strength between 7 and 28 days. As expected, most of the strength gain for the Five Star grouts was in the first day. The Five Star grouts with additives had 28 day strengths approximately 13% less than the plain Five Star Grout.

The Type K concrete mix continued to gain strength after 7 days. The highest strength was at 28 days. This mix had the highest strength gain of all the materials at 1, 7, and 28 days.

The Set 45 grout was very difficult to pour and very difficult to demold. The Set 45 adherred to the 2 in. by 2 in. forged bronze molds. The corners chipped off the cubes during demolding, therefore the strengths were low. In most samples, $^1/_4$ to $^1/_3$ of the surface area of the cube was damaged.

In general, the mixes had lower strengths than expected. The grouts were expected to reach between 4000 psi and 5000 psi at 7 days. One reason may have been that the Five Star grouts sat in the lab for approximately 1 year, the maximum amount allowed per the manufacturer. Another reason could be that the maximum amount of water was added to the grouts for workability.

4.2.2.2.2 Elastic Modulus and Poisson's Ratio

The elastic modulus and Poisson's ratio were measured for the concrete and grout using an extensometer and compressometer (Figure 4-65). Measurements were taken while loading 4 in. by 8 in. concrete and grout cylinders. The cylinders were loaded to approximately 40% of the ultimate strength, keeping the cementitious materials within the elastic range. Data was taken a minimum of two times for each sample. Three samples were used each time data was acquired. The longitudinal stress and strain were graphed and a best fit line was inserted. The slope of the line represented the elastic modulus (Figure 4-66). The transverse and longitudinal strains were graphed and a best first line was inserted (Figure 4-67). The slope of this line represented the Poisson's ratio of a sample.

Figure 4-65 Compressometer and Extensometer on a Concrete Cylinder

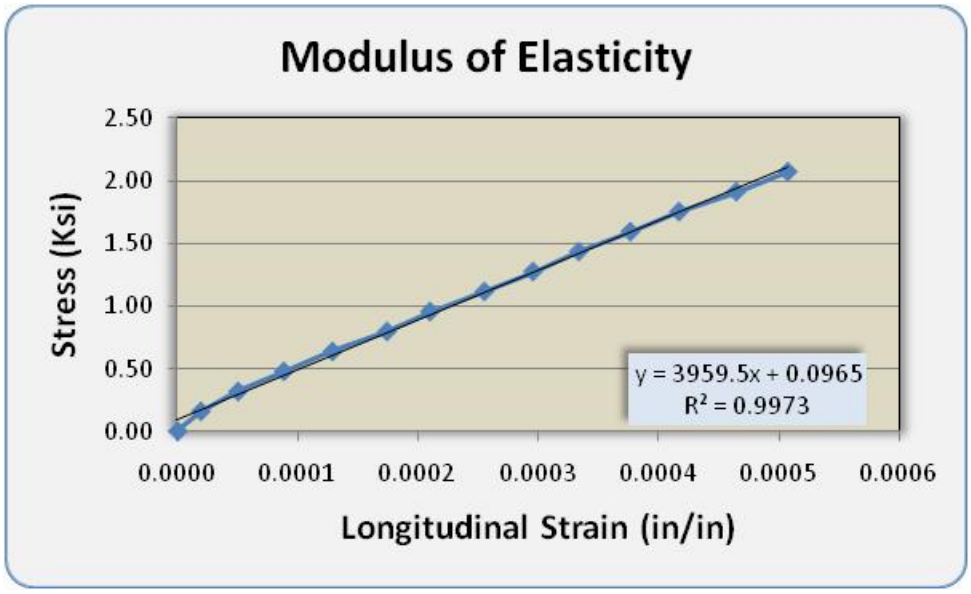

Figure 4-66 Typical Modulus of Elasticity Graph

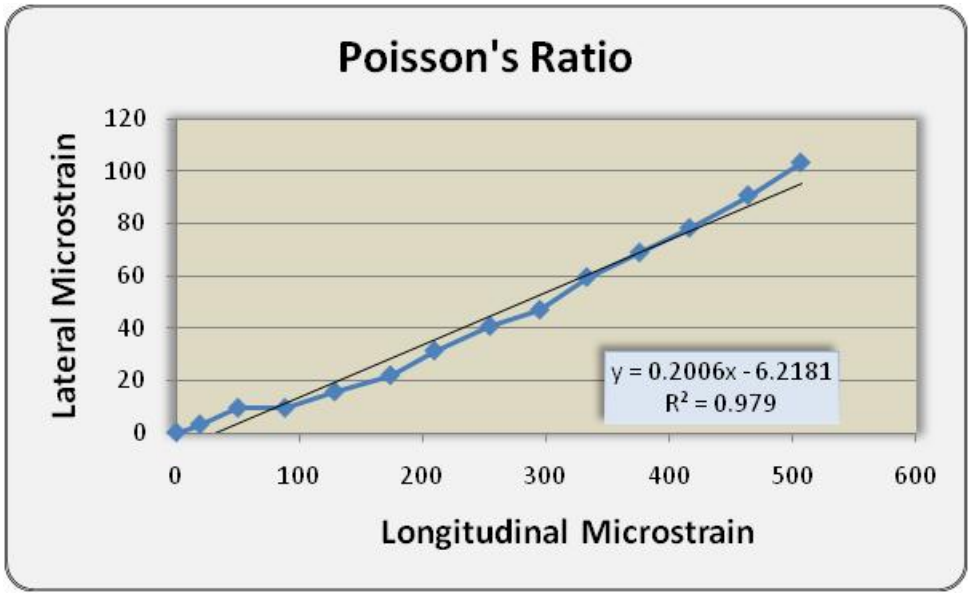

Figure 4-67 Typical Poisson's Ratio Graph

The concrete moduli and Poisson's ratios were close to the suggested values in ACI 318-08 and AASHTO LRFD, respectively (Table 4-26). (The AASHTO LRFD concrete modulus equation is the same as the ACI 318-08 equation). With the exception of the 1 day values, the predicted moduli and average measured values were within 211 ksi

(5.2%). All of the predicted values using ACI 318-08 (and AASHTO LRFD) were within one standard deviation of the average measure value. The same pattern was seen with the Poisson's ratios; the values were all within 0.02 except for the value at 1 day. The predicted AASHTO LRFD value of 0.2 was within one standard deviation of the average measured values at every point except 1 day (10%). This data confirmed past research and current design standards.

Table 4-26 Moduli and Poisson's Ratios of the Concrete

Age	Strength	Modulus of Elasticity (ksi)		Poisson's Ratio		Modulus of Elasticity	Poisson's Ratio
(Days)	(psi)	ACI 318-08	Average	AASHTO LRFD	Average	Standard Deviation	Standard Deviation
1	2090	2600	3010		0.13	157	0.015
7	3820	3520	3530		0.20	251	0.006
28	5010	4040	4020	0.20	0.19	95	0.014
42	4960	4010	3990	0.20	0.19	251	0.021
56	4970	4020	3890	0.20	0.18	57	0.017
84	4970	4020	3810	0.20	0.20	236	0.017

The Five Star grout consistently had modulus of elasticities lower than the ACI prediction but Poisson's ratios very close to the AASHTO LRFD values (Table 4-27). ACI consistently predicted moduli 20% higher. The ACI 318-08 commentary, R8.5, mentions that values typically range within 20% from the estimated value. Typical concrete has course aggregate, however the Five Star grout had only fine aggregate. This may have contributed to the lower modulus of elasticities. It must be noted that two of the three values were taken while the grout was a week old or less. The Poisson's ratios were typically between 0.16 and 0.20. The Poisson's ratios were very consistent from the first day through the end of testing.

Table 4-27 Moduli and Poisson's Ratios of the Five Star Grout

Age	Strength	Modulus of Elasticity (ksi)		Poisson's Ratio		Modulus of Elasticity	Poisson's Ratio
(Days)	(ksi)	ACI 318-08	Average	AASHTO LRFD	Average	Standard Deviation	Standard Deviation
1	3110	3180	2600		0.16	85	0.004
7	3730	3480	2770		0.20	133	0.034
14			2740		0.17	85	0.069
21			2750		0.16	260	0.030
28	3530	3380	2700	0.20	0.17	33	0.012
42			2530	0.20	0.20	61	0.006
56			2800	0.20	0.17	415	0.033

The modulus of elasticity for the Five Star grout with pea gravel was lower than the predicted values based on ACI 318-08 (Table 4-28). The values were approximately 29% lower than predicted. The Poisson's ratios were very similar throughout ranging from 0.17 to 0.18. These values are slightly less than the 0.20 AASHTO LRFD estimate.

Table 4-28 Moduli and Poisson's Ratios of the Five Star Grout with Pea Gravel

Age	Strength	Modulus of Elasticity (ksi)		Poisson's Ratio		Modulus of Elasticity	Poisson's Ratio
(Days)	(psi)	ACI 318-08	Average	AASHTO LRFD	Average	Standard Deviation	Standard Deviation
1	2510	2860	2090		0.17	139	0.027
7	3100	3170	2250		0.18	50	0.017
14			2340		0.17	148	0.025
21			2340		0.18	26	0.003
28	3050	3150	2230	0.20	0.17	60	0.012
42			2180	0.20	0.17	67	0.005
56			2200	0.20	0.17	58	0.024

The Poisson's Ratios for the Set 45 were very close to 0.20 throughout (Table 4-29). The moduli values were significantly higher for every value after the first day. At 1 day the value was within 3% of the predicted value. At 7 and 28 days the moduli were 80% to 90% higher than predicted. The moduli predictions for the Set 45 were consistently much smaller than measured values.

Table 4-29 Moduli and Poisson's Ratios of the Set 45 Grout

Age	Strength	Modulus of Elasticity (ksi)		Poisson's Ratio		Modulus of Elasticity	Poisson's Ratio
(Days)	(psi)	ACI 318-08	Average	AASHTO LRFD	Average	Standard Deviation	Standard Deviation
1	2170	2650	2720		0.23	83	0.028
7	2540	2870	5400		0.22	1320	0.067
14			5060		0.18	129	0.044
21			5520		0.19	546	0.034
28	2880	3060	5470	0.2	0.21	114	0.045
42			5210	0.2	0.18	129	0.039
56			5060	0.2	0.19	285	0.021

The moduli values for the Type K concrete were approximately half the predicted values while the Poisson's ratios averaged very close to 0.20 (Table 4-30). Both of these trends were apparent throughout the tests.

Table 4-30 Moduli and Poisson's Ratios of the Type K Concrete

Age	Strength	Modulus of Elasticity (ksi)		Poisson's Ratio		Modulus of Elasticity	Poisson's Ratio
(Days)	(psi)	ACI 318-08	Average	AASHTO LRFD	Average	Standard Deviation	Standard Deviation
1	3540	3390	1620		0.13	146	0.040
7	4520	3830	2090		0.20	46	0.038
14			2180		0.22	3	0.010
21			2060		0.18	82	0.019
28	5310	4150	2140	0.20	0.16	115	0.023
42			2070	0.20	0.18	48	0.023
56			2090	0.20	0.20	173	0.037

The Five Star grout with fibers resulted in modulus of elasticities approximately 20% less than the predicted values (Table 4-31). The Poisson's ratios were all slightly lower than the predicted value, 0.20, by about 0.02. The predictions were all within the 20% tolerance listed in ACI 318-08.

Table 4-31 Moduli and Poisson's Ratios of the Five Star Grout with Fibers

Age	Strength	Modulus of Elasticity (ksi)		Poisson's Ratio		Modulus of Elasticity	Poisson's Ratio
(Days)	(ksi)	ACI 318-08	Average	AASHTO LRFD	Average	Standard Deviation	Standard Deviation
1	2660	2940	2490		0.19	98	0.012
7	3210	3230	2560		0.17	57	0.015
14			2680		0.18	118	0.008
21			2560		0.19	100	0.014
28	3090	3170	2520	0.20	0.19	62	0.019
42			2660	0.20	0.18	93	0.013
56			2250	0.20	0.17	148	0.006

The results of the Poisson's Ratio tests demonstrate a trend. The average values for all six materials range from 0.17 to 0.20 throughout. There are slight variations early in the concrete and grout life, but the values stabilize by 7 days. The estimate of 0.20 in

AASHTO LRFD is a good estimate, though approximately 10% high, based on the results of the six materials in these tests.

The ACI 318 equation predicted modulus well for the concrete mix but was significantly off for the grout and Type K mixes. The ACI 318 equation predicted the modulus of the concrete very accurately from the first day through the end. However, the ACI 318 equation tended to predict the modulus too high for the Five Star mixes and Type K concrete mix. The Five Star with pea gravel and Type K mixes were consistently much lower than the Five Star neat and fiber mix. The Five Star mixes tended to have moduli 20% to 30% lower than ACI 318 predicted values while the Type K mix had values almost 50% of the ACI 318 predicted value. The Set 45 mix produced a modulus twice the magnitude of the value predicted by the ACI 318 equation.

4.2.2.2.3 Shrinkage

The shrinkage in the concrete and grouts was measured throughout the tests. Shrinkage in the grouts was taken for the first 7 days of testing with the ASTM C157 method and with a modified method. Shrinkage in the concrete was only found with ASTM C157 for the first 7 days. All long term data was taken using the ASTM C157 method.

4.2.2.2.3.1 Short Term

For the first 7 days, two methods of gathering shrinkage data were used. The first was ASTM C157. Shrinkage bars 3 in. by 3 in. by 11 in. long were cast for the concrete, Five Star pea gravel grout, and Type K concrete. Shrinkage bars 1 in. by 1 in. by 11 in. were used for the Set 45, Five Star grout, and Five Star fiber grout. The second method was designed by Andrei Ramniceanu and Richard Weyers through their research at Virginia Tech. The method incorporates using 3 in. by 3 in. by 11 in. shrinkage molds from the ASTM C157 test (Figure 4-68). Instead of demolding the specimens at 24 hours, the specimens are left in the molds for 7 days. The molds are coated with vacuum grease prior to pouring the cementitious materials. A screw and wing nut is placed inside the hole for the gauge studs in the end of the forms. An LVDT is then attached to each end of the form and displacements are measured continuously.

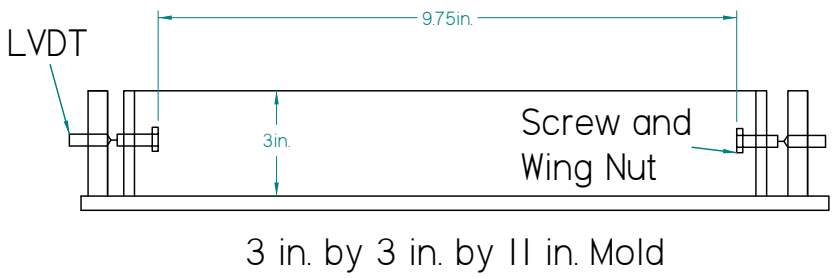

Figure 4-68 ASTM C157 Modified Shrinkage Mold

The modified method was used for the first 24 hours after pouring the grouts. This region of immediate shrinkage is not tested by the standard ASTM C157 tests. In the case of the grouts used in these tests, there was a net swelling in the first 24 hours for all samples except the Five Star control specimen. The Five Star pea gravel swelled approximately 65 με and the Five Star with fibers swelled approximately 60 με after 24 hours. The Set 45 swelled approximately 90 με while the Type K concrete swelled 400 με. The shrinkage versus time is show in Figure 4-69 for all of the grout materials.

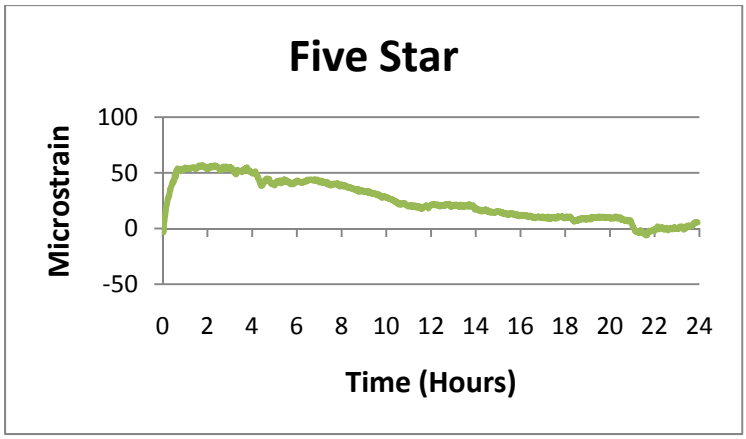
Five Star
Microstrain
100
50
0
-50
0 2 4 6 8 10 12 14 16 18 20 22 24
Time (Hours)

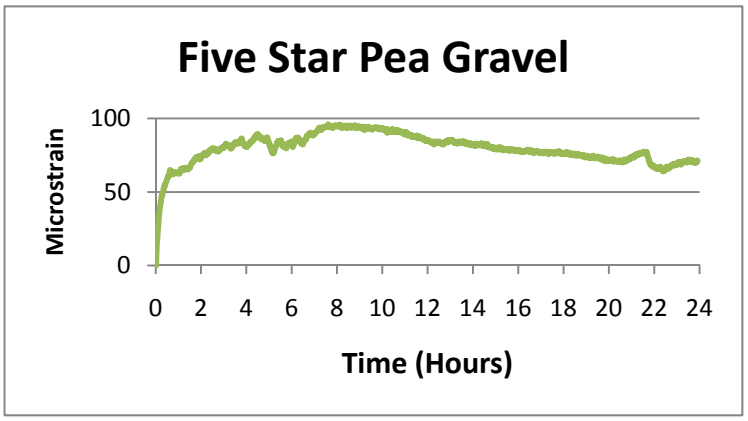
Five Star Pea Gravel
Microstrain
100
50
0
0 2 4 6 8 10 12 14 16 18 20 22 24
Time (Hours)

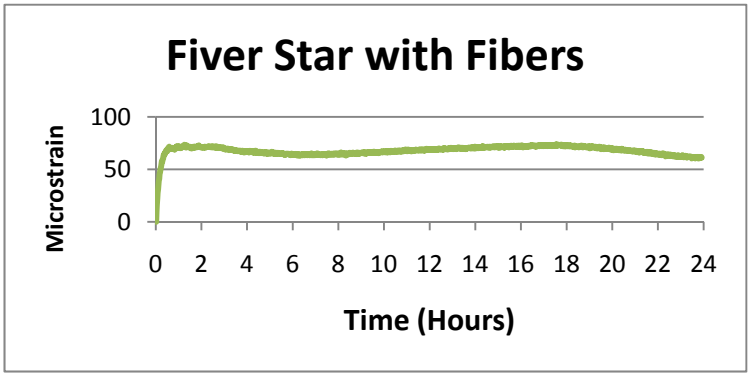
Fiver Star with Fibers
Microstrain
100
50
0
0 2 4 6 8 10 12 14 16 18 20 22 24
Time (Hours)

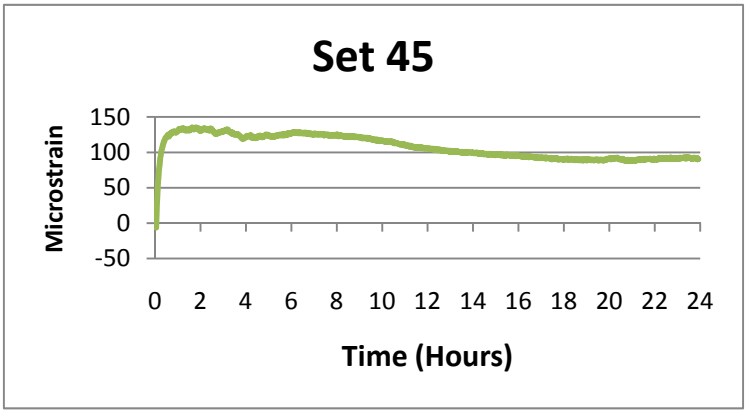
Set 45
Microstrain
150
100
50
0
-50
0 2 4 6 8 10 12 14 16 18 20 22 24
Time (Hours)

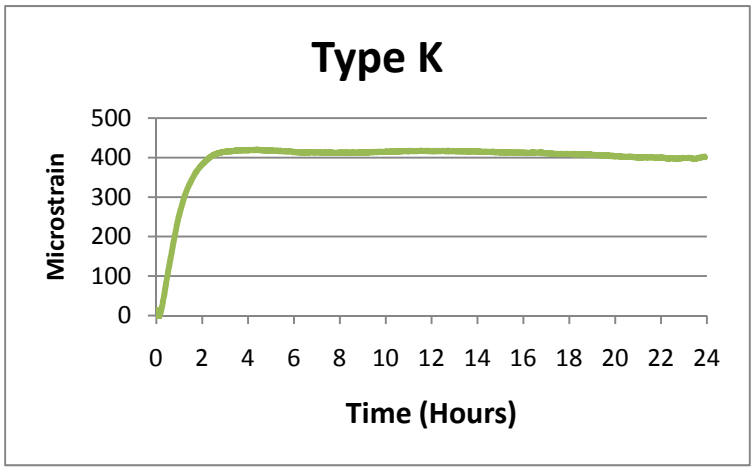

Figure 4-69 Shrinkage in the first 24 Hours

The materials all had early initial setting times and high initial strength. The fast hydration process put off a significant amount of heat. The modified shrinkage method did not take into account effects due to temperature change. Much of the early swelling was due to temperature effects. The other reason for early swelling was the early initial set.

After the first 24 hours, another 6 days of data was obtained with the modified method. This modified ASTM C157 method has never been used for shrinkage past 24 hours. Because of this, the ASTM C157 specimens were monitored during the same period and compared. Table 4-32 shows the short term shrinkage values. The full graphs are shown in Appendix C.

Table 4-32 Short Term Shrinkage

Material	Modified ASTM C157 Shrinkage			ASTM C157 Shrinkage
	24 Hour Shrinkage (με)	7 Day Shrinkage (με)	Change in Shrinkage (με)	7 Day Shrinkage (με)
Five Star Neat	5	-20	-25	-67
Five Star Pea Gravel	65	50	-15	-13
Five Star Fibers	60	75	+15	-107
Type K	400	275	-125	-163
Set 45	90	65	-35	-130

All of the values except the Five Star pea gravel grout had larger shrinkage measured by the ASTM C157 method. The Five Star pea gravel grout had almost the same value determined by both methods. The final shrinkage measurements from both methods were closest in the materials with course aggregates. The Five Star pea gravel and Type K mixes had course aggregate.

The modified method measured lower shrinkage values during the first 7 days. A possible reason for the differences is frictional reductions in the modified method. When demolding the specimens from the modified forms, the grouts had formed a bond with the steel even though the vacuum grease was still evident. Another reason for some variation is the lack of replication. Only one sample was made for the modified test of each sample. Shrinkage has a tendency to vary between samples as seen in the measurements using the ASTM C157 method.

In summary, the modified method provided trends for the grout shrinkage in the first 24 hours, however the lack of replication and newness of the test are drawbacks. These tests need further research before putting confidence in the results as shown by the comparison with the standard C157 samples. Friction may still be causing reduced readings. In addition, temperature data should be taken with future tests and taken into account during the early stage of shrinkage. The swelling effects may be primarily due to temperature effects.

4.2.2.2.3.2 Long Term

Long term shrinkage measurements were kept for all of the grouts and concretes used in the ring samples. A minimum of three measurements were taken for each material and then averaged. The standard 1 in. and 3 in. bars were used for the grout and concrete samples, respectively. A time versus average change in length plot was made for each sample. Data were recorded for the full duration of the ring tests for each material. A best fit curve was made on the plots to show the shrinkage trend for each material.

The post and rail concrete mix was poured first. A record of the shrinkage versus time was kept throughout testing. The values and a best fit curve were graphed in Figure 4-70. The concrete shrank quickly for the first 20 days. Past day 40 the mix shrank at a much slower rate. The grouts were poured on day 42 because the majority of the shrinkage appeared to have already occurred. On day 42 the strain was 733 με and on day 111 the strain was 833 με. By the end of the test the shrinkage had slowed significantly

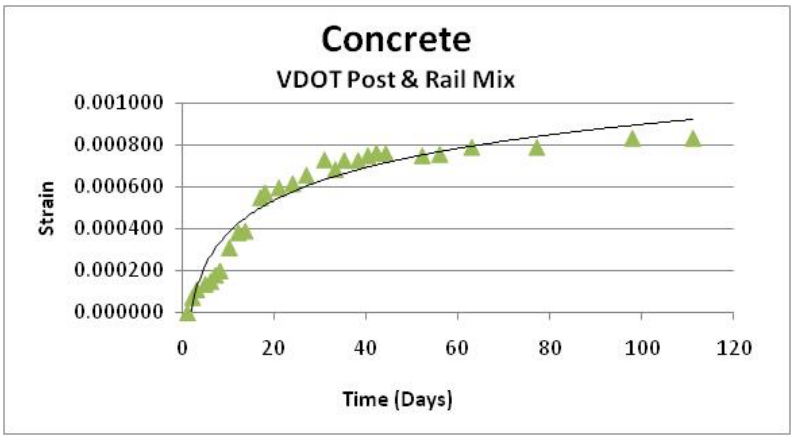

Figure 4-70 VDOT Post and Rail Concrete Shrinkage

The shrinkage for the Five Star mixes had differing trends. The neat Five Star mix (no additives) had a logarithmic shrinkage pattern with respect to time that peaked at a little over 200 με (Figure 4-71). About half of the shrinkage occurred in the first 10 days. The maximum recorded strain was 223 με. The Five Star Mix with the polypropylene

fibers had a maximum strain value of 257 με and a similar logarithmic shrinkage pattern as the neat Five Star grout (Figure 4-72). About half of the shrinkage occurred in the first 10 days.

The Five Star mix with a 3/8 in. pea gravel additive had a nearly linear shrinkage rate for the first 40 days (Figure 4-73). The strain then tapered and peaked at 140 με. The pea gravel additive reduced the maximum shrinkage value as expected. By weight, the pea gravel was approximately 40% of the mix.

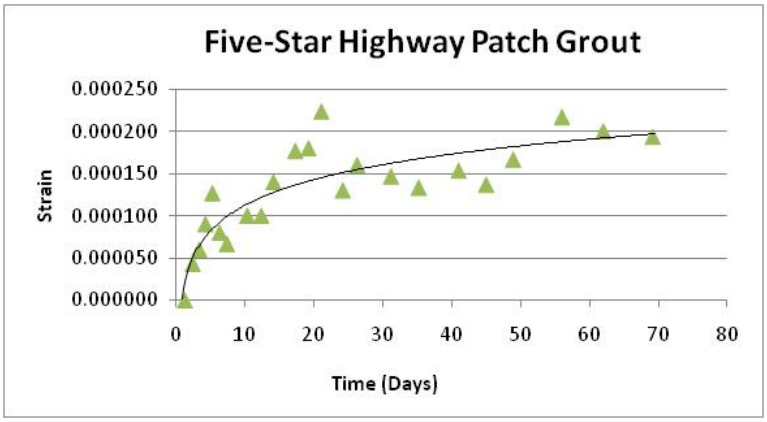

Figure 4-71 Five Star Highway Patch Grout Shrinkage

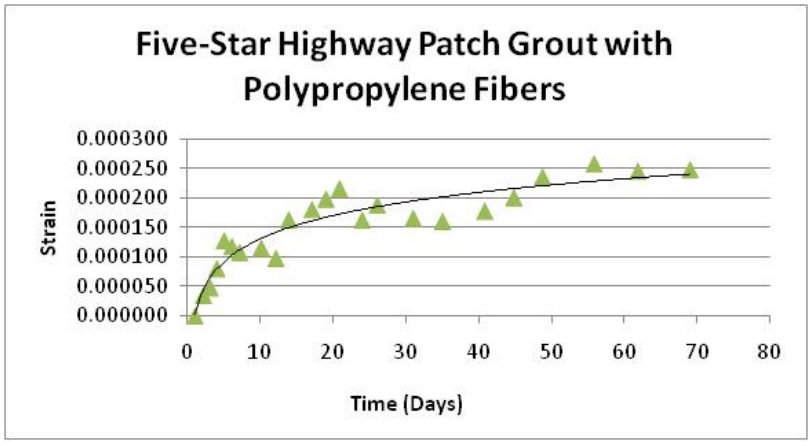

Figure 4-72 Five Star Highway Patch Grout with Polypropylene Fibers Shrinkage

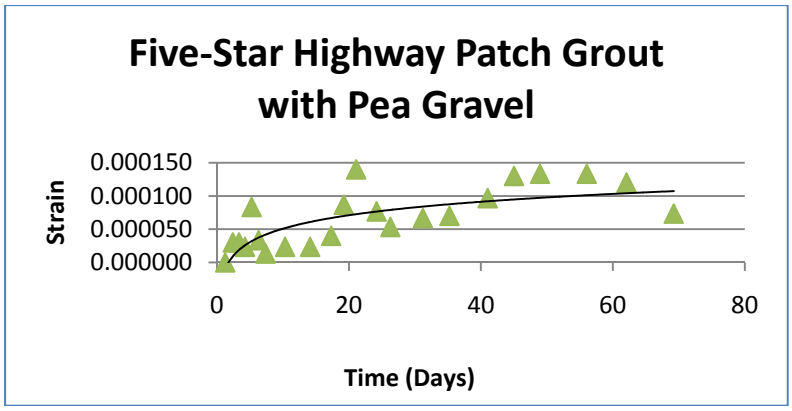

Figure 4-73 Five Star Highway Patch Grout with Pea Gravel Shrinkage

The Type K concrete mix had a similar shrinkage pattern as the post and rail concrete mix used to make the rings (Figure 4-74). The mix continued to shrink for the first 20 days at a steep rate but then began to taper between 30 and 40 days. The maximum strain was 697 με, a value 16% less than the maximum strain in the post and rail mix.

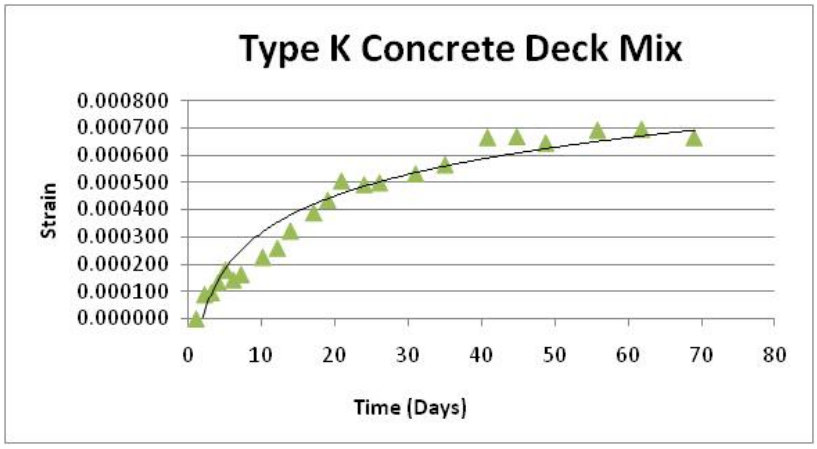

Figure 4-74 Type K Concrete Mix Shrinkage

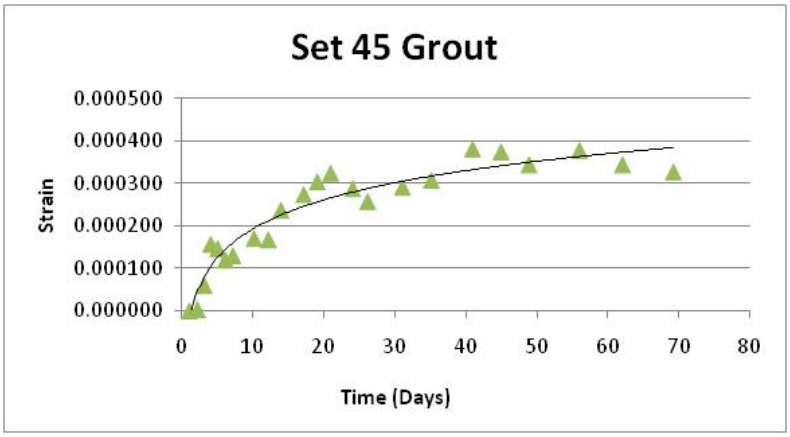

Figure 4-75 Set 45 Grout Shrinkage

The Set 45 grout had the highest shrinkage values of the grout based mixes (Figure 4-75). The maximum value was 380 με. The grout gained about half of its shrinkage in the first 10 days like the other mixes but the shrinkage values were higher thoughout.

The concrete shrank the most, as expected. The mix is not designed as a low shrinkage mix and would be expected to shrink. The rate of increase in shrinkage significantly slowed after 6 weeks. Most deck panels would not be installed earlier than 6 weeks from production so most differential shrinkage in pockets should occur primarily from the grouts.

The Type K and Set 45 mixes shrank the most. The Type K shrank nearly as much as the concrete deck mix and the Set 45 mix shrank 150% more than any of the other grouts. The Set 45 mix is better than the concrete mixes and would work as an alternative. The Type K mix did not shrink substantially less than the deck concrete and would not work as a substitute based on the shrinkage data.

All three Five Star Grouts shrank the least compared to the alternatives. The Five Star with pea gravel had the least amount of shrinkage of all the mixes. The neat and fiber mixes shrank approximately the same amount. The Five Star mix with fibers shrank 80% more and the neat mix shrank 60% more than the Five Star mix with pea gravel. Clearly the pea gravel additive helped but any of the Five Star mixes worked better than the other mixes based on shrinkage.

4.2.2.3 DEMEC Shrinkage Measurements

DEMEC readings were taken across the interface of the outer concrete and inner grout rings. Six different readings were taken around the entire diameter of the ring. These readings indicate average strain across the concrete and grout interface. In addition three readings were taken across the inner ring at even spacings (See Figure 3-27). These values measured the surface strain on each specimen.

4.2.2.3.1 DEMEC Readings on the Concrete and Grout Rings

The readings were taken at set intervals described in Table 3-5. The readings across the interfaces for each graph were averaged at each point. An average strain value was computed based on the average DEMEC readings. The data was then graphed with time on the abscissa and microstrain on the ordinate.

A typical graph of a grouted specimen with Five Star grout is shown in Figure 4-76 . Most of the specimens followed a similar strain versus time pattern. There were three main zones on the graphs: initial swelling, shrinkage, and post cracking. The initial swelling was seen within the first 7 days of the grout life. After the first week the plots tended to parallel one another and the materials began to shrink together. At some point cracking occurred and the graphs diverged. During this final stage the outer ring tended to diverge from the grouted ring. The outer ring saw slight changes while the grout ring continued to shrink.

The initial swelling of the graphs was an unexpected result attributed to the conditions of the samples and material properties. As seen with the modified ASTM C157 test, there was a swelling effect in most of the grouts. This may have contributed to some of the swelling seen in these measurements. In addition, three conditions may have contributed to the swelling: Moisture content, temperature, or confinement. The temperature remained within a 20 degree Fahrenheit range throughout the tests, so this was probably not a major factor (Appendix C.2). Confinement was present due to the bottom wooden formwork, however a plastic sheet was placed between the grout and wood. It was unlikely that a bond formed that could have caused a significant confinement problem. The moisture content in the air was fairly uniform throughout

testing, however the water content around the rings was not. The affects of ponding on the test rings were not taken into account and likely caused the swelling affects in the rings.

The ponding tests were performed on the same samples with the DEMEC points. When ponding took place the top surface with DEMEC points was inundated with approximately ¼ in. of water. Fans were used to dry the surface after the 2 hour tests but the water took between 12 and 24 hours to dry. The first ponding test was performed on 6/14/2009. The first two DEMEC readings were taken on 6/13/2009 and 6/15/2009. Therefore, the first reading was taken after the material had dried with no curing method. The second reading was taken a day after the samples had been covered with water. It has been reported that rewetting a sample after drying shrinkage has occurred can recover 100 με within one day (Mindess 2003). Most of the grouts increased in strain between 50-150 με at the beginning of the tests. The concrete rings increased in strain between 150-275 με at the beginning of the tests. The larger concrete increase may have been due to the larger surface area which could cause more reversible shrinkage.

During the second phase of the ring tests the specimens began to shrink. Both materials shrank at a similar rate until the first crack appeared. This varied for the different grouts and surface conditions. Effects of surface moisture were not as predominant because the ponding tests were done after DEMEC readings at 1 week intervals.

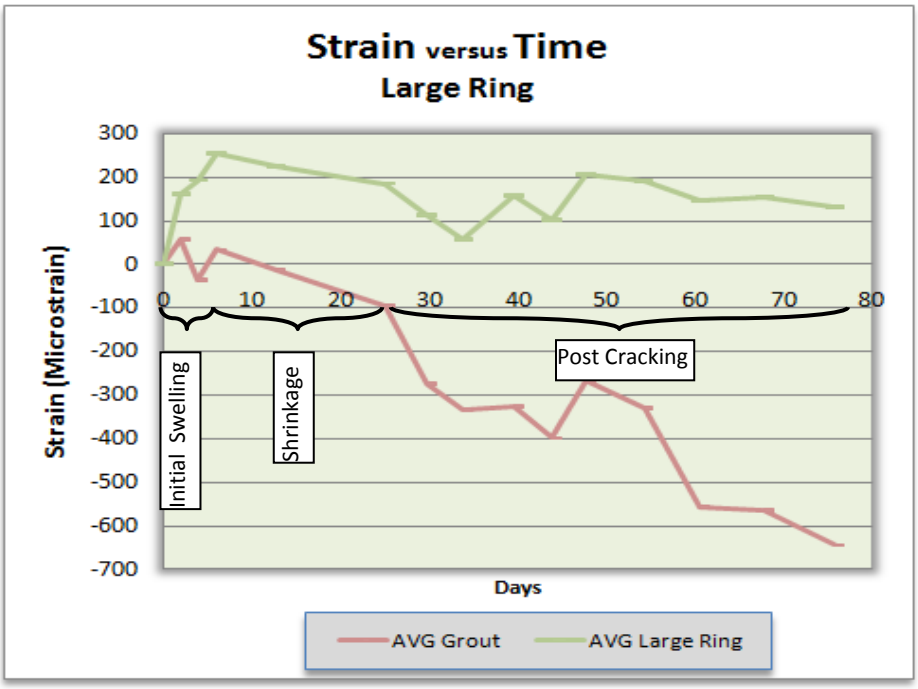

Figure 4-76 Strain versus Time for a Five Star Grout Ring Sample

The post cracking phase of the ring samples was last. It began after cracking occurred at the interface. Typically this phase showed a continuation of shrinkage for the grout ring and a slight continuation of shrinkage for the concrete ring. This was due to the release of the bond that pulled the concrete ring inward. The concrete then continued to shrink at a very slow pace. The concrete did not see significant shrinkage changes after the bond was broken.

One other location of note on the rings is between 45 and 55 days. Most of the graphs increase in strain between 50 and 150 με. These increases occur in both the grout ring and the outer ring measurements. The order of data acquisition was changed during this period without considering possible affects on the outcome. Up to this point the DEMEC readings were taken prior to performing the ponding tests. On this particular reading, the DEMEC readings were taken after the ponding test had been performed. The jump in strain is possibly due to reversible shrinkage effects. The ponding water temporarily reversed part of the shrinkage from the grout rings. The graphs have similar slopes before and after this period. This supports the idea that the

jump in the graphs was a temporary swelling effect from the presence of moisture. In addition, the strain increase is similar in magnitude to the jump that occurred during the first week of testing.

A typical strain versus time graph for Set 45 grout is shown in Figure 4-77. These grouts did not follow the same patterns as the Five Star Grouts. The Set 45 grouts had two zones. In the first zone the bond cracked, the grout shrank, and the concrete swelled. Within 1 week the materials stabilized and stopped changing in volume. The maximum shrinkage of the grout was much smaller than other materials at -79 με. The maximum swelling for the concrete followed the same patterns as the other rings.

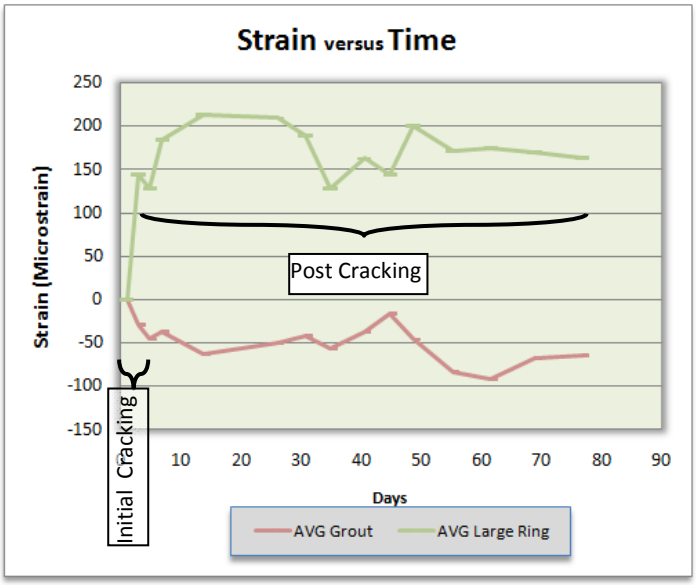

Figure 4-77 Strain versus Time for a Set 45 Ring Sample

Typical strain versus time graphs for Type K grout is shown in Figure 4-78. The grout and concrete swelled initially in these tests. Then the strain patterns became erratic but tended to parallel one another. They did not deviate from a swelling trend throughout the tests. Shrinkage was very small in these two samples.

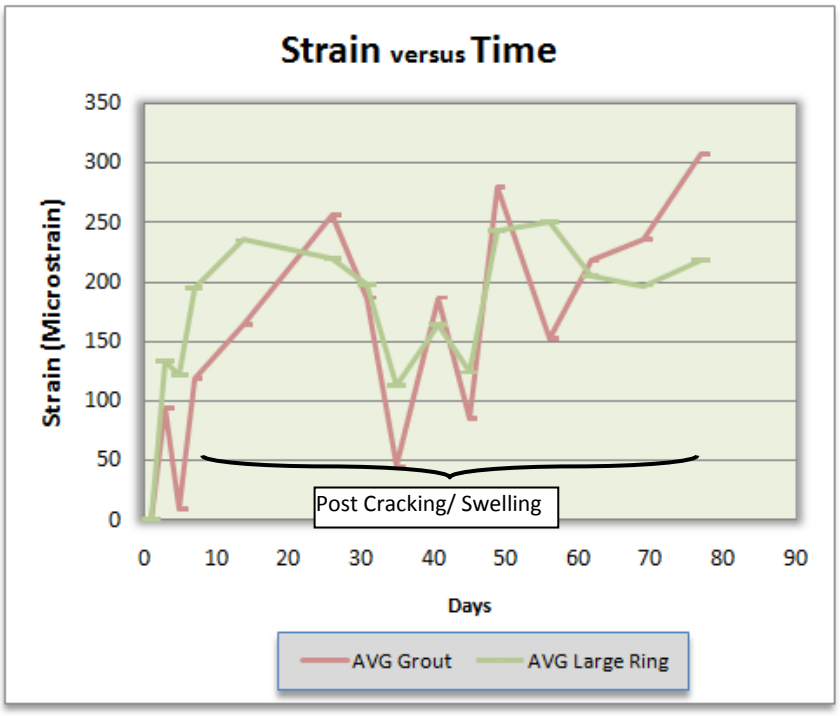

Figure 4-78 Strain versus Time for a Type K Ring Sample

4.2.2.3.2 Comparison of DEMEC Readings on the Rings

The general shrinkage trends were discussed in the previous section. The final shrinkage graphs for each sample are in Appendix C.4. Trends specific to individual grouts and surface conditions are discussed next. The description and labels for each sample type were explained in Table 3-4.

Outer Rings

The outer ring swelled during the first 7 days then slowly shrank for the remainder of the tests. Table 4-33 shows the maximum average strain, final average strain, and percent difference for each sample set.

The initial strain values for the five different pocket materials had similar ranges. The samples had maximum strains between 159 με and 285 με. The sample with Five Star grout ranged in values from 184 to 273 με. The samples with Five Star Pea Gravel

had values between 159 and 285 με. The Five Star Fibers, Type K Concrete, and Set 45 grout had initial strain values between 207 and 217 με.

The final strain values fell into two distinct groups. The final strain values for eight of the 13 samples were between 128 and 184 με. The samples with exposed aggregate (FA, FPA), epoxy (FE, FPE), and fiber grout (FF) had the smallest final strain values that ranged between 15 and 90 με.

The maximum percent difference of the maximum and final strains in the outer rings were between 28 and 51 for eight of the 13 sample types. The Five Star Epoxied (FE) and Five Star Pea Gravel Exposed Aggregate (FPA) had percent differences around 92. The Five Star Pea Gravel Epoxied (FPE), the Five Star Exposed Aggregate (FA), and the Five Star with Fibers (FF) had the second most difference at 58, 55, and 63 percent, respectively. The samples with the smallest percent difference were the Five Star Shear Key (FS) and the Set 45 Control (SC) specimens. All of the samples with the smallest final strain had the biggest percent change in strain. These samples had a better bond as indicated by the smaller swelling. The pea gravel did not make a difference in the shrinkage of the outer ring. The outer ring measurements were affected by the surface condition but not greatly affected by the type of grout.

Table 4-33 Strains in the Outer Ring

Sample Name	Maximum Average Strain (με) *	Final Average Strain (με) *	Average Percent Difference (%)
FC	**257**	**128**	**51**
FB	**228**	**139**	**40**
FA	**184**	**84**	**55**
FW	**273**	**176**	**41**
FS	**205**	**141**	**33**
FE	**211**	**18**	**91**
FPC	**285**	**184**	**34**
FPB	**245**	**150**	**40**
FPA	**159**	**15**	**92**
FPE	**211**	**90**	**58**
SC	**212**	**155**	**29**
FF	**207**	**80**	**63**
KC	**217**	**143**	**38**

***Positive values refer to swelling.**

Inner Rings

The initial swelling of the grout rings occurred in the first week after the grout was poured for the samples with Five Star grout (Table 4-34). The range for the Five Star neat grout was 64 to 132 με. The range for the Five Star with pea gravel was 41 to 93 με. The Fives Star grout with fibers had an average swelling of 114 με. The additional aggregate reduced the initial swelling but the fibers did not have an effect on swelling.

The Type K and Set 45 grout samples behaved differently in the first week. The Set 45 never swelled but instead began to shrink immediately. The Type K grout had a more erratic swelling pattern that occurred over the life of the two specimens. The initial value was at 125 με during the first week much like the Five Star grout. However, the maximum swelling did not occur during the first week for the Type K samples. It occurred near the end of the testing cycle.

Table 4-34 Strains in the Inner Ring

Sample Name	Minimum Average Strain (με)*	Maximum Average Strain (με)*	Change in Strain (Max to Min)
FC	**97**	**-523**	**-620**
FB	**69**	**-406**	**-475**
FA	**132**	**-365**	**-497**
FW	**64**	**-647**	**-711**
FS	**82**	**-306**	**-439**
FE	**108**	**-483**	**-591**
FPC	**81**	**-386**	**-467**
FPB	**41**	**-279**	**-320**
FPA	**79**	**-479**	**-558**
FPE	**93**	**-429**	**-523**
SC	**0.0**	**-151**	**-151**
FF	**114**	**-428**	**-542**
KC	**237**	**-62**	**+299**

*Negative is shrinkage and positive is swelling.

The maximum shrinkage strains were near the end of the test for every sample except the Type K and Set 45 rings. The final strain in the Five Star neat grout rings ranged from 306 to 647 με . The final strain in the Five Star pea gravel grout rings ranged from 278 to 479 με. The Five Star with fibers (FF) shrank a final amount of 428 με. The pea gravel aggregate reduced the amount of maximum shrinkage in the rings.

All of the surface conditions with Five Star neat grout reduced shrinkage except the water stops. The water stop (FW) samples shrank 647 με, the most among all samples. The Five Star exposed aggregate (FA), the Five Star shear key (FS), and the Five Star wire brushed (FB) shrank significantly less than the control specimen.

The shrinkage in the control specimen with pea gravel (FPC) shrank less than the exposed aggregate and epoxy coated rings. The wire brushed surface ring (FPB) shrank less than the pea gravel control sample (FPC). In the pea gravel samples, the addition of pea gravel affected the final shrinkage as much as the surface condition.

The Set 45 (SC) and Type K (KC) rings had maximum shrinkage strains much lower than the Five Star Samples. The Set 45 shrank a maximum of 151 με while the Type K shrank a maximum of 62 με. The Set 45 primarily shrank during the first two weeks then stagnated. The Type K had a swelling trend that prevented shrinking from

occurring. Only one out of the two Type K samples ever experienced any shrinkage strain.

The surface condition that reduced maximum shrinkage consistently was the wire brushed surface (FB). The Exposed aggregate (FE) worked well with neat Five Star grout but not extended Five Star Grout (FPE). The epoxy (FE) did not significantly affect the final strain in either sample. The shear key (FS) worked effectively with neat Five Star Grout. The Five Star fiber (FF) samples had a small affect on the strain outcome. The water stopped samples (FW) was the only condition to have a negative outcome on the final strain readings.

Comparison of Inner Ring to ASTM C157 Results

The final grout ring strains were greater than the final strain in the ASTM C157 bars in 11 of the 13 samples (Figure 4-79). The inner grout rings tended to shrink two to three times as much as the bars. Some of the difference is due to two different methods of estimating shrinkage. The ASTM had more surface area and no confining forces at any point in the tests. The ring samples had significant confinement and a different ratio of surface area to volume. Both factors would affect the results. Overall, the final magnitudes of strain followed similar patterns between the samples.

The two exceptions were the Set 45 and Type K grouts. They both shrank much more with the shrinkage bars (ASTM C157) than with the grout rings. These two samples were the ones that cracked almost immediately after pouring the grout. It appears that the grout rings do not pick up immediate shrinkage but the shrinkage bars are more sensitive to early shrinkage.

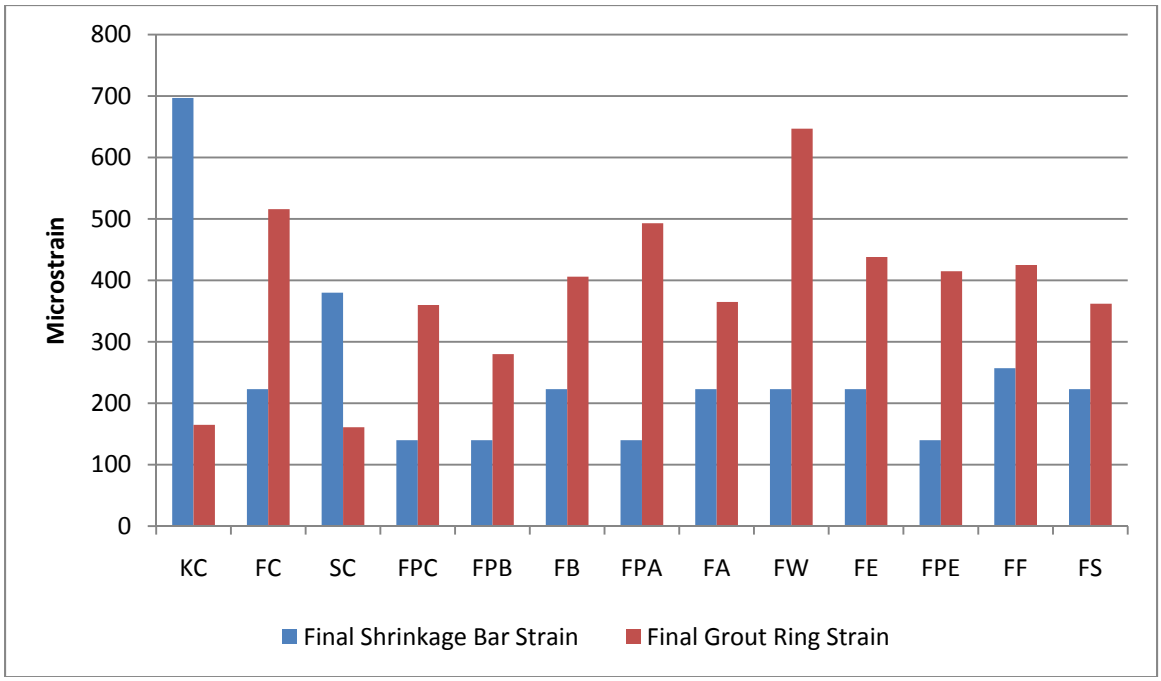

Figure 4-79 Comparison of Grout Ring and ASTM C157 Shrinkage Measurements

Final Change in Strain

The final average strains in both rings are shown in Table 4-35. As with the previous DEMEC readings, the Five Star samples followed a different pattern than the Set 45 and Type K rings.

All surface treatments except for the water stop reduced the final strain compared to the control samples. The water stopped (FW) samples had the highest final strain values. The shrinkage strain values were 28% higher than the Five Star control sample (FC). In the Five Star neat grouts, the exposed aggregate (FA), shear key (FS), wire brushed (FB), and epoxy (FE) surfaces all reduced the shrinkage strain. They ranged from 449 to 544 με compared to the control value of 644 με. In the Five Star pea gravel grouts, the wire brushed (FPB), exposed aggregate (FPA) and epoxied surfaces (FPE) ranged from 430 to 505 με while the control had shrinkage strains of 544 με. The Five Star with fibers (FF) had final values of 505 με. All of the surface preparation techniques helped reduce final shrinkage strain except the water stops. The addition of pea gravel or fibers reduced the shrinkage as much as the surface preparations.

The Type K and Set 45 had much smaller final strain values. The Type K samples increased in strain 22 με by the end of testing. The Set 45 had a final strain of 234 με. The Set 45 shrinkage value was almost half the value of the best Five Star sample. The Type K and Set 45 grouts reduced the final amount of shrinkage a significant amount compared to all the Five Star grouts.

Table 4-35 Final Strains in the Inner and Outer Ring

Sample Name	Final Strain in Grout Rings (με)*	Final Strain in Outer Rings (με)*	Final Difference in Strain
FC	**-516**	**128**	**-644**
FB	**-406**	**139**	**-544**
FA	**-365**	**84**	**-449**
FW	**-647**	**176**	**-823**
FS	**-362**	**141**	**-503**
FE	**-438**	**18**	**-456**
FPC	**-360**	**184**	**-544**
FPB	**-280**	**150**	**-430**
FPA	**-493**	**15**	**-508**
FPE	**-415**	**90**	**-505**
SC	**-79**	**155**	**-234**
FF	**-425**	**80**	**-505**
KC	**165**	**143**	**22**

*Negative is shrinkage and positive is swelling.

4.2.2.4 Cracks in the Rings

4.2.2.4.1 First Cracking

The first crack in each ring was determined with two methods: visually and with DEMEC gauges. The visual detection was based on the perception of the researcher seeing the crack without any assistance or tools. The DEMEC detection was determined by graphing the DEMEC displacements versus time and looking for a noticeable change in slope. This coincided with the loss in stiffness due to the first crack.

4.2.2.4.1.1 Visual First Cracking

Table 4-36 shows the 13 unique specimens and the point of the first crack. The size and length of the visual measurements were recorded each day for the first week

and then two times a week for 11 weeks. The crack width was measured with a crack gauge with a minimum reading of 0.005 in., however the first readings for every ring specimen were too small to measure.

The only samples with visible cracks the week after pouring were the Type K concrete and Set 45 grout samples. Of the three Type K samples built, one of them was damaged during construction. The remaining two had 50% of the interface cracked within 24 hours of pouring. One of the Set 45 specimens had a rough interface that masked any cracking. The other two specimens cracked 25% and 100%, respectively, within 4 days.

Two samples, Five Star pea gravel epoxied and Five Star water stopped, had average first cracks at 14 days. The average length of the cracks was 20% of the diameter.

The majority of the samples cracked within 19 to 24 day after the grout pour. This included the two control specimens Five Star control and Five Star pea gravel control. In addition the Five Star wire brush, Five Star pea gravel aggregate, and Five Star shear key specimens cracked during this period. At first crack, the average crack length of the pea gravel exposed aggregate and both control specimens was 25% of the diameter. The Five Star brushed and shear key specimens had approximately 13% of their diameter cracked.

The Five Star fiber specimens cracked at 31 days. These were the only samples to have a first crack in the 5 week range. They had the smallest average length of all the first cracks. The cracks averaged 6% of the diameter.

Three specimens had average first cracks occur at approximately 6 weeks after pouring. They were Five Star pea gravel brushed, Five Star aggregate, and Five Star epoxied. The Five Star pea gravel brushed had average lengths of 10% while the other two had average lengths of 20%.

The poorest performers were the Type K and Set 45 mixes. They cracked very early and had significantly long first cracks. The best performers were the Five Star

exposed aggregate and Five Star epoxied specimens. They did not crack until 6 weeks after the pour and the cracks were initially 20% of the circumference.

The pea gravel and neat control Five Star mixes cracked at almost the same time and the average lengths were about the same. The pea gravel did not have an adverse affect on the control specimens. The same trend was seen in five of the six specimens with wire brushed surfaces. One specimen never cracked but the other six specimens all had an average crack time of 20 days. The samples with epoxy or exposed aggregate and pea gravel cracked much earlier than the samples with only Five Star grout. The epoxied specimens cracked three times as early and the exposed aggregate cracked 2.25 times as early when pea gravel was included in the grout. On specimens with stronger bonds, the non pea gravel grouts extended the time to the first crack.

One other mix with delayed first cracks and very small first cracks was the Five Star with polypropylene fibers. These mixes cracked a week earlier than the best performing grouts but the cracks were shortest of any set of specimens. Their first crack lengths were approximately 6% of the diameter.

Table 4-36 First Visible Interface Cracks in the Ring Samples

Sample Name | Abbreviation		Age (Days)	Average Age (Days)	Percent of the Interface Cracked
Type K Concrete:	KC1	1	1	50%
	KC2	1		50%
Five Star Control:	FC1	31		50%
	FC2	11	20	17%
	FC3	18		10%
Set 45 Control:	SC1	4		25%
	SC2	3	3.5	100%
	SC3	---*		---*
Five Star Pea Gravel Control:	FPC1	20		50%
	FPC2	18	19.3	33%
	PFC3	20		5%
Five Star Pea Gravel Wire Brushed:	FPB1	20		17%
	FPB2	20	>39.3	12%
	PFB3	No Cracks @ 78		0%
Five Star Wire Brushed:	FB1	32		12%
	FB2	15	21.7	12%
	FB3	18		12%
Five Star Pea Gravel Exposed Aggregate:	FPA1	20		33%
	FPA2	20	20	33%
	FPA3	20		5%
Five Star Exposed Aggregate:	FA1	20		33%
	FA2	78	44.7	16%
	FA3	36		16%
Five Star Water Stopped:	FW1	20		17%
	FW2	11	14	17%
	FW3	11		25%
Five Star Epoxied:	FE1	32		33%
	FE2	62	42	5%
	FE3	32		25%
Five Star Pea Gravel Epoxied:	FPE1	20		17%
	FPE2	11	14	33%
	FPE3	11		20%
Five Star Fiber:	FF1	45		8%
	FF2	21	31	5%
	FF3	27		5%
Five Star Shear Key:	FS1	20		17%
	FS2	32	24	8%
	FS3	20		17%

*Cracks were not detectable due to a rough surface.

4.2.2.4.1.2 DEMEC First Cracking

The DEMEC graphs were explained in Section 4.2.2.3. Six DEMEC readings were taken across the interface every two days for the first week. Subsequent readings were taken on a weekly basis. In the graphs of the strain versus time there was a sudden change in slope on the grout ring measurements corresponding to the first crack. These values were identified for each sample type and are summarized in Table 4-37.

The two sets of rings to see the earliest cracking were the Type K (KC) and Set 45 (SC). The Type K rings cracked at day 3 and the Set 45 cracked immediately. All of the samples for each grout type were consistent and cracked at the same time.

The next set of samples to crack occurred in the third week of testing. Three of the four sets of Five Star pea gravel samples cracked here: the Control (FPC), the epoxied (FPE), and the exposed aggregate (FPA). The first crack in these samples occurred between the 14 and 18 day of the test. The other Five Star pea gravel sample, Five Star pea gravel wire brushed (FPB), had one sample that cracked at 49 days. The other two samples in this set cracked at 26 days. The pea gravel additive caused early cracking in the samples.

The Five Star control specimens (FC) cracked on the 28th day of the testing. The Five Star wire brushed (FB), epoxied (FE), exposed aggregate (FA), water stopped (FW), and fibers (FF) cracked between day 26 and 31. These surface treatments did not postpone the first crack on the surface of the concrete-grout interface. The Five Star shear keyed (FS) specimens did not crack on average until day 32. This was the only treatment that changed the first cracking time for the Five Star rings.

The DEMEC strain readings did not differentiate a significant difference in first cracking among the surface conditions. The pea gravel additive did contribute to earlier cracking by 10 to 12 days. The Type K and Set 45 grouts appeared to have cracking almost immediately after pouring the grout.

Table 4-37 First Interface Cracks Detected by DEMEC Strain Readings

Sample Name | Abbreviation		Age (Days)	Average Age (Days)
Type K Concrete:	KC1	3	3
	KC2	3	
Five Star Control:	FC1	26	27.7
	FC2	26	
	FC3	31	
Set 45 Control:	SC1	0	0
	SC2	0	
	SC3	0	
Five Star Pea Gravel Control:	FPC1	14	18
	FPC2	14	
	FPC3	26	
Five Star Pea Gravel Wire Brushed:	FPB1	26	34
	FPB2	26	
	FPB3	49	
Five Star Wire Brushed:	FB1	26	29
	FB2	35	
	FB3	26	
Five Star Pea Gravel Exposed Aggregate:	FPA1	14	14
	FPA2	14	
	FPA3	14	
Five Star Exposed Aggregate:	FA1	26	26
	FA2	26	
	FA3	26	
Five Star Water Stopped:	FW1	26	26
	FW2	26	
	FW3	26	
Five Star Epoxied:	FE1	35	30.7
	FE2	31	
	FE3	26	
Five Star Pea Gravel Epoxied:	FPE1	14	18
	FPE2	26	
	FPE3	14	
Five Star Fiber:	FF1	26	26
	FF2	26	
	FF3	26	
Five Star Shear Key:	FS1	35	32
	FS2	26	
	FS3	35	

4.2.2.4.1.3 Comparison of First Cracking

Table 4-38 contains a comparison of the first detected crack in each sample. The DEMEC readings were taken every 3 days for the first week, then weekly for the next 11 weeks. The visual readings were taken every day for the first week, every 3 days for the next 7 weeks, and weekly for the final 4 weeks.

Based on the span between the readings with both methods the first crack could occur within a 4 day range of the actual reading. Five of the first cracks were less than 4 days apart: Type K (KC), Set 45 (SC), Five Star pea gravel control (FPC), Five Star wire brushed (FB), and Five Star pea gravel epoxy (FPE). The first cracks in these samples were detected at the same time by both methods (Figure 4-80).

Five of the samples had first cracks detected within 5 to 10 days of one another. This included: Five Star Control (FC), Five Star pea gravel wire brushed (FPB), Five Star pea gravel exposed aggregate (FPA), Five Star shear key (FS), and Five Star Fiber (FF). The first crack in the Five Star fiber, pea gravel wire brushed, and pea gravel exposed aggregate rings were predicted by the DEMEC gauge 5 to 6 days earlier than the visual detection. This may have been due to micro cracking that occurred prior to the visual cracking. The shear key visual readings showed slow, gradual crack propagation which may have contributed to the wider range in first cracking values. The length of time to 50% cracking took a long period after the first crack. The cracking in the Five Star control specimens were 7.7 days apart which showed some slight variation in the methods.

Three samples had first cracks predicted at more than 10 days apart by the two methods. This included: Five Star exposed aggregate (FA), Five Star water stopped (FW), and Five Star epoxied (FE). The epoxied and exposed aggregate samples had DEMEC predictions 11.3 and 18.7 days prior to the visual first crack detected. This may have been due to the very slow propagation of the cracks in the samples. The length to 50% cracking took a long period after the first crack. Small microcracks may have been detected with the DEMEC readings prior to the visuals. The water stopped samples had visual detections approximately 12 days prior to DEMEC predictions. The water stops were the only sample were the DEMEC predictions were over 10 days after the visual

predictions. They were also the only sample with a physical barrier across the interface. This barrier may have caused a more gradual change in slope in the DEMEC graphs that made the first crack hard to detect.

Both of the first cracking methods, visual and DEMEC readings, gave results within 1 week of one another on most samples. Of the samples that didn't follow this trend, all but one had DEMEC first cracks occur earlier than visual first cracks. This was expected because DEMEC readings tend to detect cracking prior than visuals. The one sample that had visible cracks prior to DEMEC detection was the sample with a physical barrier between the rings, Five Star water stop rings. All of the other samples had close agreement for the first crack or their differences could be explained.

Table 4-38 Time in Days to First Interface Cracks

Sample Name	Abbreviation	First Crack - Average Age Visually (Days)	Average Age Visually 50% Cracked (Days)	First Crack - Average Age DEMEC Readings (Days)	First Crack - Average Age – Both Methods (Days)	Difference (Days)
Type K Concrete:	KC	1	1.5	3	2	-2.0
Five Star Control:	FC	20	28.7	27.7	24	-7.7
Set 45 Control:	SC	3.5	5.0	0	2	3.5
Five Star Pea Gravel Control:	FPC	19.0	26.3	18	19	1.0
Five Star Pea Gravel Wire Brushed:	FPB	>39.3	>42.3	34	37	5.3
Five Star Wire Brushed:	FB	21.7	43.7	26	24	-4.3
Five Star Pea Gravel Exposed Aggregate:	FPA	19.6	33.7	14	17	5.4
Five Star Exposed Aggregate:	FA	44.7	54.0	26	35	18.7
Five Star Water Stopped:	FW	14	23.7	26	20	-12.0
Five Star Epoxied:	FE	42	77.0	30.7	36	11.3
Five Star Pea Gravel Epoxied:	FPE	14	25.3	18	16	-4.0
Five Star Fiber:	FF	31	51.5	26	29	5.0
Five Star Shear Key:	FS	24	55.7	32	28	-8.0

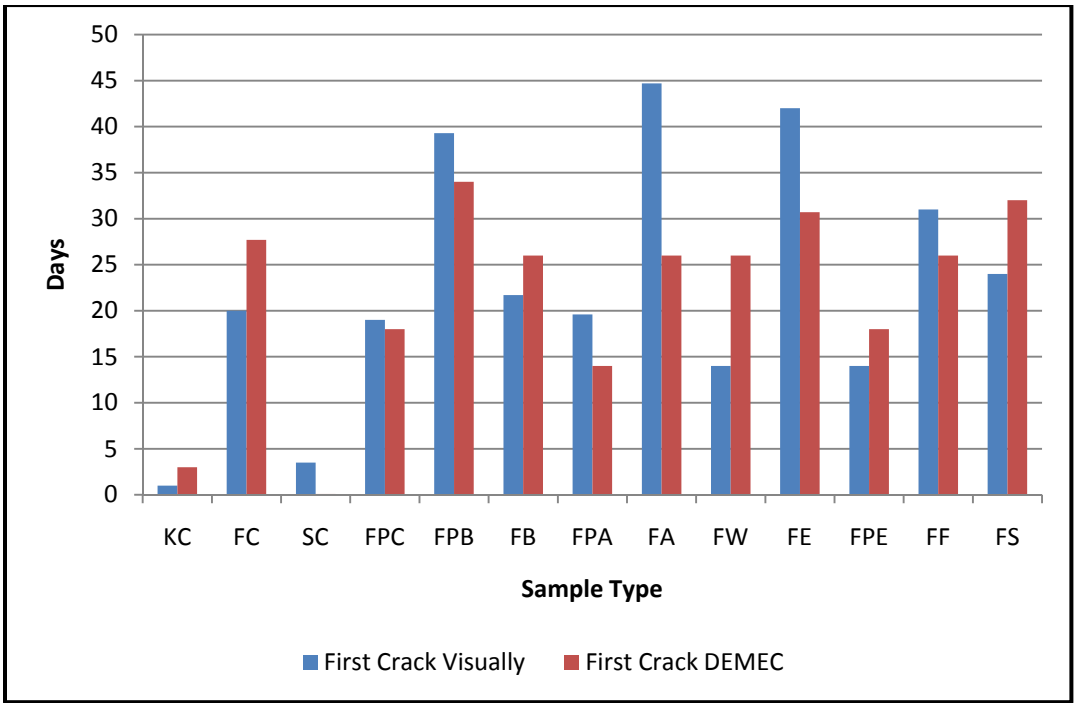

Figure 4-80 Time to First Interface Cracks

4.2.2.4.2 Long Term Cracking

Crack widths were measured the day of the last testing with crack cards. Table 4-39 summarizes the size and percent of each joint that was cracked at the end of testing. A graphical representation of the average final crack width is shown in Figure 4-81.

The Five Star control and Five Star Pea Gravel control had cracks of at least 0.005 in. wide across 50% or more of the joint interface . Only two sets of specimens, the Type K control and Set 45 control, had cracks larger than the Five Star control specimens. The Type K had cracks between 0.01 in. and 0.015 in. and the Set 45 specimens had cracks between 0.005 in. and 0.01 in. The Five Star water stopped had a similar trend to the Five Star control specimens.

Two sets of samples had no specimens with cracks large enough to measure at the end of testing. The first set, Five Star pea gravel wire brushed, had two samples that were 85% cracked and one sample with no cracking. The cracks occurred by week three in the testing but they did not grow at the end of testing. The Five Star epoxied

specimens had cracking that range from 5% to 50%. Two of the specimens slowly began to crack at week 5 and one specimen had very slight cracking during the last week of testing.

Most of the cracks in the Five Star exposed aggregate specimens and Five Star wire brushed were too small to measure at the end of testing. One Five Star exposed aggregate specimen cracked 66% and about half the cracks were 0.005 in. in thickness. One Five Star wire brushed specimen cracked 100% and 83% of the cracks were 0.005 in. in thickness. The rest of the samples had cracks too small to measure.

Three specimens, Five Star shear key, Five Star fiber, and Five Star pea gravel exposed aggregate, did not show a clear pattern. They ranged from specimens with cracks that could not be measured to specimens with predominant cracks of 0.005 in. in thickness.

The control specimens of every type of grout performed the worst in long term cracking size. The addition of fibers, water stops, or shear keys did not show a detectable difference. The presence of a wire brushed surface, exposed aggregate without pea gravel, or epoxy without pea gravel worked the best. Pea gravel had a slight negative effect on the epoxy and exposed aggregate specimens.

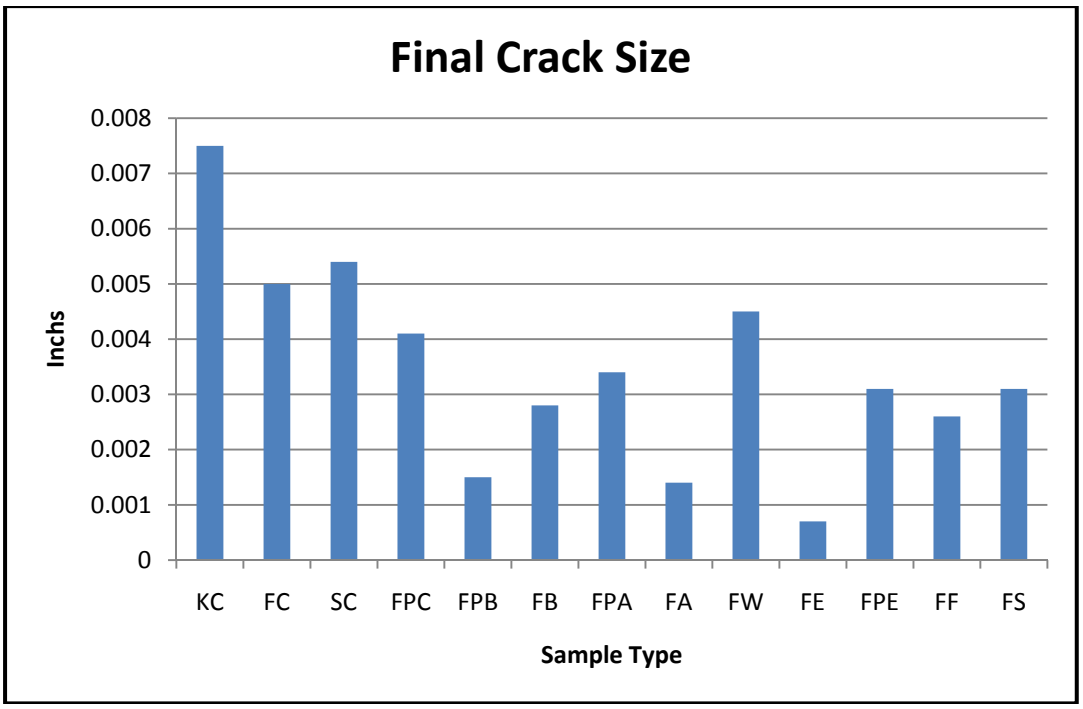

Figure 4-81 Average Size of the Final Interface Cracks

Table 4-39 Final Cracks in the Rings

Sample Name	Abbreviation	Size (Inches - % of Diameter)
Type K Concrete:	KC1	0.01 – 25%, 0.015 25%, <0.005 50%
	KC2	0.01 – 50%, 0.005 50%
Five Star Control:	FC1	0.005 – 100%
	FC2	0.005 – 100%
	FC3	0.005 – 100%
Set 45 Control:	SC1	0.01 – 33%, 0.005 – 33%, <0.005 – 33%
	SC2	0.005 – 100%
	SC3	Not Detectable – Rough Surface
Five Star Pea Gravel Control:	FPC1	0.005 – 50%, <0.005 – 50%
	FPC2	0.005 – 100%
	FPC3	0.005 – 50%, <0.005 – 25%
Five Star Pea Gravel Wire Brushed:	FPB1	<0.005 – 85%
	FPB2	<0.005 – 85%
	FPB3	No Cracks
Five Star Wire Brushed:	FB1	100% <0.005
	FB2	50% < 0.005
	FB3	83% - 0.005, 17% <0.005
Five Star Pea Gravel Exposed Aggregate:	FPA1	33% - 0.005, 60% <0.005
	FPA2	67% - 0.005, 25% <0.005
	FPA3	33% - 0.005, 50% <0.005
Five Star Exposed Aggregate:	FA1	33% - 0.005, 33% <0.005
	FA2	16% - <0.005
	FA3	50% - <0.005
Five Star Water Stopped:	FW1	75% - 0.005, 25% < 0.005
	FW2	66% - 0.005, 33% <0.005
	FW3	100% - 0.005
Five Star Epoxied:	FE1	33% < 0.005
	FE2	5% < 0.005
	FE3	50% < 0.005
Five Star Pea Gravel Epoxied:	FPE1	75% < 0.005
	FPE2	50% - 0.005, 33% < 0.005
	FPE3	66% - 0.005, 33% < 0.005
Five Star Fiber:	FF1	33% - 0.005, 66% < 0.005
	FF2	66% - 0.005, 25% < 0.005
	FF3	20% < 0.005
Five Star Shear Key:	FS1	66% - 0.005, 33% < 0.005
	FS2	33% - 0.005, 67% < 0.005
	FS3	75% < 0.005

4.2.2.5 Bond Strength of the Grouts

The bond strengths of the grouts and concrete rings were determined based on the material properties and deformations of the ASTM C157 Shrinkage bars. Just prior to the first crack, the material properties were measured for the grout and concrete of each ring specimen. The point at the first crack was the last time in testing that a bond existed around the entire perimeter of the grout-concrete interface (See Figure 3-24).

The first crack and shrinkage properties were taken from the data that was presented in the previous sections. The deformation is based on an unbonded grout ring (8 in. grout ring - See Figure 3-24) shrinking with no constraint. The average measured deformation of the grout rings, Δ, was found at the time of the first crack and the corresponding ASTM C157 shrinkage (Figure 4-71 - Figure 4-75). The shrinkage was converted to a deformation based on the ring diameter as shown in Table 4-40. An example is shown in Figure 4-82. The initial diameter of the rings was the same throughout for the concrete (18 in.) and the grout specimens (8 in.).

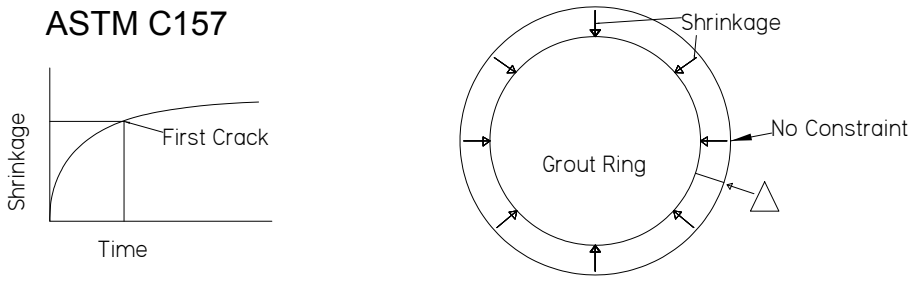

Figure 4-82 Determining the Deformation at First Crack

The material properties were measured for the grout and concrete at the time of first cracking. The modulus of elasticity of the concrete rings and the Poisson's ratio of the concrete rings changed slightly during testing (Table 4-26). The material properties of the grouts changed significantly (Table 4-27 - Table 4-31). The grout material properties at the first crack are summarized in Table 4-40. Based on these values, an average ultimate bond strength between the different rings was computed (Table 4-41,

Figure 4-83). The basic thick cylinder equation was used as shown in Equation 1 below (Riley 1999):

$$\sigma_r = \frac{\Delta(c^2-b^2)E_g E_c}{2b(E_g(1-v_c)b^2+E_g(1+v_c)c^2+E_c(1-v_g)(c^2-b^2))} \quad \text{Eq. 1}$$

where

Δ	=	Unbounded grout ring deformation (Figure 4-71 - Figure 4-75)
v_c	=	Poisson ratio of the concrete (Table 4-26)
v_g	=	Poisson ratio of the grout (Table 4-27 - Table 4-31)
E_g	=	Modulus of elasticity of the grout (Table 4-27 - Table 4-31)
E_c	=	Modulus of elasticity of the concrete (Table 4-26)
c	=	Outer radius (Concrete ring – 18 in.)
b	=	Inner radius (Grout ring – 8 in.)

Table 4-40 Grout Ring Properties at First Crack

Sample Name | Abbreviation		Unbonded Ring Deformation (in.) (Visual First Crack)	Unbonded Ring Deformation (in.) (DEMEC First Crack)	Grout Poisson's Ratio, v_g	Grout Modulus of Elasticity, E_g (ksi)
Type K	KC1	0.000000	-0.000675	0.13	1620
Concrete:	KC2	0.000000	-0.000675	0.13	1620
Five Star	FC1	-0.000976	-0.001060	0.17	2700
Control:	FC2	-0.000664	-0.001060	0.17	2740
	FC3	-0.001180	-0.000976	0.17	2740
Set 45 Control:	SC1	-0.000980	0.000000	0.22	5400
	SC2	-0.000370	0.000000	0.23	2720
	SC3	0.000000	0.000000	0.00	----
Five Star Pea	FPC1	-0.000571	-0.000151	0.18	2340
Gravel Control:	FPC2	-0.000262	-0.000151	0.18	2340
	FPC3	-0.000348	-0.000348	0.18	2340
Five Star Pea	FPB1	-0.000571	-0.000505	0.18	2340
Gravel Wire	FPB2	-0.000571	-0.000505	0.18	2340
Brushed:	FPB3	-0.000485	-0.000485	0.17	2200
Five Star Wire	FB1	-0.001100	-0.001240	0.17	2700
Brushed:	FB2	-0.001080	-0.001240	0.17	2740
	FB3	-0.001260	-0.001260	0.16	2750
Five Star Pea	FPA1	-0.000571	-0.000151	0.18	2340
Gravel Exposed	FPA2	-0.000571	-0.000151	0.18	2340
Aggregate:	FPA3	-0.000571	-0.000571	0.18	2340
Five Star	FA1	-0.001080	-0.001080	0.16	2750
Exposed	FA2	-0.001060	-0.001060	0.17	2800
Aggregate:	FA3	-0.000850	-0.001020	0.20	2530
Five Star Water	FW1	-0.001210	-0.001080	0.16	2750
Stopped:	FW2	-0.000664	-0.001060	0.17	2740
	FW3	-0.000664	-0.001060	0.17	2740
Five Star	FE1	-0.000976	-0.000883	0.17	2700
Epoxied:	FE2	-0.001330	-0.000976	0.17	2800
	FE3	-0.001060	-0.001060	0.17	2700
Five Star Pea	FPE1	-0.000085	-0.000151	0.18	2340
Gravel Epoxied:	FPE2	-0.000153	-0.000352	0.17	2340
	FPE3	-0.000153	0.000153	0.17	2340
Five Star Fiber:	FF1	-0.001310	-0.001230	0.18	2660
	FF2	-0.001400	-0.001210	0.19	2560
	FF3	-0.001210	0.000000	0.19	2520
Five Star Shear	FS1	-0.001210	-0.000894	0.16	2750
Key:	FS2	-0.000976	-0.001060	0.17	2700
	FS3	-0.001210	-0.000894	0.16	2750

Table 4-41 Bond Stress between the Rings at First Crack *

Sample Name | Abbreviation		Ring Stress (psi) (Visual First Crack)	Ring Stress (psi) (DEMEC First Crack)	Average Ring Stress (psi) (Visual First Crack)	Average Ring Stress (psi) (DEMEC First Crack)	Average Ring Stress (psi)	Tensile Strength Equation Coefficient (X_g - X_c) $f_r = X\sqrt{F}$
Type K Concrete:	KC1	0.0	-78.3	0.0	-78.3	-39.1	0.70, 0.55
	KC2	0.0	-78.3				
Five Star Control:	FC1	-168.0	-182.8	-159.2	-173.8	-166.5	2.80, 2.35
	FC2	-106.0	-169.6				
	FC3	-203.6	-169.1				
Set 45 Control:	SC1	-179.0	0.0	-78.4	0.0	-39.2	0.78, 0.55
	SC2	-56.2	0.0				
	SC3	0.0	0.0				
Five Star Pea Gravel Control:	FPC1	-92.7	-24.5	-63.9	-35.2	-49.6	0.90, 0.70
	FPC2	-42.6	-24.5				
	FPC3	-56.5	-56.5				
Five Star Pea Gravel Wire Brushed:	FPB1	-92.7	-82.1	-86.4	-79.3	-82.8	1.50, 1.17
	FPB2	-92.7	-82.1				
	FPB3	-73.7	-73.7				
Five Star Wire Brushed:	FB1	-188.5	-213.7	-192.7	-209.6	-201.2	3.39, 2.85
	FB2	-172.8	-198.2				
	FB3	-216.9	-216.9				
Five Star Pea Gravel Exposed Aggregate:	FPA1	-92.7	-24.5	-92.7	-47.3	-70.0	1.27, 0.99
	FPA2	-92.7	-24.5				
	FPA3	-92.7	-92.7				
Five Star Exposed Aggregate:	FA1	-185.6	-185.6	-169.9	-179.7	-174.8	2.94, 2.47
	FA2	-179.3	-179.3				
	FA3	-144.8	-174.3				
Five Star Water Stopped:	FW1	-208.8	-185.6	-140.2	-174.9	-157.6	2.65, 2.23
	FW2	-106.0	-169.6				
	FW3	-106.0	-169.6				
Five Star Epoxied:	FE1	-168.0	-152.0	-193.2	-167.6	-180.4	3.04, 2.55
	FE2	-228.7	-168.1				
	FE3	-182.8	-182.8				
Five Star Pea Gravel Epoxied:	FPE1	-13.9	-24.5	-19.9	-33.4	-26.6	0.48, 0.38
	FPE2	-22.9	-52.7				
	FPE3	-22.9	32.9				
Five Star Fiber:	FF1	-222.1	-207.7	-221.3	-206.2	-213.7	3.84, 3.02
	FF2	-237.0	-206.1				
	FF3	-204.8	-204.8				
Five Star Shear Key:	FS1	-208.8	-154.3	-195.2	-163.8	-179.5	3.02, 2.54
	FS2	-168.0	-182.8				
	FS3	-208.8	-154.3				

*Highlighted values were outliers at 90% but not 95% confidence level T-tests.

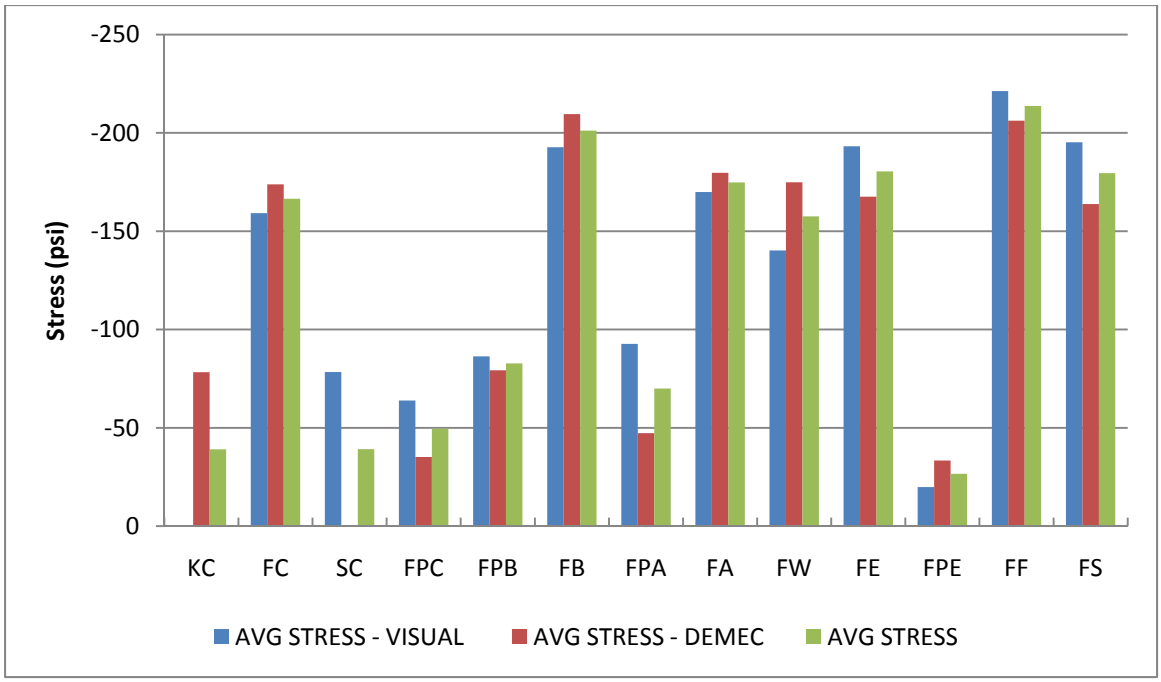

Figure 4-83 Average Stresses of the Grout Rings

Because of the spread in the data, outlier tests were performed using ASTM E 178. The details are included in Appendix C.5. A modified t-test and a Dixon's outlier test were both used to determine outliers. Ten values were identified as possible outliers by Dixon's test. Further analysis was done using the t-test. Ten outliers were identified with a 90% confidence level with the t-test, however no outliers were identified at a 95% confidence level. The ASTM recommends using a level of 95% or higher from the t-test results. Based on the results of both outlier tests, the values were all left in the analysis.

The DEMEC and visible crack detections tended to produce similar average stress levels. Two exceptions occurred: the Type K Concrete and the Set 45 grout specimens. In both sets of samples one of the detection methods produced no bond stress. These sets of samples cracked within a couple days of pouring the grout and they had two of the lowest bond strengths of any material. This method of predicting bond strength did not work well when initial cracking was during the first week after the pour.

Six specimens had average bond strengths less than 100 psi by both first cracking methods. This included the Type K (KC), Set 45 (SC), Five Star pea gravel control (FPC),

Five Star Pea Gravel Wire Brushed (FPB), Five Star Pea Gravel Exposed Aggregate (FPA), and Five Star Pea Gravel Epoxy (FPE). The Type K and Set 45 rings had cracks almost immediately which corresponded to very little bond strength. The Five Star pea gravel specimens all had bond strengths between 27 psi and 83 psi. The control specimen had a strength of 50 psi. The exposed aggregate and wire brushed specimens had higher strengths than the control by 40% and 65%, respectively. The epoxy specimen had a lower strength at cracking. In general, the pea gravel additive lowered the bond strength of the specimens.

Four specimens had bond strengths between 158 psi and 180 psi at the first crack This included the Five Star Control (FC), the Five Star Exposed Aggregate (FA), Five Star Water Stopped (FW), and Five Star Epoxied (FE). The Five Star control specimen was 167 psi, so all of these samples were within 14 psi. The exposed aggregate, water stops, and epoxy did not significantly affect the bond strength.

The two samples with the highest average bond strength were the Five Star wire brushed (FB) and the Five Star fiber (FF). The bond strength for the Five Star wire brushed was 201 psi and the bond strength for the Five Star fiber was 214 psi. These average bond strengths were 20.8% and 28.3% higher than the Five Star control.

All of the Five Star grout had higher bond strength than any of the Five Star pea gravel grouts. The highest Five Star pea gravel mix (wire brushed) had a strength about ½ the value of the lowest Five Star mix. The difference was substantial regardless of the surface condition. This was demonstrated with all four surface conditions that had pea gravel and neat grout tested. The neat grouts always had bond strengths between 2.4 and 6.8 times stronger than the grout with pea gravel.

The wire brushed condition and the fibers created the strongest bonds out of all the scenarios. In the Five Star pea gravel and neat grouts, the wire brush surface condition had the highest strength. The exposed aggregate condition consistently had the second highest bond strengths among the Five Star mixes for both the pea gravel and neat grouts. The shear key, water stop, and epoxied did not substantially change the bond performance compared to the control variables.

The concrete rupture equation estimates the tensile rupture stress of concrete to be $f_t = 6\sqrt{f_c}$. The tensile stress at first cracking was determined based on the laboratory data. The strength of the grout and concrete were both known from the material tests. A new coefficient was computed for each grout material as shown in Table 4-41. The highest coeffecients were for the Five Star and Five Star fiber grouts. They had minimum coefficients of 2.65 and 3.84 for the equation, respectively. The other grouts all had coefficients less than 1.0 because the bond was much less. The Five Star grouts without pea gravel clearly had a much higher tensile stress at first crack.

Table 4-42 Bond Stress Compared to First Crack in the Transverse Joints

Sample Name | Abbreviation		Average Ring Stress (ksi)	First Cracking Stress Lateral Joint Tests (ksi)					
			Looped Bar Joint	Embedded Bar Joint	Grout Only Post-Tensioned Joint 0.167 ksi	Pea Gravel Grout Post-Tensioned Joint 0.167 ksi	Grout Only Post-Tensioned Joint 0.340 ksi	Epoxied Grout Post-Tensioned Joint 0.340 ksi
Five Star Control:	FC1 FC2 FC3	-0.17	-0.30	-0.44	-0.13		-0.17	
Five Star Pea Gravel Control:	FPC1 FPC2 FPC3	-0.05				-0.28		
Five Star Epoxied:	FE1 FE2 FE3	-0.18						-0.17

The bond stresses from the ring samples were compared to the first cracking stresses from the lateral joint tests. Table 4-42 contains the average bond stresses for the Five Star control, Five Star pea gravel control, and Five Star epoxied ring specimens along with the first cracking in each joint. There were four joints with Five Star control, one joint with Five Star pea gravel control, and one with Five Star epoxied.

The Five Star control ring bond stress was close to the tensile stress at first crack in both post-tensioned joints. The average ring stress was 0.17 ksi while the transverse joint tensile stress was 0.15 ksi. The cast-in-place tensile stress at first crack ranged

between 0.30 ksi and 0.44 ksi. This range was twice the average grout ring stress of 0.17 ksi. Part of the reason for the difference may have been because the cast-in-place joints were tested within 7 days of pouring the grout before complete shrinkage had occurred. There were no shrinkage cracks observed in the cast-in-place joints prior to loading. The post-tensioned joints were loaded over 28 days after pouring the grout when shrinkage cracking had already been observed.

The Five Star pea gravel control grout ring cracked at a stress one fifth the size of the tensile stress in the post-tensioned transverse joint. The cracking stress in the transverse joint was 0.28 ksi while the bond stress in the grout ring was 0.05 ksi at the first crack. The stresses in these samples were significantly different. The lateral joint had not cracked due to shrinkage upon the first load. In the other three post-tensioned joints, there was significant shrinkage cracking prior to loading. Because the bond was still intact, the load induced cracking was delayed.

The Five Star epoxied transverse joint cracking stress was very close to the bond stress in the grout rings. The values ranged from 0.17 ksi to 0.18 ksi. Shrinkage cracks were apparent in the post-tensioned joint prior to loading.

The transverse joints that were cracked prior to loading cracked at a stress very close to the shrinkage bond stress in the rings. The transverse joints that cracked at a higher stress than the ring samples did not have cracking due to shrinkage prior to loading. The delay of initial cracking in the transverse joints corresponds to the delay in the first shrinkage crack.

4.2.2.6 Ponding of the Rings

Ponding tests were done on every ring sample weekly for the 12 weeks after pouring the grouts. The tests were compared with the initial ponding performance of the rings at day 2. Each test was performed for 2 hours. Table 4-43 lists the five specimens of the 38 that leaked at any point in the ponding test.

The Set 45 grouts had a propensity to leak throughout the entire tests. The specimens all leaked early in the test and continued to leak. The Set 45 grout was the only grout with consistent problems. From the ponding test the Set 45 grout failed.

Two other specimens developed small leaks. The Five Star pea gravel control specimen #3 developed a small leak toward the end of the test. The leak grew to about ¼ of the interface by the end of the testing. The Five Star pea gravel wire brushed ring developed a leak early in the testing. This leak was not consistent during every ponding test. It never grew any larger and appeared near an imperfection created during the grout pour. These two specimens appeared to be anomalies because the other two specimens in their group did not leak and the leaks were small and inconsistent.

All of the Five Star and Type K grouts performed well during ponding testing. Based on ponding all of these grout types and all the surface techniques are acceptable. The ponding test did not differentiate the grouts with the exception of the Set 45.

Table 4-43 Ponding Results in the Ring Tests

Specimen	Age at First Leak (Days)	Size of the Leak (% of Grout/Concrete Interface)
Set 45 Grout #1	Day 7	100%
Set 45 Grout #2	Day 7	100%
Set 45 Grout #3	Day 2	90% (100% by Day 22)
Five Star Pea Gravel Control #3	Day 45	5% (25% by Day 62)
Five Star Pea Gravel Wire Brushed #3	Day 2	16%

4.2.2.7 Grout Performance Summary

Table 4-44, summarizes the performances of each set of samples. The final data for each category is averaged and the best performers in each category are highlighted. The rows with the most highlighted boxes performed the best as compared to the other samples. A choice can be made as to which grout is best based on the factors that seem most important to a bridge owner. For this research, all factors were considered when analyzing the best and worst performers.

The trends in these boxes show that the Type K, Set 45, and Five Star Pea Gravel control specimens performed the worst. If a standard grout is to be used without a surface alteration in the blockout, then Five Star or Five Star with fibers should be used.

An equivalent highway patch grout with similar material characteristics would also be acceptable.

A wire brushed surface or an epoxied surface worked the best. Other good options are the Five Star shear key and Five Star exposed aggregate. The water stop and Five Star Fibers were acceptable. The choice to add a pea gravel extension did not greatly affect the overall outcome. The pea gravel did affect individual characteristics such as bond strength and shrinkage.

Table 4-44 Summary of Ring Tests

Samples	Average First Crack (Days)	Stress Average at First Crack (psi)	Final Shrinkage Bar Strain (με)	Final Shrinkage (First 24 Hr Included)	Final Grout Ring Strain (με)	Ponding Leaks	Final Percent Cracked	Final Average Crack Size (In.)
Type K Concrete:	2	-39.1	697	297	165		100%	0.0075
Five Star Control:	24	-166.5	223	218	516		100%	0.005
Set 45 Control:	2	-39.2	380	290	79	3 Samples - ~100% Leaked	100%	0.0054
Five Star Pea Gravel Control:	19	-49.6	140	75	360	1 Sample - 25% Leaked	92%	0.0041
Five Star Pea Gravel Wire Brushed:	37	-82.8	140	75	280	1 Sample - 16% Leaked	57%	0.0015
Five Star Wire Brushed:	24	-201.2	223	218	406		83%	0.0028
Five Star Pea Gravel Exposed Aggregate:	17	-70	140	75	493		89%	0.0034
Five Star Exposed Aggregate:	35	-174.8	223	218	365		44%	0.0014
Five Star Water Stopped:	20	-157.6	223	218	647		100%	0.0045
Five Star Epoxied:	36	-180.4	223	218	438		29%	0.0007
Five Star Pea Gravel Epoxied:	16	-26.6	140	75	415		86%	0.0031
Five Star Fiber:	29	-213.7	257	197	425		70%	0.0026
Five Star Shear Key:	28	-179.5	223	218	362		92%	0.0031

*Yellow (Dark) highlights are the best performers in a category

**Red (Light) highlights are the second best (acceptable) performers in each category

5 Finite Element Analysis

5.1 Finite Element Modeling

Finite element modeling was done of the transverse joint models and the ring samples. The software package Abaqus was used for all of the models. They were built as analytical representations of the transverse joint and ring laboratory tests. The modeling techniques and results for each type are explained below.

5.1.1 Transverse Joint Models

The deck panels used in the three transverse joint tests were tested and modeled as a double cantilever system. After building the models, the results were compared to the theoretical stresses and strains expected in the bridge.

5.1.1.1 Modeling Methods

5.1.1.1.1 Two Dimensional Trials

The objective of this finite element model was to accurately predict the stress levels along the girder line of a deck panel system. The first step was to choose a modeling program and method. The Abaqus finite element package was chosen for all of the finite element models because of its availability, applicability, and flexibility. It had the option of modeling with many types of elements and could be done with two or three dimensions.

The methods used for the models were chosen after reviewing past literature and doing trial runs on bridge models. The first decision was to use two dimensional modeling instead of three dimensional modeling because of the computational efficiency. Past research by Sullivan showed that two dimensional modeling provides good results when modeling girder lines with deck panels (Sullivan 2007). The objective of the modeling was to find a method that produced the same results as the tests in the longitudinal direction of the bridge. Simple spans with steel girders and concrete decks were investigated to confirm this assumption. Stresses in the joints and girders were measured and compared to theoretical values from mechanics equations (Table 5-1).

At the same time an element type had to be chosen for use on the models. All of the bridge parts were primarily tested for bending. Two different types of plane stress elements were considered: a 4 node (CPS4R – 4 node quadratic plane stress, reduced integration) and an 8 node (CPS8R – 8 node quadratic plane stress, reduced integration) element. The decision was made to use the 8 node element because parasitic shear would not occur in these quadratic elements. Quadratic plane stress elements were used on all parts of the bridge because they provide accurate results in a bending situation. This included separate elements for the girder flanges, web, haunch, deck, and reinforcing bars. In the deck panel analysis, the stresses and strains along the girder lines were the focus. Simply supported beam models were created with a composite deck system on a W21x101 steel girder. All of the elements were constrained, or connected, at the intersection of the different parts (flanges, web, haunch, and deck slab). The results were close to the theoretical when using 8-node plane stress elements with a width of 3.375 in. The height was set either with the same dimension as the width (i.e. Girder and Deck Sections) or with the maximum height of the section (i.e. Flange and Haunch Sections). Beam theory stresses and deflections for the simply supported condition were compared to the finite element results and the 8 node element models were within 6% for a composite bridge deck (Table 5-1). The beam theory results for deformation and stress were conservative.

The only time 4 node elements worked efficiently was for the prestressing strand. The prestressing strands were placed in the model to apply an initial compressive force to the deck system. They did not contribute to the bending strength. The 4 node elements provided good results, were computationally efficient, and prevented internal errors from occurring within the Abaqus processor.

Table 5-1 Verification of the Abaqus Models

Model (All Models were 2-Dimensional and loaded with a point load a midspan)	Maximum Abaqus Stress	Maximum Theoretical Stress	% Difference
W21x101 Beam, 20 ft, Simply Supported, 8 – Node Quadratic Elements, 20 Elements x 5 Elements	0.279 ksi	0.301 ksi	-7.3%
W21x101 Beam, 20 ft, Simply Supported, 8 – Node Quadratic Elements, 240 Elements x 23 Elements	0.279 ksi	0.301 ksi	-7.3%
W21x101 Beam and 8 in x 42 in Deck, 20 ft, Simply Supported, 8 – Node Quadratic Elements, 20 Elements x 9 elements	0.173 ksi	0.158 ksi	9.5%
W21x101 Beam and 8 in x 42 in Deck, 50 ft, Simply Supported, 8 – Node Quadratic Elements, 20 Elements x 9 Elements	0.418 ksi	0.433 ksi	-3.5%
W21x101 Beam and 8 in x 42 in Deck, 50 ft, Simply Supported, 8 – Node Quadratic Elements, 20 Elements x 9 Elements, 100 psi in the Deck	0.102 ksi	0.101 ksi	0.1%
W21x101 Beam and 8 in x 42 in Deck, 50 ft, Simply Supported, 8 – Node Quadratic Elements, 20 Elements x 9 Elements, 100 psi in the Deck, Spring Constrained to the Haunch	0.154 ksi	0.145 ksi	5.8%

The deck panels were built in steps and therefore required staged finite element models. In the first stage, prior to attaching the deck panels to the bridge girders, a post-tensioning force was added to some of the decks. In the second stage of the finite element model, springs were used to constrain the bridge deck to the girders. In the final stage, the service load vehicle was applied to the model.

The springs were given non-linear properties based on a force versus displacement relationship (Figure 5-1). Initially, the springs were designed with a very small stiffness (0.001 k/in) to simulate a free condition. This constant was chosen because it was the largest value that created a condition that behaved as an unconstrained system and was computationally efficient. After the stress was applied, the springs were given a very large spring constant (1,000,000 k/in) to simulate a fixed condition. This constant was chosen because it was large enough to create a

constrained system without making the model unstable or computationally inefficient. The point where the non-linear behavior began was computer based on the axially deformed mechanics equation, $\Delta = PL/AE$. The post tensioning load applied, length of the deck, cross sectional area of the deck, and the modulus of elasticity of the concrete had been identified. This resulted in a deflection value for the system upon applying the post-tensioning force. Any deflection in the panels beyond this point resulted in a fixed condition because of the high spring constant.

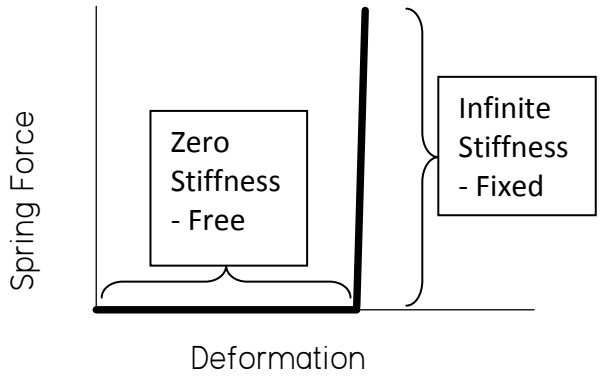

Figure 5-1 Spring Stiffness for the Post-Tensioned Deck Connections

5.1.1.2 Analysis of the Transverse Joint Tests

The model for the deck panels is shown in Figure 5-2. The models were made of the transverse joint tests from the laboratory specimens (Figure 3-6). Each test was modeled as a single girder line system. The tests were built with two girders and a 7 ft wide deck. The models were built with one girder and a 3.5 ft wide deck. The models were a simply supported system with a cantilever. A roller was placed at midspan, a pin at the restrained end, and a load at the other end. The load level applied to the model was half the load applied to the actual system, 37.75 kips.

The finite element mesh is shown in Figure 5-3. The elements are all rectangular and vary in height based on the physical constraints of the parts. The dense elements in the middle of the deck correspond to the embedded elements from the post-tensioned

strands. The material properties for the deck are the same as the transverse joints presented in Appendix B.1.

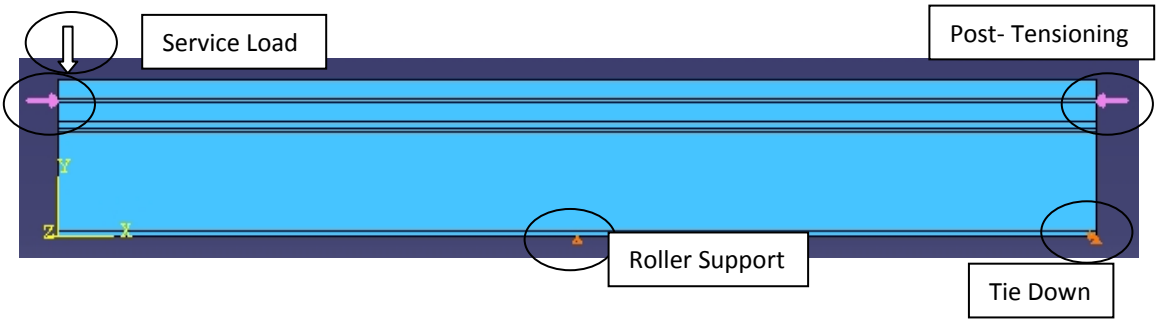

Figure 5-2 Abaqus Model for the Deck Panels

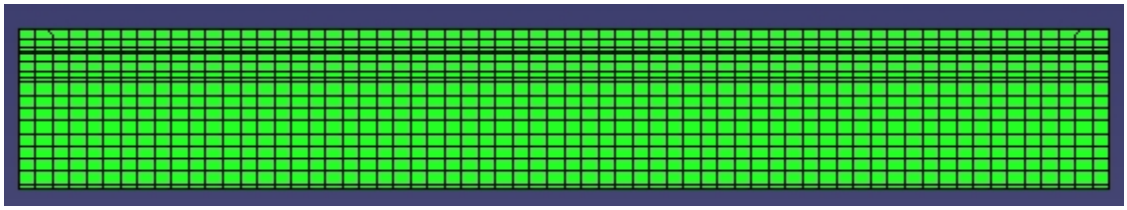

Figure 5-3 Finite Elements for the Deck Panel Models

The stresses in the results were highest at the roller support in the middle of the specimen. The stresses in the deck were highest at the top surface as expected. The neutral axis occurred near the top flange as predicted by beam theory results. Figure 5-4 demonstrates a typical in plane, primary stress distribution in the models.

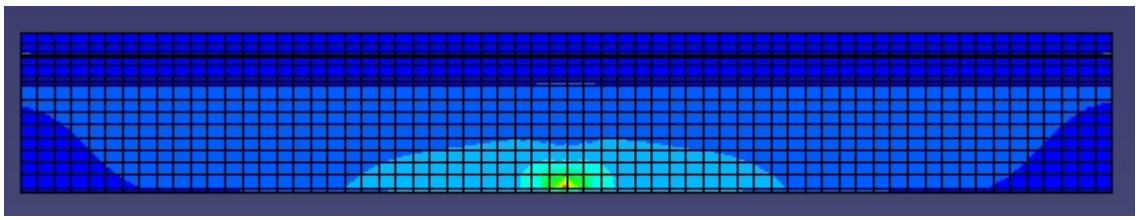

Figure 5-4 Typical Stress Distribution in the Abaqus Deck Panel Models

During testing, creep and shrinkage effects were not investigated because the models were tested a few weeks after constructing the bridge decks. The long term losses were not considered on the models. Immediate losses were measured and taken into account when applying the longitudinal load to the deck panels.

In all of the models, the strains, stresses and deflections at key points were recorded. In the transverse joints laboratory tests, these same values were monitored at the location of the joints and at the edge of the cantilevered system. Strain profiles were then compared between the tested, the design, and the finite element values for short term effects.

The strains and stresses at key locations are shown in Table 5-2 through Table 5-4. The joint with 340 psi of compressive stress in the slab had model results very close to the laboratory results. The stresses and strains throughout the model were close to the test and theoretical values. All of the values except the stress at the top of the joint were within 4% of the actual test readings. The stress at the top was 12% higher in the Abaqus model. It must be noted that in the theoretical computations and the Abaqus model, cracking was not taken into account. There was slight cracking in the deck surface of the laboratory model.

The stresses and strains in the 167 psi laboratory joint did not match the Abaqus model closely. The values ranged between -20% and 21% different. What must be noted is that the last 30% of the load in this model caused surface cracking in the panels. The panels were not expected to do this and the Abaqus model was built assuming no cracking. This was the main source of error in the model.

The cast-in-place Abaqus model did not closely agree with the laboratory results. They ranged from -90% to 20% difference. As expected, the strains and stresses were higher in the bottom of the girder and lower in the deck panels. This was because cracking occurred very early in the test. The model assumes an uncracked situation. The stresses and strains were redistributed in the laboratory tests but not in the Abaqus model.

Table 5-2 Comparison of the 340 psi Joint Results

	Final Stress and Strains (Post-Tensioning and Service Loads Added)				
	Theoretical	Abaqus		Laboratory Tests	
		Reading	%Difference	Reading	% Difference
$\sigma_{joints\text{-}top}$	0.216 ksi	0.193 ksi	-11%	0.17 ksi	12%
$\sigma_{girder\text{-}bottom}$	6.94 ksi	7.18 ksi	3.5%	6.90-7.08 ksi	3.9% : 1.4%
$\varepsilon_{joints\text{-}top}$	36.3 με	40.9 με	13%	39.9 με	2.4%
$\varepsilon_{girder\text{-}bottom}$	241 με	242 με	0.4%	238-244 με	-0.9% : 1.7%

Table 5-3 Comparison of the 167 psi Joint Results

	Final Stress and Strains (Post-Tensioning and Service Loads Added)				
	Theoretical	Abaqus		Laboratory Tests	
		Reading	%Difference	Reading	% Difference
$\sigma_{joints\text{-}top}$	0.389 ksi	0.356 ksi	-8.5%	0.28 ksi	21%
$\sigma_{girder\text{-}bottom}$	6.79 ksi	7.01 ksi	3.2%	8.38 ksi	-20%
$\varepsilon_{joints\text{-}top}$	71.0 με	68.6 με	-3.4%	64 με	6.7%
$\varepsilon_{girder\text{-}bottom}$	241 με	242 με	0.4%	289 με	-19%

Table 5-4 Comparison of the Cast-in-Place Joint Results

	Final Stress and Strains (Service Loads Added)				
	Theoretical	Abaqus		Laboratory Tests	
		Reading	%Difference	Reading	% Difference
$\sigma_{joints\text{-}top}$	0.55 ksi	0.55 ksi	0%	0.30-0.44 ksi	-45%: -25%
$\sigma_{girder\text{-}bottom}$	6.79 ksi	6.89 ksi	1.5%	7.98-8.73 ksi	19% : 29%
$\varepsilon_{joints\text{-}top}$	103 με	109 με	5.8%	10-20 με	-90%: -81%
$\varepsilon_{girder\text{-}bottom}$	241 με	242 με	0.4%	275-301 με	14% : 20%

The Abaqus model will work for an uncracked post-tensioned deck. Further investigation would be needed to model a cracked deck panel system. The goal of the research was to build transverse joints that do not crack.

In the future this would work well for designing a deck panel system and predicting the stresses and strains in the deck and steel girder system. The stresses in the model could be compared to the expected cracking stresses. If the stresses in the Abaqus model exceed the cracking stress, a designer would be aware of a potential problem. The most applicable situation would be in a post-tensioned deck panel system. It must be noted that time dependent effects were not taken into account.

One use of the model would be for the demonstration bridge. The level of stress designed for the bridge can be compared to the recommended level computed from the finite element model. The model will be used to check the design and to compare the bridge performance during future testing. The strain profile from the finite element model will be compared to the strain profiles obtained from the live load test in the future.

5.1.2 Grout Ring Models

The concentric grout and concrete rings from Section 4.2 were modeled in Abaqus. The goal was to model the stress and deformation relationship given a strain rate. Thirteen unique grout and surface conditions were modeled with a 2-dimensional finite element model in Abaqus. The strain rates were input based on the test data. The stress at first crack was computed with the finite element model. The deformation predictions of the model at first crack were then compared to the values from the laboratory tests.

5.1.2.1 Two Dimensional Modeling

5.1.2.1.1 Abaqus Ring Models

The objective of these models was to replicate the shrinkage performance of the models in the laboratory. The rings consisted of two layers of cementitious materials: grout and concrete. Plane stress elements were used because the stress was only of interest in the plane of the rings. All measurements from the laboratory tests were of the surface strain in the grout rings. A typical bridge deck may run hundreds of feet

long, a minimum of 30 ft wide, and approximately 8 in. thick. Their thickness is very thin compared to the total cross sectional area. The ratio of the cross sectional area to the thickness was 375 for the Virginia bridge.

The element selection was done after deciding to use the plane stress elements. In the case of the rings, they would all shrink radially about the center point of the sample. Elements were laid out concentrically about the center point. Two different types of plane stress elements were investigated: a 4 node (CPS4R – 4 node quadratic plane stress, reduced integration) and an 8 node (CPS8R – 8 node quadratic plane stress, reduced integration) element. Initial tests were run on both elements with a ring sample and a uniform unit compressive load on the outside. The think walled cylinder equation was used to compute the expected deformation in a concrete ring under a uniform compressive stress (Figure 5-5). The theoretical deflections calculated using the thick walled theory were compared to the values obtained from the models with both element types. Numerous different Poisson ratio, modulus of elasticity, and concrete compressive strength combinations were used. The ring was tested with 25, 80, and 200 elements along the outside diameter. The 8 node plane stress elements with 200 elements on the outer diameter returned values within approximately 5% of the theoretical values. The 4 node elements were slightly higher (Table 5-5). Therefore, the 8 node elements were chosen.

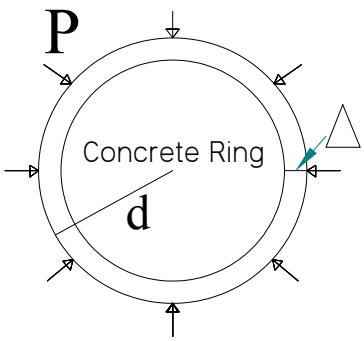

$$\Delta = (1 - v)Pd/E$$

Where

Δ	=	Uniform Displacement of the Ring
v	=	Poisson's Ratio of the Ring
P	=	External Uniform Pressure
d	=	Original Diameter of the Ring
E	=	Modulus of Elasticity of the Ring

Figure 5-5 Verification of the Abaqus Model with Thick Walled Cylinders

The concrete rings were 18 in. in diameter and the grout rings were 8 in. in diameter. The elements were laid out in the model as concentric rings. The 80 element layout was used because it was shown to be precise enough but not too small to be computationally inefficient. On the outer edge the elements were 0.7 in by 0.5 in. As they moved in, the elements became more rectangular in shape. An example is shown in Figure 5-6.

Table 5-5 Verification of the Abaqus Ring Models

Model (All Models are 2-Dimensional, plane stress, and have a unit load applied around the circumference.)*	Abaqus Interface displacement (in.)	Theoretical Interface displacement (in.)	% Difference
4-node, 25 elements per diameter	0.00102	0.00085	20%
4-node, 100 elements per diameter	0.00184	0.0016	15%
4-node, 200 elements per diameter	.000663	.000615	7.8%
8-node, 200 elements per diameter	.000622	.000615	1.2%

*This is a representative sample of the verification models.

The ring models were made with 8 node quadratic plane stress elements (Figure 5-6). The thickness of all the elements was 4 in., the same as the laboratory specimens. The shrinkage of concern was the "in-plane" shrinkage of the grout. Concrete shrinkage was not taken in account because, as observed in the lab, it had nearly stopped shrinking.

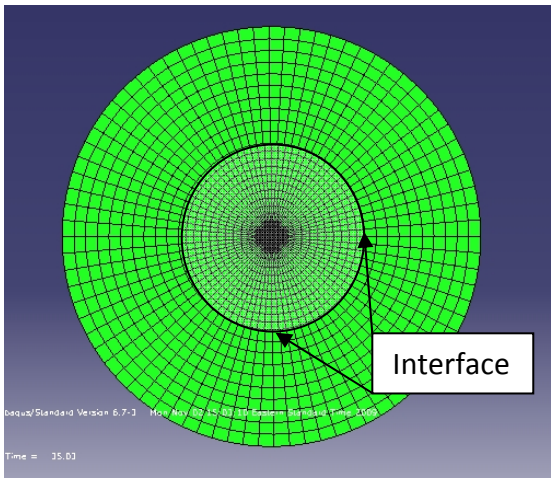

Figure 5-6 Finite Element Layout for the Rings

The rings models were modeled with two materials that were homogenous throughout: i.e. the Poisson's ratio, modulus of elasticity, and the compressive strength were constant (Table 5-6). Because of this, the ring models would result in the same

stress patterns throughout the rings. Based on symmetry and the material properties, the samples acted axisymmetric.

The shrinkage was applied to the grout ring by using the internal swelling function in Abaqus. This built in function is based on a linear strain rate multiplied by a factor of 1/3. A negative strain value was computed since the strain was shrinkage and not swelling. The strain for each grout was computed using the unbounded strains found from the ASTM C157 results for each grout material (Figure 5-7). In every case, the stress at the concrete-grout interface at first crack was approximately 25% higher than the value using thick walled cylinder equations. Abaqus predicted the stress too high in all cases, so the rate was reduced to match the laboratory results.

In every model, the strain of the grouts closely followed a logarithmic curve however, in Abaqus the strain rate was linear. The results were only accurate at the point of first crack. In order to model the shrinkage of the grouts throughout the tests, a nonlinear shrinkage function would be needed.

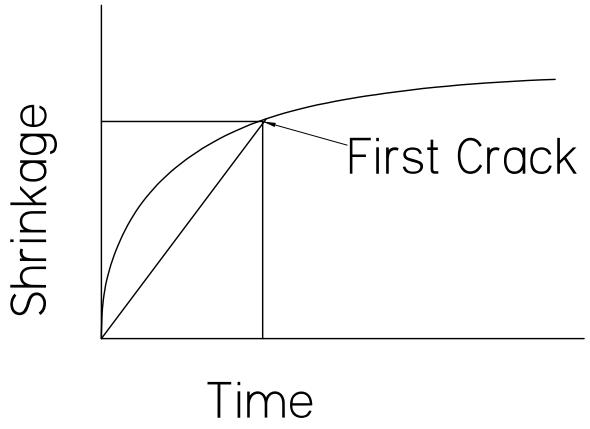

Figure 5-7 ASTM C157 Shrinkage versus Time Graph

The center of the ring was assumed to have no shrinkage. Horizontal, transverse, and rotational fixity was enforced at the center of each model. The interface

between the materials was expected to have a perfect bond until the first crack appeared. A constraint was placed between the grout and concrete model.

The models resulted in a stress and deformation at the grout-concrete interface at first cracking. The stress values were compared to the laboratory predictions to ensure they matched. The change in diameter of the grout-concrete interface was expected to compare with the range of values measured in the laboratory for each sample.

Table 5-6 Ring Material Properties for the Finite Element Model

Sample Name | Abbreviation		Concrete Poisson's Ratio, V_c	Concrete Modulus of Elasticity, E_c (ksi)	Grout Poisson's Ratio, V_g	Grout Modulus of Elasticity, E_g (ksi)	Computed Strain Rate (ε/day)
Type K Concrete:	KC1	0.13	3010	0.13	1620	-0.000146
	KC2	0.13	3010	0.13	1620	
Five Star Control:	FC1	0.19	4020	0.17	2700	-0.000446
	FC2	0.20	3530	0.17	2740	
	FC3	0.19	4020	0.17	2740	
Set 45 Control:	SC1	0.13	3010	0.22	5400	-0.000093
	SC2	0.13	3010	0.23	2720	
	SC3	0.0	0	0.00	----	
Five Star Pea Gravel Control:	FPC1	0.19	4020	0.18	2340	-0.00000754
	FPC2	0.19	4020	0.18	2340	
	FPC3	0.19	4020	0.18	2340	
Five Star Pea Gravel Wire Brushed:	FPB1	0.19	4020	0.18	2340	-0.00000845
	FPB2	0.19	4020	0.18	2340	
	FPB3	0.20	3810	0.17	2200	
Five Star Wire Brushed:	FB1	0.19	4020	0.17	2700	-0.0000228
	FB2	0.20	3530	0.17	2740	
	FB3	0.19	4020	0.16	2750	
Five Star Pea Gravel Exposed Aggregate:	FPA1	0.19	4020	0.18	2340	-0.0000117
	FPA2	0.19	4020	0.18	2340	
	FPA3	0.19	4020	0.18	2340	
Five Star Exposed Aggregate:	FA1	0.19	4020	0.16	2750	-0.0000133
	FA2	0.20	3810	0.17	2800	
	FA3	0.19	4020	0.20	2530	
Five Star Water Stopped:	FW1	0.19	4020	0.16	2750	-0.0000216
	FW2	0.20	3530	0.17	2740	
	FW3	0.20	3530	0.17	2740	
Five Star Epoxied:	FE1	0.19	4020	0.17	2700	-0.0000131
	FE2	0.18	3900	0.17	2800	
	FE3	0.19	4020	0.17	2700	
Five Star Pea Gravel Epoxied:	FPE1	0.19	4020	0.18	2340	-0.00000535
	FPE2	0.20	3530	0.17	2340	
	FPE3	0.20	3530	0.17	2340	
Five Star Fiber:	FF1	0.18	3900	0.18	2660	-0.0000203
	FF2	0.19	4020	0.19	2560	
	FF3	0.19	4020	0.19	2520	
Five Star Shear Key:	FS1	0.19	4020	0.16	2750	-0.0000168
	FS2	0.19	4020	0.17	2700	
	FS3	0.19	4020	0.16	2750	

5.1.2.1.2 Abaqus Ring Model Results

The ring data from the laboratory tests resulted in average deflection measurements at six locations on the edge of the grout ring. These measurements were used to find the stress level at the first crack. This stress level and time to the stress level were used to build the shrinkage models in Abaqus. Once the shrinkage was determined, the ring models were run to determine the stress throughout the life of the grout. When the stress reached the critical cracking value, then the time to first crack was known.

The deformations of the top surface of the laboratory rings were measured with DEMEC points. The range of deformations was substantial because they depended on finding the time right before the first crack occurred. The two different methods to determine the age at first crack, visually and with DEMEC strains, produced a range of values. Table 5-7 contains the average values from the two methods. At the first crack, the samples did not crack around the entire diameter. As discussed previously (Section 4.2.2.4.1), the first cracks were very small and only occurred at 10% to 25% of the interface (Figure 5-8). The maximum measured deformation in the rings was greater than the average deformation measured in the rings at the first crack. The Abaqus model was derived to provide a continuous stress and deformation around the entire interface. Therefore, both the average and maximum deformations at first crack in the rings are reported and compared to the values from the Abaqus models (Table 5-7, Figure 5-9).

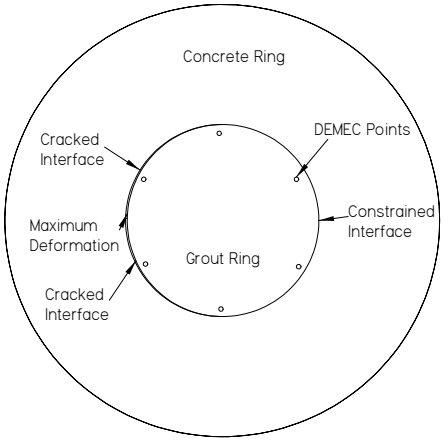

Figure 5-8 First Cracking Pattern in the Grout Rings

Table 5-7 Comparison of Laboratory and Abaqus Deformations at First Crack

		Deformations of the Grout-Concrete Interface at First Cracking		
Sample Name | Abbreviation		**Range of Average Ring Deformations (in.)**	**Range of Maximum Ring Deformations (in.)**	**Abaqus Ring Deformations (in.)**
Type K Concrete:	KC	0.0 0.000521	0.0 0.000072	-0.000176
Five Star Control:	FC	-0.000161 -0.000284	-0.000277 -0.000409	-0.000215
Set 45 Control:	SC	-0.000114 0.0	-0.000197 0.0	-0.0000876
Five Star Pea Gravel Control:	FPC	-0.000172 0.000015	-0.000150 -0.000327	-0.000083
Five Star Pea Gravel Wire Brushed:	FPB	0.000028 -0.000336	-0.000739 -0.000761	-0.000151
Five Star Wire Brushed:	FB	-0.000044 -0.000099	-0.000528 -0.000624	-0.000345
Five Star Pea Gravel Exposed Aggregate:	FPA	-0.000071 -0.000453	-0.000375 -0.000682	-0.000127
Five Star Exposed Aggregate:	FA	0.000021 -0.000604	-0.000206 -0.001044	-0.000271
Five Star Water Stopped:	FW	-0.000034 -0.000294	-0.000208 -0.000556	-0.000289
Five Star Epoxied:	FE	-0.000424 -0.000960	-0.000714 -0.001218	-0.000305
Five Star Pea Gravel Epoxied:	FPE	0.000035 0.000059	-0.000088 -0.000121	-0.000045
Five Star Fiber:	FF	0.000080 -0.000411	-0.000042 -0.000545	-0.000377
Five Star Shear Key:	FS	-0.000165 -0.000341	-0.000382 -0.000449	-0.000272

*Positive values are swelling.

** Highlighted Values Fall Outside the Average Deformation Range

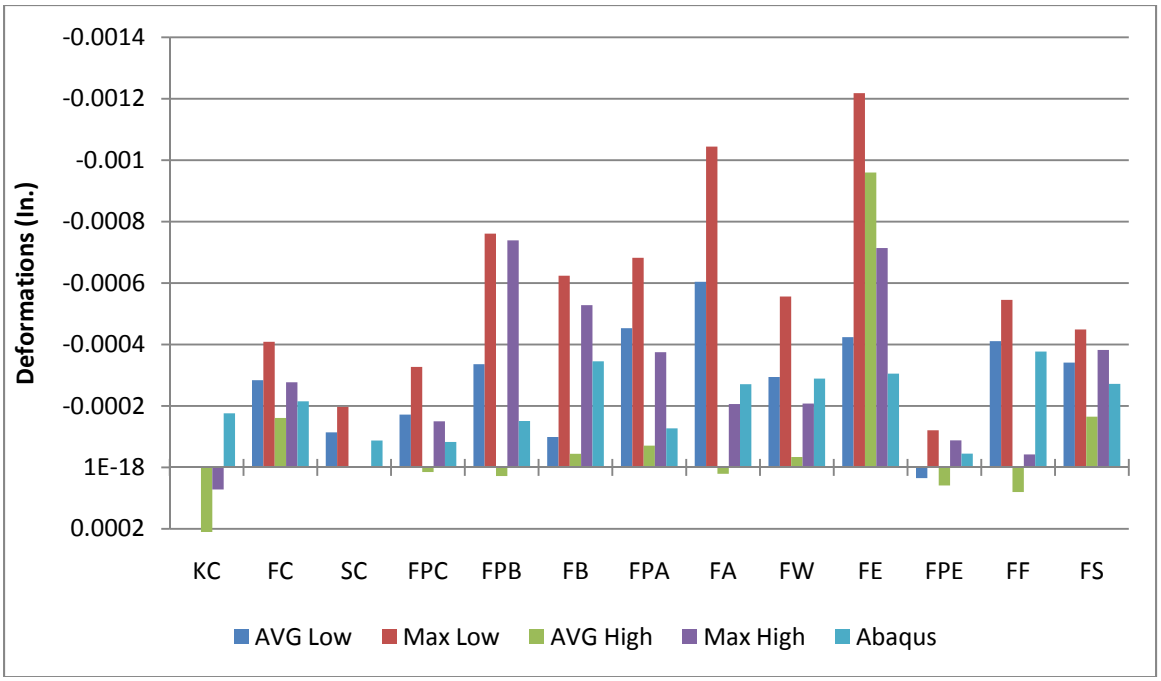

Figure 5-9 Deformations at the Concrete-Grout Interface

The deformations and stresses at the grout-concrete interface were recorded for each Abaqus model. The graphical results were viewed in Abaqus to ensure uniform values at similar radii in the ring (Figure 5-10). The stress values in the model matched the stress values computed from the laboratory tests. The deformation values at the interface are shown in Table 5-7. The Abaqus results were expected to fall close to the range of measured results from the laboratory samples.

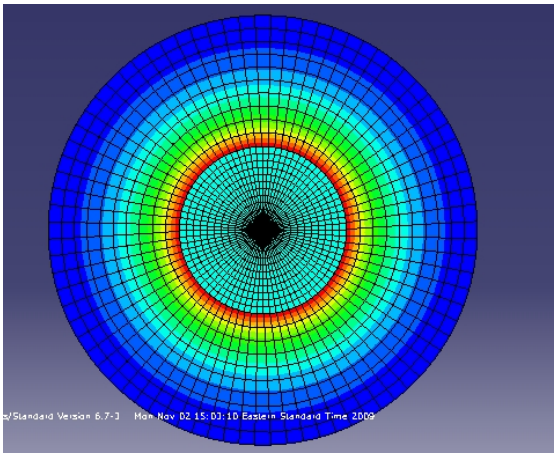

Figure 5-10 Uniform Stress output from Abaqus for a Ring Sample

Nine of the thirteen samples had deformation values predicted by the Abaqus models within the average deformation range observed from the laboratory. Table 5-7 shows the range of average and maximum deformations at the first crack and the predicted deformation based on the Abaqus model. The average deformations should be closer to the Abaqus values because the Abaqus models predict a uniform stress around the ring. The maximum deformation values demonstrate the range of values due to uneven cracking at the interface.

The Type K ring was one sample that did not have agreement between the laboratory and Abaqus model. The problem with this model was that the shrinkage values used in the model did not take into account the significant swelling that took place within the first 24 hours for this grout. The first crack occurred when the Type K rings had a net swelling, therefore the shrinkage rate available from the ASTM C157 bars did not correspond well to the actual behavior.

The Five Star pea gravel epoxy specimens did not fall within the deformation range measured in the laboratory because the deformations were very small and some swelling occurred. The Abaqus model predicted deformations in the middle of the range between the average and maximum values. The Abaqus prediction was within the range of observed values.

The Five Star wire brush specimens had Abaqus predicted deformations higher than the observed average deformations. The Abaqus predictions were right between the average and the maximum observed deformations. The Abaqus prediction was still within the range of observed values.

The Five Star epoxied Abaqus model was the only one to predict deformations below all of the average and maximum observed values. Of all the laboratory samples, this one had the latest and smallest first cracks. In addition, the cracks never developed very large. The first cracking measurements are not as precise because the first crack was extremely hard to identify. The Abaqus modeling did not prove accurate in a very slow shrinkage situation with only minute cracks.

In general, the Abaqus models predict an average deformation of the ring interface within the range of the observed values in the laboratory. Most of the laboratory rings did not crack across the entire interface with the same size crack at the same time. The Abaqus model only captures an average deformation with a similar stress observed at the interface in the laboratory. These models provide a good estimate of the deformation to be expected at the grout-concrete interface.

5.1.2.2 Prediction Models

The Abaqus modeling techniques may be used to predict average stress and deformation estimates for different size shear pockets when the material properties are known. In many cases, square, rectangular, or oblong shear pockets are used. If an ultimate strain and the material properties are available for the grout, then the stress level and deformation may be estimated. These deformations and stresses could be compared to the average deformation and stresses computed at first cracking from this research. This would provide an estimate for if and when the pocket would crack. By adjusting the blockout dimensions and material types, the model would help predict performance. This would be very useful for a designer working on deck panel blockouts.

Figure 5-11 is an example of how the design process could work. A designer would pick a few combinations of blockout sizes and grout materials. In this case, they are labeled A, B, and C. The shrinkage expected during the life span of the grout is input

into the model along with the Poisson's ratio and modulus of the grout and concrete. The result would be a maximum deformation and stress for each material. These values could be compared to the stresses and deformations observed at first cracking in laboratory tests.

For these three examples, the first cracking would occur at the limit labeled First Crack Limit. Any part of the model with deformations above this value would be expected to crack. The time to first cracking could be estimated on the horizontal axis of the graph. In this problem, blockout A and B would crack because their final deformation would be greater than the limit. Blockout C would never crack because the final deformation is less than the limit. The blockout size and material used in C would be the best design choice.

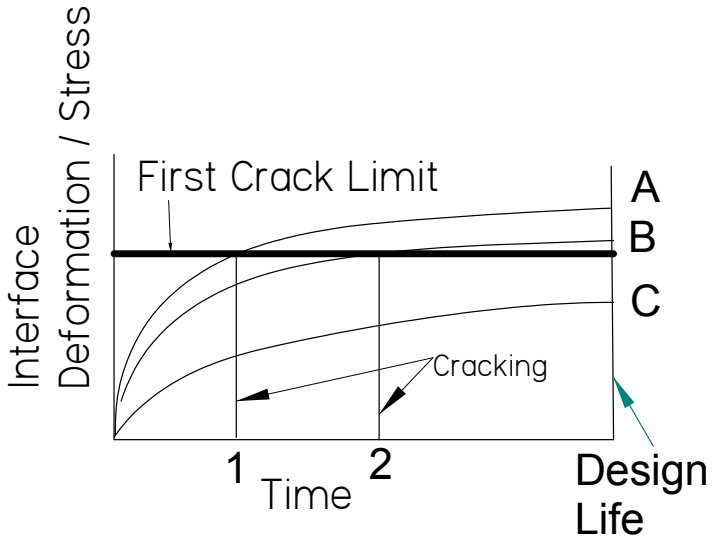

Figure 5-11 Sample Design of a Blockout

6 Conclusion and Recommendation

At the beginning of this research project a list of research needs was developed (See Table 2-6). Table 6-1 is a summary of each research need and the results. Following this summary table is a more detailed list of conclusions drawn from the transverse joint and grout ring tests. Each section is broken into the construction, performance, and design of the specimens.

6.1 Transverse Joint Tests

6.1.1 Construction

The general construction processes were similar to methods from previous research or traditional deck construction. Some of the specific forming methods, materials, and procedures did deviate. The following conclusions were drawn from the construction of the transverse joint tests.

1) The panels were easy to build in the precast plant, however the addition of suspended parts or complex geometry slowed the process. In particular, the HSS sections, the water stops, the anchor bolt assembly, and the post tensioned anchors took more time to install.
2) Fiberboard formwork contained the grout, was easy to adjust, and stiff enough to withstand the self weight of the deck panels.
3) The looped bar joints and post-tensioned joints had sufficient tolerances and were quick to install. The embedded bar joint did not have sufficient tolerance to align the rebar and was difficult to setup.

Table 6-1 Summary of Research Results

Research Need	Research Results
1. Construction Methods for Joints and Haunches	1. During construction a list was developed of the procedures followed, materials used, and manpower needed. 2. The optimum grout material for the transverse joints was a neat Five Star grout. Forming the transverse joints without protrusions through the deck surface worked best. 3. The easiest joints to build were the looped reinforcing bar joint followed by the post-tensioned joints.
2. Performance of Grouts Used in the Shear Pockets	1. The ring models revealed that Five Star Highway Patch grout performed the best. Set 45 performed the worst. Polypropylene fibers can improve grout performance. Adding a pea gravel provides mixed results. 2. A surface preparation technique will reduce cracking, increase bond strength, and prevent leaking. 3. The wire brushed and epoxy surfaces performed best. The water stop prevents leaks but cracks. The exposed aggregate was acceptable. 4. A finite element model was created to help predict the first crack and deformation in the grout rings.
3. Compare Post-Tensioned and Cast-In-Place Transverse Joints	1. The post-tensioned joint with 0.340 ksi of effective stress performed best. 2. The looped reinforcing joint was acceptable.
4. Negative Moment (Tensile) Tests on Transverse Joints	1. The cast-in-place joints cracked. The looped joint performed better than the embedded bar joint. 2. Providing a sufficient level of post-tensioning ensured a good product. A low level of post-tensioning produced a bad joint.
5. Post-Tensioning Level in Transverse Joints	1. A tensile cracking stress of 0.130 ksi was the point of first crack at the concrete-grout bond interface. 2. The post-tensioned design methods worked but the tensile strength of the transverse joints was less than predicted. 3. A finite element model was created that predicts the stresses in an uncracked post-tensioned system.
6. Stiffness Loss in Transverse Joints Over the Design Life	1. The cast-in-place joints transferred very little strain throughout the cyclical tests. By the end of the test, the embedded bar joint lost significant stiffness. 2. The 0.167 ksi post-tensioned joint maintained a linear stiffness for approximately 2/3 of the design load. After cracking the strain remained constant. The behavior remained consistent throughout testing. 3. The 0.340 ksi post-tensioned joint had a nearly linear strain distribution throughout testing. The joint stiffness was maintained.
7. Implement the Results on a Real Bridge	1. Based on the transverse joint results a post-tensioned bridge was designed. 2. The design documents were created and transmitted to the bridge owner, VDOT.
8. Monitor the Behavior of a Real Bridge Designed With Deck Panels	1. A suggested instrumentation plan was created for the Virginia bridge.

4) Using threaded rods to hold up the wooden formwork created weak points in the grouted joints. Tying the formwork to the reinforcing bars prevented weak points in the top surface of the deck slab.

5) Adding a pea gravel to the joint did not take additional time, but workability suffered and segregation occurred when the mix was not placed within 15 minutes.

6) Installing post-tensioning was not difficult, however seating losses were significant given the short (18 ft) deck panels.

7) Having a sufficiently large workforce was essential at all stages because of the time dependent nature of installing the panels. This was particularly true when setting the panels, pouring the grout, and post-tensioning the deck panels.

6.1.2 Performance

The transverse joints in the deck panels were exposed to 1,000,000 cycles of the truckload. This value was the expected 75 year design life for the rural bridge in Virginia. The transverse joint tests were based on the expected loading conditions of the Virginia bridge. A number of observations were made for the best joint to use on this bridge.

1) The concrete-grout interface is the weakest point in all of the joints. The tensile strength of this joint is weaker than the tensile strengths of the concrete and grouts tested.
2) Shrinkage cracking will occur between the concrete and grout interface if no surface preparation technique is used regardless of the joint type.
3) Imperfections due to tie rods or formwork will cause cracking in the grouts.
4) Reinforced joints under tensile forces will crack under HS-20 loading primarily between the concrete and grout. Cracking occurs immediately upon loading.

5) In the post-tensioned transverse joints, cracking was first observed at a net stress level of 0.13 ksi (precompression minus the load induced stress). This corresponds to a tensile strength of $1.5\sqrt{f'c}$ in the transverse joint. F'c is the weakest compressive stress between the grout in the joint and concrete panels.
6) A post-tensioning level of 0.340 ksi effective stress prevented significant cracking in the top surface of the joint and resulted in linear strain behavior at the transverse joint.
7) A post-tensioning level of 0.167 ksi resulted in significant cracking in the top surface of the joint and a non-linear strain response at the transverse joint.
8) The embedded bar joint cracked significantly. The concrete at the transverse joint carried almost no strain.
9) The looped reinforcing bar joint had minor cracks between both grout-concrete interfaces. At the transverse joint, the concrete carried a small amount of strain.
10) Reinforced joints and post-tensioned joints that crack will leak water. A level of 0.340 ksi prevented any leaks from occurring in the transverse joints.
11) The neutral axis based on the strain measurements remained constant for a post-tensioning joint with 0.340 ksi of initial stress. The reinforced joints and 0.167 ksi post-tensioned joints had neutral axes that moved toward the neutral axis of the girder, away from the deck, during cyclical loading.
12) The surface strain under the maximum service load remained constant for the 0.340 ksi joint. The embedded bar experienced the largest increase in surface strain during the tests followed closely by the 0.167 ksi joints. The looped bar joint had consistent surface strains.

The post-tensioned joint with 0.340 ksi of initial stress in the joint performed the best based on cracking, deformation, ponding, and strain distribution measurements. This joint is recommended for future transverse joints. The model developed by Bowers et al. is acceptable for designing the tranverse joints, however the tensile

strength of the concrete should be reduced to $1.5\sqrt{f'c}$. (F'c is the weakest compressive stress of the concrete and grout). This should eliminate or greatly reduce cracking.

The looped reinforcing bar joint had minor cracking and the second smallest leaks during testing. If post-tensioning was not an option, then the looped reinforcing bar joint would provide satisfactory performance. The top surface of the joint should be covered in an impermeable barrier to increase its life span and reduce effects from leaks.

The 0.167 ksi joints and embedded bar joints did not perform well based on leaking, extensive cracking and large deformations. These joints are not recommended for transverse joints in full depth deck panels.

6.1.3 Finite Element Analysis

The finite element models were made of the six transverse joints. The following conclusions were drawn from the plane stress models for each joint.

1) The plane stress, 8-node element accurately predicted the stress and strains due to applied loads in the post-tensioned uncracked joints.
2) The reinforced concrete joints are not accurately modeled after cracking. A more detailed cracking model would be necessary to predict stresses and strains in the deck panels.
3) The finite element models could be adjusted for different continuous applications. The stress and strains could be predicted using this uncracked model. If the stresses are higher than the tensile limits, then the finite element model will predict cracking. Time dependent redistributions were not considered but could be added to the model.

6.1.4 Transverse Joint Recommendations

The best transverse joints in these tests were the post-tensioned joints with 0.340 ksi of effective stress. The stress value was reduced by short term losses and 2 months

of long term losses. Approximately 5% of the stress in the deck was lost during the 2 months of long term losses. The post-tensioned joint performed the best on all measures.

The grout-concrete interface is the weakest point in tension. The maximum tension value should be designed near $1.5\sqrt{f'c}$ (f'c is the weakest compressive strength of the concrete and grout) in order to prevent any surface cracking in the deck from service loading. This tension value is based on a Five Star Highway patch grout poured next to a 6000 psi highway deck concrete.

The looped reinforcing bar joint performs satisfactory but cracking is expected. The cracks will primarily occur between the grout-concrete interface. The cracking allowed very little water penetration and remained relatively small compared to cracks in the other joints.

Shrinkage cracks will occur if grout is poured next to concrete in transverse joints with no surface treatment in the joint. A sealant or driving surface will be necessary if shrinkage cracks are allowed to form in the decking.

6.2 Grout Ring Tests

A number of conclusions have been drawn based on the performance of the various grouts and surface conditions of the grout rings and test panels. By changing the materials used in the blockouts, the performance can be improved. The best conditions are reported for different applications.

6.2.1 Construction

A number of conclusions have been drawn through the construction of the shear pockets in the tests panels and ring samples. They are as follows:

1) When adding a surface preparation technique, the construction sequence must be carefully coordinated because the grout sets up fast. Adding another step, such as coating the blockout with epoxy, requires precise timing.

2) Adding a pea gravel to the grout does not take additional time, however adding polypropylene fibers creates segregation problems.
3) The wire brushed surface is the least time dependent and easiest to apply to the blockouts outside of the control, wetted condition.
4) The water stopped, shear key, and exposed aggregate surface conditions require no extra field work but do require more work for the precaster. These surfaces may increase the cost of the panels.
5) The Set 45 grout was not applicable to shear pockets. The time to initial set was less than 5 minutes and the surface heat of hydration at 5 minutes was measured at over 180˚ Fahrenheit.
6) Type K concrete took longer to mix than the traditional grouts and the set time was similar to a standard concrete mix.

6.2.2 Performance

The grout rings performed differently depending on the grouts and surface condition combination. Many of the combinations were acceptable. It would be up to the designer to determine which design criteria was most important. Shrinkage, bond strength, crack size, and ponding were all criteria for picking the best combination. The conclusions for the grouting materials, the ring testing procedures, and the ring properties are listed below.

Material Properties

1) An extensometer was used to measure the grout and concrete Poisson's ratios throughout testing. The Poisson's Ratios were between 0.18-0.20 after the grouts had cured for at least 7 days. The values were constant from this point forward. The assumption of a 0.20 Poisson's ratio for concrete is also accurate for grouts except during the first few days of curing.
2) The modulus of elasticity for the grouted materials was not closely predicted with the ACI 318-08 equation $57\sqrt{f'c}$. The compressometer measured moduli

20% to 50% higher for the Five Star Grouts and Type K grouts. The Set 45 modulus was about twice the predicted value.

3) The Five Star and Set 45 grouts shrank ¼ and ½ as much as the concrete bridge deck mix. The grouts shrink less than concrete. The Type K concrete shrank as much as the deck concrete.
4) The ASTM C157 modified method detected swelling effects in all of the grouts during the first 24 hours, except the neat Five Star grout. A swelling effect helps compensate for the long term shrinkage effects.
5) The ASTM C157 modified method measured lower shrinkage values during days 1 through 7 than the ASTM C157 method.

Ring Testing Method

1) The rings should not be ponded and tested for surface strain simultaneously unless the effects of a wetting and drying cycle are desired. Separate rings should be made for each test because of the susceptibility of concrete and grout to moisture.
2) A six week curing period from the end of the concrete pour until the grout pour removed concrete shrinkage as a variable. Over 90% of the concrete shrinkage had occurred at 6 weeks.
3) The visual and DEMEC crack detection methods both worked effectively, however readings should be taken at closer intervals. Readings every day would provide a better indication of the time and deformation of the first crack. The DEMEC method in particular predicts microcracking prior to the visual method. A shorter data interval would provide more precise results.
4) The ponding test did not reveal leaks in the majority of the samples. A testing period of 6 to 12 months may be necessary to measure long term effects.

Ring Results

1) Based on the ring tests, the control condition (wetted surface) with Five Star grout had the largest cracks and the longest cracks. The transverse joint blockouts on the panel specimens had similar results.
2) The Set 45 grout was the only grout type to leak at the entire grout-concrete interface. All three samples had 100% leakage during the test. The Set 45 grout performed the worst of all grouts
3) Both Type K concrete specimens had the largest cracks of any material. The Type K performed similar to the Five Star control specimens.
4) The concrete and grout rings will swell 50-150 με when wetted for 24 hours. The shrink and swell effect may negatively affect the bond strength. The differential shrinkage rates of the concrete and grout may create larger stresses at the interface.
5) In general, pea gravel helped reduce shrinkage in the grout but reduced the bond strength, and increased the amount of cracking.
6) Water stopped blockouts never leaked but always cracked. The final strains were the largest of all ring samples but the crack progression was gradual as compared to the sudden cracking in most samples.
7) The wire brushed surface reduced the effects of interface cracking the most. The final strain was smallest in these rings. The wire brushed condition had the smallest final cracks and one of the two highest final stresses.
8) The epoxy and exposed aggregate had some of the smallest final cracks. This was confirmed by earlier results on the deck panel blockouts.
9) The fiber grout had one of the two highest final stresses.
10) The wire brushed surface had the best final results followed by the epoxied surface. The exposed aggregate and fiber grout performed well.
11) The Five Star and Five Star fiber grouts performed the most consistently of all the grouts in terms of shrinkage, crack distribution, crack size, and ponding.

12) The bond stress between the concrete-grout was consistently less than the modulus of rupture predicted by ACI 318-08, $Fr = 7.5\sqrt{f'c}$. This confirmed the results from the bond strength in the transverse joint tests; the tensile strength is reduced at a concrete-grout interface. Most of the tensile bond stresses ranged from $0.5\sqrt{f'c}$. to $4.0\sqrt{f'c}$. The Five Star grout with or without fibers had tensile bond stresses close to the upper limit. The Five Star pea gravel, Set 45, and Type K grouts had tensile bond stresses close to the lower limit.

6.2.3 Finite Element Analysis

The two-dimensional plane stress finite element models predicted the average deformation at the grout-concrete interface between the rings. The models predicted the values best for the rings that had a distinct first crack over the majority of the grout-concrete interface. For these cases, the results fell within the range of the observed results. The grouts that had very small cracking over a period of several days were not easily predicted by the model. A more detailed non-linear model would be needed to predict gradual, progressive cracking.

This finite element model predicts the stress levels at the grout-concrete interface given the shrinkage rate of the grout material and the dimensions of the blockouts. The average stress and deformation at first crack has been recorded for a number of specimens. The values can be compared and the time to first cracking can be predicted. The blockouts can be designed with different materials and surface conditions to prevent cracking. The finite element models will predict the performance.

6.2.4 Design Recommendations

The Five Star grout was preferred over the Set 45 or Type K materials. The pea gravel reduced shrinkage but also decreased the bond strength. The pea gravel is an acceptable substitute but a neat grout is recommended.

An epoxied, wire brushed, or exposed aggregate surface helped reduce cracking and increase bond strengths when pea gravel was not used. The fibers perform well

and do not require a surface preparation technique. Any of the surface preparation techniques will reduce cracking amount and size and prevent water infiltration better than the control (wetted) condition.

A number of factors should be taken into account when selecting a grout and surface condition. A designer should consider the amount of time needed to prepare the surfaces in the field versus time needed in the precast plant. The availability of highway patch grouts and the importance of reducing the cracks must be considered. The finite element model may be used to estimate the stresses and the time to cracking. A number of grouts and surface conditions could be considered depending on the priorities of the project.

6.3 Recommendations

The following recommendations have been derived from this research project:

Transverse Joint Tests

1. Post-tensioned joints perform better than cast-in-place joints under service loads
2. The tensile rupture strength at the interface between the grout and concrete should be designed as $1.5\sqrt{f'c}$.
3. Five Star Highway Patch grout or an equivalent worked best inside the joints.
4. The best cast-in-place joint is a looped bar joint and should be chosen if post-tensioning the deck is not an option.

Grout Ring Tests

1. A grout with equivalent material properties as Five Star Highway Patch grout should be used in deck panel blockouts.
2. A roughened (wire brushed or exposed aggregate) or an epoxied surface should be used with a grout equivalent to Five Star Highway Patch grout.

3. The tensile rupture strength at the interface between Five Star Highway Patch grout and a deck concrete should be designed as $2.5\sqrt{f'c}$.
4. Alternate grouts used on bridge decks should not be designed with a tensile rupture strength greater than $0.5\sqrt{f'c}$.
5. Set 45 grout or an equivalent is not recommended for blockouts in deck panels.

6.4 Contributions of the Research

At a time with limited resources and a large need for investment in the infrastructure, new efficient rehabilitation methods are paramount. Full depth precast deck panels for bridge rehabilitation can be both quick and cost effective. They have application on rehabilitation and new deck construction and have the potential for significant costing savings.

The final results of this research project have increased the knowledge base for implementing full depth concrete bridge decks. The joints and blockouts traditionally have had long term performance and durability problems. The results of this research have shown which joints will work for deck panels over an interior bent, what construction techniques are viable, and what grouting techniques work best in blockouts.

In particular, this was the first time transverse joints have been tested head-to-head in a research project. The joints were tested under the same conditions with the same loading and compared. In addition, this was the first time post-tensioned and cast-in-place transverse joints were tested together. Field studies have been reported on the different joint types but this research provided a controlled comparison. Lastly, these tests were one of the first on transverse joints in worst case negative bending.

The construction techniques for the deck panels and joints were carefully documented. The number of people and amount of time needed for each step was recorded. This will help provide an estimate for the amount of resources needed for the

construction of deck panels. It also provides a basic outline of what needs to be done to build the panels and which procedures work effectively. Additionally, it demonstrates the importance of preparing the surfaces correctly and pouring the correct grout in the joints and blockouts. The construction procedures and methods were shown to contribute to the performance of the final product.

The grouting study was the first one done on both a variety of grouting types and a variety of surface preparation conditions. The combination of samples provided an estimate of which grouts work best based on cracking, leaking, and bond stress. A basic design procedure was suggested based on the results. Additionally, the Poisson's Ratio, Modulus of Elasticity, and shrinkage of the grouts was directly compared. This provided additional information on highway patch grouts that was previously unavailable.

6.5 Future Research

The future of full depth deck panels will depend on implementing the results on real bridges and monitoring the performance. In particular, this research should be applied to the Virginia bridge the panel design was based upon. A correlation could be made between the performance of the transverse joints and blockout pockets in the field and laboratory. The costs and labor estimates could also be recorded.

Another topic of interest would be an economic comparison of full depth deck panel and traditional cast-in-place decks. The assumptions about construction efficiency, cost savings to the user, and increased material costs for the panels should be investigated. A more detailed comparison of a number of bridges may show the real economics behind the systems.

The grout ring tests were done for the first time with this research program. A number of procedures may need further investigation to improve the test. In particular, the techniques to gather surface strains and pond the surface could be improved. The cracking and ponding tests should also be run concurrently on separate samples. This would help show the contribution of water to the shrinkage and swelling of the grout.

References

AASHTO. (2002). "Standard Specifications for Highway Bridges." American Association of State Highway and Transportation Officials, Washington, DC.

AASHTO. (2007). *AASHTO LRFD Bridge Design Specifications*
American Association of State Highway and Transportation Officials.

ACI-318. (2008). *Building Code Requirements for Structural Concrete*, ACI, Farmington Hills, MI.

Au, A., Lam, C., and Tharmabala, B. (2008). "Investigation of prefabricated bridge using reduced-scale models." *PCI Journal*, 53(6), 67-95.

Babaei, K., Fouladgar, A., and Nicholson, R. T. "Nighttime Bridge Deck Replacement with Full Depth Precast Concrete Panels at Route 7 over Route 50, Fairfax County, Virginia." *Transportation Research Board 80th Annual Meeting*, Washington, D.C., 17.

Badie, S. S., Amgad F. Girgis, Krissachai Sriboonma, Mather K Tadros. "Extending Spacing of Horizontal Shear Connection Pockets from 24 to 48 inches for Steel Girders." *PCI National Bridge Conference 2006*.

Badie, S. S., Baishya, M. C., and Tadros, M. K. (1998). "NUDECK - an efficient and economical precast prestressed bridge deck system." *PCI Journal*, 43(5), 56-83.

Badie, S. S., Maher K Tadros, Amgad F Girgis. (2006b). "Full-Depth, Precast-Cocnrete Bridge Deck Panel Systems." NCHRP, ed., National Research Council.

Badie, S. S., and Tadros, M. K. (2008). *Full-depth precast concrete bridge deck panel systems* Transportation Research Board, Washington, D.C. :.

Badie, S. S. M. K. T. a. R. M. M. U. (2009). "Full-Depth, Precast Concrete Bridge Deck Panel Systems." *Concrete International*, 31(4), 53-58.

Badwan, I. Z., and Liang, R. Y. (2007). "Performance evaluation of precast posttensioned concrete multibeam deck." *Journal of Performance of Constructed Facilities*, 21(5), 368-374.

Biswas, M. (1986). "Precast Bridge Deck Design Systems." *Journal of the Prestressed Concrete Institute*, 31(2), 40-94.

Biswas, M., Iffland, JSB, Schofield, RE, and Gregory, AE. (1974). "Innovations in construction and maintenance of transportation facilities : proceedings of the sixth summer meeting of the Highway Research Board in cooperation with the Washington State Department of Highways, August 6-8, 1973, Olympia, Washington." *0309022975*, Transportation Research Board, National Research Council, Washington :.

Biswas, M., Osegueda, R. A., and Noel, J. S. (1984). "Scale-Model Tests for Full-depth Precast Concrete Panel-Decked Composite Bridge Span." *0361-1981*, Transportation Research Board, Washington, DC, USA, Minneapolis, MN, USA.

Bowers, S. (2007). "Recommendations for longitudinal post-tensioning in full-depth precast concrete bridge deck panels," Virginia Tech, Blacksburg.

Carter III, J. W., Pilgrim, T., Hubbard, F. K., Poehnelt, T., and Oliva, M. (2007). "Wisconsin's use of full-depth precast concrete deck panels keeps interstate 90 open to traffic." *PCI Journal*, 52(1), 16-30.

CBS-News. (2005). "Gridlock Driving Up Wasted Time, Drivers Spent 3.7B Hours, 2.3B Gallons Gas In Traffic Delays In 2003." CBS News.

Chang, S.-P., and Shim, C.-S. (2000). "Continuous Composite Bridges with Precast Decks." *Structures and Buildings*, 14(1), 123-132.

Culmo, M. P. (2000). "Rapid bridge deck replacement with full-depth precast concrete slabs." *Transportation Research Record*(1712), 139-146.

Dinitz, A. M., Michael S. Stenko. (2008). "First Successful Accelerated Bridge Deck Replacement Utilizing MMA Polymer Concrete." Concrete Bridge Conference, National Concrete Bridge Conference, St Louis.

Fallaha, S., Sun, C., Lafferty, M. D., and Tadros, M. K. (2004). "High performance precast concrete NUDECK panel system for Nebraska's skyline bridge." *PCI Journal*, 49(5), 40-50.

Gulyas, R. J. (1996). "Precast bridge decks: Keyway grouting data." *Concrete International*, 18(8), 45-48.

Gulyas, R. J., and Champa, J. T. (1997). "Use of composite testing for evaluation of keyway grout for precast prestressed bridge beams." *ACI Materials Journal*, 94(3), 244-250.

Gulyas, R. J., Wirthlin, G. J., and Champa, J. T. (1995). "Evaluation of keyway grout test methods for precast concrete bridges." *PCI Journal*, 40(1), 44-57.

Gutzwiller, M. J., Lee, R. H., and Scholer, C. F. (1971). "Precast, prestressed concrete for bridge decks."

Hanna, K. E., George Morcous, Maher K. Tadros. (2008). "Standardized Precast Prestressed Concrete Panels for Bridge Decks." 2008 Concrete Bridge Conference, National Concrete Bridge Council, St Louis, MO.

Harrison, A., and LeBlanc, N. D. "Design and construction of a bridge with a full-width, full-depth precast concrete deck slab on steel girders." Boston, MA, United States.

Harrison, A., and LeBlanc, N. D. (2005b). "Design and construction of a full-width, full-depth precast concrete deck slab on steel girder bridge." *Transportation Research Record*(1907), 55-66.

Issa, M. (2002). "Experimental Evaluation of Full Depth Precast/Prestressed Concrete Bridge Deck Panels. Project IB-H1, FY 98." United States.

Issa, M. A., Anderson, R., Domagalski, T., Asfour, S., and Islam, M. S. (2007). "Full-scale testing of prefabricated full-depth precast concrete bridge deck panel system." *ACI Structural Journal*, 104(3), 324-332.

Issa, M. A., Idriss, A.-T., Kaspar, I. I., and Khayyat, S. Y. (1995a). "Full depth precast and precast, prestressed concrete bridge deck panels." *PCI Journal*, 40(1), 59-80.

Issa, M. A., Ribeiro Do Valle, C. L., Abdalla, H. A., Islam, S., and Issa, M. A. (2003). "Performance of transverse joint grout materials in full-depth precast concrete bridge deck systems." *PCI Journal*, 48(4), 92-103.

Issa, M. A., Yousif, A. A., and Issa, M. A. (1995b). "Construction procedures for rapid replacement of bridge decks." *Concrete International*, 17(2), 49-52.
Issa, M. A., Yousif, A. A., and Issa, M. A. (2000). "Experimental behavior of full-depth precast concrete panels for bridge rehabilitation." *ACI Structural Journal*, 97(3), 397-407.
Issa, M. A., Yousif, A. A., Issa, M. A., Kaspar, I. I., and Khayyat, S. Y. (1995c). "Field performance of full depth precast concrete panels in bridge deck reconstruction." *PCI Journal*, 40(3), 82-108.
Issa, M. A., Yousif, A. A., Issa, M. A., Kaspar, I. I., and Khayyat, S. Y. (1998). "Analysis of full depth precast concrete bridge deck panels." *PCI Journal*, 43(1), 74-85.
Kassner, B. L., Brown, M. C., and Schokker, A. J. (2007). *Material investigation of the full-depth, precast concrete deck panels of the old Woodrow Wilson Bridge*, M. C. Brown and A. J. Schokker, translator, Virginia Transportation Research Council, Charlottesville, Va. :.
Khalil, H. A.-H., Ahmad. (2008). "Accelerated Construction And Innovations 24Th Street Bridge Over I-80/I-29 Council Bluffs, Iow." Concrete Bridge Conference, National Concrete Bridge Committee, St. Louis, MO.
Knudsen, C. V. (1980). "RE-DECKING A BRIDGE WITH PRECAST CONCRETE." *Civil Engineering (New York)*, 50(4), 75-77.
Lutz, J. G. (1984). "WOODROW WILSON MEMORIAL BRIDGE, WASHINGTON, D. C. : CONCRETE DECK RECONSTRUCTION." *TRNews (Transportation Research Board)*(111), 2-7.
Markowski, S. M. (2005). "Experimental and Analytical Study of Full Depth Prestressed Precast Concrete Deck Panels for Highway Bridges," University of Wisconsin-Madison, Madison, WI.
Menkulasi, F., and Roberts-Wollmann, C. L. (2005). "Behavior of horizontal shear connections for full-depth precast concrete bridge decks on prestressed I-girders." *PCI Journal*, 50(3), 60-73.
Mindess, S. (2003). *Concrete*, J. F. Young and D. Darwin, translator, Prentice Hall, Upper Saddle River, NJ :.
Nottingham, D. (1996). "Joint grouting in Alaskan bridges and dock decks." *Concrete International*, 18(2), 45-48.
PCI. (2003). *PCI Bridge Design Manual*, PCI Institute, Chicago, IL.
PCI, C. (2006). "State of the Art Report on Full-Depth Precast Concrete Bridge Deck Panels." PCI.
Potter, J. L. (2003). "State-of-the-Practice for Full-Depth Precast Concrete Bridge Deck Design, Detailing and Utilization." 2003 PCI Bridge Conference.
Precast/Prestressed, P. P. C. I. N. E. R. (2002). "Full Depth Precast Concrete Deck Slabs."
Rawles, R. H., Jr. (1973). "DALLAS BRIDGE HAS POST-TENSIONED CONCRETE DECK." *Civil Engineering (New York)*, 43(4), 74-77.
Riley, W. F., Sturges, L.D., & Morris, D. H. (1999). *Mechanics of Materilas*, John Wiley, New York.

Scholz, D. P. (2004). "PERFORMANCE CRITERIA RECOMMENDATIONS FOR MORTARS USED IN FULL-DEPTH PRECAST CONCRETE BRIDGE DECK PANEL SYSTEMS," Virginia Tech, Blacksburg, VA.

Scholz, D. P., Wallenfelsz, J. A., Lijeron, and Roberts-Wollmann, C. L. (2007). *Recommendations for the connection between full-depth precast bridge deck panel systems and precast I-beams*, Virginia Transportation Research Council, Charlottesville, Va. .

Shahawy, M. A. (2003). "Prefabricated Bridge Elements and Systems to Limit Traffic Disruption During Construction." *NCHRP Sythesis 324*, 324, 58.

Shim, C. S., and Chang, S. P. (2002). "Cracking of continuous composite beams with precast decks." *Journal of Constructional Steel Research*, 59(2), 201-214.

Slavis, C. (1983). "PRECAST CONCRETE DECK MODULES FOR BRIDGE DECK RECONSTRUCTION." *Journal of the Prestressed Concrete Institute*, 28(4), 120-135.

Sprinkel, M., Weyers, R., Blevins, C., Ramniceanu, A., and Weyers, S. (2009). "Failure and Repair of Deck Closure Pour on I81." Transportation Research Board.

Sullivan, S. (2007). "Construction and Behavior of Precast Bridge Deck Panel Systems," Virginia Tech, Blacksburg, VA.

Swartz, B. D. a. A. J. S. (2008). "Design Guide Development for Post-Tensioned Bridge Decks." *PTI Journal*, 6(2), 7-20.

Tadros, M. K. (1998). *Rapid replacement of bridge decks*, M. C. Baishya, translator, National Academy Press, Washington, D.C. :.

The Fort Miller CO., I. (2002). "Precast Composite Deck Systems." A. F. M. G. Company, ed., Schuylerville, NY.

US-News. (2007). "Traffic is making millions sick and tired. The bad news? It's going to get worse unless things change in a real big way." US News.

VDOT. (2007a). "Strategic Plan, Service Area Plan, 2008-2010 Biennial." V. T. Department, ed., Virginia Transportation Department, 86.

VDOT. (2007b). "Structure and Bridge Manuals." V. D. o. Transportation, ed.

Versace, J. D., Julio A. Ramirez. (2004). "Implementation of Full-Width Precast Bridge Deck Panels: A Synthesis Study." *Project No. C-36-56OOO, File No. 7-4-66, SPR-2794*, Purdue University, West Lafayette, Indiana.

Wallenfelsz, J. A. (2006). "Horizontal Shear Transfer for Full Full-Depth Bridge Deck Concrete Deck Panels," Virginia Tech, Blacksburg, VA.

Wenzlick, J. (2005). "Deck Replacement with Precast Reinforced Concrete Segments." Missouri Department of Transportation, Jefferson City.

Yamane, T., Tadros, M. K., Badie, S. S., and Baishya, M. C. (1998). "Full depth precast, prestressed concrete bridge deck system." *PCI Journal*, 43(3), 50-66.

Zaki, A. R., and Mailhot, G. (2003). "Deck Reconstruction of Jacques Cartier Bridge Using Precast Prestressed High Performance Concrete Panels." *PCI Journal*, 48(5), 20-33.

Appendix A - VDOT Bridge Preliminary Design

A.1 Construction Drawings

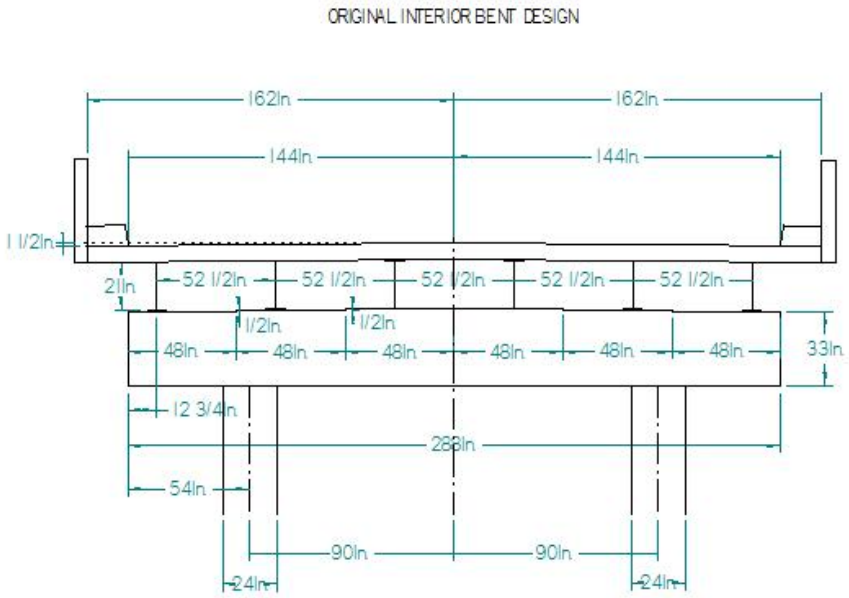

The Current Deck Layout for the Virginia Replacement Bridge

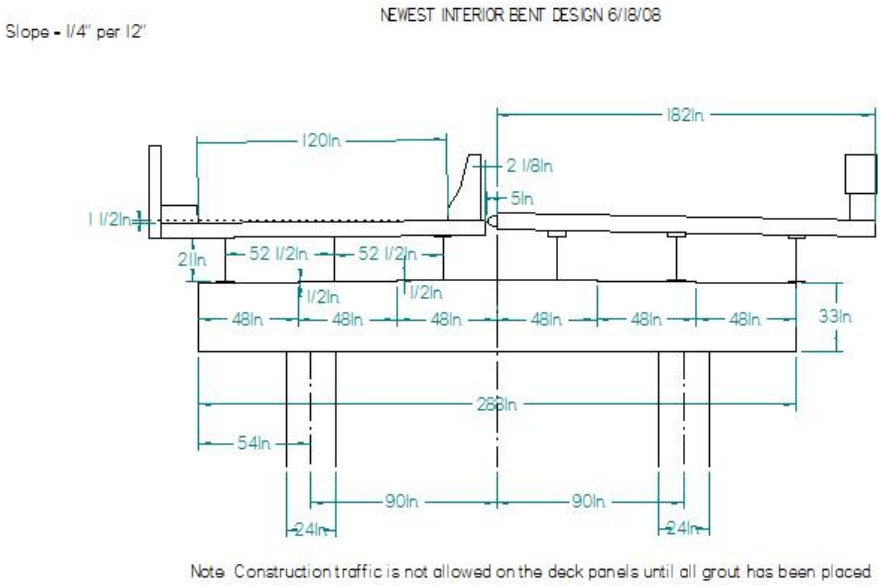

Phase 1 Construction for the Virginia Replacement Bridge

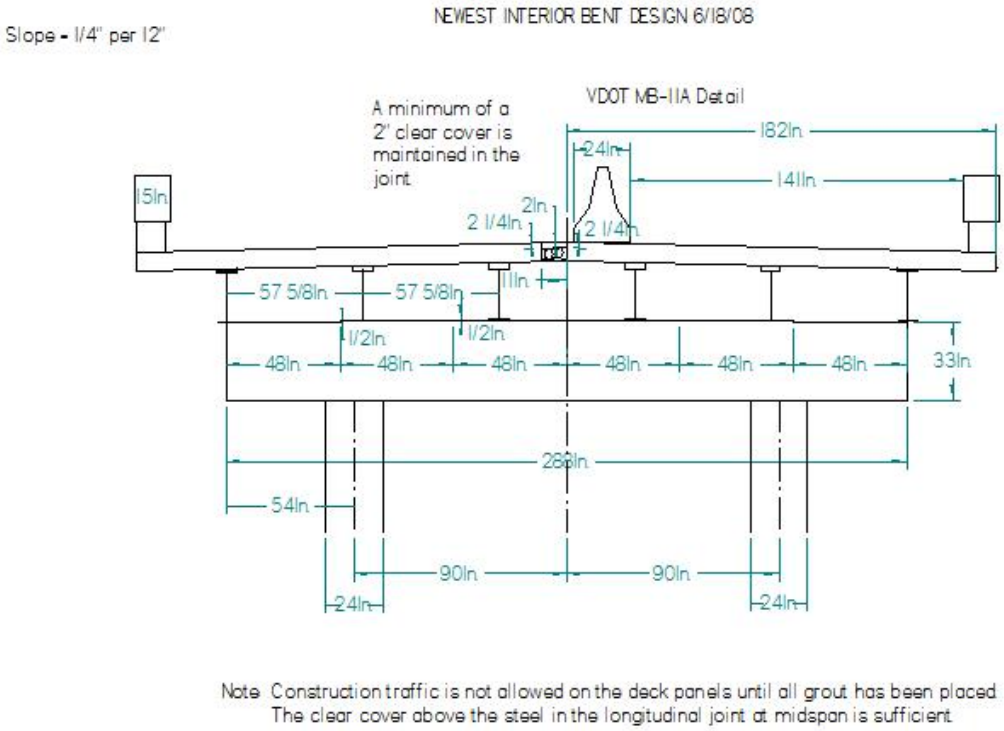

Phase 2 Construction for the Virginia Replacement Bridge

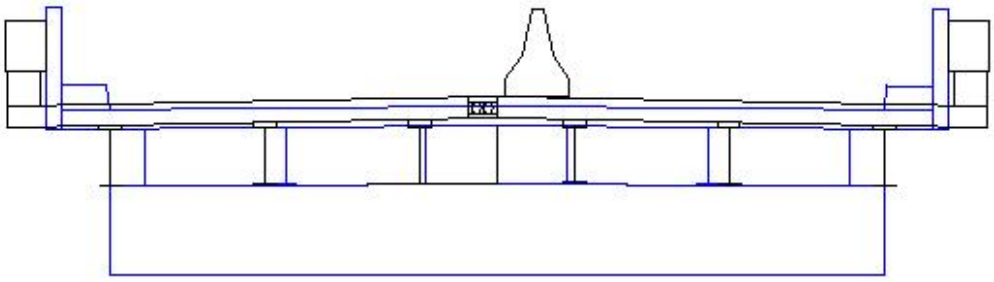

Superimposed View of the Old and New Decks on the Virginia Replacement Bridge

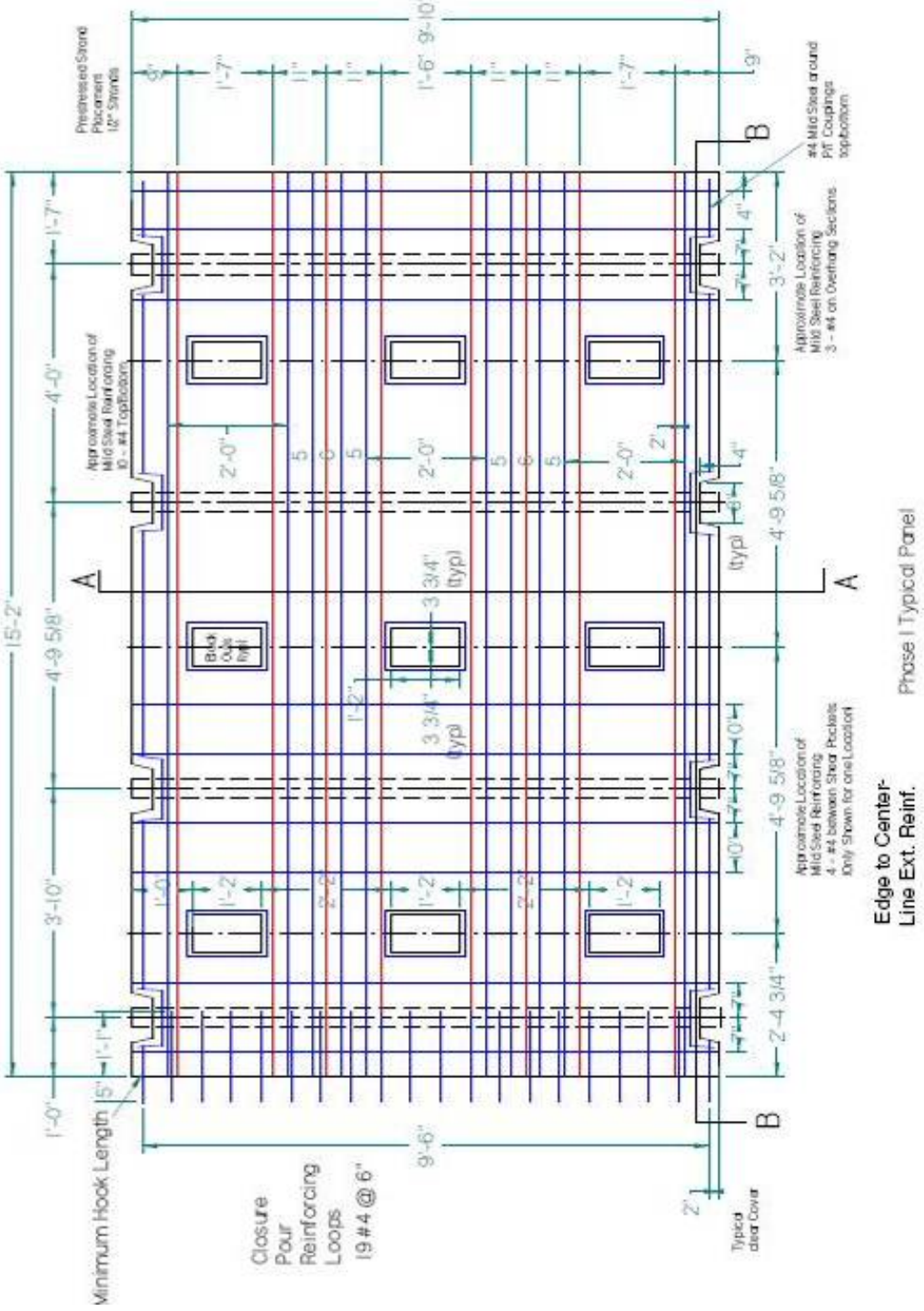

Phase 1 Typical Panel Plan View

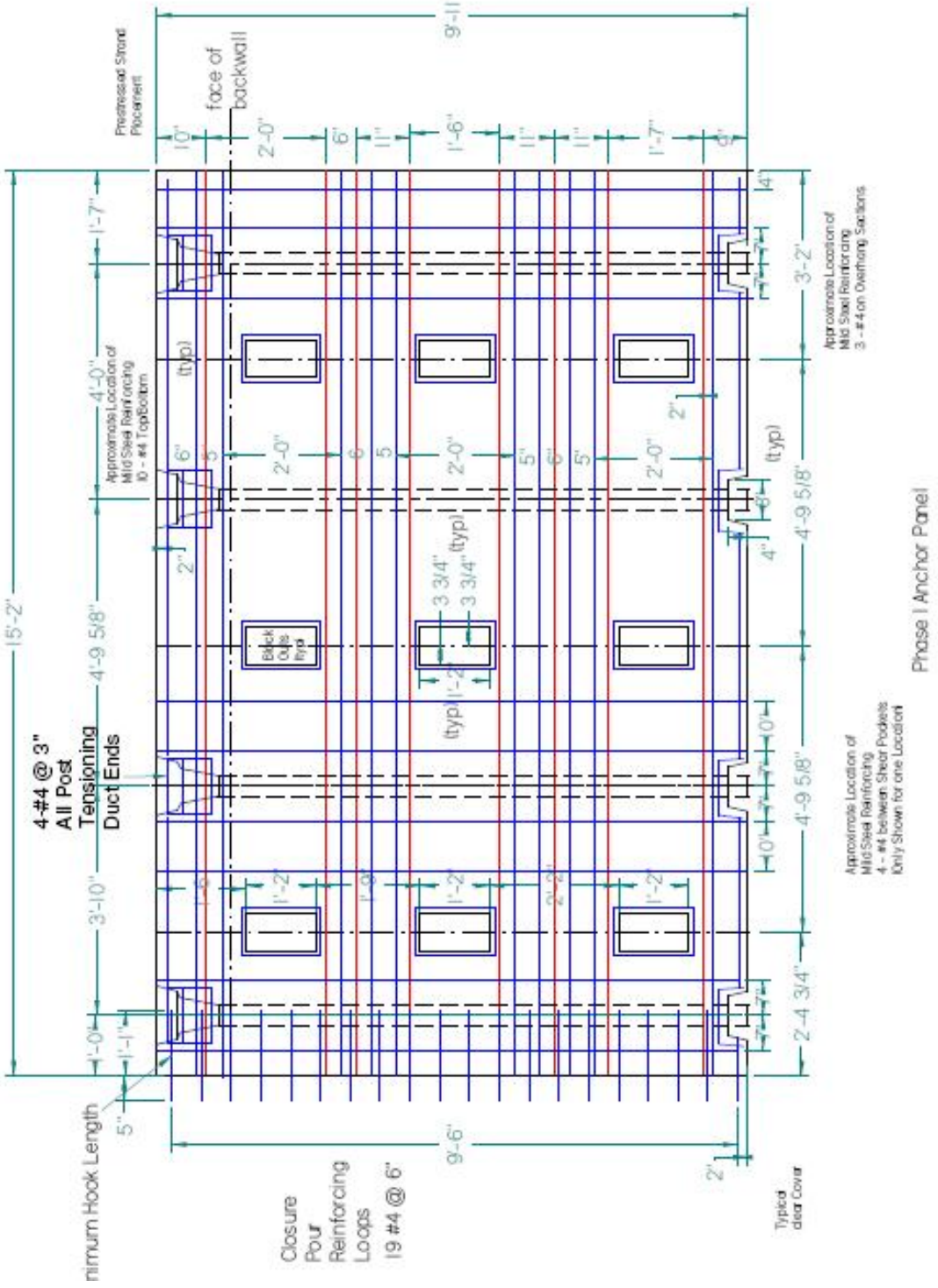

Phase 1 Anchor Panel Plan View

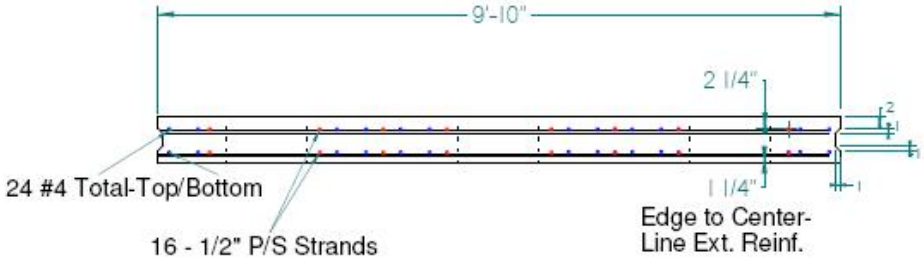

Section A-A

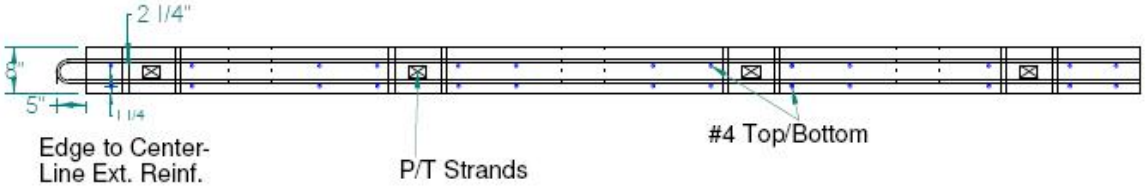

Section B-B

Phase 1 Typical Elevation View

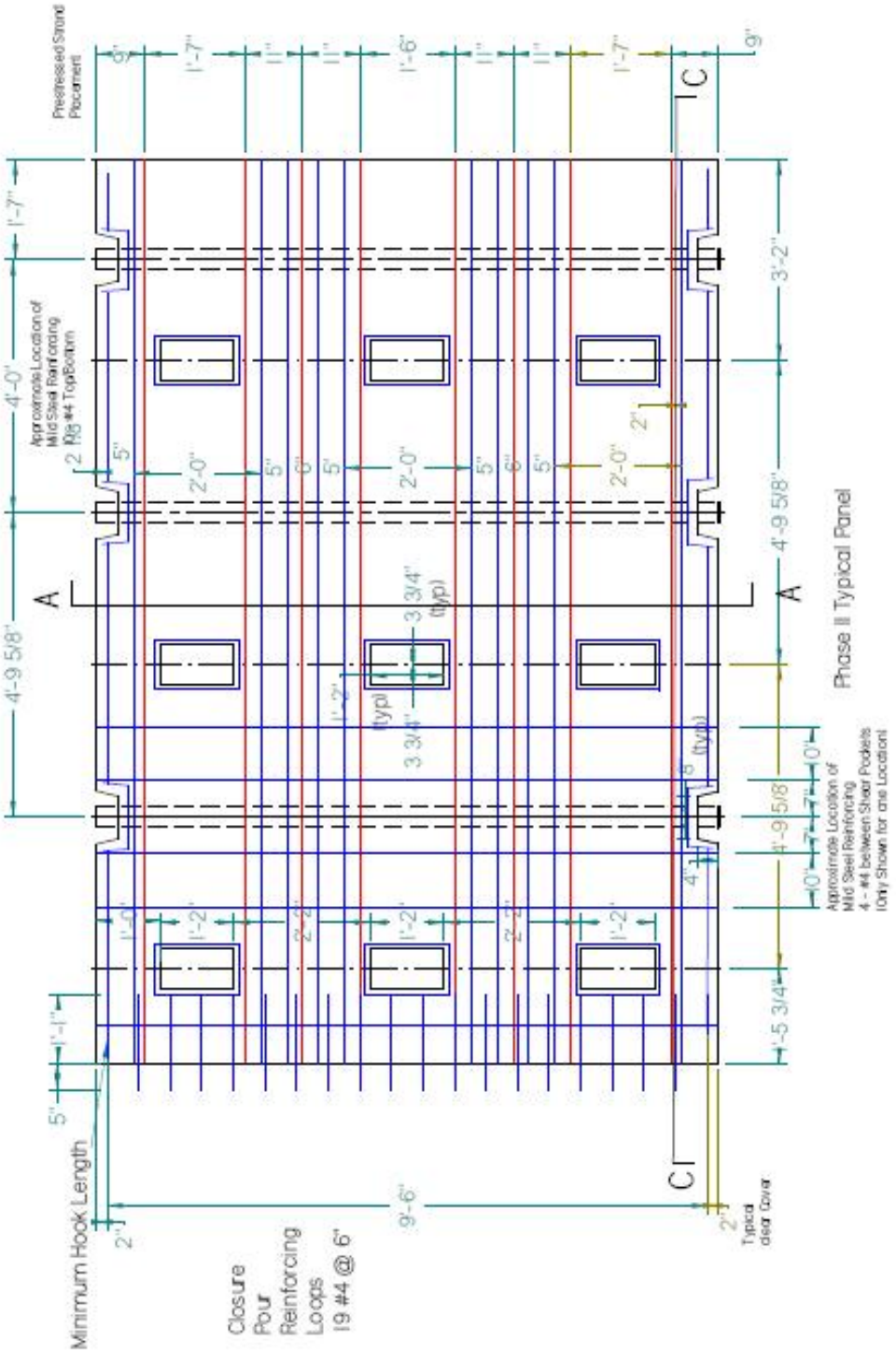

Phase 2 Typical Panel Plan View

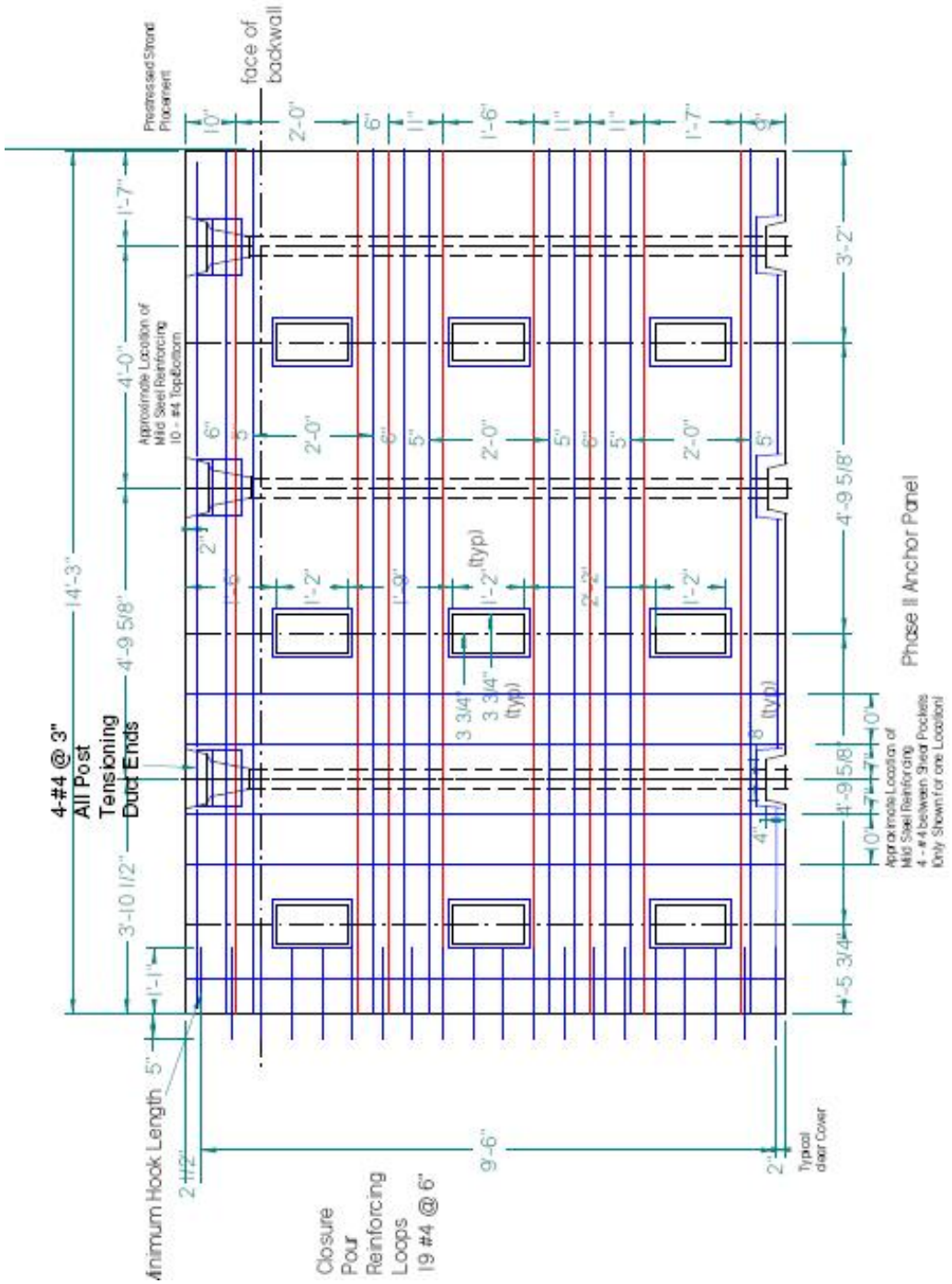

Phase 2 Anchor Panel Plan View

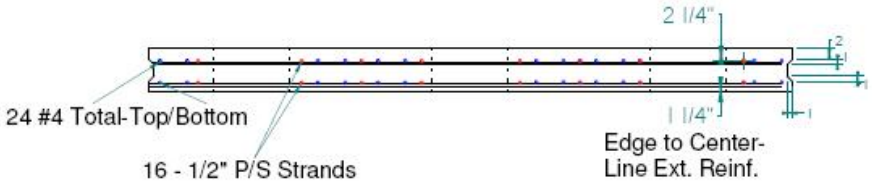

Section A-A

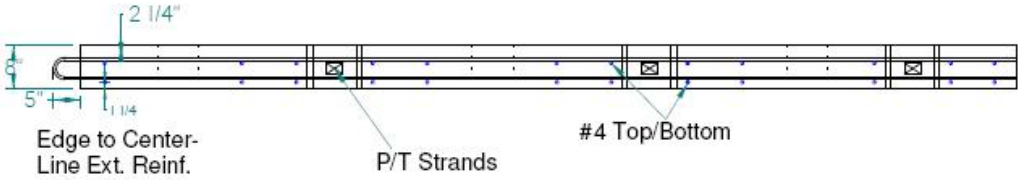

Section C-C

Phase 2 Typical Elevation View

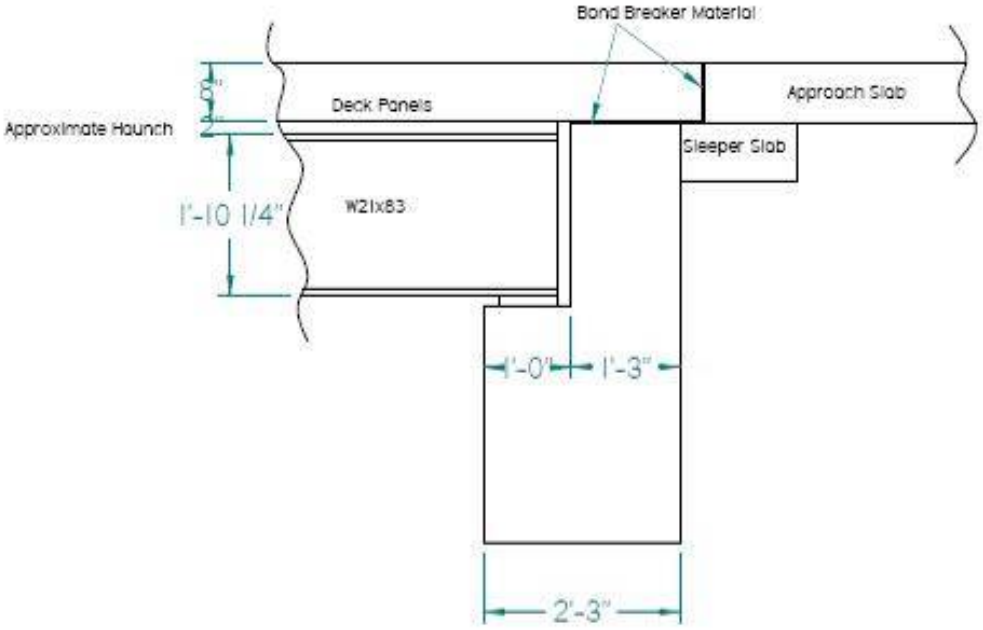

Elevation View of the End Bent Connection

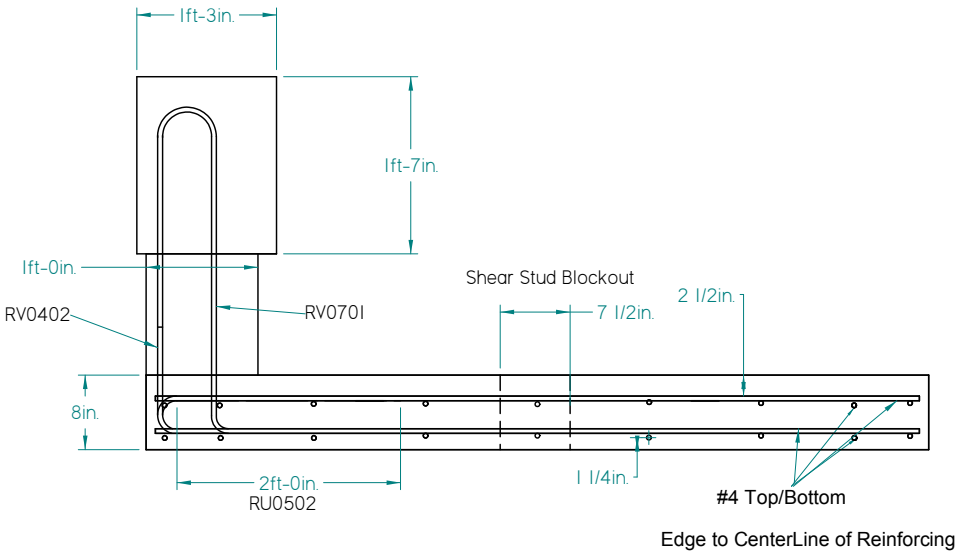

Typical Section Near the Kansas Corral Rails
Use the Standard Kansas Corral Rail Detail with the Dimensions Shown Above. Only the steel extending into the slab is shown above. The remaining steel is the same as the standard detail.

Elevation View of a Barrier Curb

A.2 Transverse Deck Design Calculations

A.2.1 Transverse Deck Analysis

Sample Calculation
Live Load Analysis in the Transverse Direction Using 16 kip point loads (Design Vehicle Tire Loads) - Multiple locations were analyzed to find the worse case locations for the vehicles.

The following is a sample calculation for 1 iteration of the design.

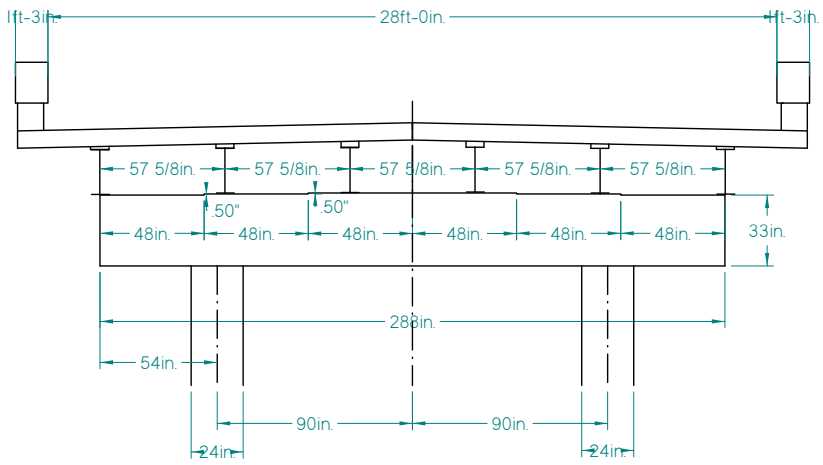

This analysis is to determine the interior and exterior moments on the deck.

Model this as a continuous beam with 10 global degrees of freedom. Each element has 4 local degrees of freedom. Only moments are being considered in this case.

ORIGIN:= 1

A 1 foot strip section is being used for analysis and design of the slab.

b := 12 Inches

h := 7.5 Inches

$I := \frac{1}{12} \cdot b \cdot h^3$ In^4

fc := 600(psi

$E := 57 \cdot \sqrt{fc}$ ksi

Mat := (E I) all spans

$$CON := \begin{matrix} \text{Nodes} & & \text{Mat} \\ 1 & 2 & \end{matrix} \begin{pmatrix} 1 & 2 & 1 \\ 2 & 3 & 1 \\ 3 & 4 & 1 \\ 4 & 5 & 1 \\ 5 & 6 & 1 \\ 6 & 7 & 1 \\ 7 & 8 & 1 \end{pmatrix}$$

Restraints

$$R := \begin{pmatrix} 0 & 0 \\ 1 & 0 \\ 1 & 0 \\ 1 & 0 \\ 1 & 0 \\ 1 & 0 \\ 1 & 0 \\ 0 & 0 \end{pmatrix} \qquad ID := \begin{pmatrix} 1 & 2 \\ 0 & 3 \\ 0 & 4 \\ 0 & 5 \\ 0 & 6 \\ 0 & 7 \\ 0 & 8 \\ 9 & 10 \end{pmatrix}$$

$L := (38 \quad 57.6 \quad 57.6 \quad 57.6 \quad 57.6 \quad 57.6 \quad 38)$ inches

4x4 generic k matrix

$$K(E, I, L) := E \cdot I \begin{bmatrix} \frac{12}{(L)^3} & \frac{6}{(L)^2} & \frac{-12}{(L)^3} & \frac{6}{(L)^2} \\ \frac{6}{(L)^2} & \frac{4}{L} & \frac{-6}{(L)^2} & \frac{2}{L} \\ \frac{-12}{(L)^3} & \frac{-6}{(L)^2} & \frac{12}{(L)^3} & \frac{-6}{(L)^2} \\ \frac{6}{(L)^2} & \frac{2}{L} & \frac{-6}{(L)^2} & \frac{4}{L} \end{bmatrix}$$

$$k1 := K\left(Mat_{1,1}, Mat_{1,2}, L_{1,1}\right)$$

$$k2 := K\left(Mat_{1,1}, Mat_{1,2}, L_{1,2}\right)$$

$$k3 := K\left(Mat_{1,1}, Mat_{1,2}, L_{1,3}\right)$$

$$k4 := K\left(Mat_{1,1}, Mat_{1,2}, L_{1,4}\right)$$

$$k5 := K\left(Mat_{1,1}, Mat_{1,2}, L_{1,5}\right)$$

$$k6 := K\left(Mat_{1,1}, Mat_{1,2}, L_{1,6}\right)$$

$$k7 := K\left(Mat_{1,1}, Mat_{1,2}, L_{1,7}\right)$$

A Transformations - 10 DOF

$$A1 := \begin{pmatrix} 1 & 0 & 0 & 0 & 0 & 0 & 0 & 0 & 0 & 0 \\ 0 & 1 & 0 & 0 & 0 & 0 & 0 & 0 & 0 & 0 \\ 0 & 0 & 0 & 0 & 0 & 0 & 0 & 0 & 0 & 0 \\ 0 & 0 & 1 & 0 & 0 & 0 & 0 & 0 & 0 & 0 \end{pmatrix} \quad A4 := \begin{pmatrix} 0 & 0 & 0 & 0 & 0 & 0 & 0 & 0 & 0 & 0 \\ 0 & 0 & 0 & 0 & 1 & 0 & 0 & 0 & 0 & 0 \\ 0 & 0 & 0 & 0 & 0 & 0 & 0 & 0 & 0 & 0 \\ 0 & 0 & 0 & 0 & 0 & 1 & 0 & 0 & 0 & 0 \end{pmatrix}$$

$$A2 := \begin{pmatrix} 0 & 0 & 0 & 0 & 0 & 0 & 0 & 0 & 0 & 0 \\ 0 & 0 & 1 & 0 & 0 & 0 & 0 & 0 & 0 & 0 \\ 0 & 0 & 0 & 0 & 0 & 0 & 0 & 0 & 0 & 0 \\ 0 & 0 & 0 & 1 & 0 & 0 & 0 & 0 & 0 & 0 \end{pmatrix} \quad A5 := \begin{pmatrix} 0 & 0 & 0 & 0 & 0 & 0 & 0 & 0 & 0 & 0 \\ 0 & 0 & 0 & 0 & 0 & 1 & 0 & 0 & 0 & 0 \\ 0 & 0 & 0 & 0 & 0 & 0 & 0 & 0 & 0 & 0 \\ 0 & 0 & 0 & 0 & 0 & 0 & 1 & 0 & 0 & 0 \end{pmatrix} \quad A7 := \begin{pmatrix} 0 & 0 & 0 & 0 & 0 & 0 & 0 & 0 & 0 & 0 \\ 0 & 0 & 0 & 0 & 0 & 0 & 0 & 1 & 0 & 0 \\ 0 & 0 & 0 & 0 & 0 & 0 & 0 & 0 & 1 & 0 \\ 0 & 0 & 0 & 0 & 0 & 0 & 0 & 0 & 0 & 1 \end{pmatrix}$$

$$A3 := \begin{pmatrix} 0 & 0 & 0 & 0 & 0 & 0 & 0 & 0 & 0 & 0 \\ 0 & 0 & 0 & 1 & 0 & 0 & 0 & 0 & 0 & 0 \\ 0 & 0 & 0 & 0 & 0 & 0 & 0 & 0 & 0 & 0 \\ 0 & 0 & 0 & 0 & 1 & 0 & 0 & 0 & 0 & 0 \end{pmatrix} \quad A6 := \begin{pmatrix} 0 & 0 & 0 & 0 & 0 & 0 & 0 & 0 & 0 & 0 \\ 0 & 0 & 0 & 0 & 0 & 0 & 1 & 0 & 0 & 0 \\ 0 & 0 & 0 & 0 & 0 & 0 & 0 & 0 & 0 & 0 \\ 0 & 0 & 0 & 0 & 0 & 0 & 0 & 1 & 0 & 0 \end{pmatrix}$$

$$\underset{\sim}{K} := A1^{T} \cdot k1 \cdot A1 + A2^{T} \cdot k2 \cdot A2 + A3^{T} k3 \cdot A3 + \left(A4^{T} \cdot k4 \cdot A4\right) + A5^{T} \cdot k5 \cdot A5 + A6^{T} \cdot k6 \cdot A6 + A7^{T} \cdot k7 \cdot A7$$

K Matrix

$$K = \begin{pmatrix} 407.347 & 7.74\times 10^{3} & 7.74\times 10^{3} & 0 & 0 & 0 & 0 & 0 & 0 & 0 \\ 7.74\times 10^{3} & 1.961\times 10^{5} & 9.803\times 10^{4} & 0 & 0 & 0 & 0 & 0 & 0 & 0 \\ 7.74\times 10^{3} & 9.803\times 10^{4} & 3.254\times 10^{5} & 6.468\times 10^{4} & 0 & 0 & 0 & 0 & 0 & 0 \\ 0 & 0 & 6.468\times 10^{4} & 2.587\times 10^{5} & 6.468\times 10^{4} & 0 & 0 & 0 & 0 & 0 \\ 0 & 0 & 0 & 6.468\times 10^{4} & 2.587\times 10^{5} & 6.468\times 10^{4} & 0 & 0 & 0 & 0 \\ 0 & 0 & 0 & 0 & 6.468\times 10^{4} & 2.587\times 10^{5} & 6.468\times 10^{4} & 0 & 0 & 0 \\ 0 & 0 & 0 & 0 & 0 & 6.468\times 10^{4} & 2.587\times 10^{5} & 6.468\times 10^{4} & 0 & 0 \\ 0 & 0 & 0 & 0 & 0 & 0 & 6.468\times 10^{4} & 3.254\times 10^{5} & -7.74\times 10^{3} & 9.803\times 10^{4} \\ 0 & 0 & 0 & 0 & 0 & 0 & 0 & -7.74\times 10^{3} & 407.347 & -7.74\times 10^{3} \\ 0 & 0 & 0 & 0 & 0 & 0 & 0 & 9.803\times 10^{4} & -7.74\times 10^{3} & 1.961\times 10^{5} \end{pmatrix}$$

$$\text{LOAD} := \begin{array}{c} \begin{matrix} w & P1 & a1 & P2 & a2 & P3 & a3 & P4 & a4 \end{matrix} \\ \begin{pmatrix} 0 & 0 & 0 & 0 & 0 & 0 & 0 & 0 & 0 \\ 0 & -16 & .5833 & 0 & 0 & 0 & 0 & 0 & 0 \\ 0 & -16 & .67 & 0 & 0 & 0 & 0 & 0 & 0 \\ 0 & -16 & .5 & 0 & 0 & 0 & 0 & 0 & 0 \\ 0 & -16 & .75 & 0 & 0 & 0 & 0 & 0 & 0 \\ 0 & -16 & 0 & 0 & 0 & 0 & 0 & 0 & 0 \\ 0 & 0 & 0 & 0 & 0 & 0 & 0 & 0 & 0 \end{pmatrix} \end{array}$$

Locations (% of span length)

Loads (Kips)

This will find the FEF and FEM for a beam with a dist. load and up to 4 point loads.

Positive loads are up. Positive moments are counterclockwise.

$$
\begin{aligned}
&\text{FEF2DBEAM}(m, CON, L, LOAD) := \\
&\quad R_4 \leftarrow 0 \\
&\quad a1 \leftarrow LOAD_{m,3} \cdot L_m \\
&\quad a2 \leftarrow LOAD_{m,5} \cdot L_m \\
&\quad a3 \leftarrow LOAD_{m,7} \cdot L_m \\
&\quad a4 \leftarrow LOAD_{m,9} \cdot L_m \\
&\quad b1 \leftarrow L_m - a1 \\
&\quad b2 \leftarrow L_m - a2 \\
&\quad b3 \leftarrow L_m - a3 \\
&\quad b4 \leftarrow L_m - a4 \\
&\quad R_1 \leftarrow \left(-LOAD_{m,1} \cdot \frac{(L_m)}{2} + \left[(-LOAD_{m,2} \cdot b1^2 \cdot \frac{(3 \cdot a1 + b1)}{(L_m)^3}\right] + \left[-LOAD_{m,4} \cdot b2^2 \cdot \frac{(3 \cdot a2 + b2)}{(L_m)^3}\right] + \left[-LOAD_{m,6} \cdot b3^2 \cdot \frac{(3 \cdot a3 + b3)}{(L_m)^3}\right] + \left[\left(-LOAD_{m,8}\right) \cdot b4^2 \cdot \frac{(3 \cdot a4 + b4)}{(L_m)^3}\right]\right. \\
&\quad R_3 \leftarrow -LOAD_{m,1} \cdot L_m + (-LOAD_{m,2} + (-LOAD_{m,4} + (-LOAD_{m,6} + (-LOAD_{m,8} - R_{1,1} \\
&\quad R_2 \leftarrow -LOAD_{m,1} \cdot \frac{(L_m)^2}{12} + (-LOAD_{m,2} \cdot a1 \cdot \frac{b1^2}{(L_m)^2} + \left[-LOAD_{m,4} \cdot a2 \cdot \frac{b2^2}{(L_m)^2}\right] + \left[[-(LOAD]_{m,6} \cdot a3 \cdot \frac{b3^2}{(L_m)^2}\right] + [-(LOAD]_{m,8} \cdot a4 \cdot \frac{b4^2}{(L_m)^2} \\
&\quad R_4 \leftarrow LOAD_{m,1} \cdot \frac{(L_m)^2}{12} + LOAD_{m,2} \cdot a1^2 \cdot \frac{b1}{(L_m)^2} + LOAD_{m,4} \cdot a2^2 \cdot \frac{b2}{(L_m)^2} + \left[LOAD_{m,6} \cdot a3^2 \cdot \frac{b3}{(L_m)^2}\right] + LOAD_{m,8} \cdot a4^2 \cdot \frac{b4}{(L_m)^2} \\
&\quad R
\end{aligned}
$$

Location of Point Loads

$$L := L^T$$

$$F1 := \begin{pmatrix} 0 \\ 0 \\ 0 \\ 0 \end{pmatrix}$$

These forces and moments were added manually because of their location on the cantilever.

$$FEF2 := FEF2DBEAM(2, CON, L, LOAD) \qquad FEF2 = \begin{pmatrix} 6.019 \\ 93.343 \\ 9.981 \\ -130.662 \end{pmatrix}$$

$$FEF3 := FEF2DBEAM(3, CON, L, LOAD) \qquad FEF3 = \begin{pmatrix} 4.077 \\ 67.243 \\ 11.923 \\ -136.523 \end{pmatrix}$$

$$FEF4 := FEF2DBEAM(4, CON, L, LOAD) \qquad FEF4 = \begin{pmatrix} 8 \\ 115.2 \\ 8 \\ -115.2 \end{pmatrix}$$

$$FEF5 := FEF2DBEAM(5, CON, L, LOAD) \qquad FEF5 = \begin{pmatrix} 2.5 \\ 43.2 \\ 13.5 \\ -129.6 \end{pmatrix}$$

$$FEF6 := FEF2DBEAM(6, CON, L, LOAD) \qquad FEF6 = \begin{pmatrix} 16 \\ 0 \\ 0 \\ 0 \end{pmatrix}$$

$$F7 := \begin{pmatrix} 0 \\ 0 \\ 0 \\ 0 \end{pmatrix}$$

Total FEF/FEM matrix

$$FEF := \begin{pmatrix} F1_1 \\ F1_2 \\ F1_4 + FEF2_2 \\ FEF2_4 + FEF3_2 \\ FEF3_4 + FEF4_2 \\ FEF4_4 + FEF5_2 \\ FEF5_4 + FEF6_2 \\ FEF6_4 + F7_2 \\ F7_3 \\ F7_4 \end{pmatrix} \qquad Q := -FEF$$

Fixed End Forces/Moments (K-ft, K) Positive is up. CCW is positive Moments

Deflections

$D := K^{-1} \cdot Q$

$D =$

	1	
1	0.03713837	Inches
2	-0.00097733	Radians
3	-0.00097733	Radians
4	0.00051141	Radians
5	-0.00008773	Radians
6	0.0001692	Radians
7	0.00052418	Radians
8	-0.00026209	Radians
9	-0.00995949	Inches
10	-0.00026209	Radians

$Q =$

	1
1	0
2	0
3	-93.343
4	63.419
5	21.323
6	72
7	129.6
8	0
9	0
10	0

Element Forces

Individual Bar Forces/Moments
+ Up,Forces; CCW = -, Moments
Force K

Moment K-In
Force K

Moment K-In

$f1 := (k1 \cdot A1 \cdot D) + F1$

$$f1 = \begin{pmatrix} 0 \\ 1.358 \times 10^{-14} \\ 0 \\ 9.862 \times 10^{-14} \end{pmatrix}$$

$f2 := k2 \cdot A2 \cdot D + FEF2$

$$f2 = \begin{pmatrix} 4.45 \\ -0 \\ 11.55 \\ -127.72 \end{pmatrix}$$

$f3 := k3 \cdot A3 \cdot D + FEF3$

$$f3 = \begin{pmatrix} 5.504 \\ 127.72 \\ 10.496 \\ -114.795 \end{pmatrix}$$

Unfactored Live Loads ONLY

$$f4 = \begin{pmatrix} 8.274 \\ 114.795 \\ 7.726 \\ -98.988 \end{pmatrix}$$

$f4 := k4 \cdot A4 \cdot D + FEF4$

$$f5 = \begin{pmatrix} 4.836 \\ 98.988 \\ 11.164 \\ -50.853 \end{pmatrix}$$

$f5 := (k5 \cdot A5 \cdot D) + FEF5$

$f6 := (k6 \cdot A6 \cdot D) + FEF6$

$$f6 = \begin{pmatrix} 16.883 \\ 50.853 \\ -0.883 \\ -3.506 \times 10^{-14} \end{pmatrix}$$

$$f7 = \begin{pmatrix} 0 \\ 3.41 \times 10^{-14} \\ 0 \\ 2.21 \times 10^{-15} \end{pmatrix}$$

$f7 := (k7 \cdot A7 \cdot D) + F7$

Maximum Positive Loads are found using free body diagrams of the shear and moments of each individual element and its respective forces.

The Dead Load Analysis was done with the same method. The major differences in loading are shown below. There is a continuous self weight and dead load due to the barriers on the cantilevers.

$$LOAD := \begin{pmatrix} w & P1 & a1 & P2 & a2 & P3 & a3 & P4 & a4 \\ -.0125 & -.394 & .171 & 0 & 0 & 0 & 0 & 0 & 0 \\ -.0125 & 0 & 0 & 0 & 0 & 0 & 0 & 0 & 0 \\ -.0125 & 0 & 0 & 0 & 0 & 0 & 0 & 0 & 0 \\ -.0125 & 0 & 0 & 0 & 0 & 0 & 0 & 0 & 0 \\ -.0125 & 0 & 0 & 0 & 0 & 0 & 0 & 0 & 0 \\ -.0125 & 0 & 0 & 0 & 0 & 0 & 0 & 0 & 0 \\ -.0125 & -.394 & .171 & 0 & 0 & 0 & 0 & 0 & 0 \end{pmatrix}$$

Locations (% of span length)

Loads (Kips, Kips/Inch)

Element Forces

$f1 := (k1 \cdot A1 \cdot D) + F1$

$$f1 = \begin{pmatrix} 0 \\ -7.418 \times 10^{-15} \\ 0.869 \\ -20.649 \end{pmatrix}$$

$f2 := k2 \cdot A2 \cdot D + FEF2$

$$f2 = \begin{pmatrix} 0.74 \\ 20.65 \\ -0.02 \\ 1.07 \end{pmatrix}$$

$f3 := k3 \cdot A3 \cdot D + FEF3$

$$f3 = \begin{pmatrix} 0.266 \\ -1.068 \\ 0.454 \\ -4.361 \end{pmatrix}$$

$f4 := k4 \cdot A4 \cdot D + FEF4$

$$f4 = \begin{pmatrix} 0.36 \\ 4.361 \\ 0.36 \\ -4.361 \end{pmatrix}$$

$$f5 = \begin{pmatrix} 0.454 \\ 4.361 \\ 0.266 \\ 1.068 \end{pmatrix}$$

$f5 := (k5 \cdot A5 \cdot D) + FEF5$

$$f6 = \begin{pmatrix} -0.017 \\ -1.068 \\ 0.737 \\ -20.649 \end{pmatrix}$$

$f6 := (k6 \cdot A6 \cdot D) + FEF6$

$f7 := (k7 \cdot A7 \cdot D) + F7$

$$f7 = \begin{pmatrix} 0.869 \\ 20.649 \\ 0 \\ -4.47 \times 10^{-15} \end{pmatrix}$$

Individual Bar Forces/Moments
+ Up,Forces; CCW = -, Moments
Force K

Moment K-In
Force K

Moment K-In

Unfactored Dead Loads ONLY

A.2.2 Transverse Deck Design

Deck Panel Design - Transverse Direction

Layout

ta := 8 Inches *Actual panel depth*

t := 7.5 Inches *Depth used for design*

S := 4.8 fee *Girder Spacing*

Girders := 6

Overhang := 3.8 Inches

SBC := 14 *Inches (Width of the Barrier Curb from the edge of the slab-the kansas type used actually extends 15" but the last inch is past the edge of the slab.)*

W21x83

bf := 8.36 Inches

Properties

gc := 150 pcf

$wc := gc \cdot \frac{ta}{12}$

wc = 100 plf *Slab weight*

wcl := 50 plf *Construction weight*

wp := 394 plf *Kansas Corral Barrier (6.5" cg from the edge of the deck)*

Pll := 16 kips *Point Load-HS20 Wheel*

fci := 4 ksi

$Eci := 57 \cdot \sqrt{fci \cdot 1000}$ ksi

Eci = 3605 ksi

fc := 6 ksi

$Ec := 57 \cdot \sqrt{fc \cdot 1000}$ ksi

Ec = 4415 ksi

db := .5 Inches *Diameter of P/S strands*

fsu := 270 ksi

fsy := 243 ksi

Es := 28500 ksi

As := .153 in^2 *Area of P/S strands*

ϕb := 1.0 *Factor for bending*

Load Factors *AASHTO LFD 2002*

$\gamma := 1.3$

$\beta dl := 1.0$

$\beta cl := 1.0$

$\beta ll := 1.67$

Loading

Dead Loads

This is solved using a continuous beam analysis with the self weight and construction loads as continuous loads. The barrier was added as a point load 6.5" from the edge of the slab.

Mdlext := 20.6
Mdlintn := 4.3 k-in/ft
Mdlintp := 3.9

Live Loads

A continuous beam analysis was done with the worst case tire loads. The positive, negative, and overhang moments were computed.

Multi-presence factors 3.12.1 AASHTO 2002

MPF2 := 1 *2 lanes or less*
MPF3 := .9 *3 lanes*

Impact Factors AASHTO 2002

IF := 1.3

Effective Slab Width AASHTO 3.24.3.2

X := 1 fee

Wpm := (4 + .06·S)·12 Wpm = 51.456 Inches

Wnm := (4 + .06·S)·12 Wnm = 51.456 Inches

Wo := (3.2 + .35·X)·12 Wo = 42.6 Inches

Mllext := 192 k-in/ft

Mllintn := 156.6 k-in/ft

Mllintp := 159.2 k-in/ft

No impact factors, multi-presence factors or effective width factors were used in this analysis.

$Mllext := Mllext \cdot IF \cdot \frac{MPF2 \cdot 12}{Wo}$ Mllext = 70.31 k-in/ft

$Mllintn := Mllintn \cdot IF \cdot MPF2 \cdot \frac{12}{Wnm}$ Mllintn = 47.495 k-in/ft

$Mllintp := Mllintp \cdot IF \cdot MPF2 \cdot \frac{12}{Wpm}$ Mllintp = 48.283 k-in/ft

Impact factors, mulit-presence factors and effective width factors were used in this analysis. All of the limiting values were with 2 lanes or less.

Strand Design

Allowable Stresses AASHTO 2002 9.15

$fci := -.6 \cdot fci$ $fci = -2.4$ ksi

$fti := 0$ $fti = 0$ ksi

$fcs1 := -.4 \cdot fc$ $fcs1 = -2.4$ ksi Prestress and DL

$fcs2 := -.6 \cdot fc$ $fcs2 = -3.6$ ksi Live and Dead Loads

$fts := \frac{6 \cdot \sqrt{fc \cdot 1000}}{1000}$ $fts = 0.465$ ksi

Service Load Moments

$Mneg := \frac{Mllintn}{12} + \frac{Mdlintn}{12}$ $Mneg = 4.321$ k-ft/ft

$Mpos := \frac{Mllintp}{12} + \frac{Mdlintp}{12}$ $Mpos = 4.349$ k-ft/ft

$Mext := \frac{Mllext}{12} + \frac{Mdlext}{12}$ $Mext = 7.58$ k-ft/ft

Section Properties - 1 foot wide strip

$Ac := t \cdot 12$ $Ac = 90$ in^2

$Ic := \frac{1}{12} \cdot 12 \cdot t^3$ $Ic = 421.875$ in^4

$Sc := \frac{Ic}{\frac{t}{2}}$ $Sc = 112.5$ in^3

f = M/S Stresses at Service Loads without P/A term-Use for initial design.

$fneg := \frac{Mneg \cdot 12}{Sc}$ $fneg = 0.461$

$fpos := \frac{Mpos \cdot 12}{Sc}$ $fpos = 0.464$

$fext := \frac{Mext \cdot 12}{Sc}$ $fext = 0.809$

Find the limiting tension stress from these equations and then add enough strands to bring the stress level within the limits.

$fp := \max(fneg, fpos, fext) - fts$ Stress needed from the strands.

$fp = 0.344$ ksi

$Pe := fp \cdot Ac$ $Pe = 30.94$ K/ft Initially assume 30% jacking and 15% time Losses.

$Pstrand := fsu \cdot .7 \cdot As \cdot .85$ $Pstrand = 24.579$ K

$Prqd := \frac{Pe}{Pstrand}$ $\frac{Pe}{Pstrand} = 1.259$ strands / foot required

Panel Width	Min Strands	Min Pe
7	S7 := floor(7·Prqd) + 1 = (9)	S7·Pe = 278.457
8	S8 := floor(8·Prqd) + 1 = (11)	S8·Pe = 340.336
9	S9 := floor(9·Prqd) + 1 = (12)	S9·Pe = 371.276
10	S10 := floor(10·Prqd) + 1 = (13)	S10·Pe = 402.216
11	S11 := floor(11·Prqd) + 1 = (14)	S11·Pe = 433.155
12	S12 := floor(12·Prqd) + 1 = (16)	S12·Pe = 495.035

Losses Calculations PCI Bridge Manual 8.6 Same as AASHTO 2002 except Creep which is similar.

More exact calculations are used to determine the losses and the stressing forces.

Wp := 120 Inches Choose a panel width.

Ap := Wp·t Ap = 900 in^2

Strands:= 16 Choose a number of strands.

Elastic Shortening

$$fcgp := \frac{As \cdot .7 \cdot fsu \cdot Strands}{Ap} \qquad fcgp = 0.514$$

$$\Delta fpes := \frac{Es}{Eci} \cdot fcgp \qquad \Delta fpes = 4.064 \quad ksi$$

Shrinkage

H := 70 % Fig 3.12.2 PCI Bridge Manual

$\Delta fpsr := 17 - .15 \cdot H$ $\Delta fpsr = 6.5$ ksi

Creep of Concrete

fcdp := 0 Prestressing resultant force at the centroid of the concrete.

$\Delta fpcr := 12 \cdot fcgp - 7fcdp$ $\Delta fpcr = 6.169$ ksi

Relaxation of Prestressing Steel

-Before Transfer

t1 := 1 day

fi := .75·fsu fi = 202.5 ksi

$$\Delta fpr1 := \frac{\log(24 \cdot t1)}{45} \cdot \left(\frac{fi}{fsu} - .55 \right) \cdot fi \qquad \Delta fpr1 = 1.242 \quad ksi$$

–AfterTransfe

$\Delta fpr2 := 6 - .12 \cdot \Delta fpes - .06 \cdot (\Delta fpsr + \Delta fpcr)$ $\Delta fpr2 = 4.752$ ksi

$\Delta fpr := \Delta fpr1 + \Delta fpr2$ $\Delta fpr = 5.994$ ksi

Total Losses at Transfer

$\Delta fpi := \Delta fpes + \Delta fpr$ $\Delta fpi = 5.306$ ksi

Stress in tendon after transfer

$fpt := .75 \cdot fsu - \Delta fp$ $fpt = 197.194$ ksi

Prestressing force after transfer per panel

$Pi := Strands \cdot As \cdot fpt$ $Pi = 482.73$ kips

Total Losses at Service Loads

$\Delta fpt := \Delta fpes + \Delta fpsr + \Delta fpcr + \Delta fpr2$ $\Delta fpt = 21.485$ ksi

Stress in tendon affter all losses

$fpe := .75 \cdot fsu - \Delta fp$ $fpe = 181.015$

Effective P/S force per panel

$Pe := Strands \cdot As \cdot fpe$ $Pe = 443.124$ kips

Stress Check

Transfer Length

$lt := 60 \cdot \frac{db}{12}$ $lt = 2.5$ fee

The transfer length is sufficient. The critical section over the exterior girder is 38" from the edge of the slab. This is greater than lt.

-Transfer Stress

$fc1 := \frac{-Pi}{Ap}$ $fc1 = -0.536$ ksi < fci $fci = -2.4$ ksi

-Service Stress

$ft1 := \frac{-Pe}{Ap} + \frac{Mpos \cdot 12}{Sc}$ $ft1 = -0.029$

$ft2 := \frac{-Pe}{Ap} + \frac{Mneg \cdot 12}{Sc}$ $ft2 = -0.031$

$ft3 := \frac{-Pe}{Ap} + \frac{Mext \cdot 12}{Sc}$ $ft3 = 0.316$ < fts $fts = 0.465$ ksi

$fc11 := \frac{-Pe}{Ap} - \frac{Mdlintp}{Sc}$ $fc11 = -0.527$

$fc12 := \frac{-Pe}{Ap} - \frac{Mdlintn}{Sc}$ $fc12 = -0.531$

$fc13 := \frac{-Pe}{Ap} - \frac{Mdlext}{Sc}$ $fc13 = -0.676$ > fcs1 $fcs1 = -2.4$ ksi

$fc21 := \frac{-Pe}{Ap} - \frac{Mpos \cdot 12}{Sc}$ $fc21 = -0.956$

$fc22 := \frac{-Pe}{Ap} - \frac{Mneg \cdot 12}{Sc}$ $fc22 = -0.953$

$fc23 := \frac{-Pe}{Ap} - \frac{Mext \cdot 12}{Sc}$ $fc23 = -1.301$ > fcs2 $fcs2 = -3.6$ ksi

Flexural Strength

Applied Loads

$$Muext := \gamma \cdot \left(\beta dl \cdot Mdlext \cdot \frac{wc}{wc + wcl} + \beta cl \cdot Mdlext \cdot \frac{wcl}{wc + wcl} + \beta ll \cdot Mllext \right)$$

$Muext = 179.488$ k-in/ft

$$Muintn := \gamma \cdot \left(\beta dl \cdot Mdlintn \cdot \frac{wc}{wc + wcl} + \beta cl \cdot Mdlintn \cdot \frac{wcl}{wc + wcl} + \beta ll \cdot Mllintn \right)$$

$Muintn = 108.779$ k-in/ft

$$Muintp := \gamma \cdot \left(\beta dl \cdot Mdlintp \cdot \frac{wc}{wc + wcl} + \beta cl \cdot Mdlintp \cdot \frac{wcl}{wc + wcl} + \beta ll \cdot Mllintp \right)$$

$Muintp = 109.893$ k-in/ft

The dead load and construction loads were added together previously. They are seperated based on the continuous loading entered at the beginning in the loading section.

Capacity

$Ast := As \cdot Strand$ $Ast = 2.448$ in^2

$\beta 1 := .85 - (fc - 4) \cdot .0$ $\beta 1 = 0.75$

$b := Wp$ $b = 120$ In

$dp := t - 1.5 - \frac{db}{2}$ $dp = 5.75$ In A two inch cover is required but a half inch is accounted for in the sacrificial surface.

$\gamma s := .2$

$$p := \frac{\frac{Ast}{2}}{b \cdot dp}$$ $p = 1.774 \times 10^{-3}$

$$fsus := fsu \cdot \left[1 - \frac{\gamma s}{\beta 1} \cdot \left[p \cdot \frac{fsu}{(fc)} \right] \right]$$ $fsus = 261.954$ ksi

$fsumax := S \cdot 12 \cdot \frac{3}{db} + \frac{2}{3} \cdot fpe$ $fsumax = 466.276$ ksi

$ld := \left(fsus - \frac{2 \cdot fpe}{3} \right) \cdot \frac{db}{12}$ $ld = 5.887$ ft

The strands are fully developed at the interior section but not over the exterior girder. This is addressed in the cantilever check later.

$Lint := \frac{38}{12} + \frac{8}{2}$ $Lint = 7.167$ ft

$Lext := \frac{38}{12}$ $Lext = 3.167$ ft

$\phi := 1.0$

$\phi Mn := \frac{\phi}{12} \cdot \left[As \cdot \frac{Strands}{2} \cdot fsus \cdot (dp) \cdot \left(1 - .6 \cdot p \cdot \frac{fsus}{fc} \right) \right]$ $\phi Mn = 146.497$ k-ft/ft

$\frac{\max(Muintn, Muintp, Muext)}{12} = 14.957$ **Passes** in flexure

Mild Steel

Maximum Steel AASHTO 8.16.3.1

$fy := 60$ ksi

$\rho b := \frac{.85 \cdot \beta 1 \cdot fc}{fy} \cdot \left(\frac{87000}{87000 + fy \cdot 1000} \right)$ $\rho b = 0.038$

$\rho b := \rho b \cdot .75$ $\rho b = 0.028$

$Asmax := \rho b \cdot 12 \cdot t$ $Asmax = 2.547$ in^2/ft

Minimum Steel AASHTO 8.17.1

$fr := \frac{-7.5 \cdot \sqrt{fc \cdot 1000}}{1000}$ $fr = -0.581$ ksi

$fpem := \frac{-Pe}{Ap}$ $fpem = -0.492$ ksi

$Mcr := \frac{Sc \cdot (fr + fpem)}{\frac{b}{12}}$ $Mcr = -12.075$ k-ft/ft

$Mcr < \phi Mn$ OK

Without including the P/S strand reinforcing. AASHTO 8.16.3.2

$Mcr1 := \frac{Sc \cdot (fr)}{\frac{b}{12}}$ $Mcr1 = -6.536$ k-in/ft

$\phi Mn := 1.2 \cdot Mcr1$ k-ft/ft

$Mn := \frac{\phi Mn}{.9}$ k-ft/ft

$Y := Asmin \cdot fy \cdot t - \frac{Asmin^2 \cdot fy^2}{1.7 \cdot fc \cdot 12} - -Mn$ $root(Y, Asmin) \rightarrow \left(1.9389488775152231772 \cdot 10^{-2} \quad 15.280610511224847768\right)$

$Asmin := .0193$ in^2/ft

#4 @ 12"
#3 @ 6"

Minimum Mild Steel (Transverse to the P/T) AASHTO 9.24

$Arqd := .11$ in^2/ft

Use #4 @ 18" Minimum Transverse Panel Direction
or #3 @ 12"

Punching Shear Not Required AASHTO LFD 8.20 - This is the LRFD method.

$l := 1($ lr

$w := 2($ lr

$Atire := 20($ in^2

$Pressure := .12$ ksi

$Vu := 1.3 \cdot 1.67 \cdot PressureAtire$ $Vu = 54.275$ K

$\beta c := \frac{w}{l}$ $\beta c = 2$

$dv := dp$ $dv = 5.75$ lr

$bo := 2 \cdot (l + w)$ $bo = 60$ in^2

$\phi c := .9$

$\phi V := \phi c \cdot \min\left[\left(.063 + \frac{.126}{\beta c}\right) \cdot \sqrt{fc} \cdot bo \cdot dv, .126 \cdot \sqrt{fc} \cdot bo \cdot dv\right]$

$\phi V = 95.831$ K

OK

Flexural Strength-Cantilever

Applied Loads

The limiting case is located at 1/2 the width of the girder.

$Muext := \frac{Muext}{12}$

$Muext = 14.957$

Capacity

$Lcant := \frac{38}{12}$ Fee — The length of the embedded strand from the edge of the deck to the critical location.

$Ast := As \cdot Strands$ $Ast = 2.448$ in^2

$\beta 1 := .85 - (fc - 4) \cdot .05$ $\beta 1 = 0.75$

$b := Wp$ $b = 120$ lr

$dp := t - 1.5 - \frac{db}{2}$ $dp = 5.75$ lr — A two inch cover is required but a half inch is accounted for in the sacrificial surface.

$\gamma s := .28$

$p := \frac{\frac{Ast}{2}}{b \cdot dp}$ $p = 1.774 \times 10^{-3}$

$fsus := fsu \cdot \left[1 - \frac{\gamma s}{\beta 1} \cdot \left[p \cdot \frac{fsu}{(fc)} \right] \right]$ $fsus = 261.954$ ksi

$fsumax := S \cdot 12 \cdot \frac{3}{db} + \frac{2}{3} \cdot fpe$ $fsumax = 466.276$ ksi

$ld := \left(fsus - \frac{2 \cdot fpe}{3} \right) \cdot \frac{db}{12}$ $ld = 5.887$ ft

$fsus := fsus \cdot \frac{Lext}{ld}$ $fsus = 140.918$ ksi

$\phi := 1.0$

$\phi Mn := \frac{\phi}{12} \cdot \left[As \cdot \frac{Strands}{2} \cdot fsus \cdot (dp) \cdot \left(1 - .6 \cdot p \cdot \frac{fsus}{fc} \right) \right]$ $\phi Mn = 80.582$ k-ft/ft

Passes in flexure

Applied Loads

The limiting case is located at 1/2 the width of the girder.

$Muext = 14.957$

Capacity

$Lcant := \frac{14}{12}$ Fee — The length of the embedded strand from the edge of the deck to the critical location.

$Ast := As \cdot Strands$ $Ast = 2.448$ in^2

$\beta 1 := .85 - (fc - 4) \cdot .05$ $\beta 1 = 0.75$

$b := Wp$ $b = 120$ lr

$dp := t - 1.5 - \frac{db}{2}$ $dp = 5.75$ lr — A two inch cover is required but a half inch is accounted for in the sacrificial surface.

$\gamma s := .28$

$$p := \frac{\frac{Ast}{2}}{b \cdot dp} \qquad p = 1.774 \times 10^{-3}$$

$$fsus := fsu \cdot \left[1 - \frac{\gamma s}{\beta 1} \cdot \left[p \cdot \frac{fsu}{(fc)} \right] \right] \qquad fsus = 261.954 \quad ksi$$

$$fsumax := S \cdot 12 \cdot \frac{3}{db} + \frac{2}{3} \cdot fpe \qquad fsumax = 466.276 \quad ksi$$

$$ld := \left(fsus - \frac{2 \cdot fpe}{3} \right) \cdot \frac{db}{12} \qquad ld = 5.887 \quad ft$$

$$fsus := fsus \cdot \frac{Lcant}{ld} \qquad fsus = 51.917 \quad ksi$$

$$\phi := 1.($$

$$\phi Mn := \frac{\phi}{12} \cdot \left[As \cdot \frac{Strands}{2} \cdot fsus \cdot (dp) \cdot \left(1 - .6 \cdot p \cdot \frac{fsus}{fc} \right) \right] \qquad \phi Mn = 30.169 \quad k\text{-}ft/ft$$

Passes in flexure

The capacity is sufficient at the barrier curb. If not Add mild steel.

Reinforcing Limits-Cantilever

These are the same as above.

A.3 Transverse Joint Design

A.3.1 Longitudinal Analysis

This spreadsheet will take the service load moments from Q-Con and factor them with the given load factors. This is done to get around the LRFD setup in Q-Con. The data for the HS-20 vehicle and the Dead Loads are used. The Lane loadings are zeroed out in Q-Con.

INTERIOR		Load Factors	
Load Type	DF	Strength I	Service I
Live Load	0.436	2.171	1
Dead Load		1.3	1
Impact Factor		1.3	

AASHTO 2002 Standard Specification

Moments (k-ft) (LL are all per lane from Q-Con)

	Span 1		Span 2		Span 3	
	Max +	Max -	Max +	Max -	Max +	Max -
LL	365.44	-363.07	306.58	-363.07	365.44	-363.07
DL	78.06	-99.68	27.03	-99.68	78.06	-99.68
Factored Strength	**551.52**	**-576.70**	**412.70**	**-576.70**	**551.52**	**-576.70**
Factored Service	**237.52**	**-258.10**	**160.81**	**-258.10**	**237.52**	**-258.10**

EXTERIOR		Load Factors	
Load Type	DF	Strength IA	Service I
Live Load	0.436	2.171	1
Dead Load		1.3	1
Impact Factor		1.3	

Moments (k-ft) (LL are all per lane from Q-Con)

Moments (k-ft)

	Span 1		Span 2		Span 3	
	Max +	Max -	Max +	Max -	Max +	Max -
LL	365.44	-363.07	306.58	-363.07	365.44	-363.07
DL	84.29	-107.64	29.19	-107.64	84.29	-107.64
Factored Strength	**559.62**	**-587.06**	**415.50**	**-587.06**	**559.62**	**-587.06**
Factored Service	**243.75**	**-266.07**	**162.97**	**-266.07**	**243.75**	**-266.07**
Factored Serv LL	**159.46**	**-158.43**	**133.78**	**-158.43**	**159.46**	**-158.43**

A.3.2 Longitudinal Strength Design

Embedded Rebar Design

Based on the AASHTO 2002 Bridge Manual
Section 10.50

Negative Moment Sections
Exterior Girder

Es,s	29000	ksi
Es,g	29000	ksi
Fy,s	60	ksi
fy,g	50	ksi

Girder Dimensions		
As,girder	28.5	in2
Ix	2381.87	in4
C.G. (Gird)	10.6875	Inches
d	21.375	Inches
t/b	0.065	In/In
tw	0.5	Inches
tf	0.75	Inches
bf	12.375	Inches
lambda	12500	

bs	66.8	Inches
ts	8	Inches
Clear Cover,t	4	Inches
Clear Cover,b	0	Inches
D,steel,t	0.75	Inches
As,slab,t	1.54	In^2
D,steel,b	0.50	Inches
As,slab,b	0.00	In^2

Top Steel **#6 @ 18"**

C.G. (composite)	11.42	Inches
Ig	2681.16	In^4
I1	283.95	
I2	2397.21	
Sx,t1	20.35	
Sx,t2	171.80	
Sx,c	234.75	
Fcr	50.00	
Rb	1.00	
Φ	0.90	
ΦMn	8829.72 735.81	K-In K-ft

C1	13.95
C2	11.42

***Originally Designed for the real W21x83 Girder
Tested with a W21x101 Girder

Strength **Passes**

Looped Bar Design
Based on the AASHTO 2002 Bridge Manual
Section 10.50

Negative Moment Sections
Exterior Girder

Es,s	29000	ksi
Es,g	29000	ksi
Fy,s	60	ksi
fy,g	50	ksi

Girder Dimensions		
As,girder	28.5	in2
Ix	2381.87	in4
C.G. (Gird)	10.6875	Inches
d	21.375	Inches
t/b	0.09989	In/In
tw	0.5	Inches
tf	0.75	Inches
bf	12.375	Inches
lambda	12500	

bs	66.8	Inches
ts	8	Inches
Clear Cover,t	3	Inches
Clear Cover,b	1	Inches
D,steel,t	0.5	Inches
As,slab,t	1.31	In^2
D,steel,b	0.50	Inches
As,slab,b	1.31	In^2

This is based on the actual design-not the test setup.

Top Steel **#4 @ 10" throughout**

Bottom Steel **#4 @ 10" throughout**

C.G. (composite)	11.84	Inches
Ig	2839.42	In^4

C1	14.54
C2	11.84

I1	419.70
I2	2419.72

Sx,t1	28.88
Sx,t2	166.47
Sx,c	239.82
Fcr	50.00
Rb	1.00

Φ	0.90	
ΦMn	9050.56 754.21	K-In K-ft

***Originally Designed for the real W21x83 Girder
Tested with a W21x101 Girder

Strength **Passes**

Post-Tensioned Stress Design

				SS analysis				Continuous span analysis						
Girder Type	Girder Spacing (ft)	Span Length (ft)	# strands in deck	Initial comp. in deck (ksi)	Final compression in deck			Tension at top of deck over middle support					6*sqrt(f'c) (ksi)	Total stress vs. 6*sqrt(f'c)
					top (ksi)	middle (ksi)	bottom (ksi)	due to force redist (ksi)	due to LL (ksi)	DFM	LL*factors	Final values (ksi)		
W21X83	4.8	32/32.5/32	2	-0.133	-0.138	-0.071	-0.00311	0.169	0.862	0.4365	0.301	0.33	0.42	OK
W21X83	4.8	32/32.5/32	4	-0.266	-0.268	-0.19	-0.112	0.194	0.865	0.4365	0.302	0.23	0.42	OK
W21x83	4.8	32/32.5/33	6	-0.399	-0.394	-0.306	-0.219	0.218	0.863	0.4365	0.301	0.13	0.42	OK
W21x83	4.8	32/32.5/34	8	-0.532	-0.514	-0.418	-0.322	0.239	0.861	0.4365	0.301	0.03	0.42	OK
TEST SETUP														
W21x101	4.8	19	2	-0.164					0.588	1	0.588	0.42	0.42	OK
W21x101	4.8	19	3	-0.246					0.588	1	0.588	0.34	0.42	OK
W21x101	4.8	19	4	-0.328					0.588	1	0.588	0.26	0.42	OK
TEST SETUP – 2 MONTHS OF LONG-TERM LOSSES														
W21x101	4.8	19	2	-0.164	-0.154	-0.123	-0.093		.588	1	0.588	0.43	0.42	NO
W21x101	4.8	19	3	-0.246	-0.233	-0.198	-0.164		.588	1	0.588	0.36	0.42	OK
W21x101	4.8	19	4	-0.328	-0.312	-0.273	-0.234		.588	1	0.588	0.28	0.42	OK

Short Term Losses in the Post Tensioned Deck Panels

P/T 1 Panels

Panel Dimensions

Width	84	Inches
Height	8	Inches
Area	672	In^2
Ec	4415.20	ksi
fy	6000	ksi
I	395136	In^4
r^2	588	In^2

Strand Values

fu	270	ksi
Area (Used)	0.167	In^2
Area (Desig	0.153	In^2
Es	28500	ksi
n	6.45	
k	0.000200	
Slip	0.10	Inches
Length	18.25	Feet

Desired Force in Strands (completion of construction-No Long Term Losses)

Percent of Ultimate	**61.2**	%
P	**27.60**	**Kips**

Spacing of Strands from the Centerline

1	16.5	Inches
2	16.5	Inches
3	17.5	Inches
4	17.5	Inches

Force with Elastic Shortening			**Average**
P4	30.40	kips	30.99
P3	30.79	kips	
P2	31.18	kips	
P1	31.59	kips	
Average	**30.99**	**kips**	**68.7%**

Length to Pull the Strands

Seating D	**Elastic De**	**Total**		
0.25	1.40	1 10/16	1.65	Inches
0.25	1.42	1 11/16	1.67	Inches
0.25	1.43	1 11/16	1.68	Inches
0.25	1.45	1 11/16	1.70	Inches

Friction Losses

P4	-0.101	kips
P3	-0.101	kips
P2	-0.101	kips
P1	-0.101	kips

Seating Losses

Live End

P4	-2.17	kips
P3	-2.17	kips
P2	-2.17	kips
P1	-2.17	kips

Creep Losses

Short Term	-0.29	kips

Shrinkage Losses

Short Term	0.00	kips

Relaxation Losses

Short Term	-0.235	kips

Short Term Losses in the Post Tensioned Deck Panels

P/T 2 Panels

Panel Dimensions

Width	84	Inches
Height	8	Inches
Area	672	In^2
Ec	4415.20	ksi
fy	6000	ksi
I	395136	In^4
r^2	588	In^2

Strand Values

fu	270	ksi
Area (Used)	0.167	In^2
Area (Desig	0.153	In^2
Es	28500	ksi
n	6.45	
k	0.000200	
Slip	0.10	Inches
Length	18.25	Feet

Desired Force in Strands (completion of construction-No Long Term Losses)

Percent of Ultimate	**61.0**	%
P	**27.50**	**Kips**

Spacing of Strands from the Centerline

1	16.5	Inches
2	16.5	Inches
3	17.5	Inches
4	17.5	Inches
5	18.5	Inches
6	18.5	Inches
7	19.5	Inches
8	19.5	Inches

Force with Elastic Shortening			**Average**
P8	30.30	kips	30.89
P7	30.68	kips	
P6	31.08	kips	
P5	31.49	kips	
P4	31.91	kips	32.58
P3	32.35	kips	
P2	32.80	kips	
P1	33.28	kips	
Average	**31.74**	**kips**	**70.4%**

Length to Pull the Strands

Seating D	**Elastic De**	**Total**		
0.25	1.39	1 10/16	1.64	Inches
0.25	1.41	1 11/16	1.66	Inches
0.25	1.43	1 11/16	1.68	Inches
0.25	1.45	1 11/16	1.70	Inches
0.25	1.47	1 11/16	1.72	Inches
0.25	1.49	1 12/16	1.74	Inches
0.25	1.51	1 12/16	1.76	Inches
0.25	1.53	1 12/16	1.78	Inches

Friction Losses

P8	-0.100	kips
P7	-0.100	kips
P6	-0.100	kips
P5	-0.100	kips
P4	-0.100	kips
P3	-0.100	kips
P2	-0.100	kips
P1	-0.100	kips

Seating Losses

Live End

P8	-2.17	kips
P7	-2.17	kips
P6	-2.17	kips
P5	-2.17	kips
P4	-2.17	kips
P3	-2.17	kips
P2	-2.17	kips
P1	-2.17	kips

Creep Losses

Short Term	-0.29	kips

Shrinkage Losses

Short Term	0.00	kips

Relaxation Losses

Short Term	-0.235	kips

A.3.3 Horizontal Shear Design

Shear Stud Design (Actual Bridge Design 8/23/07)

Stud Diameter, d	0.875	Inches	α	7850	@ 2,000,000 Cycles
Stud Height, H	5	Inches	Zr	6.01016	Kips
H/d >= 4	YES		ΣZr	48.0813	Kips
# of Studs/X-Sec.	8				
Asr	0.59	In^2/ft			

Span #	Spans 1/3 Interior (21Wx83)										
	0	0.1	0.2	0.3	0.4	0.5	0.6	0.7	0.8	0.9	1
Shear Vr (K)	29.73	25.17	23.82	20.5	24.15	24.39	21.69	25.28	27.01	29.1	32.1

Fatigue Design

Vr, Average Shear	29.73	25.17	23.82	20.50	24.15	24.39	21.69	25.28	27.01	29.10	32.10
Q	256.38	256.38	256.38	256.38	256.38	256.38	256.38	256.38	256.38	256.38	256.38
I	5842.98	5842.98	5842.98	5842.98	5842.98	5842.98	5842.98	5842.98	5842.98	5842.98	5842.98
Sr	1.30	1.10	1.05	0.90	1.06	1.07	0.95	1.11	1.19	1.28	1.41
Pitch	36.86	43.54	46.00	53.45	45.37	44.93	50.52	43.35	40.57	37.66	34.14
Chosen Pitch	40	40	40	40	40	40	40	40	40	40	40
A_r^s	2.832	2.832	2.832	2.832	2.832	2.832	2.832	2.832	2.832	2.832	2.832
fr	10,000	10,000	10,000	10,000	10,000	10,000	10,000	10,000	10,000	10,000	10,000
Zr	6.01016	6.01016	6.01016	6.01016	6.01016	6.01016	6.01016	6.01016	6.01016	6.01016	6.01016
Nc	4.71	4.71	4.71	4.71	4.71	4.71	4.71	4.71	4.71	4.71	4.71

Shear Stud Design *(Actual Bridge Design 8/23/07)*

Stud Diameter, d	0.875	Inches	α	7850	@ 2,000,000 Cycles
Stud Height, H	5	Inches	Zr	6.01016	Kips
H/d >= 4	YES		ΣZr	48.0813	Kips
# of Studs/X-Sec.	8				
Asr	0.59	In^2/ft			

Span #	Spans 1/3 Interior (21Wx83)										
	0	0.1	0.2	0.3	0.4	0.5	0.6	0.7	0.8	0.9	1
Strength Design											
Force in Slab, P	1215	1215	1215	1215	1215	1215	1215	1215	1215	1215	1215
Steel Area	24.3	24.3	24.3	24.3	24.3	24.3	24.3	24.3	24.3	24.3	24.3
Fy	50000	50000	50000	50000	50000	50000	50000	50000	50000	50000	50000
f'c	6000	6000	6000	6000	6000	6000	6000	6000	6000	6000	6000
Eff Flange width, b	57.6	57.6	57.6	57.6	57.6	57.6	57.6	57.6	57.6	57.6	57.6
ts, Slab Thickness	7.5	7.5	7.5	7.5	7.5	7.5	7.5	7.5	7.5	7.5	7.5
P1	1215000	1215000	1215000	1215000	1215000	1215000	1215000	1215000	1215000	1215000	1215000
P2	2203200	2203200	2203200	2203200	2203200	2203200	2203200	2203200	2203200	2203200	2203200
P3	141600	141600	141600	141600	141600	141600	141600	141600	141600	141600	141600
Su	51406.1	51406.1	51406.1	51406.1	51406.1	51406.1	51406.1	51406.1	51406.1	51406.1	51406.1
Ec	4695982	4695982	4695982	4695982	4695982	4695982	4695982	4695982	4695982	4695982	4695982
N	31.05	31.05	31.05	31.05	31.05	31.05	31.05	31.05	31.05	31.05	31.05
Total Needed/Span	63	63	63	63	63	63	63	63	63	63	63
Shear Conn. Zone	32	32	32	32	32	32	32	32	32	32	32
Pitch	55.85	55.85	55.85	55.85	55.85	55.85	55.85	55.85	55.85	55.85	55.85
Chosen Pitch	40	40	40	40	40	40	40	40	40	40	40
Limiting Pitch	40	40	40	40	40	40	40	40	40	40	40

Span 2 Interior (21Wx83)										
0	0.1	0.2	0.3	0.4	0.5	0.6	0.7	0.8	0.9	1

1215	1215	1215	1215	1215	1215	1215	1215	1215	1215	1215	Kips
24.3	24.3	24.3	24.3	24.3	24.3	24.3	24.3	24.3	24.3	24.3	In^2
50000	50000	50000	50000	50000	50000	50000	50000	50000	50000	50000	psi
6000	6000	6000	6000	6000	6000	6000	6000	6000	6000	6000	psi
57.6	57.6	57.6	57.6	57.6	57.6	57.6	57.6	57.6	57.6	57.6	Inches
7.5	7.5	7.5	7.5	7.5	7.5	7.5	7.5	7.5	7.5	7.5	Inches
1215000	1215000	1215000	1215000	1215000	1215000	1215000	1215000	1215000	1215000	1215000	pounds
2203200	2203200	2203200	2203200	2203200	2203200	2203200	2203200	2203200	2203200	2203200	pounds
141600	141600	141600	141600	141600	141600	141600	141600	141600	141600	141600	pounds
51406.1	51406.1	51406.1	51406.1	51406.1	51406.1	51406.1	51406.1	51406.1	51406.1	51406.1	pounds
4695982	4695982	4695982	4695982	4695982	4695982	4695982	4695982	4695982	4695982	4695982	psi
31.05	31.05	31.05	31.05	31.05	31.05	31.05	31.05	31.05	31.05	31.05	Connectors
63	63	63	63	63	63	63	63	63	63	63	Connectors
32	32	32	32	32	32	32	32	32	32	32	feet
55.85	55.85	55.85	55.85	55.85	55.85	55.85	55.85	55.85	55.85	55.85	Inches
40	40	40	40	40	40	40	40	40	40	40	Inches
40	40	40	40	40	40	40	40	40	40	40	Inches

Span 2 Interior (21Wx83)										
0	0.1	0.2	0.3	0.4	0.5	0.6	0.7	0.8	0.9	1
32	29.77	25.87	24.41	21.2	24.13	21.2	24.41	25.87	29.77	32

												Averages
32.00	29.77	25.87	24.41	21.20	24.13	21.20	24.41	25.87	29.77	32.00	Kips	**26.07**
256.38	256.38	256.38	256.38	256.38	256.38	256.38	256.38	256.38	256.38	256.38	In^3	**256.38**
5842.98	5842.98	5842.98	5842.98	5842.98	5842.98	5842.98	5842.98	5842.98	5842.98	5842.98	In^4	**5842.98**
1.40	1.31	1.14	1.07	0.93	1.06	0.93	1.07	1.14	1.31	1.40	Kips/Inch	**1.14**
34.24	36.81	42.36	44.89	51.69	45.41	51.69	44.89	42.36	36.81	34.24	Inches	**42.81**
40	40	40	40	40	40	40	40	40	40	40	Inches	40

2.832	2.832	2.832	2.832	2.832	2.832	2.832	2.832	2.832	2.832	2.832	In^2
10,000	10,000	10,000	10,000	10,000	10,000	10,000	10,000	10,000	10,000	10,000	psi
6.01016	6.01016	6.01016	6.01016	6.01016	6.01016	6.01016	6.01016	6.01016	6.01016	6.01016	Kips
4.71	4.71	4.71	4.71	4.71	4.71	4.71	4.71	4.71	4.71	4.71	Connectors

A.4 Specifications

Grout Specifications for the Deck Panels

1. Product Composition

1.1 Neat Mortars: The product shall be composed of all fine particles and have a consistency of a powder. Water shall be the only additive required.

1.2 Neat mortars must comply with the specifications set forth in Section 2 through Section 9.

2. Compressive Strength

2.1 The product shall meet the following time-based criteria for compressive strength based on ASTM C 109:

- 1 hour: No strength
- 1 day: Minimum 4000 psi
- 7 day: Minimum 5000 psi

2.2 If a 7 day compressive strength is not available for a product, the following criteria shall be used:

- 28 day: Minimum 6000 psi

3. Splitting Tensile Strength

3.1 The product shall meet the following time-based criteria for splitting tensile strength based on ASTM C 496:

- 1 day: Minimum 200 psi
- 7 day: Minimum 400 psi

3.2 If a 7 day splitting tensile strength is not available for a product, the following criteria shall be used:

- 28 day: Minimum 600 psi

3.3 If no splitting tensile strength information is available for a product, the following criteria shall be used:

- 1 day compressive strength divided by 15 must be greater than 300 psi
- 7 day compressive strength divided by 15 must be greater than 400 psi
- 28 day compressive strength divided by 15 must be greater than 500 psi
- (in lieu of 7 day strength)

4. Shrinkage

4.1 The product shall meet the following criteria for shrinkage based on either ASTM C157 or ASTM C 596. Neat mortars shall be evaluated with 1 in. square cross section prisms.

- 28 day: Maximum 0.04% (400 microstrain)

5. Sulfate Resistance

5.1 The product shall meet the following criteria for sulfate resistance based on ASTM C 1012. Neat mortars shall be evaluated with 1 in. square cross section prisms.

- 28 week: 0.10% (1000 microstrain)

6. Freeze-Thaw Resistance

6.1 The product shall meet the following criteria for freeze-thaw resistance based on ASTM C 666, Procedure A:

- 300 Cycles: Minimum 80% Durability Factor

7. Scaling Resistance

7.1 The product shall meet the following criteria for scaling resistance based on ASTM C 672:

- 25 Cycles: 0 Scaling Rating (no scaling)

8. Mixing Procedure

8.1 The powder shall be added to the specified minimum water content. An additional water amount shall be supplied after approximately 80% of the product has been added to the initial water. This additional water amount may be specified by the manufacturer or may be taken as the difference between the specified maximum water content and the specified minimum water content. The specified maximum water content for a specific product shall not be exceeded. No water shall be added to the product once pouring has commenced.

9. Flow

9.1 The product shall be tested according to 9.2 on site, after mixing and immediately before pouring the product.

9.2 The product shall be tested on a standard flow table specified by ASTM C 230. The testing procedure shall follow ASTM C 1437 with the following modifications:

- The average diameter of the product shall be measured after the mold is lifted to determine the product's flow under its own self weight.
- The table shall then be dropped 10 times in 15 seconds.
- The average diameter of the product shall be measured after the 10 drops
- If either the self weight or 10 drops causes the product's diameter to exceed the diameter of the table, then that measurement shall be recorded as the diameter of the table.

9.3 The product shall meet the following criteria for flow based on the procedure in 9.2:

- Minimum average diameter from self weight flow: 7 in.
- Minimum average diameter after 10 drops: 9 in.

10. Grout Placement

10.1 The product shall be placed in a series of separate pours.

- The product shall be placed in the shear key joints between the panels prior to post-tensioning the panels.
- After post-tensioning the panels a grout product shall be placed in the post-tensioning ducts. This product shall be a type of grout specifically produced for grouting post-tensioned ducts. The product shall be approved by the engineer prior to placement.
- After placing a grout product in the post-tensioned ducts and welding the shear studs to the girders, product shall be placed in the shear pockets and haunches. Each girder line may be poured separately. The blockouts and haunches must be free of any debris or deleterious material.
- Once the leveling bolts are removed, the product shall be placed in the leveling bolt cavities.

10.2 The ambient temperature shall be within the following limits during mixing and placement:

- The temperature range recommended by the grout manufacturer
- A minimum of 35˚ F.
- A maximum of 90˚ F.

10.3 Any bonding surface for the grout shall be wetted to a saturated surface dry condition immediately prior to placing the grout. The surfaces should be clean of any oils or deleterious materials.

11. Curing

11.1 The product shall be cured at a temperature above 35˚ F until it reaches the minimum strengths in 2. Compressive Strength.

11.2 The product does not need cover unless it is raining. When raining, cover the grout for a minimum of 1 hour after the initial set.

Construction Traffic

1. Grouting

1.1 During the grout placement no vehicular traffic is permitted on the deck.

1.2 Traffic may commence on the deck panels once the one day strength of 2.1 is met on all of the grout from section 10.1.

Construction Procedures

1. Lifting the Panels

1.1 The panels shall be lifted at a minimum of three points. The supports will have a minimum lifting capacity of 12,000 pounds.

2. Panel Elevation

2.1 The panels shall have a minimum of four cast in place barrels and leveling bolts to adjust the panel elevations. A minimum of a 1 in. haunch should be maintained throughout. The bolts shall not be removed until the grout in the haunch obtains its minimum 1 day compressive strength from Grout Specifications for Deck Panels.

3. Bracing the Girders

3.1 Fully brace the steel girders prior to placing the panels.

Testing Equipment & Procedures

1. Precast Panels

1.1 An initial stage 1 precast panel shall be constructed prior to producing the remaining panels. The panel shall be inspected by the researchers prior to making the rest of the panels. The test panel shall be transported to the bridge and left on the construction site. This panel shall be grouted at the same time as the deck panels on the bridge. The researchers will need access to the test panel throughout the construction process.

1.2 During the casting of the precast panels vibrating wire gauges (VWG) shall be placed in the panels. A team of researchers from Virginia Tech shall coordinate with the contractor and precaster to place the gauges prior to the pour.

1.3 The team of researchers from Virginia Tech shall document the casting of the precast panels at the precast plant. This shall include recording data from the stressing operation and taking concrete samples during the pour.

1.4 The quantity of retarder placed on the shear pockets shall be measured. The shear pocket surfaces shall be checked for the amount of exposed aggregate prior to placing the shear studs and grouting around them.

1.5 The researchers shall be provided copies of the stressing information recorded by the post-tensioning contractor when the strands are stressed.

2. Girders

2.1 Prior to placing the girders on the bents, strain gauges shall be applied to the inside of the girder flanges and the web. Initial strain data shall be gathered from the girders while they are stored on site.

2.2 After the girders are placed and prior to installing the panels, twangers shall be applied to the steel girders. Twangers shall be applied to the midpoint of each span on the bottom flange of the girders. A wire shall be run from the Twanger to a weight on the ground directly beneath the girder.

2.3 Data shall be recorded from the strain gauges and twangers during the installation of the deck panels.

3. Grouting

3.1 Grout cubes shall be made during the grouting processes. Flow measurements shall also be taken while grouting.

4. Surface Treatment

4.1 Prior to applying any surface treatment to the panels, the shear pockets shall be inspected for cracks.

5. Ponding Tests

5.1 Prior to applying the surface treatment and opening up the panels to traffic, a ponding test shall be run on the stage I and stage 2 lanes.

5.2 The ponding tests consists of placing a ½ in. strip of construction adhesive around the edge of the deck and applying approximately ¼ in. of water to the surface of the deck. The bottom of the panels shall be monitored for leaks for approximately 2 hours.

Post-Tensioning

1. Certifications

1.1 At least one person shall be certified on Bonded Post-tensioning Systems as defined by PTI

2. Post-tensioned Ducts

2.1 The post-tensioned system shall be shown on shop drawings by the contractor and approved. The drawings shall show details about the methods and materials that shall be used. The contractor shall determine the details and type of system to meet the requirements of the drawings.

2.2 A water and air tight seal must be made between the post-tensioned ducts in the panel joints. The coupler should smoothly connect the ducts with no kinks or bumps. Duct tape is not an acceptable material for coupling the duct.

2.3 The plastic materials used in the ducts should contain antioxidant stabilizers and have an environmental stress cracking of not less than 192 hours as determined by ASTM D 1693 “Standard Test Method for Environmental Stress-Cracking of Ethylene Plastics”, Condition C.

2.4 Ducts shall be supported at intervals not to exceed 24 in.

2.5 The ducts shall be free of any deleterious material that would impair bonding between the grout and the strands.

2.6 Vents shall be attached to the duct and shall be tight enough to prevent leakage of any grout. The minimum diameter of the vents shall be ½ in.

3. Grouting Plan

3.1 A grouting plan with the location of grout inlets shall be approved prior to grouting.

3.2 The mixer shall be capable of mixing grout free of lumps and evenly distributing the cement.

3.3 Under normal conditions, the grouting equipment should be capable of grouting one duct in no more than 20 minutes.

4. Post-tensioning Anchorages

4.1 The post-tensioned anchorage system shall be placed at the location shown on the plans.

4.2 The post-tensioning anchorage system shall meet the requirements in the AASHTO LRFD Bridge Construction Specifications, Sec 10.3.2.3, Special Anchorage Device Acceptance Test.

5. Strands

5.1 The strands used in the precast panels shall come from a certified PC Strand Manufacturing Plant as defined by the PTI Certification Committee. The strands shall meet the requirements of ASTM A416 for low relaxation strands.

5.2 Each lot of strands shall include a mill certification and test report.

5.3 For each lot of strands four - 4 ft sections shall be provided for testing.

5.4 During the time from manufacture to grouting, strands shall be protected against physical damage and deleterious materials such as water and grease.

5.5 The strands shall not need a direct application of a corrosion inhibitor unless the grout is not placed inside the duct within 15 days of stressing the strands.

6. Stressing

6.1 Stressing may not begin until the grout in the joints reaches a minimum compressive strength of 4000 psi.

6.2 Strands shall be tensioned with a hydraulic jack to the force shown on the drawings.

6.3 Elongation values shall be approved prior to stressing by the engineer. This shall include confirmation of the seating losses, friction loss, and elastic shortening losses.

6.4 The sequence of stressing shall be done as shown on the drawings unless prior approval is given by the engineer.

6.5 The jacking system shall provide a method of measuring tendon elongation and jacking stress. Elongation measurements shall be made to the nearest 1/8 in. The two measurements shall produce stress levels within 5% of one another.

References

AASHTO LRFD Bridge Construction Specifications, 1999 Interim Edition

AASHTO LRFD Bridge Design Specifications, 2001 Interim Edition

Corven, John and Alan Moreton, "Post-tensioning Tendon Installation and Grouting Manual, US Department of Transportation", Federal Highway Administration, May 26, 2004, http://www.fhwa.dot.gov/BRIDGE/pt/pttoc.cfm

PTI Certification Committee, Post-tensioning Institute, 5th Edition, 2007. http://www.post-tensioning.org/certification_program.php

Scholz, Don P., "Performance criteria recommendations for mortars used in full-depth precast concrete bridge deck panel systems", Thesis, Virginia Tech, 2004.

Utah Department of Transportation. "Draft – Full Depth Precast Concrete Deck Panel Specifications." March 31, 2008.

Appendix B - Documents for the Test Panels

B.1 Material Properties for the Panel Tests

Deck Panel Concrete

Reinforced Concrete and Post-Tensioned #1 Joints			
Days	Note	Strength (psi)	Modulus of Elasticity (ksi)
14		7313	
35		7613	
39	First Day of R/C Tests	8329	5138
164	Last Day of P/T Tests	8648	6449

Post-Tensioned #2 Joints			
Days	Note	Strength (psi)	Modulus of Elasticity (ksi)
28		7149	5579
102	First Day of Tests	7945	5703
124	Last Day of Tests	8197	6068

Reinforced Concrete Joints - Grout		
Days	Note	Strength (psi)
2		5138
7	Day of First Test	4642
28		4746

Post-Tension Joints #1 (167 psi)		
Joint Neat Grout		
Days	Note	Strength (psi)
7		3358
28	Day of First Test	3967
67	Last Day of Test	4579

Post-Tension Joints #1 (167 psi)		
Joint Extended Grout		
Days	Note	Strength (psi)
7		3583
28	Day of First Test	4704
67	Last Day of Test	5446

Post-Tension Joints #1 (167 psi)		
Tendon Grout		
Days	Note	Strength (psi)
2		3135
28	Day of First Test	4225
67	Last Day of Test	4675

Post-Tension Joints #1 (167 psi)		
Haunch Grout		
Days	Note	Strength (psi)
28	Day of First Test	6554
67	Last Day of Test	7667

Post-Tension Joints #2 (340 psi)		
Joint Grout		
Days	Note	Strength (psi)
2		4025
10	Post-Tensioning	4754
69	Day of First Test	5363

Post-Tension Joints #2 (340 psi)		
Tendon Grout		
Days	Note	Strength (psi)
2		3946
60	Day of First Test	5171
82	Last Day of Test	6508

Post-Tension Joints #2 (340 psi)		
Haunch Grout		
Days	Note	Strength (psi)
2		3833
52	Day of First Test	4796
74	Last Day of Test	6000

B.2 Measured Stresses in the Deck Panels

Post-Tensioned Transverse Joint Test #1 (0.167 Ksi Effective Stress)

	Live End Force	Measured Seating Losses	Measured Elastic Shortening	Final Force	Strand Stress (ksi)	% f_{pu}
Strand 1	32	6	0.65	25.35	152	56.2
Strand 2	31	2.3	0.7	28.05	168	62.2
Strand 3	31.8	2.1	0.1	29.65	178	65.8
Strand 4	30.7	1.8	0.05	28.86	173	64.0
Slab				**111.91**	**0.167**	**62.1**

Post-Tensioned Transverse Joint Test #2 (0.340 Ksi Effective Stress)

	Live End Force	Measured Seating Losses	Measured Elastic Shortening	Final Force	Strand Stress (ksi)	% f_{pu}
Strand 1	31.3	2.7	1.3	27.4	164	60.7
Strand 2	32.1	2.9	2.1	27.1	162	60.1
Strand 3	32.2	4.7	0.6	26.9	161	59.8
Strand 4	32.1	0.7	0.1	31.3	187	69.3
Strand 5	32.0	2.9	0.1	29.0	174	64.3
Strand 6	32.3	3.4	0.0	28.9	173	64.1
Strand 7	32.9	3.0	0.0	29.8	179	66.2
Strand 8	31.9	3.7	0.0	28.2	169	62.5
Slab				**228.6**	**0.340**	

B.3 Load Computations for the Transverse Joint Tests

Stress levels for the Transverse Joint Tests
DESIGN VALUES

Virginia Bridge

6 - W21x83 Steel Girders

1 Girder Line on the Virginia Bridge

$S_v := 57.6$	inches	Girder Spacing
$t_v := 7.5$	inches	Slab Thickness
$h_v := 1.5$	inches	Haunch Thickness
$d_v := 21.4$	inches	Girder Height
$NA_v := 8.05$	inches	Neutral Axis from the Top of the Slab
$I_{vna} := 6652.5$	in^2	Moment of Inertia about the neutral axis
$Fyv := 50$	ksi	Yield strength of the steel girder

Test Bridge

2 - W21x101 Steel Girders

1 Girder Line on the Test Bridge

$S_t := 42$	inches	Girder Spacing
$t_t := 7.5$	inches	Slab Thickness
$h_t := 1.5$	inches	Haunch Thickness
$d_t := 21.375$	inches	Girder Height
$NA_t := 10.20$	inches	Neutral Axis from the Top of the Slab
$I_{tna} := 7152.24$	in^2	Moment of Inertia about the neutral axis
$F_{yt} := 50$	ksi	Yield strength of the steel girder

Loading on the Virginia Bridge System

$M_{maxext} := 266.07$	k – ft	Maximum moment on the Virginia Bridge (Exterior Girder)
$M_{maxint} := 258.1$	k – ft	Maximum moment on the Virginia Bridge (Interior Girder)
$M_{max} := \max(M_{maxext} M_{maxint})$		
$M_{max} = 266.07$	k – ft	Design Moment for the Test Setup

Equivalent Stress Calculation on the 2 Girder Test Setup

$$\sigma_v := \frac{M_{max} \cdot NA_v \cdot 12}{I_{vna}}$$

Maximum tensile stress in the deck over an interior bent.
All numbers are based on 1 Girder Line.

$\sigma_v = 3.864$ ksi

$$M_t := \frac{\sigma_v \cdot I_{tna}}{NA_t \cdot 12}$$

$M_t = 225.761$ k – ft

Moment needed in the test setup for an equivalent maximum tensile stress in the deck.
All numbers are based on 1 Girder Line.

$M_{t_2} := M_t \cdot 2$ k – ft

Moment applied to the system with 2 Girder lines (the as built condition.)

$M_t = 451.522$ k – ft

Load Applied to the Test Setup

$Cant := 5.5$ ft

Cantilever length in the test bridge.

$L_{cant} := 75.5$ ft

Length of the cantilever from the CL of the joint to the load application or tie down point.

$M_{dl} := 34.8$ k – ft

Dead Load Moment - From self weight
In a typical situation the DL moment would not apply but in this setup, due to the construction sequence of removing the cantilever support after constrution, the DL moment was included.

$M_{ll} := Cant \cdot L_{cant}$

Live Load Moment - Applied with the actuator.

$M_{ll} = 415.25$ k – ft

$M_{total} := M_{ll} + M_{dl}$

Total load applied to the transverse joint

$M_{total} = 450.05$ k – ft

Stress levels for the Transverse Joint Tests
ACTUAL TEST VALUES (AS BUILT)

Virginia Bridge

6 - W21x83 Steel Girders

1 Girder Line on the Virginia Bridge

$S_v := 57.6$	inches	Girder Spacing
$t_v := 7.5$	inches	Slab Thickness
$h_v := 1.5$	inches	Haunch Thickness
$d_v := 21.4$	inches	Girder Height
$NA_v := 8.06$	inches	Neutral Axis from the Top of the Slab
$I_{vna} := 6652.49$	in^2	Moment of Inertia about the neutral axis
$Fyv := 50$	ksi	Yield strength of the steel girder

Test Bridge

2 - W21x101 Steel Girders

1 Girder Line on the Test Bridge

$S_t := 42$	inches	Girder Spacing
$t_t := 7.5$	inches	Slab Thickness
$h_t := 1.5$	inches	Haunch Thickness
$d_t := 21.375$	inches	Girder Height
$NA_t := 9.68$	inches	Neutral Axis from the Top of the Slab
$I_{tna} := 7775$	in^2	Moment of Inertia about the neutral axis
$F_{yt} := 50$	ksi	Yield strength of the steel girder

Loading on the Virginia Bridge System

$M_{maxext} := 266.07$	k – ft	Maximum moment on the Virginia Bridge (Exterior Girder)
$M_{maxint} := 258.1$	k – ft	Maximum moment on the Virginia Bridge (Interior Girder)
$M_{max} := \max(M_{maxext}, M_{maxint})$		
$M_{max} = 266.07$	k – ft	Design Moment for the Test Setup

Equivalent Stress Calculation on the 2 Girder Test Setup

$$\sigma_v := \frac{M_{max} \cdot NA_v \cdot 12}{I_{vna}}$$

Maximum tensile stress in the deck over an interior bent.
All numbers are based on 1 Girder Line.

$\sigma_v = 3.868$ ksi

$$M_t := \frac{\sigma_v \cdot I_{tna}}{NA_t \cdot 12}$$

$M_t = 258.924$ k – ft

Moment needed in the test setup for an equivalent maximum tensile stress in the deck.
All numbers are based on 1 Girder Line.

$M_t := M_t \cdot 2$ k – ft

Moment applied to the system with 2 Girder lines (the as built condition.)

$M_t = 517.847$ k – ft

Load Applied to the Test Setup

$Cant := 5.5$ ft

Cantilever length in the test bridge.

$L_{cant} := 75.5$ ft

Length of the cantilever from the CL of the joint to the load application or tie down point.

$M_{dl} := 34.8$ k – ft

Dead Load Moment - From self weight
In a typical situation the DL moment would not apply but in this setup, due to the construction sequence of removing the cantilever support after constrution, the DL moment was included.

$M_{ll} := Cant \cdot L_{cant}$

Live Load Moment - Applied with the actuator.

$M_{ll} = 415.25$ k – ft

$M_{total} := M_{ll} + M_{dl}$

Total load applied to the transverse joint

$M_{total} = 450.05$ k – ft

B.4 Construction Drawings for the Test Panels

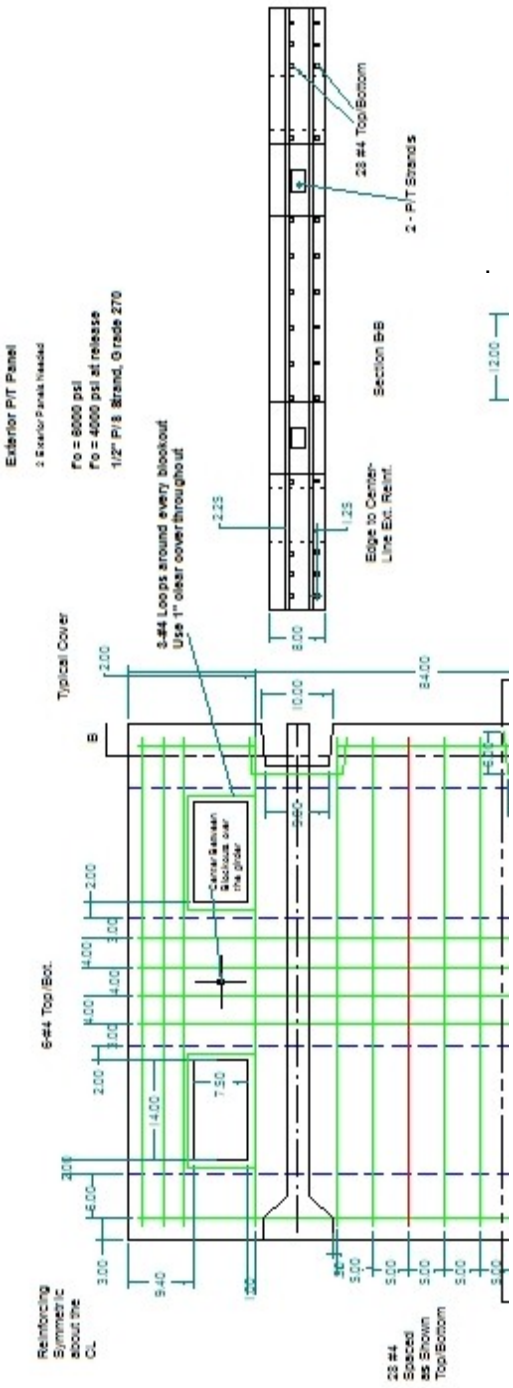

Exterior Post-tensioning Panel

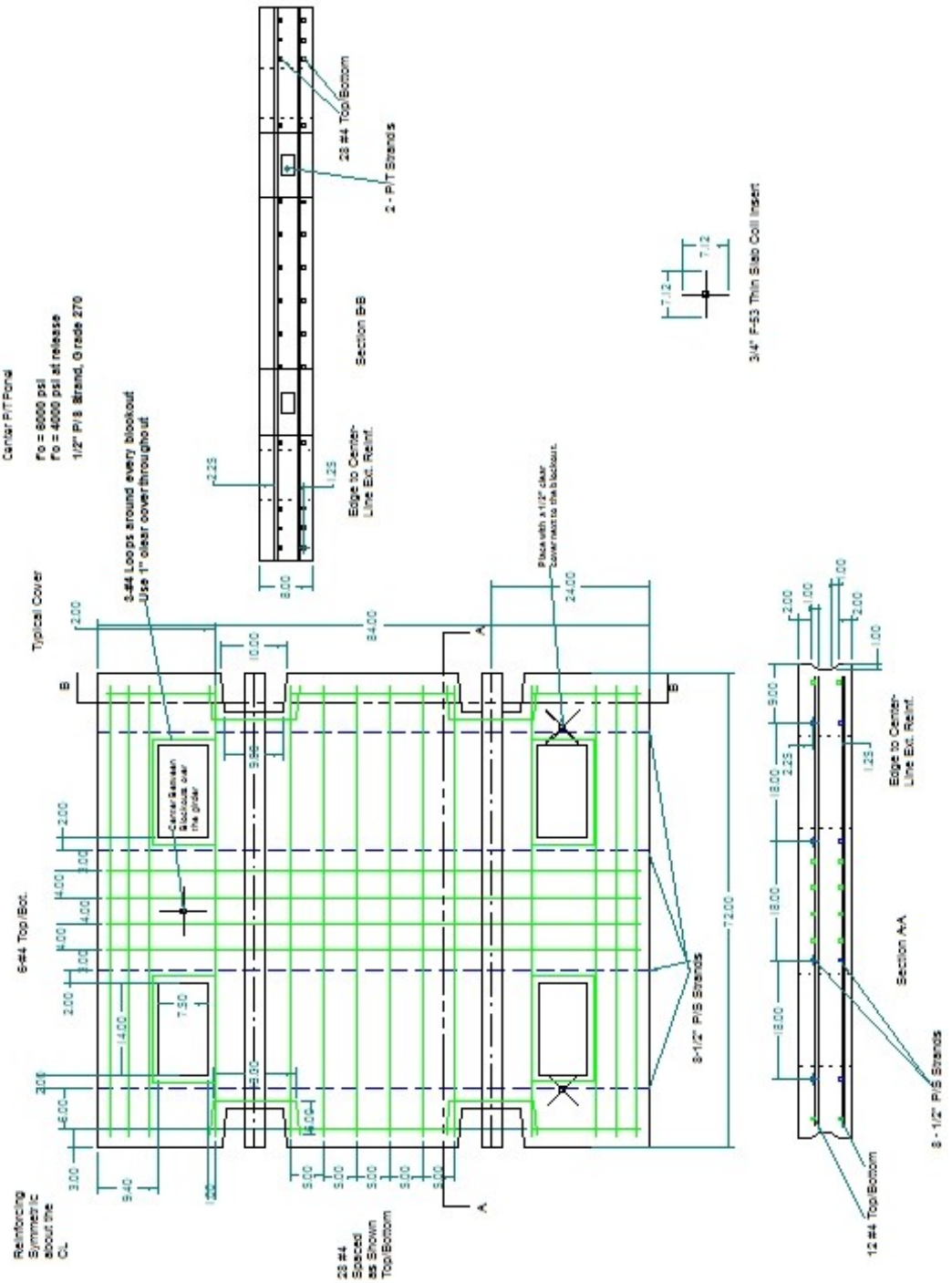

Interior Post-tensioning Panel

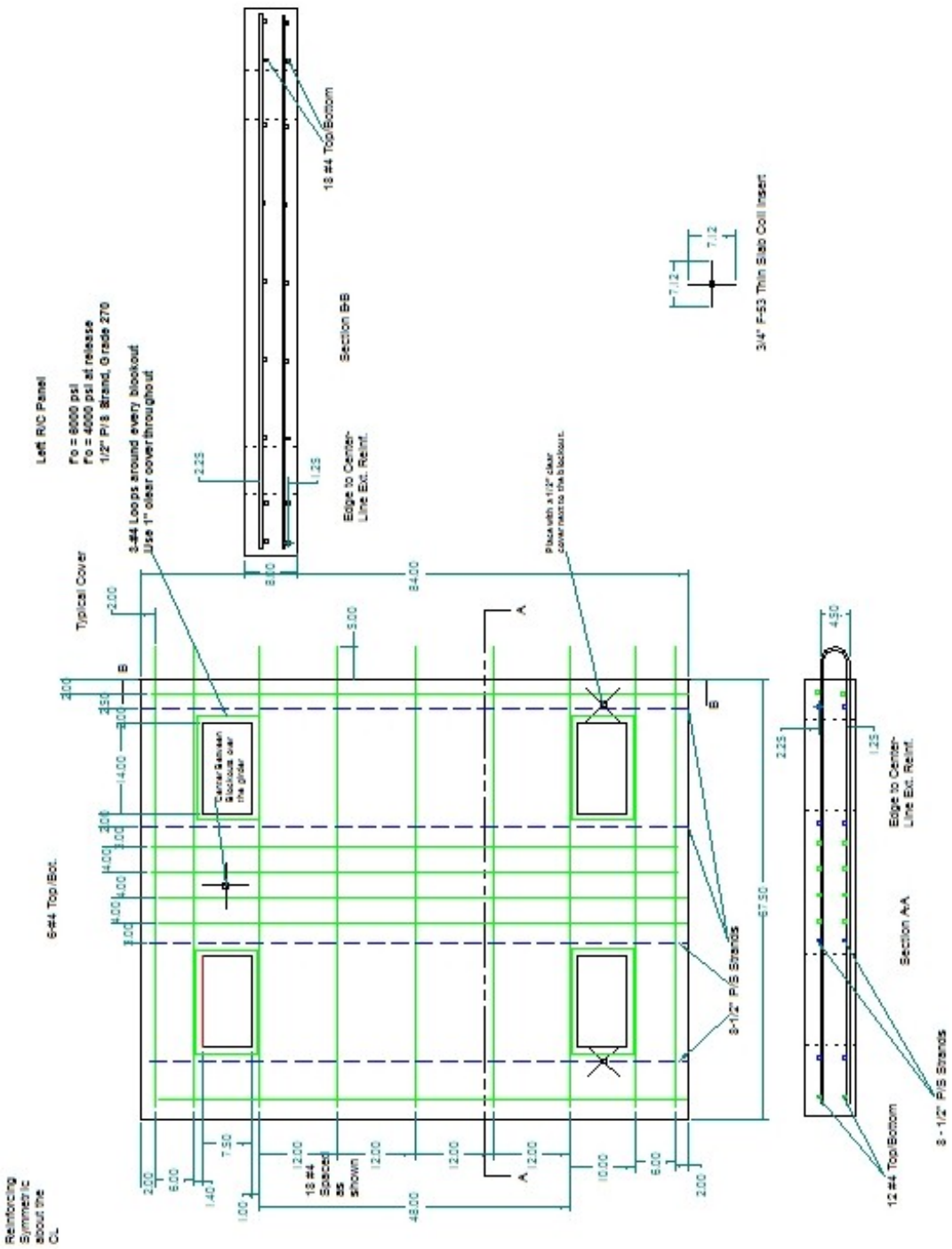

Looped Reinforcing Exterior Panel

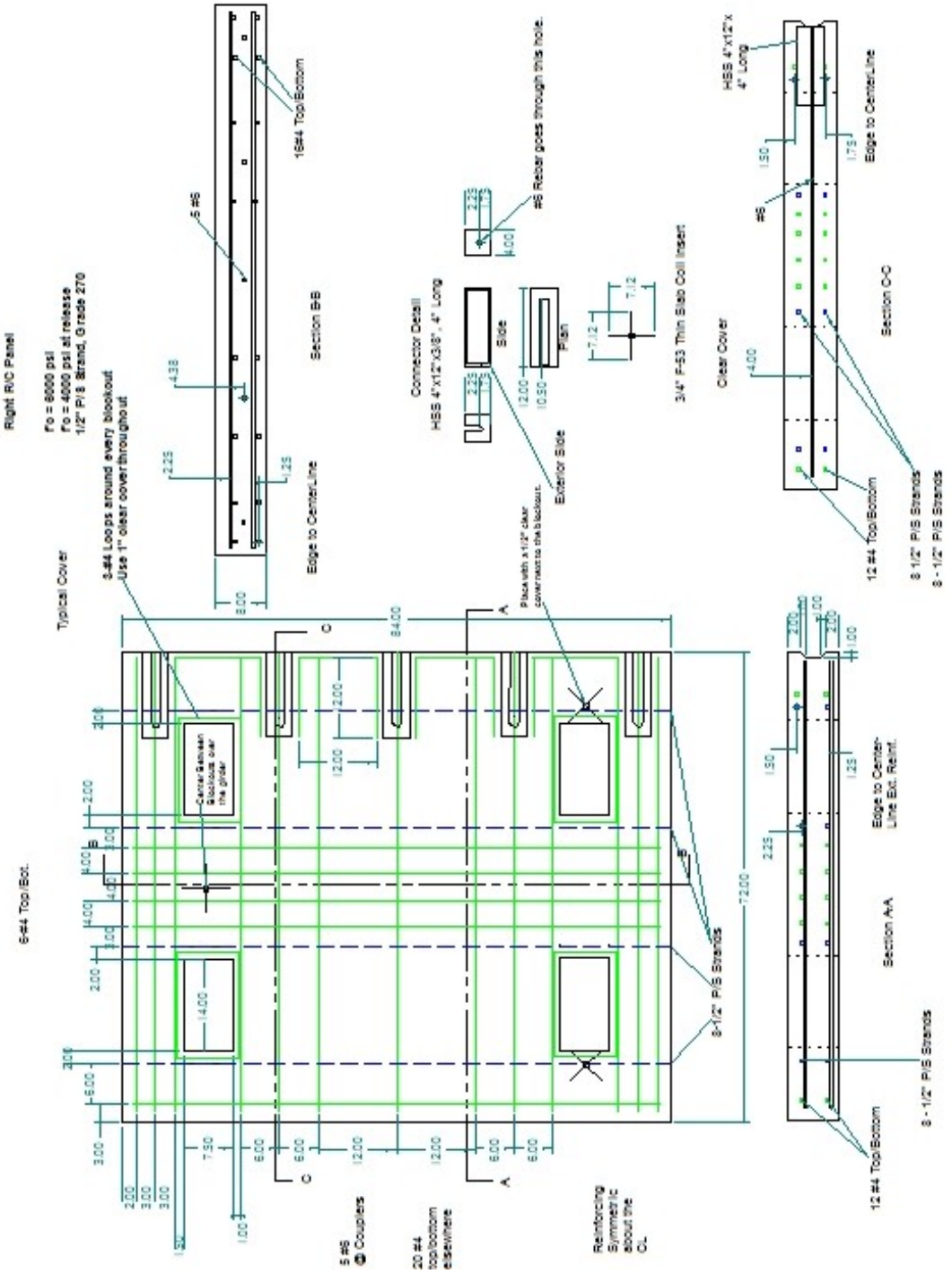

Embedded Reinforcing Exterior Panel

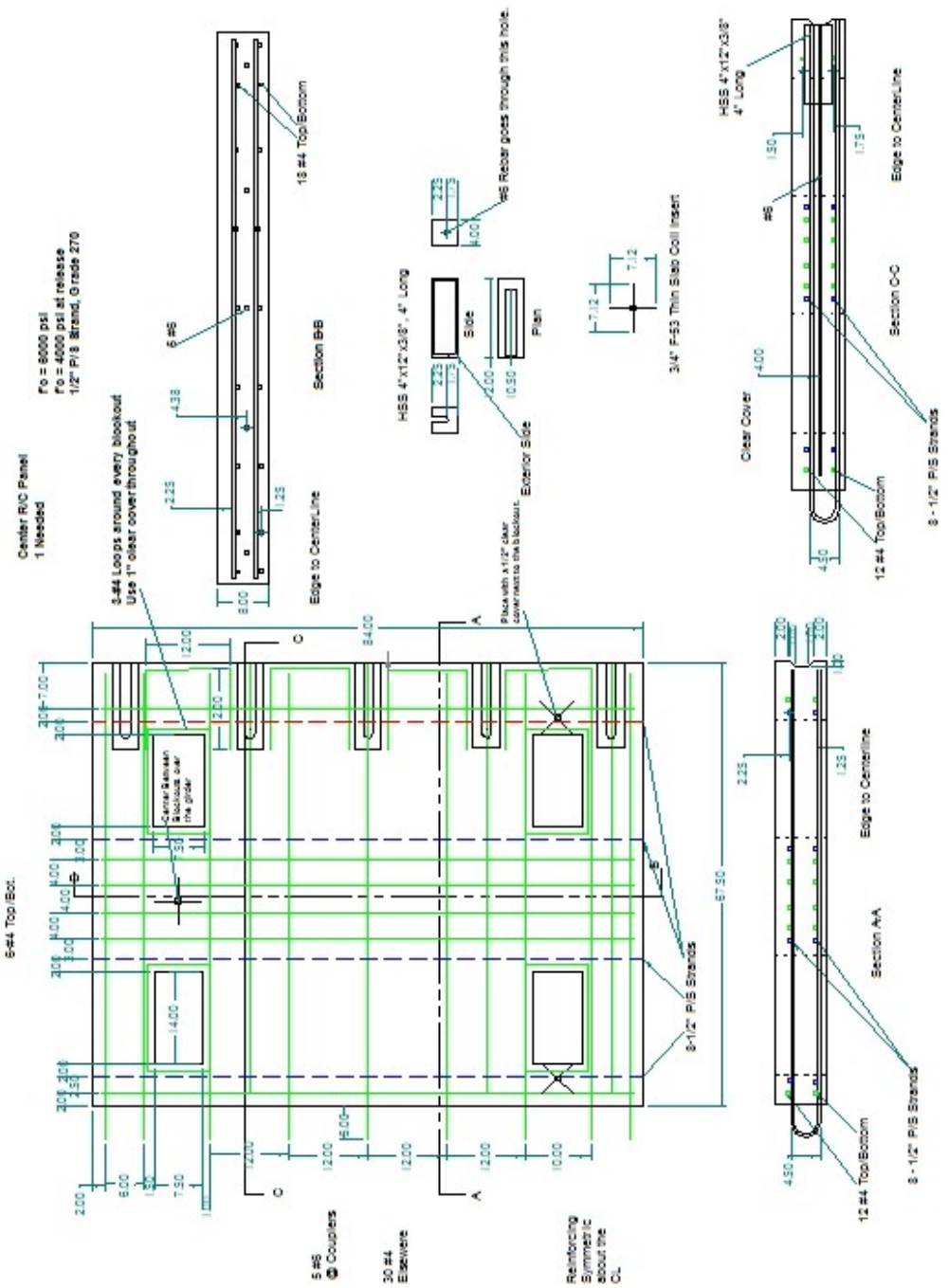

Looped and Embedded Reinforcing Interior Panel

Additional items requested:

1) Strength of the concrete at release.
2) 30 concrete cylinders
3) 8 - 30’ additional pieces of ½”strand (Total Length = 120’)
4) 5 – 5’ additional pieces of ½” strand (Total Length = 25’)

Notes

1) Use 3 - F-53 Thin Slab Coil Inserts (Dayton-Superior), ¾” diameter, 3” high per panel
2) Place 3 - #4 rebar loops around every blockout.
3) Fy = 60 ksi for all reinforcing bars.
4) F’c = 6 ksi for all concrete
5) Use Grade 270 Prestressing strands.
6) Stress the strands to 75% of ultimate.
7) All units are in inches on these details.
8) Use Williams 6” neoprene dumbbell water stops or equivalent.

Typical Blockout Reinforcing Detail

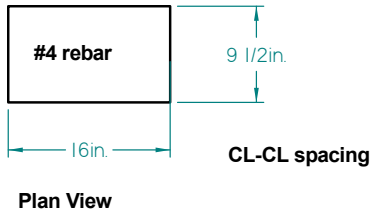

Plan View

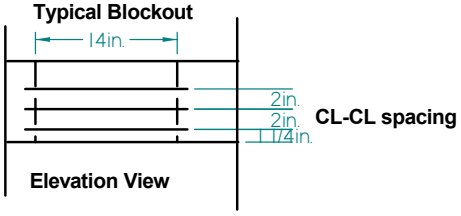

Lifting Hooks

#6 Minimum size rebar

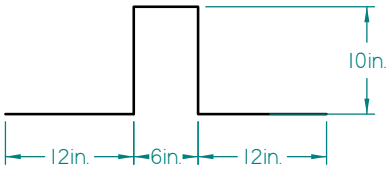

Bridge Deck Panels			
Bill of Materials			
Material Type	**Dimensions**	**Length**	**# Required**
F-53 Thin Slab coil Inserts	From Supplier	From Supplier	9
P/S Strands	1/2" Diameter	84"	24 Strands
P/T Duct (4 Strand)	From VSL	7'	6
P/T Duct Ends (4 Strand)	From VSL	From VSL	4
Lateral Reinforcing	#4 Rebar	80"	36
Lateral Reinf.	#4 Rebar	25"	8
Lateral Reinf.	#4 Rebar	17"	16
Longitudinal Reinf.	#4 Rebar	70"	84
Blockout Reinf.	#4 Rebar	16" x 9.5" Loop	36
P/T Blockout Reinf	#4 Rebar	6" x 13" x 6" Angles	16
P/T Anchor Zone Reinf.	#4 Rebar	5" x 12" Loop	16
Water Stops	6" Neoprene	88"	
Water Stop Corners	6" Neoprene	From Supplier	8
Retarder		5 ft^2 Surface Area	

Notes for the Precast Panels

B.5 Cost Estimate of the Test Panels

Cost Estimate

Precast Panels

The costs are based on the testing procedures used in the laboratory at Virginia Tech.
These Procedures are all based on three 19' long, 2 girder lab tests.
The numbers were compared to a similar lab test and adjusted as needed

Precast Costs	Quantities	Area	Price	$/panel	$/ft²	Notes
Panels	3	126. ft2	9200.00	3066.67	73.02	*The price is high for a number of reasons: Every panel was different, an entire stressing bed was used for only 3 test panels, a full crew was used for these small test panels and a full size truck was used to transport a partial load. The price should go down with the full bridge. The price did not include any profit for the precaster.*

Lab Materials	Quantities		Quantity/ft²
Grout (5 Star Hwy Patch)	40	50 lb Bags Total	0.32
Joints	12		
Ducts	4		
Haunches	24		
Strands (Oversized)	8	1/2" x 32' Grade 270	0.06
Formwork	1	1/2" x 8' x 4' Sheet of Plywood	0.01
	3	2" x 2" x 8' sawn lumber	0.02
	72	1/4" washer/nut sets	0.57
	36	1/4" threaded rod	0.29
B-14 Coil Leveling Bolts	9	3/4" x 14"	0.07
Haunch Material	72	1/2" x 3 1/2" fiber formwork	0.57
Shear Studs	96	7/8" x 5 1/2"	0.76
Ferrules	96	7/8"	0.76

Procedures

Process	Manpower	Time	Installation Rate		Notes
	(People)	*(Hours)*	*Units Installed/Hour*		*(A breakdown of what each person did)*
Installing Haunch Fiberboard	1	3	12.67	ft/hour	1 Person cutting, gluing, and clamping the boards to the top flange
Making Joint Formwork	2	4	3.50	ft/hour	2 People measuring and cutting the plywood and threaded rod
Placing Panels	3	3	1.00	Panel/Hour	1 Crane, 1 Guiding, 1 Monitoring haunches/Adjusting leveling bolts
Placing Joint Formwork	3	2	7.00	ft/hour	1 Holding, 2 Lining up the bolts, Tightening the nuts, Oiling forms
Making Haunch Formwork	1	3	1.33	Form/Hour	1 Cutting plywood, Making wooden wedges, Tying wire to formwork
Installing Haunch Formwork	1	1	0.25	Form/Hour	1 Placing formwork and wedges, Oiling
Joint Grout	6	1	14.00	ft/hour	1 Mixing, 1 Making Cubes, 1 Moving Grout, 1 Pouring, 1 Guiding, 1 Vibrating
Formwork Removal	1	1	---		1 Removing haunch and joint formwork
Installing Tendons	2	1	152.00	ft/hour	1 Threading through end plates, 1 Guiding through joints
Stressing Tendons	3	6	1.33	Tendons/hour	1 Stressing, 1 Measuring values, 1 Overseeing
Grouting Ducts	5	1	38.00	ft/hour	1 Mixing, 1 Making Cubes, 1 Moving Grout, 1 Pumping, 1 Monitoring
Shear Studs	2	3	32.00	studs/hour	1 Welding, 1 Marking the girder and laying out materials
Cleaning Haunches	2	1	38.00	ft/hour	1 Breaking ferrules, 1 Vacuuming the particles in the haunches
Grouting Haunches	7	2	19.00	ft/hour	1 Mixing, 1 Making Cubes, 2 Moving Grout, 1 Pouring, 1 Guiding, 1 Vibrating
Removing Leveling Bolts	1	1	9.00	bolts/hour	1 Person with an air wrench

Dimensions		
Bridge Length	19	feet
Girders	2	W 21x101
Joints	2	Lateral PT
Length	7	feet
Tendon Ducts	2	

B.6 Stresses in the Top of the Transverse Joints

Stress Levels in the Bridge Deck at First Crack

During testing the decks cracked at different stress levels. The stress level of the first crack is computed here.

$Lc := 5.5$	ft	Length of the cantilever.
$P := 75.5$	kips	Load applied in the test to each cantilever

Transverse Joint Test #1 - Cast-in-Place Joints

$fy := 50$	ksi	Girder Yield Stress
$f_c := 8330$	psi	Concrete Strength on First Day of Testing
$f_g := 4642$	psi	Plain grout strength - first day of testing
$f_{pg} := 0$	psi	Pea gravel grout strength - first day of testing
$E_s := 29000$	ksi	Elastic Mod of Steel
$E_c := 57\cdot\sqrt{f_c\cdot 1000}$	ksi	Elastic Mod of Concrete
$E_c = 1.645\times 10^5$	ksi	
$n := \frac{E_s}{E_c}$		Ratio of Elasticities
$n = 0.176$		
$A_d := 84\cdot 8$	in^2	Area of the Deck Concrete
$A_d = 672$		
$I_{nac} := 86681$	in^4	Moment of Inertia with respect to the actual concrete strength.
$C1 := 9.68$	in	Distance from the N.A. to the top of the slab
$P_{app} := 0$	ksi	Force applied to the deck
$f_{ts} := \frac{P\cdot Lc\cdot 12}{\frac{I_{nac}}{C1}} - \frac{P_{app}}{A_d}$	ksi	Stress level in the top of the slab under service load (+ is tension, - is compression)
$f_{ts} = 0.556$	ksi	

$M_{rconc} := 6\cdot\frac{\sqrt{f_c}}{1000}$ $\quad$ $M_{rgrout} := 6\cdot\frac{\sqrt{f_g}}{1000}$ $\quad$ $M_{rpg} := 6\cdot\frac{\sqrt{f_{pg}}}{1000}$

$M_{rconc} = 0.548$ ksi $\quad$ $M_{rgrout} = 0.409$ ksi $\quad$ $M_{rpg} = 0$ ksi

Cracking should occur when the tensile strength is greater than the modulus of rupture.

Stress at First Crack

$P1 := 40$ kips — Load applied at first crack for the looped reinforcing bar joint

$P2 := 60$ kips — Load applied at first crack for the Embedded bar joint

$$f_{ts1} := \frac{P1 \cdot Lc \cdot 12}{\frac{I_{nac}}{C1}} - \frac{P_{app}}{A_d} \quad \text{ksi}$$

Stress level in the top of the slab at cracking
Looped Reinforcing Bars
(+ is tension, - is compression)

$f_{ts1} = 0.295$ ksi

$$f_{ts2} := \frac{P2 \cdot Lc \cdot 12}{\frac{I_{nac}}{C1}} - \frac{P_{app}}{A_d} \quad \text{ksi}$$

Stress level in the top of the slab at cracking
Embedded Reinforcing Bars
(+ is tension, - is compression)

$f_{ts2} = 0.442$ ksi

Transverse Joint Test #2 - Post-Tensioning Joints

$f_y := 50$	ksi	Girder Yield Stress
$f_c := 8330$	psi	Concrete Strength on First Day of Testing
$f_g := 3967$	psi	Plain grout strength - first day of testing
$f_{pg} := 4704$	psi	Pea gravel grout strength - first day of testing
$E_s := 29000$	ksi	Elastic Mod of Steel
$E_c := 57 \cdot \sqrt{f_c \cdot 1000}$	ksi	Elastic Mod of Concrete
$E_c = 1.645 \times 10^5$	ksi	
$n := \frac{E_s}{E_c}$		Ratio of Elasticities
$n = 0.176$		
$A_d := 84 \cdot 8$	in^2	Area of the Deck Concrete
$A_d = 672$		
$I_{nac} := 86681$	in^4	Moment of Inertia with respect to the actual concrete strength.
$C1 := 9.68$	in	Distance from the N.A. to the top of the slab
$P_{app} := 111.9$	kips	Force applied to the deck
$f_{ts} := \frac{P \cdot Lc \cdot 12}{\frac{I_{nac}}{C1}} - \frac{P_{app}}{A_d}$	ksi	Stress level in the top of the slab under service load (+ is tension, - is compression)
$f_{ts} = 0.39$	ksi	

$M_{rconc} := 6 \cdot \frac{\sqrt{f_c}}{1000}$ $\quad M_{rgrout} := 6 \cdot \frac{\sqrt{f_g}}{1000}$ $\quad M_{rpg} := 6 \cdot \frac{\sqrt{f_{pg}}}{1000}$

$M_{rconc} = 0.548$ ksi $\quad M_{rgrout} = 0.378$ ksi $\quad M_{rpg} = 0.412$ ksi

Cracking should occur when the tensile strength is greater than the modulus of rupture.

Stress at First Crack

$P1 := 40$ kips — Load applied at first crack for the Neat Grout 167 psi joint

$P2 := 60$ kips — Load applied at first crack for the Pea Gravel 167 psi joint

$$f_{ts1} := \frac{P1 \cdot Lc \cdot 12}{\frac{I_{nac}}{C1}} - \frac{P_{app}}{A_d} \quad \text{ksi}$$

Stress level in the top of the slab at cracking Plain 167 psi joint
(+ is tension, - is compression)

$f_{ts1} = 0.128$ ksi

$$f_{ts2} := \frac{P2 \cdot Lc \cdot 12}{\frac{I_{nac}}{C1}} - \frac{P_{app}}{A_d} \quad \text{ksi}$$

Stress level in the top of the slab at cracking Pea Gravel 167 psi joint
(+ is tension, - is compression)

$f_{ts2} = 0.276$ ksi

Transverse Joint Test #3 - Post-Tensioning Joints

$f_y := 50$	ksi	Girder Yield Stress
$f_c := 7945$	psi	Concrete Strength on First Day of Testing
$f_g := 4754$	psi	Plain grout strength - first day of testing
$f_{pg} := 0$	psi	Pea gravel grout strength - first day of testing
$E_s := 29000$	ksi	Elastic Mod of Steel
$E_c := 57 \cdot \sqrt{f_c \cdot 1000}$	ksi	Elastic Mod of Concrete
$E_c = 1.607 \times 10^5$	ksi	
$n := \frac{E_s}{E_c}$		Ratio of Elasticities
$n = 0.18$		
$A_d := 84 \cdot 8$	in^2	Area of the Deck Concrete
$A_d = 672$		
$I_{nac} := 88232$	in^4	Moment of Inertia with respect to the actual concrete strength.
$C1 := 9.76$	in	Distance from the N.A. to the top of the slab
$P_{app} := 228.6$	kips	Force applied to the deck
$f_{ts} := \frac{P \cdot Lc \cdot 12}{\frac{I_{nac}}{C1}} - \frac{P_{app}}{A_d}$	ksi	Stress level in the top of the slab under service load (+ is tension, - is compression)
$f_{ts} = 0.211$	ksi	

$M_{rconc} := 6 \cdot \frac{\sqrt{f_c}}{1000}$ $\quad M_{rgrout} := 6 \cdot \frac{\sqrt{f_g}}{1000}$ $\quad M_{rpg} := 6 \cdot \frac{\sqrt{f_{pg}}}{1000}$

$M_{rconc} = 0.535$ ksi $\quad M_{rgrout} = 0.414$ ksi $\quad M_{rpg} = 0$ ksi

Cracking should occur when the tensile strength is greater than the modulus of rupture.

Stress at First Crack

$P1 := 70$ kips — Load applied at first crack for the Neat Grout 340 psi joint

$P2 := 70$ kips — Load applied at first crack for the Epoxied 340 psi joint

$$f_{ts1} := \frac{P1 \cdot Lc \cdot 12}{\frac{I_{nac}}{C1}} - \frac{P_{app}}{A_d} \quad \text{ksi}$$

Stress level in the top of the slab at cracking
Plain 340 psi joint
(+ is tension, - is compression)

$f_{ts1} = 0.171$ ksi

$$f_{ts2} := \frac{P2 \cdot Lc \cdot 12}{\frac{I_{nac}}{C1}} - \frac{P_{app}}{A_d} \quad \text{ksi}$$

Stress level in the top of the slab at cracking
Epoxied 340 psi joint
(+ is tension, - is compression)

$f_{ts2} = 0.171$ ksi

B.7 Strain Levels in the Deck Panels

Steel and Rebar Only - NA in the Web of the Girder
Simulates a completely cracked deck slab.
Embedded Reinforcing Bars

$As := 1.1$ in^2

$E_s := 29000$ ksi

$b_f := 12.3$ in

$d := 21.4$ in

$H := 1.5$ in

$DK := 8$ in

$t_w := 0.5$ in

$t_f := 0.8$ in

$I := 2642.52$ in^4 Cracked Section - Rebar Included

$M := 207.5$ $k - ft$ Service Load Applied

$c := 11.27$ in Guess this value and iterate until Forces are equal.

$$\varepsilon_s := -\frac{\frac{M \cdot 12 \cdot c}{I}}{E_s}$$ Strain in the Steel and Top of the Concrete Slab

$$\varepsilon_c := \frac{-\varepsilon_s \cdot (d + H + DK - c)}{c}$$

$$SL := \left(\frac{-\varepsilon_s + \varepsilon_c}{d + H + DK} \right)$$ $SL = 0.00003249$ Slope of Strain Distribution

$$C := \left[b_f \cdot E_s \cdot \int_0^{t_f} \left(\varepsilon_s + SL \cdot y \right) dy \right] + t_w \cdot E_s \cdot \int_{t_f}^{c} \left(\varepsilon_s + SL \cdot y \right) dy$$ Compressive and Tensile Forces

$$T := \left[t_w \cdot E_s \cdot \int_c^{(d - t_f)} \left(\varepsilon_s + SL \cdot y \right) dy \right] + \left[b_f \cdot E_s \cdot \int_{(d - t_f)}^{d} \left(\varepsilon_s + SL \cdot y \right) dy \right] + As \cdot E_s \cdot \left[\varepsilon_s + SL \cdot \left(d + H + \frac{DK}{2} \right) \right]$$

$T = 127$ kips Equilibrium should be reached

$C = -127$ kips

$\varepsilon_s = -0.000366$ Final Strains in the Concrete and Steel

$\varepsilon_c = 0.000638$

$\varepsilon_{BSG} := \varepsilon_s + SL \cdot t_f$ $\varepsilon_{BSG} = -0.00034$ Strains at the level of the VWGs, the steel, and the Strain Gauge on the bottom flange. VWG locations measured in the precast plant.

$\varepsilon_{VWG} := \varepsilon_c - SL \cdot 2.25$ $\varepsilon_{VWG} = 0.000565$

$\varepsilon_{steel} := \varepsilon_c - SL \cdot 4$ $\varepsilon_{steel} = 0.000508$

Steel and Rebar Only - NA in the Web of the Girder
Simulates a completely cracked deck slab.
Looped Reinforcing Bars

$As1 := .8835 \quad in^2$

$As2 := .8835 \quad in^2$

$E_s := 29000 \quad ksi$

$b_f := 12.3 \quad in$

$d := 21.4 \quad in$

$H := 1.5 \quad in$

$DK := 8 \quad in$

$t_w := 0.5 \quad in$

$t_f := 0.8 \quad in$

$I := 2800 \quad in^4$ Cracked Section - Rebar Included

$M := 207.5 \quad k - ft$ Service Load Applied

$c := 11.58 \quad in$ Guess this value and iterate until Forces are equal.

$\varepsilon_s := -\frac{M \cdot 12 \cdot c}{I \cdot E_s}$ Strain in the Steel and Top of the Concrete Slab

$\varepsilon_c := \frac{-\varepsilon_s \cdot (d + H + DK - c)}{c}$

$SL := \left(\frac{-\varepsilon_s + \varepsilon_c}{d + H + DK}\right)$ $SL = 0.00003067$ Slope of Strain Distribution

$C := \left[b_f \cdot E_s \cdot \int_0^{t_f} (\varepsilon_s + SL \cdot y)\, dy\right] + t_w \cdot E_s \cdot \int_{t_f}^{c} (\varepsilon_s + SL \cdot y)\, dy$ Compressive and Tensile Forces

$T := \left[t_w \cdot E_s \cdot \int_c^{(d - t_f)} (\varepsilon_s + SL \cdot y)\, dy\right] + \left[b_f \cdot E_s \cdot \int_{(d - t_f)}^{d} (\varepsilon_s + SL \cdot y)\, dy\right] + \left[As1 \cdot E_s \cdot \left[\varepsilon_s + SL \cdot (d + H + DK \cdot .15625)\right]\right] + As2 \cdot E_s \cdot \left[\varepsilon_s + SL \cdot (d + H + DK \cdot .71875)\right]$

$T = 124 \quad kips$ Equilibrium should be reached

$C = -124 \quad kips$

$\varepsilon_s = -0.000355$ Final Strains in the Concrete and Steel

$\varepsilon_c = 0.000592$

$\varepsilon_{BSG} := \varepsilon_s + SL \cdot t_f \quad \varepsilon_{BSG} = -0.000331$

$\varepsilon_{VWG} := \varepsilon_c - SL \cdot 2.25 \quad \varepsilon_{VWG} = 0.000523$

Strains at the level of the VWGs/the top steel, and the Strain Gauge on the bottom flange. VWG locations measured in the precast plant. The VWG location was the same as the top steel.

Complete Composite Behavior - NA in Haunch
Simulating the Post-Tensioned Slabs and the Uncracked Cast-in-Place Joints

$As := .33$ in^2 $B := 42$ in

$E_s := 29000$ ksi $f_c := 7945$ psi

$b_f := 12.3$ in $E_c := 57\sqrt{f_c}$

$d := 21.375$ in $E_c = 5081$ ksi

$H := 1.5$ in $E_{pt} := 29500$ ksi

$DK := 8$ in

$t_w := 0.5$ in

$t_f := 0.75$ in

$I := 7728.91$ in^4

$M := 207.625$ $k - ft$

$c := 21.65$ in Guess this value and iterate until Forces are equal.

$$\varepsilon_s := -\frac{\frac{M \cdot 12 \cdot c}{I}}{E_s}$$

$$\varepsilon_c := \frac{-\varepsilon_s \cdot (d + H + DK - c)}{c}$$

$$SL := \left(\frac{-\varepsilon_s + \varepsilon_c}{d + H + DK}\right) \qquad SL = 0.00001112$$

Sum forces in the bottom flange, web, top flange, and part of the haunch.

$$C := \left[b_f E_s \cdot \int_0^{t_f} \left(\varepsilon_s + SL \cdot y\right) dy\right] + \left[t_w \cdot E_s \cdot \int_{t_f}^{d - t_f} \left(\varepsilon_s + SL \cdot y\right) dy\right] + \left[b_f E_s \cdot \int_{d - t_f}^{d} \left(\varepsilon_s + SL \cdot y\right) dy\right] + b_f E_c \cdot \int_d^c \left(\varepsilon_s + SL \cdot y\right) dy$$

$C = -100$ $kips$

Sum forces in part of the haunch, rebar, and deck.

$$T := \left[b_f E_c \cdot \int_c^{d+H} \left(\varepsilon_s + SL \cdot y\right) dy\right] + \left[As \cdot E_{pt} \cdot \left[\varepsilon_s + SL \cdot \left(d + H + \frac{DK}{2}\right)\right]\right] + \left[B \cdot E_c \cdot \int_{d+H}^{d+H+DK} \left(\varepsilon_s + SL \cdot y\right) dy\right]$$

$T = 100$ $kips$

$C = -100$ $kips$

$\varepsilon_s = -0.000241$

$\varepsilon_c = 0.000103$

$\varepsilon_{BSG} := \varepsilon_s + SL \cdot t_f$ $\varepsilon_{BSG} = -0.000232$

$\varepsilon_{VWG} := \varepsilon_c - SL \cdot 2$ $\varepsilon_{VWG} = 0.00008$

Strains at the level of the VWGs and the Strain Gauge on the bottom flange.
VWG locations measured in the precast plant.

Appendix C - Grout Testing

C.1 Material Data Sheets

C.1.1 Five Star Grout

FIVE STAR

HIGHWAY PATCH

Fast Traffic Area Repair

PRODUCT DESCRIPTION

Five Star® Highway Patch is a one component, fast setting hydraulic cement material ideal for horizontal repairs of concrete in traffic areas.

ADVANTAGES

- High early strength
- One component/ease of use
- Open to traffic in two hours
- Freeze/thaw resistance
- Resistant to salts
- Cold weather installation
- Coarse aggregate extension

USES

- Highways and bridges
- Parking decks and ramps
- Airport runways and taxiways
- Expansion joint rebuild
- Dowel bar retrofit
- Cold weather repairs

PACKAGING AND YIELD

Five Star Highway Patch is packaged in heavy-duty polyethylene lined bags each weighing 50 lb (22.7 kg) yielding approximately 0.40 cubic feet (11.3 liters) and approximately 0.66 cubic feet (16.9 liters) with an 80% coarse aggregate extension. Also available in 3000 lb (1363 kg) bulk bags.

SHELF LIFE

One year in original unopened packaging when stored in dry conditions; high relative humidity will reduce shelf life.

TYPICAL PROPERTIES AT 70°F (21°C)	
Compressive Strength, ASTM C 109	
2 Hours	2000 psi (13.8 MPa)
3 Hours	3500 psi (24.1 MPa)
1 Day	5000 psi (34.5 MPa)
7 Days	7000 psi (48.3 MPa)
Bond Strength, ASTM C 882	
1 Day	1500 psi (10.4 MPa)
7 Days	2000 psi (13.8 MPa)
Length Change, ASTM C 157	
28 Days Wet	+0.05%
28 Days Dry	-0.05%
Freeze/Thaw Resistance, ASTM C 666A	
Relative Durability Factor	90%
Flexural Strength, ASTM C 78	
3 Hours	400 psi
Chloride Ion Permeability, ASTM C 1202	
28 Days	Very Low (<1000 Coulombs)
Working Time at 70°F (21°C)	10 minutes

The data shown above reflects typical results based on laboratory testing under controlled conditions. Reasonable variations from the data shown above may result. Test methods are modified where applicable.

PLACEMENT GUIDELINES

1. **SURFACE PREPARATION:** All horizontal and vertical surfaces in contact with Five Star® Highway Patch shall be free of oil, grease, laitance, and other contaminants. All horizontal and vertical concrete surfaces must be clean, sound and rough to ensure a good bond. Remove all oxidation from exposed reinforcing steel and for additional protection, coat reinforcing steel with Five Star® AC Coat. A perimeter edge and minimum depth of one inch (25 mm) should be provided for a durable repair. Featheredging is not desirable. Soak concrete surfaces prior to application with liberal quantities of potable water, leaving the concrete saturated and free of standing water or use Five Star® Bonding Adhesive. Surfaces shall be conditioned to between 35°F and 90°F (2°C and 32°C) at time of placement.
2. **MIXING:** Mix Five Star Highway Patch thoroughly for approximately four to five minutes to a uniform consistency with a mortar mixer (stationary barrel with moving blades) or a drill and paddle mixer. Mix Five Star Highway Patch with 2 1/4 to 3 quarts potable water per 50 lb. bag. Adjust consistency if necessary, but do not exceed maximum water content stated on the package or an amount that will cause segregation. Do not mix more material than can be placed in 10 minutes. Addition of coarse aggregate, meeting ASTM C 33, should be used for pours greater than 2 inches (50 mm) in depth. Always add mixing water first to mixer followed by repair material.
3. **PLACEMENT PROCEDURES:** When bonding adhesive is not used, firmly work Five Star Highway Patch into substrate and place full depth from one side of the repair to the other. Where this is not practical, placement must be continuous to prevent cold joints between pours. Finish as necessary.

   SPECIAL CONDITIONS: For use in cold temperatures, Five Star Highway Patch must be maintained at a temperature of at least 35°F (2°C) until a compressive strength of at least 1000 psi (6.9 MPa) is obtained. Faster strength gain will occur when the Five Star Highway Patch and mixing water have been conditioned to a higher temperature prior to placement. In hot temperatures, Five Star Highway Patch should be kept as cool as possible, but not exceeding 90°F (32°C). Chilled water should be used for mixing to help maintain sufficient working time.
4. **POST-PLACEMENT PROCEDURES:** Five Star Highway Patch shall be immediately coated with an approved curing compound meeting the water retention properties of ASTM C 309. In-service operation may begin immediately after the required strength has been reached.

NOTE: PRIOR TO APPLICATION, READ ALL PRODUCT PACKAGING THOROUGHLY. *For more detailed placement procedures, refer to Design-A-Spec™ installation guidelines or call the Five Star Engineering and Technical Service Center at (800) 243-2206.*

CONSIDERATIONS

- Never exceed the maximum water content as stated on the package or an amount that will cause segregation.
- Temperature of surfaces must be between 35°F and 90°F (2°C and 32°C) at time of placement. For cold and hot weather placement, call the Five Star Products Engineering and Technical Service Center.
- Repair material shall be protected from freezing until it reaches 1000 psi (6.9 MPa).
- Placement shall be continuous to avoid cold joints.

CAUTION

Irritant, toxic, strong sensitizer. International Agency for Research on Cancer has determined that there is sufficient evidence for the carcinogenicity of inhaled crystalline silica to humans. Take appropriate measures to avoid breathing dust. Avoid contact with eyes and contact with skin. In case of contact with eyes, immediately flush with plenty of water for at least 15 minutes. Immediately call a physician. Wash skin thoroughly after handling. Keep product out of reach of children. **PRIOR TO USE, REFER TO MATERIAL SAFETY DATA SHEET.**

For worldwide availability, additional product information and technical support, contact your local Five Star distributor, local sales representative, or you may call Five Star's Engineering and Technical Service Center at (800) 243-2206.

WARRANTY: "FIVE STAR PRODUCTS INC. (FSP) PRODUCTS ARE MANUFACTURED TO BE FREE OF MANUFACTURING DEFECTS AND TO MEET FSP'S CURRENT PUBLISHED PHYSICAL PROPERTIES WHEN APPLIED IN ACCORDANCE WITH FSP'S DIRECTIONS AND TESTED IN ACCORDANCE WITH ASTM AND FSP STANDARDS. HOWEVER, SHOULD THERE BE DEFECTS OF MANUFACTURING OF ANY KIND, THE SOLE RIGHT OF THE USER WILL BE TO RETURN ALL MATERIALS ALLEGED TO BE DEFECTIVE, FREIGHT PREPAID TO FSP, FOR REPLACEMENT. THERE ARE NO OTHER WARRANTIES BY FSP OF ANY NATURE WHATSOEVER, EXPRESS OR IMPLIED, INCLUDING ANY WARRANTY OF MERCHANTABILITY OR FITNESS FOR A PARTICULAR PURPOSE IN CONNECTION WITH THIS PRODUCT. FSP SHALL NOT BE LIABLE FOR DAMAGES OF ANY SORT, INCLUDING PUNITIVE, ACTUAL, REMOTE, OR CONSEQUENTIAL DAMAGES, RESULTING FROM ANY CLAIMS OF BREACH OF CONTRACT, BREACH OF ANY WARRANTY, WHETHER EXPRESSED OR IMPLIED, INCLUDING ANY WARRANTY OF MERCHANTABILITY OR FITNESS FOR A PARTICULAR PURPOSE OR FROM ANY OTHER CAUSE WHATSOEVER. FSP SHALL ALSO NOT BE RESPONSIBLE FOR USE OF THIS PRODUCT IN A MANNER TO INFRINGE ON ANY PATENT HELD BY OTHERS."

Five Star Products, Inc.
Corporate Headquarters
750 Commerce Drive
Fairfield, CT 06825 USA
Tel: 203-336-7900 • Fax: 203-336-7930
http://www.fivestarproducts.com

ISO 9001

©2008 Five Star Products, Inc. (03/09)
American Owned & Operated

C.1.2 Five Star Grout with Fibers

Fibers were added to the grout at a ratio of 1 pound of fibers to 1 cubic yard of Fiver Star Grout. The fibers were 1-1/2 in. long polypropylene fibers bought from a local construction supply store.

C.1.3 Type K Concrete Mix

Concrete Mix Design
Weight of Materials - 1 cubic yard

Spring 2009

The methods from ACI 211.1 have been used for the initial design of the mix

Coarse Aggregate

NMS	0.375	Inches	(Need to pick a CA)
FM	0		(Need to determine from sand)
% CA	0.5		(Table 6.3.6 - 'assuming there is no sand added')
DRUW	95	pcf	(need to dry in the oven, dry rod, and determine)
WT. CA	1282.5	lb/yd^3	

Water

Slump	6	Inches	
W/C	0.45		(Table 6.3.4(a))
Air Ent. ?	No		
Air %	2	%	
WT. H2O	688.5	lb/yd^3	(Table 6.3.3 - NOT used - Forced to be 50% CA & 50% W-C)

Cement

WT. Cem.	1530	lb/yd^3	http://www.ctscement.com/TypeK_data.asp

Fine Aggregate

Vol. FA	0.001986	ft^3	(Unit weights are assumed here - Check)
(BSGod)fa	0	lb/yd^3	(Dry Specific Gravity of Sand)
WT. FA	0	lb/yd^3	

Adjusted Weights

SMCfa	0	%	
SMCca	-1	%	
TMCfa	0	%	Assuming Dry
TMCca	0	%	Assuming Dry
(H20)fa	0	lbs	
(H20)ca	-12.825	lbs	

Batch Weights

Total Vol.	0.88	ft^3
Total Vol.	0.032593	yd^3

Water	701.325	lb/yd^3
FA	0	lb/yd^3
CA	1282.5	lb/yd^3
Cement	1530	lb/yd^3

Water	22.86	lb
FA	0.00	lb
CA	41.80	lb
Cement	49.87	lb

C.1.4 Set 45 Highway Grout

PRODUCT DATA

3 03 01 00 **Maintenance of Concrete**

SET® 45 AND SET ®45 HW

Chemical-action repair mortar

Description

Set ® 45 is a one-component magnesium phosphate-based patching and repair mortar. This concrete repair and anchoring material sets in approximately 15 minutes and takes rubber-tire traffic in 45 minutes. It comes in two formulations: Set ® 45 Regular for ambient temperatures below 85° F (29° C) and Set ® 45 Hot Weather for ambient temperatures ranging from 85 to 100° F (29 to 38° C).

Yield

A 50 lb (22.7 kg) bag of mixed with the required amount of water produces a volume of approximately 0.39 ft ³ (0.011 m ³); 60% extension using 1/2" (13 mm) rounded, sound aggregate produces approximately 0.58 ft ³ (0.016 m ³).

Packaging

50 lb (22.7 kg) multi-wall bags

Color

Dries to a natural gray color

Shelf Life

1 year when properly stored

Storage

Store in unopened containers in a clean, dry area between 45 and 90° F (7 and 32° C).

Features

- Single component
- Reaches 2,000 psi compressive strength in 1 hour
- Wide temperature use range
- Superior bonding
- Very low drying shrinkage
- Resistant to freeze/thaw cycles and deicing chemicals
- Only air curing required
- Thermal expansion and contraction similar to Portland cement concrete
- Sulfate resistant

Where to Use

APPLICATION

- Heavy industrial repairs
- Dowel bar replacement
- Concrete pavement joint repairs
- Full-depth structural repairs
- Setting of expansion device nosings
- Bridge deck and highway overlays
- Anchoring iron or steel bridge and balcony railings
- Commercial freezer rooms
- Truck docks
- Parking decks and ramps
- Airport runway-light installations

Benefits

Just add water and mix

Rapidly returns repairs to service

From below freezing to hot weather exposures

Bonds to concrete and masonry without a bonding agent

Improved bond to surrounding concrete

Usable in most environments

Fast, simple curing process

More permanent repairs

Stable where conventional mortars degrade

LOCATION

- Horizontal and formed vertical or overhead surfaces
- Indoor and outdoor applications

How to Apply

Surface Preparation

1. A sound substrate is essential for good repairs. Flush the area with clean water to remove all dust.
2. Any surface carbonation in the repair area will inhibit chemical bonding. Apply a pH indicator to the prepared surface to test for carbonation.
3. Air blast with oil-free compressed air to remove all water before placing Set ® 45.

Technical Data

Composition

Set ® 45 is a magnesium-phosphate patching and repair mortar.

Test Data

Typical Compressive Strengths*, psi (MPa) — ASTM C 109, modified

	Plain Concrete 72° F (22° C)	Set ® 45 Regular 72° F (22° C)	Set ® 45 Regular 36° F (2° C)	Set ® 45 HW 95° F (35° C)
1 hour	—	2,000 (13.8)	—	—
3 hour	—	5,000 (34.5)	—	3,000 (20.7)
6 hour	—	5,000 (34.5)	1,200 (8.3)	5,000 (34.5)
1 day	500 (3.5)	6,000 (41.4)	5,000 (34.5)	6,000 (41.4)
3 day	1,900 (13.1)	7,000 (48.3)	7,000 (48.3)	7,000 (48.3)
28 day	4,000 (27.6)	8,500 (58.6)	8,500 (58.6)	8,500 (55.2)

NOTE: Only Set ® 45 Regular formula, tested at 72° F (22° C), obtains 2,000 psi (13.8 MPa) compressive strength in 1 hour.

PROPERTY	RESULTS		TEST METHODS
Modulus of Elasticity, psi (MPa)			ASTM C 469
	7 days	**28 days**	
Set ® 45 Regular	4.18×10^6 (2.88×10^4)	4.55×10^6 (3.14×10^4)	
Set ® 45 Hot Weather	4.90×10^6 (3.38×10^4)	5.25×10^6 (3.62×10^4)	
Freeze/thaw durability test, % RDM, 300 cycles, for Set ® 45 and Set 45 ® HW		80	ASTM C 666, Procedure A (modified**)
Scaling resistance to deicing chemicals, Set ® 45 and Set 45 ® HW			ASTM C 672
5 cycles		0	
25 cycles		0	
50 cycles		1.5 (slight scaling)	
Sulfate resistance			ASTM C 1012
Set ® 45 length change after 52 weeks, %		0.09	
Type V cement mortar after 52 weeks, %		0.20	
Typical setting times, min, for Set ® 45 at 72° F (22° C), and Set ® 45 Hot Weather at 95° F (35° C)			Gilmore ASTM C 266, modified
Initial set		9 - 15	
Final set		10 - 20	
Coefficient of thermal expansion,* both Set ® 45 Regular and Set ® 45 Hot Weather coefficients		7.15×10^{-6}/° F (12.8×10^{-6}/° C)	CRD-C 39
Flexural Strength, psi (MPa), 3 by 4 by 16" (75 by 100 by 406 mm) prisms, 1 day strength,			ASTM C 78, modified
Set ® 45 mortar		550 (3.8)	
Set ® 45 mortar with 3/8" (9 mm) pea gravel		600 (4.2)	
Set ® 45 mortar with 3/8" (9 mm) crushed angular noncalcareous hard aggregate		650 (4.5)	

* All tests were performed with neat material (no aggregate)

**Method discontinues test when 300 cycles or an RDM of 60% is reached.

***Determined using 1 by 1 by 11" (25 mm by 25 mm by 279 mm) bars. Test was run with neat mixes (no aggregate). Extended mixes (with aggregate) produce lower coefficients of thermal expansion.

Test results are averages obtained under laboratory conditions. Expect reasonable variations.

Mixing

1. Set ® 45 must be mixed, placed, and finished within 10 minutes in normal temperatures (72° F [22° C]). Only mix quantities that can be placed in 10 minutes or less.

2. Do not deviate from the following sequence; it is important for reducing mixing time and producing a consistent mix. Use a minimum 1/2" slow-speed drill and mixing paddle or an appropriately sized mortar mixer. Do not mix by hand.

3. Pour clean (potable) water into mixer. Water content is critical. Use a maximum of 4 pts (1.9 L) of water per 50 lb (22.7 kg) bag of Set ® 45. Do not deviate from the recommended water content.

4. Add the powder to the water and mix for approximately 1 - 1-1/2 minutes.

5. Use neat material for patches from 1/2 - 2" (6 - 51 mm) in depth or width. For deeper patches, extend a 50 lb (22.7 kg) bag of Set ® 45 HW by adding up to 30 lbs (13.6 kg) of properly graded, dust-free, hard, rounded aggregate or noncalcareous crushed angular aggregate, not exceeding 1/2" (6 mm) in accordance with ASTM C 33, #8. If aggregate is damp, reduce water content accordingly. Special procedures must be followed when angular aggregate is used. Contact your local BASF representative for more information. (Do not use calcareous aggregate made from soft limestone. Test aggregate for fizzing with 10% HCL).

Application

1. Immediately place the mixture onto the properly prepared substrate. Work the material firmly into the bottom and sides of the patch to ensure good bond.

2. Level the Set ® 45 and screed to the elevation of the existing concrete. Minimal finishing is required. Match the existing concrete texture.

Curing

No curing is required, but protect from rain immediately after placing. Liquid-membrane curing compounds or plastic sheeting may be used to protect the early surface from precipitation, but never wet cure Set ® 45.

For Best Performance

- Color variations are not indicators of abnormal product performance.
- Regular Set ® 45 will not freeze at temperatures above -20° F (-29° C) when appropriate precautions are taken.
- Do not add sand, fine aggregate, or Portland cement to Set ® 45.
- Do not use Set ® 45 for patches less than 1/2" (13 mm) deep. For deep patches, use Set ® 45 Hot Weather formula extended with aggregate, regardless of the temperature. Consult your BASF representative for further instructions.
- Do not use limestone aggregate.
- Water content is critical. Do not deviate from the recommended water content printed on the bag.
- Precondition these materials to approximately 70° F (21° C) for 24 hours before using.
- Protect repairs from direct sunlight, wind, and other conditions that could cause rapid drying of material.
- When mixing or placing Set ® 45 in a closed area, provide adequate ventilation.
- Do not use Set ® 45 as a precision nonshrink grout.
- Never featheredge Set ® 45; for best results, always sawcut the edges of a patch.
- Prevent any moisture loss during the first 3 hours after placement. Protect Set ® 45 with plastic sheeting or a curing compound in rapid-evaporation conditions.
- Do not wet cure.
- Do not place Set ® 45 on a hot (90° F [32° C]), dry substrate.
- When using Set ® 45 in contact with galvanized steel or aluminum, consult your local BASF sales representative.
- Make certain the most current versions of product data sheet and MSDS are being used; call Customer Service (1-800-433-9517) to verify the most current versions.
- Proper application is the responsibility of the user. Field visits by BASF personnel are for the purpose of making technical recommendations only and not for supervising or providing quality control on the jobsite.

C.1.5 VDOT Post and Rail Bridge Deck Mix

Concrete Class	Design Compressive Strength at 28 days (psi)	Aggregate Size (No.)	Max Laboratory Premeability at 28 Days (Coulombs)	Nominal Max. Aggregate Size (in.)	Minimum Cementitios Material (lbs/Yd^3)	Max Water / Cement Ratio (lb/lb)	Consistancy (Slump)	Air Content (%)
A4	4,000	7,8, or 78	2500	½	635	0.45	2-5	7 +/- 2

C.2 Environmental Conditions During the Tests

	Time	Temperature (°F)	Humidity (%)	Notes
5/1/2009 (Concrete Pour)	4:00 PM	73	68%	*For the first 7 days the concrete specimens were left covered with burlap and plastic. The burlap was kept moist and the temperature in the lab remained in the low 70s. Light Rain Occurred nearly every afternoon in May = Humid environment.
5/2/2009	1:00 PM	69	77%	
5/7/2009	4:00 PM	73	100%	
5/11/2009	5:30 PM	72	100%	
5/18/2009	8:30	65	37%	
6/1/2009	8:30 AM	70		
6/12/2009 (Grout Pour)	8:00 AM	72	100%	Misty Morning that Turned Sunny by 12:00 PM
	3:00 PM	82	65%	
6/13/2009	Afternoon	Low 80's	~100%	Afternoon rains each day (Lab Doors Open)
6/14/2009		57-79		
6/15/2009		61-76	~100%	
6/16/2009		62-67	~100%	
6/17/2009		62-73	~100%	
6/18/2009		64-82	~100%	
6/19/2009		60-85		
6/19-6/30		60 –Mid 80's	~60%	Dry Weather with Lower Humidity (2 Days with Trace precipitation)
7/8/2009		55-81	~60%	Mist/Fog Morning
7/13/2009		61-81	~60%	Mist/Fog Morning
7/17/2009		63-80	~100%	Heavy Rain
7/23/2009		57-80		Trace Rain
7/27/2009		63-81	~100%	Heavy Rain
7/31/2009		64-77	~100%	Light Rain
8/7/2009		56-79		
8/13/2009		59-83	~100%	Heavy Fog
8/20/2009		65-75	~100%	Light Rain
8/28/2009		64-70		Trace

C.3 Modified ASTM C157 Shrinkage Measurements

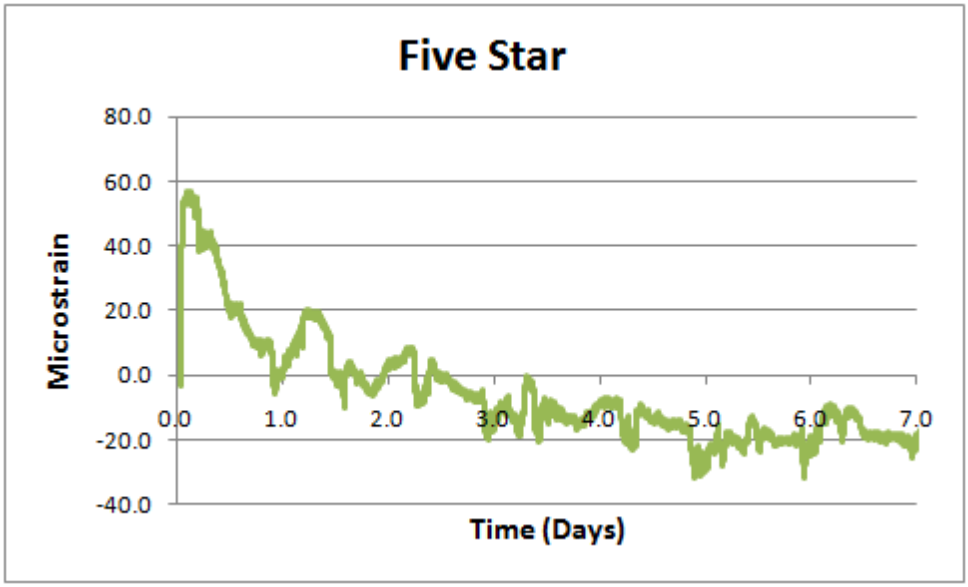

Five Star Modified ASTM C157 Shrinkage

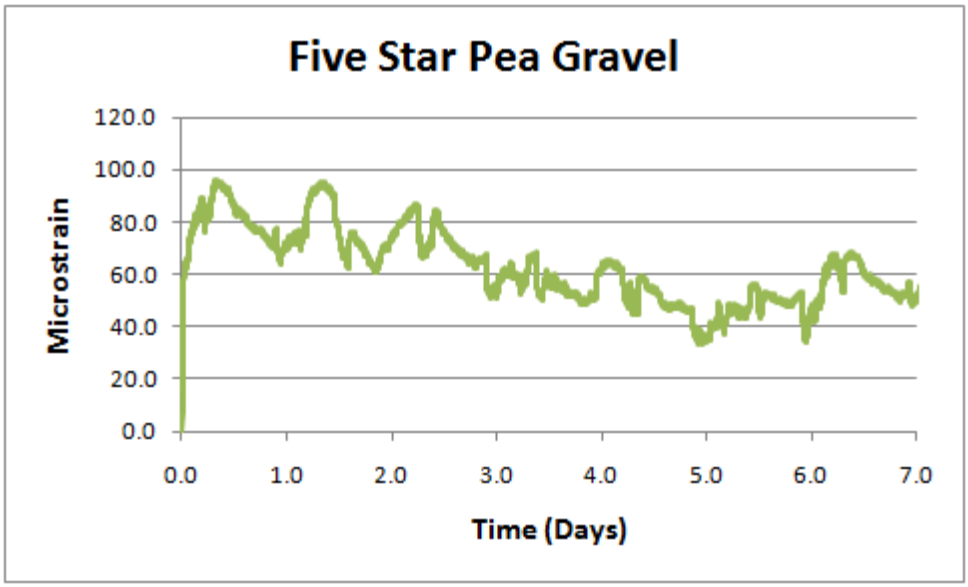

Five Star Pea Gravel Modified ASTM C157 Shrinkage

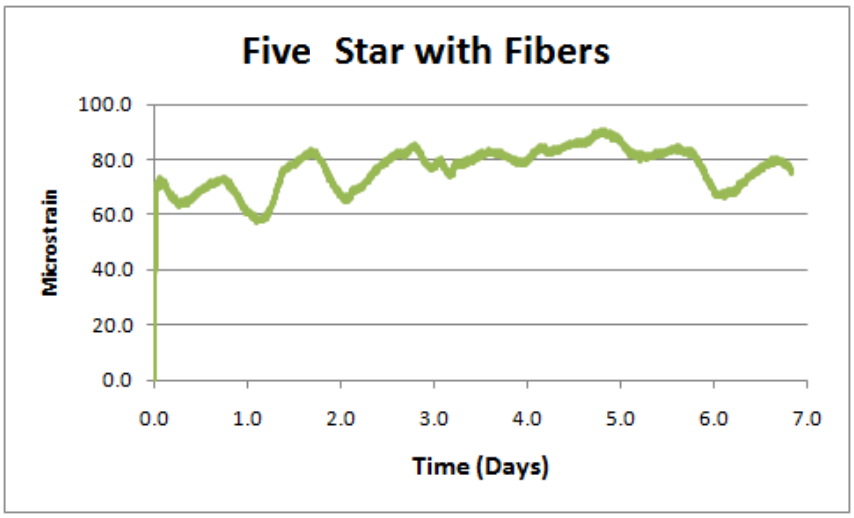

Five Star Fiber Modified ASTM C157 Shrinkage

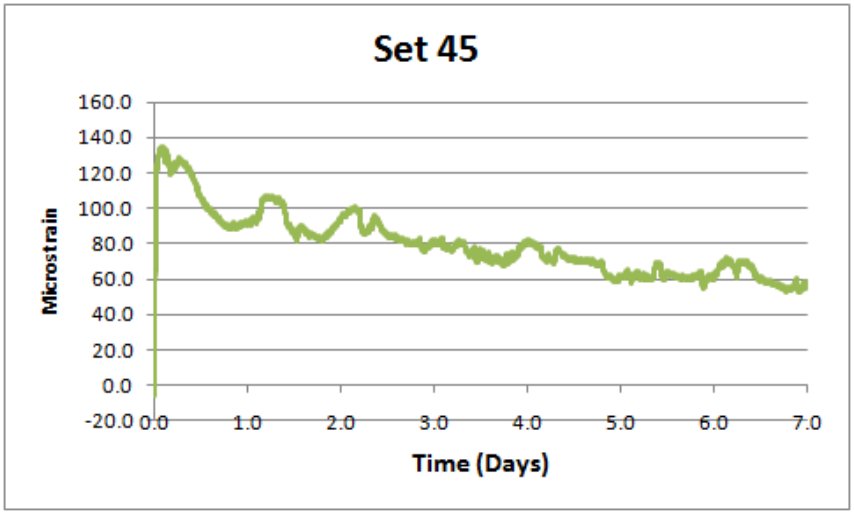

Set 45 Modified ASTM C157 Shrinkage

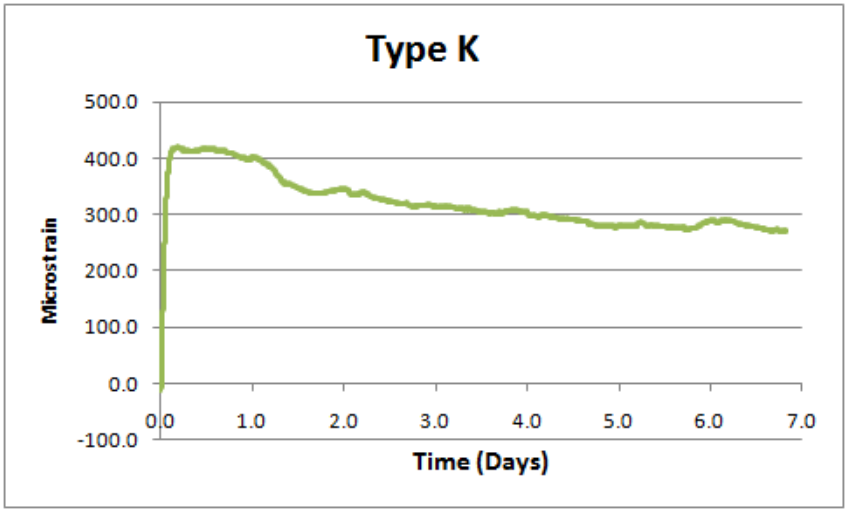

Type K Modified ASTM C157 Shrinkage

C.4 Deflection versus Time for the Rings

C.4.1 Five Star Control Specimens

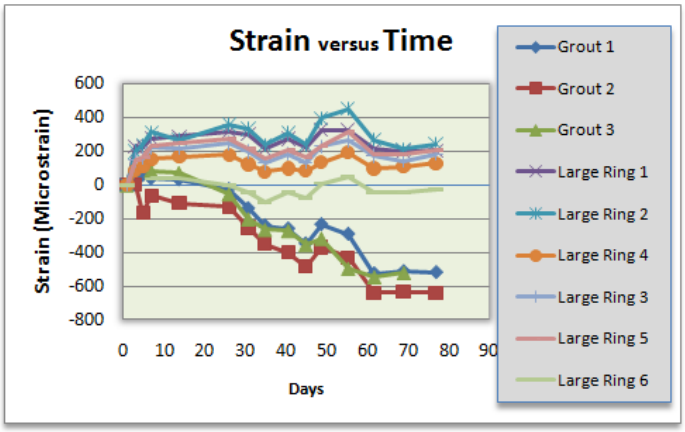

Five Star Control #1

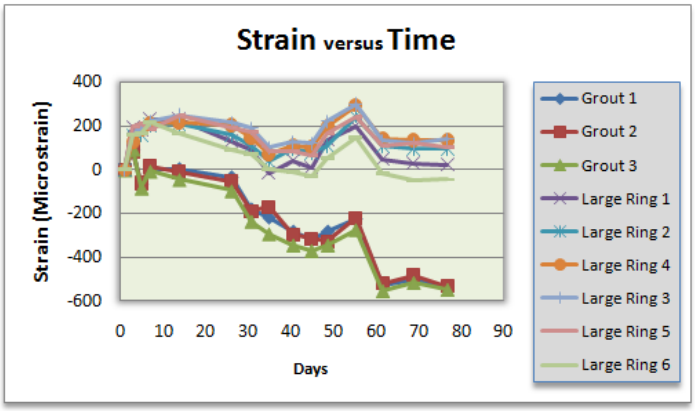

Five Star Control #2

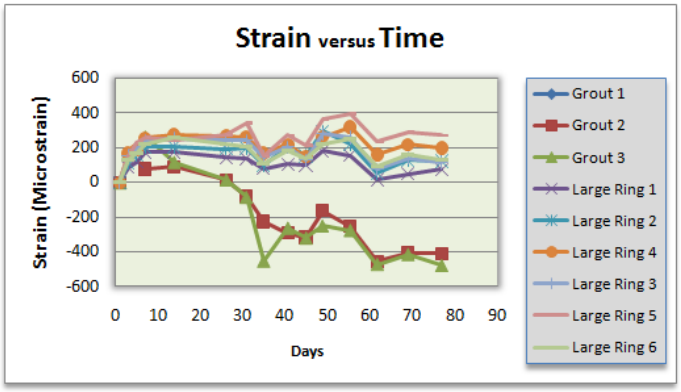

Five Star Control #3

C.4.2 Five Star Pea Gravel Control Specimens

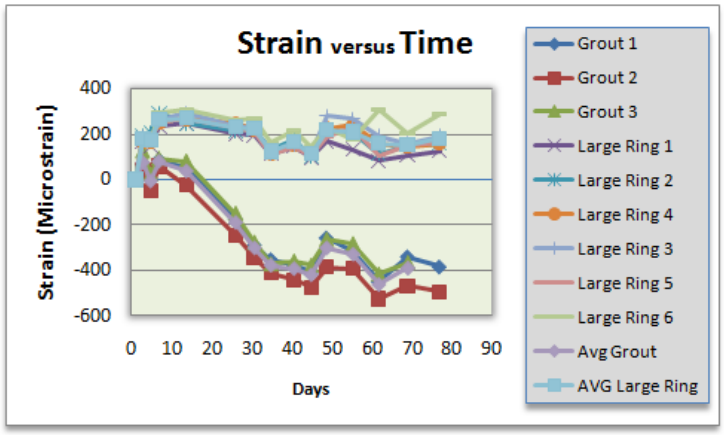

Five Star Pea Gravel Control #1

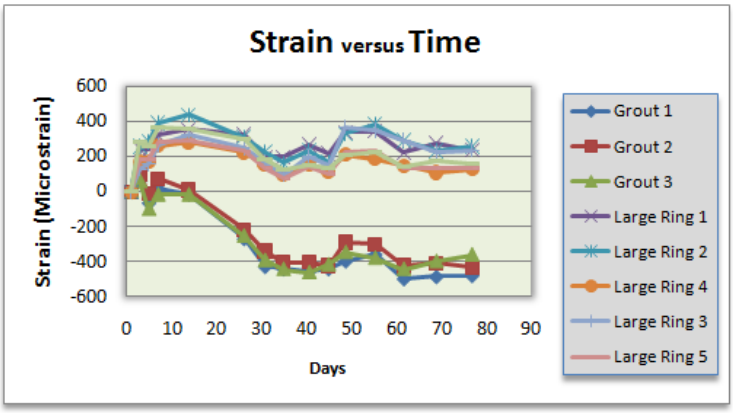

Five Star Pea Gravel Control #2

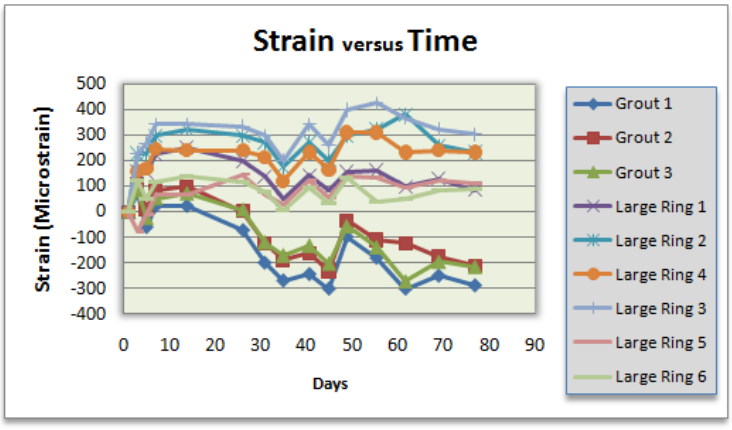

Five Star Pea Gravel Control #3

C.4.3 Set 45 Control

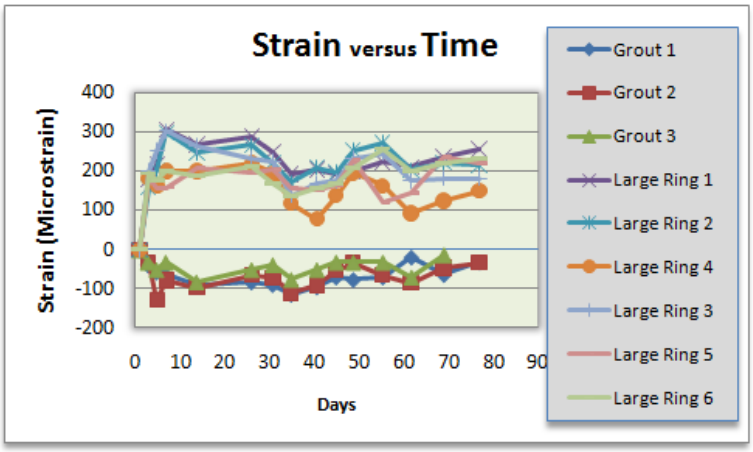

Set 45 Control #1

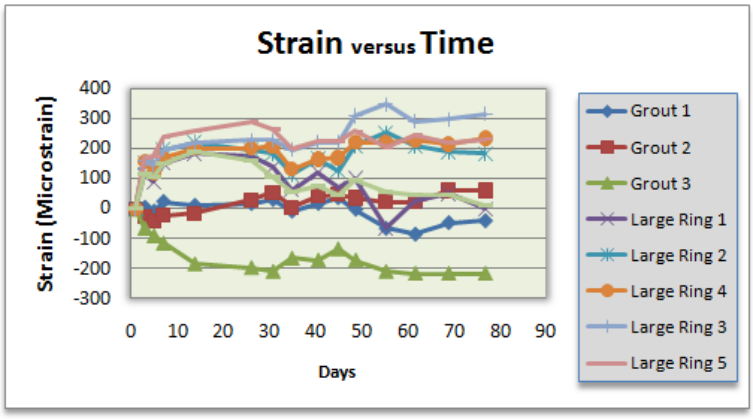

Set 45 Control #2

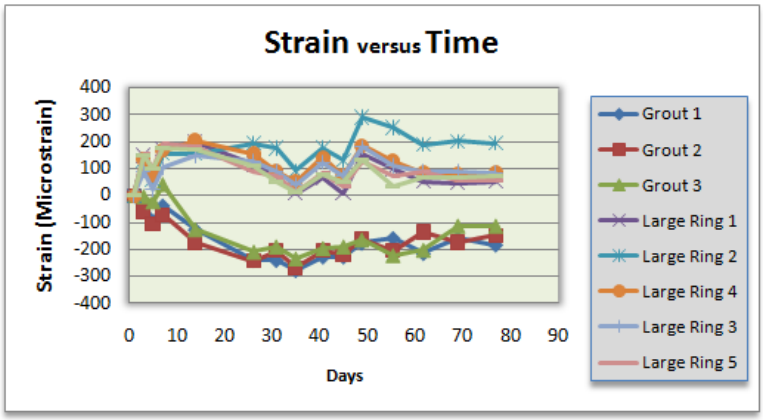

Set 45 Control #3

C.4.4 Type K Control

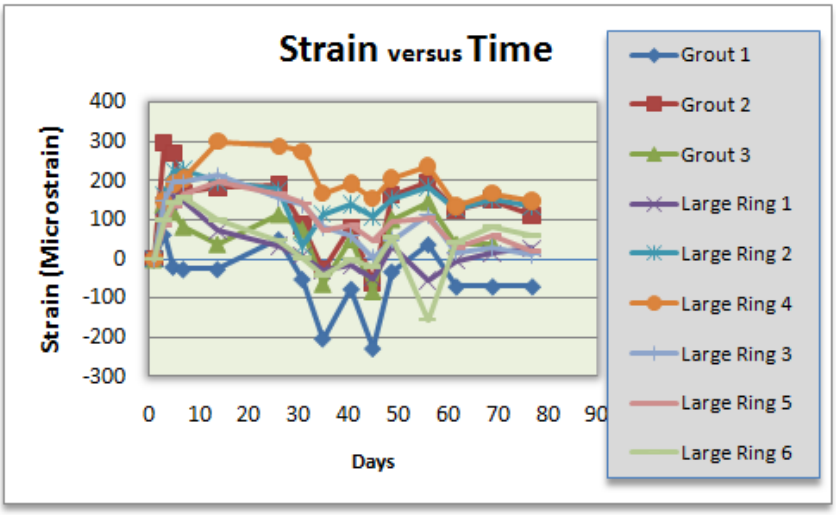

Type K Control #1

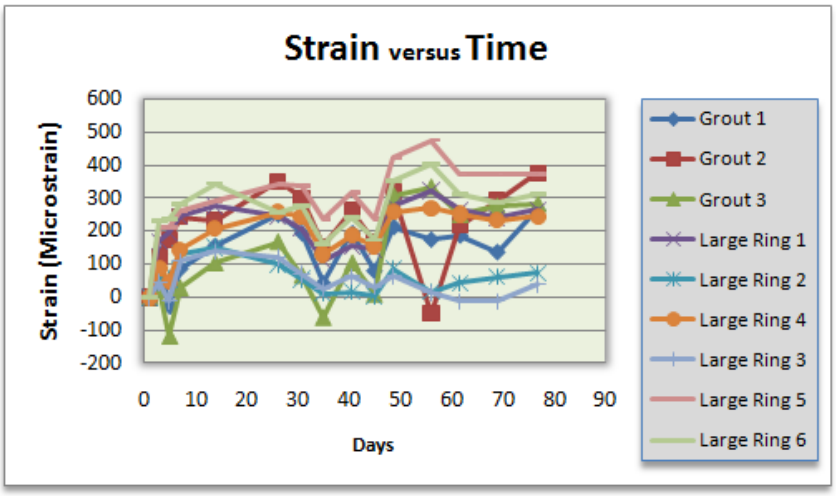

Type K Control #2

C.4.5 Five Star Fiber Control

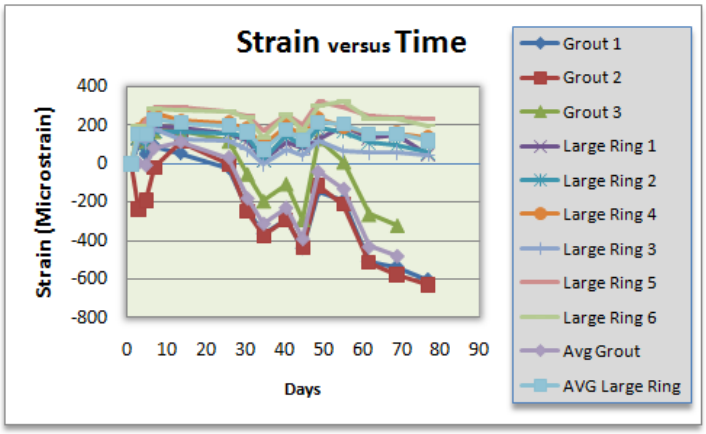

Five Star Fiber Control #1

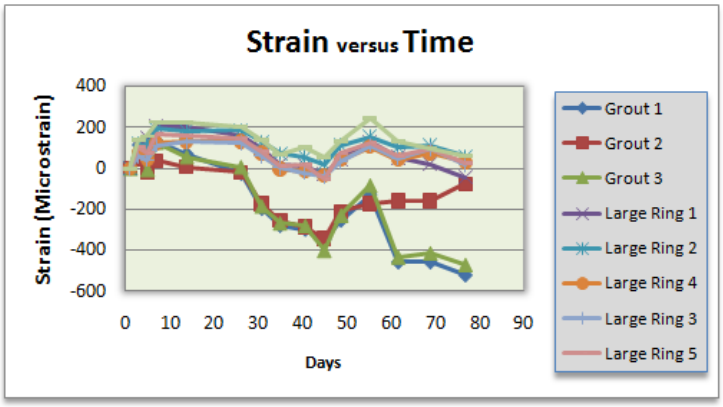

Five Star Fiber Control #2

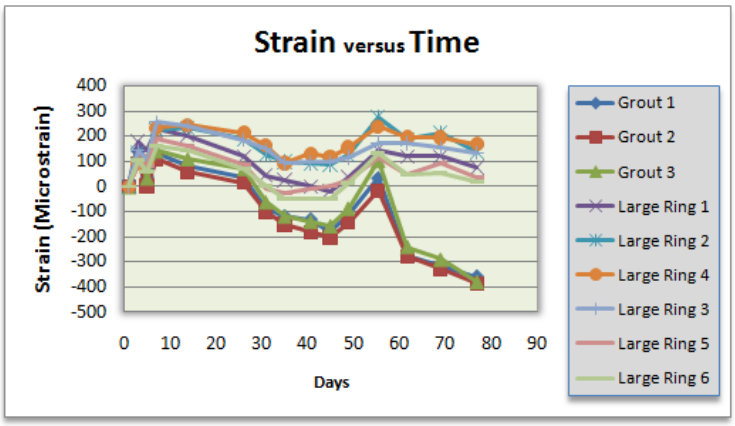

Five Star Fiber Control #3

C.4.6 Five Star Exposed Aggregate

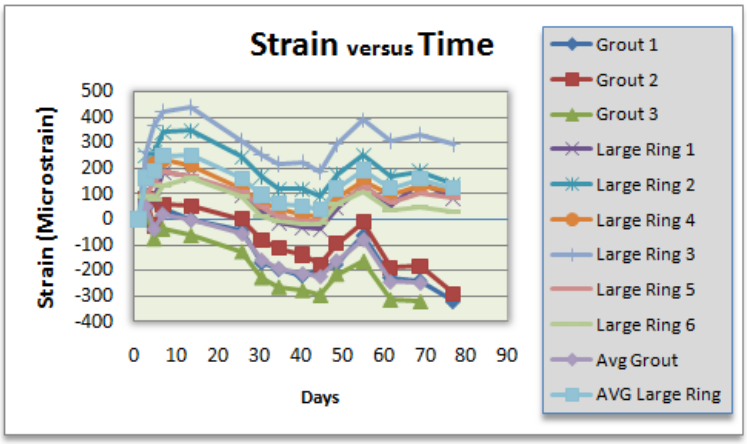

Five Star Exposed Aggregate #1

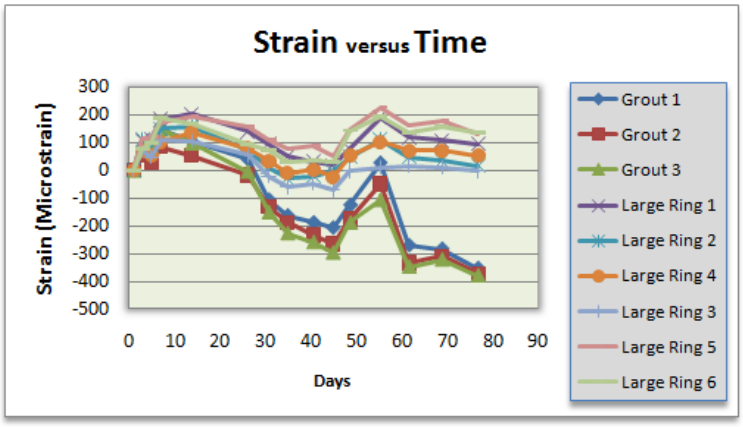

Five Star Exposed Aggregate #2

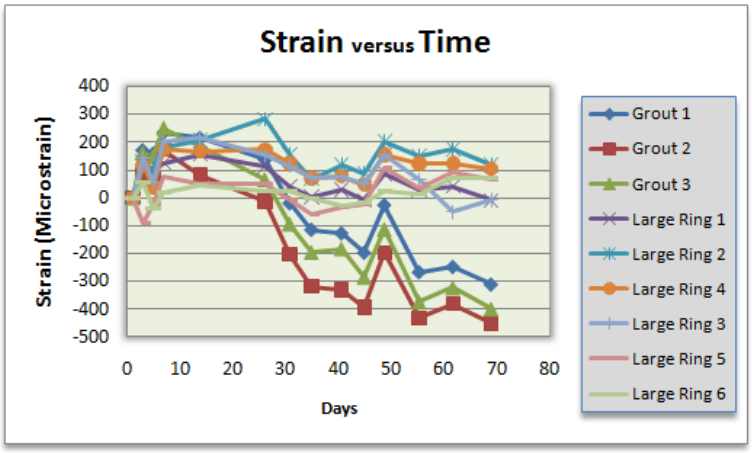

Five Star Exposed Aggregate #3

C.4.7 Five Star Pea Gravel Exposed Aggregate

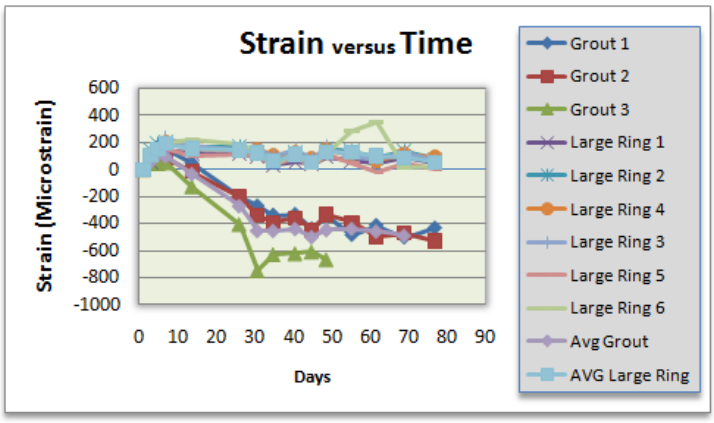

Five Star Pea Gravel Exposed Aggregate #1

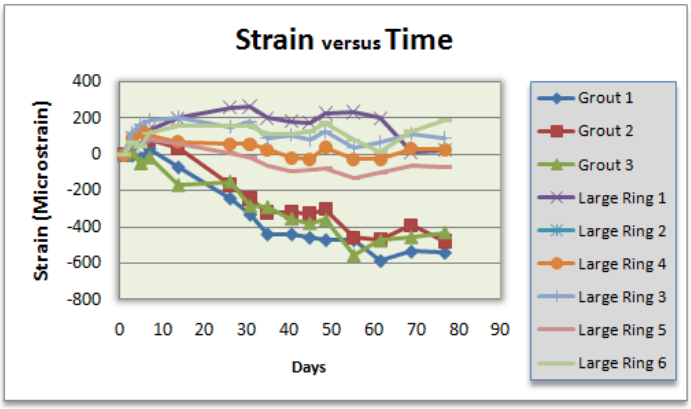

Five Star Pea Gravel Exposed Aggregate #2

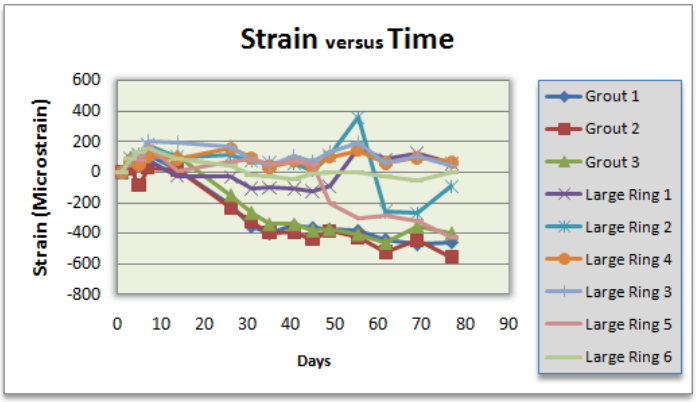

Five Star Pea Gravel Exposed Aggregate #3

C.4.8 Five Star Wire Brush

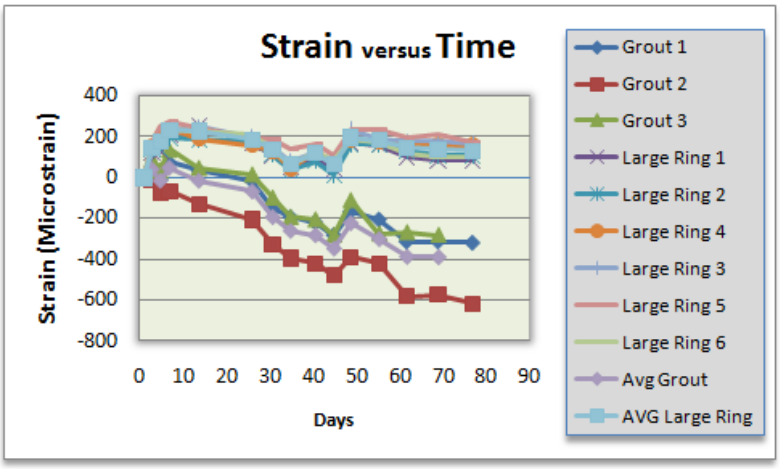

Five Star Wire Brush #1

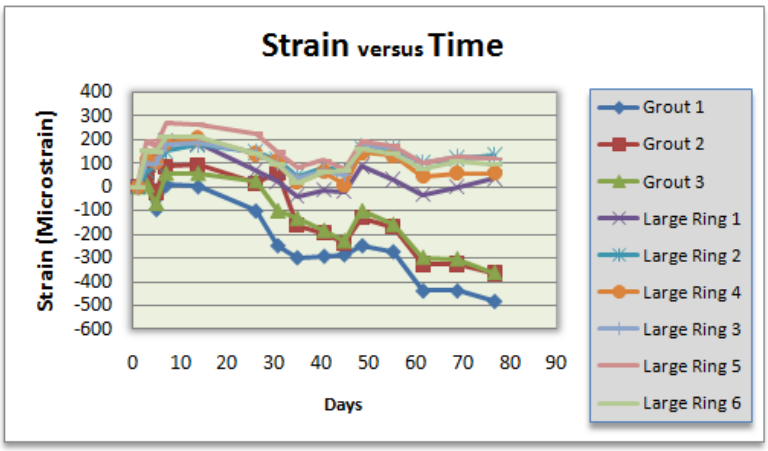

Five Star Wire Brush #2

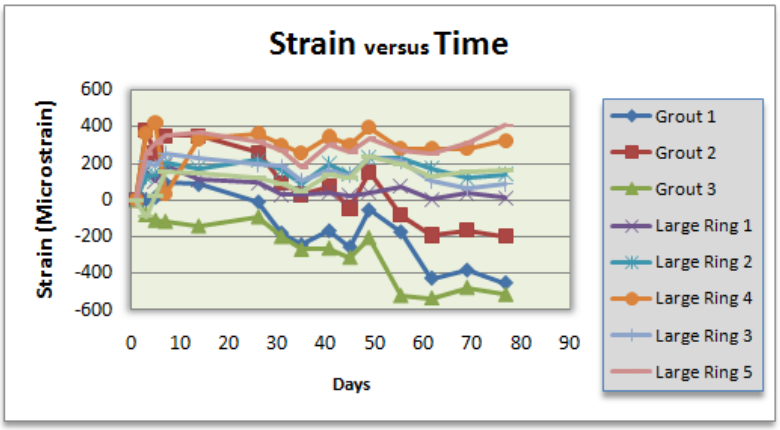

Five Star Wire Brush #3

C.4.9 Star Pea Gravel Wire Brush

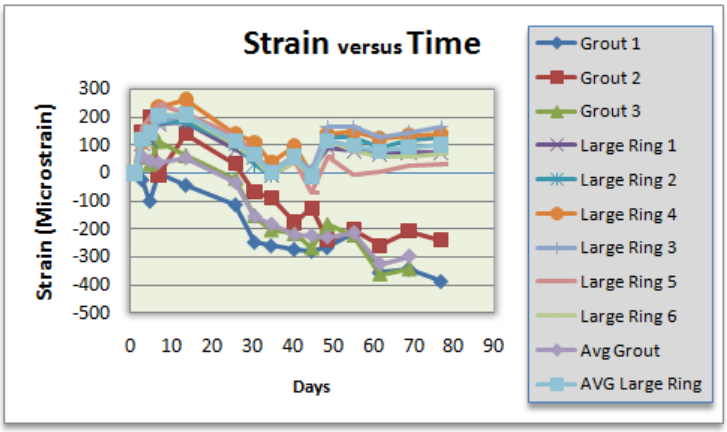

Five Star Pea Gravel Wire Brush #1

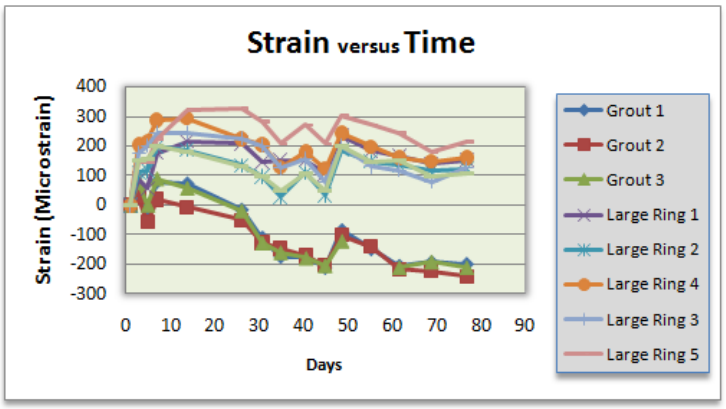

Five Star Pea Gravel Wire Brush #2

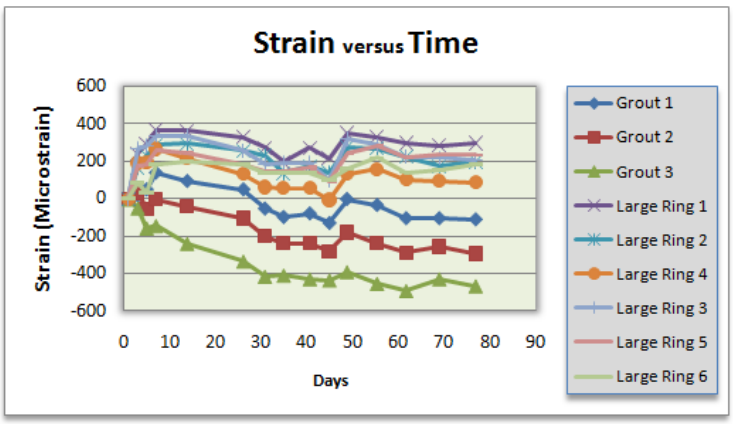

Five Star Pea Gravel Wire Brush #3

C.4.10 Five Star Epoxy

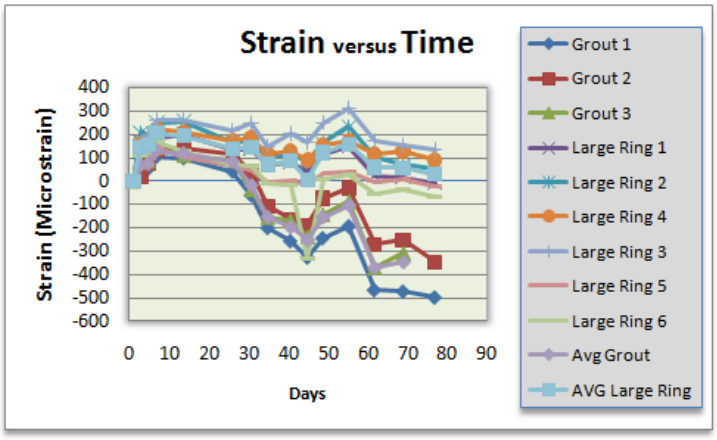

Five Star Epoxy #1

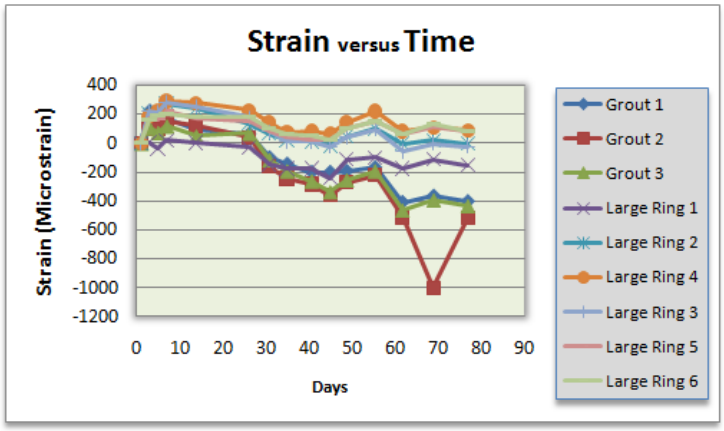

Five Star Epoxy #2

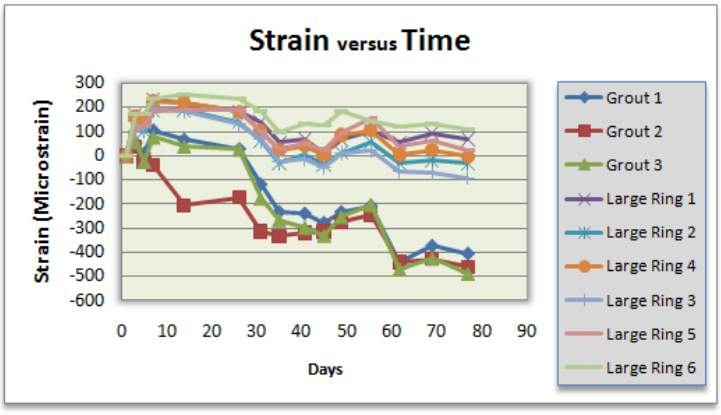

Five Star Epoxy #3

C.4.11 Five Star Pea Gravel Epoxy

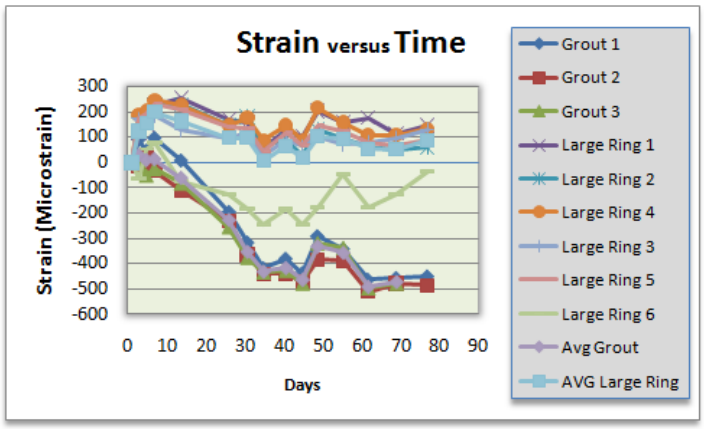

Five Star Pea Gravel Epoxy #1

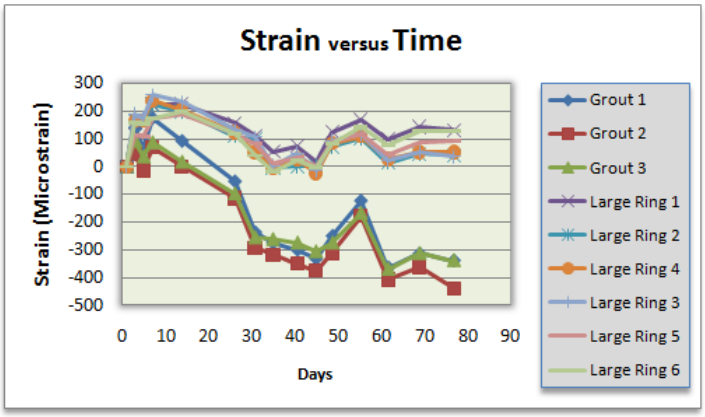

Five Star Pea Gravel Epoxy #2

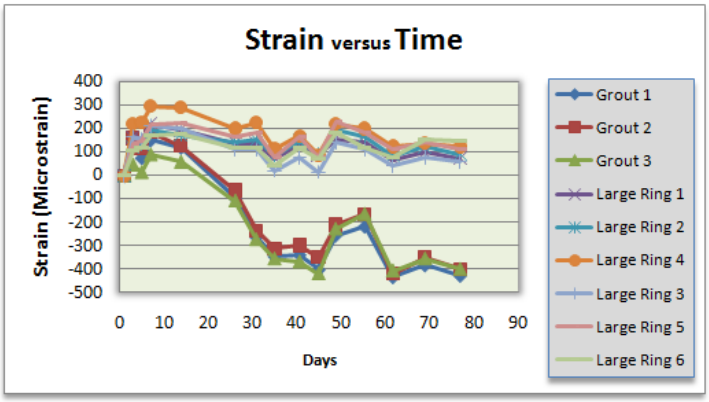

Five Star Pea Gravel Epoxy #3

C.4.12 Five Star Shear Key

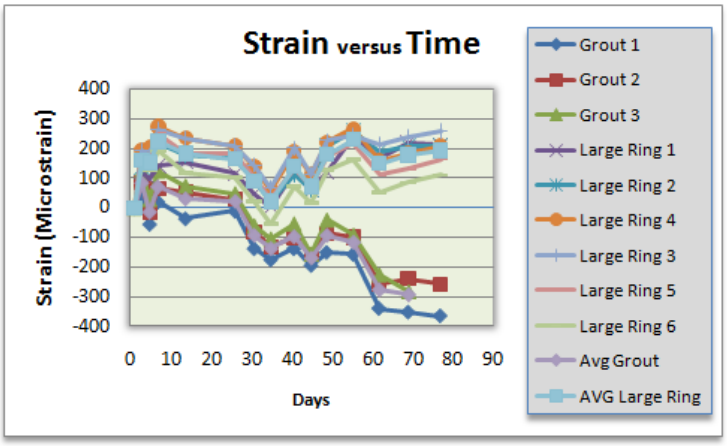

Five Star Shear Key #1

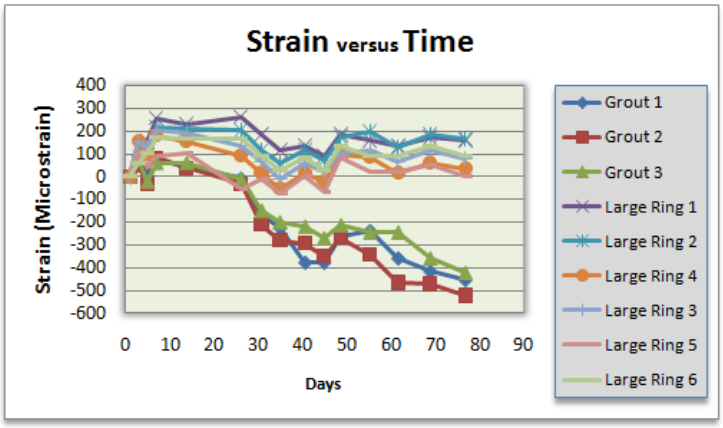

Five Star Shear Key #2

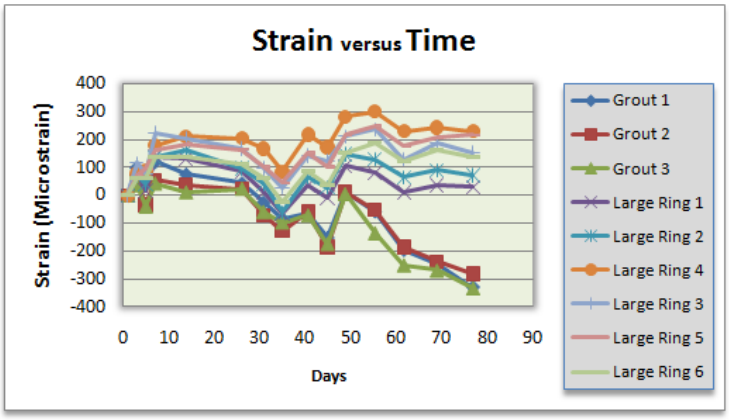

Five Star Shear Key #3

C.4.13 Five Star Water Stop

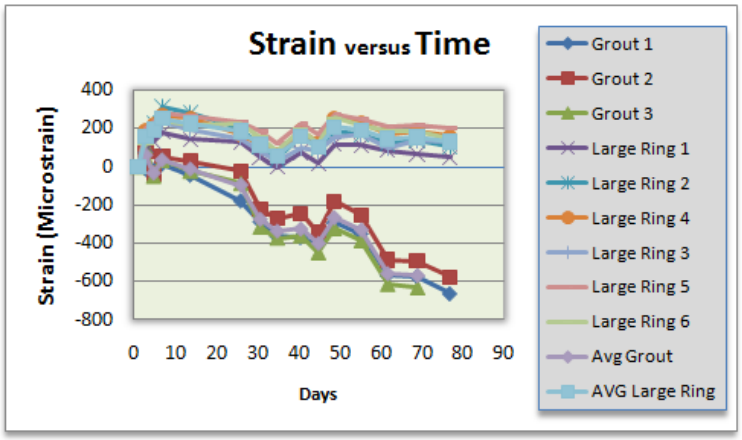

Five Star Water Stop #1

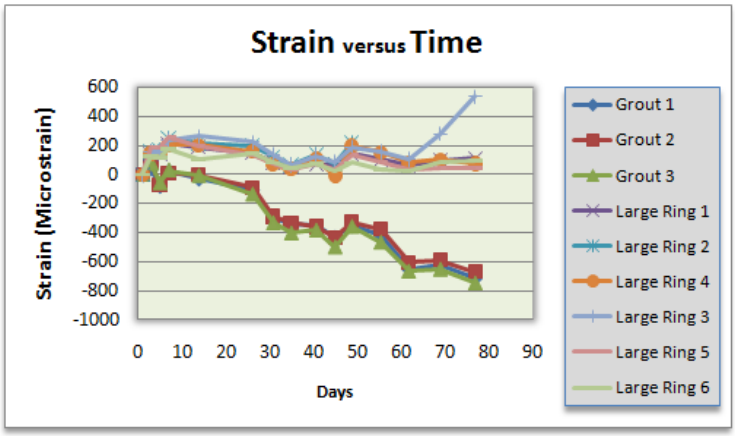

Five Star Water Stop #2

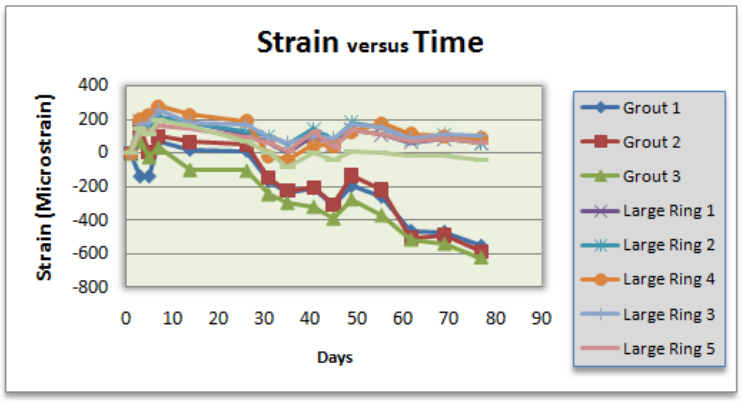

Five Star Water Stop #3

C.5 Outlier Tests for the Ring Data

C.5.1 Dixon Outlier Test

Sample Name	Ring Stress Visual	Ring Stress DEMEC	AVG Ring Stress (Ksi)	AVG Ring Stress (Ksi)	Standard Deviation (Visual)	Standard Deviation (DEMEC)	r-statistic (Visual)	r-statistic (DEMEC)	r-critical (98% Confiden	r-critical (90% Confiden	98% Visual Outlier?	98% DEMEC Outlier?	90% Visual Outlier?	90% DEMEC Outlier?
Type K Concrete:	0.0	-78.3	0.0	-78.3					0.988	0.941	NO	NO	NO	NO
	0.0	-78.3			0.0	0.0			0.988	0.941	NO	NO	NO	NO
Five Star Control:	-203.6	-182.8					0.365	0.964	0.988	0.941	NO	NO	NO	Yes
	-168	-169.6	-159.2	-173.8										
	-106	-169.1			49.4	7.8	0.635	0.036	0.988	0.941	NO	NO	NO	NO
Set 45 Control:	-179	0							0.988	0.941	NO	NO	NO	NO
	-56.2	0	-78.4	0.0					0.988	0.941	NO	NO	NO	NO
	0	0			91.5	0.0			0.988	0.941	NO	NO	NO	NO
Five Star Pea Gravel Control:	-92.7	-56.5					0.723	1.000	0.988	0.941	NO	Yes	NO	Yes
	-56.5	-24.5	-63.9	-35.2					0.988	0.941	NO	NO	NO	NO
	-42.6	-24.5			25.9	18.5	0.277	0.000	0.988	0.941	NO	NO	NO	NO
Five Star Pea Gravel Wire Brushed:	-92.7	-82.1					0.000	0.000	0.988	0.941	NO	NO	NO	NO
	-92.7	-82.1	-86.4	-79.3					0.988	0.941	NO	NO	NO	NO
	-73.7	-73.7			11.0	4.8	1.000	1.000	0.988	0.941	Yes	Yes	Yes	Yes
Five Star Wire Brushed:	-216.9	-216.9					0.644	0.171	0.988	0.941	NO	NO	NO	NO
	-188.5	-213.7	-192.7	-209.6					0.988	0.941	NO	NO	NO	NO
	-172.8	-198.2			22.4	10.0	0.356	0.829	0.988	0.941	NO	NO	NO	NO
Five Star Pea Gravel Exposed Aggregate:	-92.7	-92.7					0.000	1.000	0.988	0.941	NO	Yes	NO	Yes
	-92.7	-24.5	-92.7	-47.2					0.988	0.941	NO	NO	NO	NO
	-92.7	-24.5			0.0	39.4	0.000	0.000	0.988	0.941	NO	NO	NO	NO
Five Star Exposed Aggregate:	-185.6	-185.6					0.154	0.558	0.988	0.941	NO	NO	NO	NO
	-179.3	-179.3	-169.9	-179.7					0.988	0.941	NO	NO	NO	NO
	-144.8	-174.3			22.0	5.7	0.846	0.442	0.988	0.941	NO	NO	NO	NO
Five Star Water Stopped:	-208.8	-185.6					1.000	1.000	0.988	0.941	Yes	Yes	Yes	Yes
	-106	-169.6	-140.3	-174.9					0.988	0.941	NO	NO	NO	NO
	-106	-169.6			59.4	9.2	0.000	0.000	0.988	0.941	NO	NO	NO	NO
Five Star Epoxied:	-228.7	-182.8					0.756	0.477	0.988	0.941	NO	NO	NO	NO
	-182.8	-168.1	-193.2	-167.6					0.988	0.941	NO	NO	NO	NO
	-168	-152			31.7	15.4	0.244	0.523	0.988	0.941	NO	NO	NO	NO
Five Star Pea Gravel Epoxied:	-22.9	-52.7					0.000	0.702	0.988	0.941	NO	NO	NO	NO
	-22.9	-32.9	-19.9	-36.7					0.988	0.941	NO	NO	NO	NO
	-13.9	-24.5			5.2	14.5	1.000	0.298	0.988	0.941	Yes	NO	Yes	NO
Five Star Fiber:	-237	-207.7					0.463	0.552	0.988	0.941	NO	NO	NO	NO
	-222.1	-206.1	-221.3	-206.2					0.988	0.941	NO	NO	NO	NO
	-204.8	-204.8			16.1	1.5	0.537	0.448	0.988	0.941	NO	NO	NO	NO
Five Star Shear Key:	-208.8	-182.8					0.000	1.000	0.988	0.941	NO	Yes	NO	Yes
	-208.8	-154.3	-195.2	-163.8					0.988	0.941	NO	NO	NO	NO
	-168	-154.3			23.6	16.5	1.000	0.000	0.988	0.941	Yes	NO	Yes	NO

C.5.2 ASTM E 178 T-test Outlier Analysis

Sample Name		Ring Stress Visual	Ring Stress DEMEC	AVG Ring Stress (Ksi)	AVG Ring Stress (Ksi)	Standard Deviation (Visual)	Standard Deviation (DEMEC)	t-statistic (Visual)	t-statistic (DEMEC)	t-critical (95% Confiden	t-critical (90% Confiden	95% Visual Outlier?	95% DEMEC Outlier?	90% Visual Outlier?	90% DEMEC Outlier?
Type K Concrete:	KC1	0	-78.3	0.0	-78.3			0.000	0.000	1.155	1.153	NO	NO	NO	NO
	KC2	0	-78.3			0.0	0.0	0.000	0.000	1.155	1.153	NO	NO	NO	NO
Five Star Control:	FC1	-168	-182.8	-159.2	-173.8			0.178	1.154	1.155	1.153	NO	NO	NO	Yes
	FC2	-106	-169.6					1.077	0.545	1.155	1.153	NO	NO	NO	NO
	FC3	-203.6	-169.1			49.4	7.8	0.899	0.609	1.155	1.153	NO	NO	NO	NO
Set 45 Control:	SC1	-179	0	-78.4	0.0			1.099	0.000	1.155	1.153	NO	NO	NO	NO
	SC2	-56.2	0					0.243	0.000	1.155	1.153	NO	NO	NO	NO
	SC3	0	0			91.5	0.0			1.155	1.153	NO	NO	NO	NO
Five Star Pea Gravel Control:	FPC1	-92.7	-24.5	-63.9	-35.2			1.112	0.577	1.155	1.153	NO	NO	NO	NO
	FPC2	-42.6	-24.5					0.825	0.577	1.155	1.153	NO	NO	NO	NO
	FPC3	-56.5	-56.5			25.9	18.5	0.287	1.155	1.155	1.153	NO	NO	NO	Yes
Five Star Pea Gravel Wire Brushed:	FPB1	-92.7	-82.1	-86.4	-79.3			0.577	0.577	1.155	1.153	NO	NO	NO	NO
	FPB2	-92.7	-82.1					0.577	0.577	1.155	1.153	NO	NO	NO	NO
	FPB3	-73.7	-73.7			11.0	4.8	1.155	1.155	1.155	1.153	NO	NO	Yes	Yes
Five Star Wire Brushed:	FB1	-188.5	-213.7	-192.7	-209.6			0.189	0.410	1.155	1.153	NO	NO	NO	NO
	FB2	-172.8	-198.2					0.892	1.140	1.155	1.153	NO	NO	NO	NO
	FB3	-216.9	-216.9			22.4	10.0	1.081	0.730	1.155	1.153	NO	NO	NO	NO
Five Star Pea Gravel Exposed Aggregate:	FPA1	-92.7	-24.5	-92.7	-47.2			0.000	0.577	1.155	1.153	NO	NO	NO	NO
	FPA2	-92.7	-24.5					0.000	0.577	1.155	1.153	NO	NO	NO	NO
	FPA3	-92.7	-92.7			0.0	39.4	0.000	1.155	1.155	1.153	NO	NO	NO	Yes
Five Star Exposed Aggregate:	FA1	-185.6	-185.6	-169.9	-179.7			0.715	1.036	1.155	1.153	NO	NO	NO	NO
	FA2	-179.3	-179.3					0.428	0.077	1.155	1.153	NO	NO	NO	NO
	FA3	-144.8	-174.3			22.0	5.7	1.143	0.960	1.155	1.153	NO	NO	NO	NO
Five Star Water Stopped:	FW1	-208.8	-185.6	-140.3	-174.9			1.155	1.155	1.155	1.153	NO	NO	Yes	Yes
	FW2	-106	-169.6					0.577	0.577	1.155	1.153	NO	NO	NO	NO
	FW3	-106	-169.6			59.4	9.2	0.577	0.577	1.155	1.153	NO	NO	NO	NO
Five Star Epoxied:	FE1	-168	-152	-193.2	-167.6			0.795	1.015	1.155	1.153	NO	NO	NO	NO
	FE2	-228.7	-168.1					1.123	0.030	1.155	1.153	NO	NO	NO	NO
	FE3	-182.8	-182.8			31.7	15.4	0.328	0.985	1.155	1.153	NO	NO	NO	NO
Five Star Pea Gravel Epoxied:	FPE1	-13.9	-24.5	-19.9	-14.8			1.155	0.223	1.155	1.153	NO	NO	Yes	NO
	FPE2	-22.9	-52.7					0.577	0.870	1.155	1.153	NO	NO	NO	NO
	FPE3	-22.9	32.9			5.2	43.6	0.577	1.093	1.155	1.153	NO	NO	NO	NO
Five Star Fiber:	FF1	-222.1	-207.7	-221.3	-206.2			0.050	1.033	1.155	1.153	NO	NO	NO	NO
	FF2	-237	-206.1					0.974	0.069	1.155	1.153	NO	NO	NO	NO
	FF3	-204.8	-204.8			16.1	1.5	1.024	0.964	1.155	1.153	NO	NO	NO	NO
Five Star Shear Key:	FS1	-208.8	-154.3	-195.2	-163.8			0.577	0.577	1.155	1.153	NO	NO	NO	NO
	FS2	-168	-182.8					1.155	1.155	1.155	1.153	NO	NO	Yes	Yes
	FS3	-208.8	-154.3			23.6	16.5	0.577	0.577	1.155	1.153	NO	NO	NO	NO

Sample Name		Ring Stress Visual	Ring Stress DEMEC	AVG Ring Stress (Ksi)	AVG Ring Stress (Ksi)	Standard Deviation (Visual)	Standard Deviation (DEMEC)	t-statistic (Visual)	t-statistic (DEMEC)	t-critical (95% Confiden	t-critical (90% Confiden	95% Visual Outlier?	95% DEMEC Outlier?	90% Visual Outlier?	90% DEMEC Outlier?
Type K Concrete:	KC1	0.0	29.4	0.0	8.3	0.0	29.8	0.000	0.707	1.155	1.153	NO	NO	NO	NO
	KC2	0.0	-12.8					0.000	0.429	1.155	1.153	NO	NO	NO	NO
Five Star Control:	FC1	-174.8	-87.4	-47.1	-69.0	116.0	16.0	1.101	1.152	1.155	1.153	NO	NO	NO	NO
	FC2	-18	-60.8					0.251	0.510	1.155	1.153	NO	NO	NO	NO
	FC3	51.6	-58.7					0.851	0.642	1.155	1.153	NO	NO	NO	NO
Set 45 Control:	SC1	-61.7	0	-50.2	0.0	16.3	0.0	0.707	0.000	1.155	1.153	NO	NO	NO	NO
	SC2	-38.6	0					0.707	0.000	1.155	1.153	NO	NO	NO	NO
	SC3	-----	-----*							1.155	1.153	NO	NO	NO	NO
Five Star Pea Gravel Control:	FPC1	-84.1	-15.1	-53.1	-24.3	35.5	19.6	0.872	0.470	1.155	1.153	NO	NO	NO	NO
	FPC2	-60.9	-11					0.219	0.679	1.155	1.153	NO	NO	NO	NO
	FPC3	-14.4	-46.8					1.091	1.148	1.155	1.153	NO	NO	NO	NO
Five Star Pea Gravel Wire Brushed:	FPB1	-49.2	-72.9	-22.4	-114.7	24.9	108.7	1.078	0.384	1.155	1.153	NO	NO	NO	NO
	FPB2	-17.9	-33					0.179	0.751	1.155	1.153	NO	NO	NO	NO
	FPB3	0	-238.1					0.898	1.135	1.155	1.153	NO	NO	NO	NO
Five Star Wire Brushed:	FB1	-233.1	-141.3	-107.4	-89.2	116.7	45.1	1.077	1.155	1.155	1.153	NO	NO	NO	Yes
	FB2	-2.4	-63.5					0.899	0.570	1.155	1.153	NO	NO	NO	NO
	FB3	-86.7	-62.8					0.177	0.585	1.155	1.153	NO	NO	NO	NO
Five Star Pea Gravel Exposed Aggregate:	FPA1	-167.8	-81.2	-110.7	-61.0	52.1	61.7	1.096	0.328	1.155	1.153	NO	NO	NO	NO
	FPA2	-98.6	-110					0.233	0.795	1.155	1.153	NO	NO	NO	NO
	FPA3	-65.8	8.3					0.863	1.123	1.155	1.153	NO	NO	NO	NO
Five Star Exposed Aggregate:	FA1	-63.3	-86.2	-177.3	-35.4	100.2	44.0	1.138	1.154	1.155	1.153	NO	NO	NO	Yes
	FA2	-251.5	-11.4					0.740	0.545	1.155	1.153	NO	NO	NO	NO
	FA3	-217.1	-8.6					0.397	0.609	1.155	1.153	NO	NO	NO	NO
Five Star Water Stopped:	FW1	-74.6	-122.7	-35.0	-91.8	36.5	28.6	1.086	1.080	1.155	1.153	NO	NO	NO	NO
	FW2	-2.8	-86.5					0.883	0.185	1.155	1.153	NO	NO	NO	NO
	FW3	-27.6	-66.2					0.203	0.894	1.155	1.153	NO	NO	NO	NO
Five Star Epoxied:	FE1	-58.2	-137	-209.7	-122.9	147.5	12.7	1.027	1.107	1.155	1.153	NO	NO	NO	NO
	FE2	-352.9	-112.3					0.971	0.837	1.155	1.153	NO	NO	NO	NO
	FE3	-218	-119.5					0.056	0.270	1.155	1.153	NO	NO	NO	NO
Five Star Pea Gravel Epoxied:	FPE1	-106.8	-22	-15.9	-18.8	79.7	51.4	1.140	0.063	1.155	1.153	NO	NO	NO	NO
	FPE2	17	-68.5					0.413	0.967	1.155	1.153	NO	NO	NO	NO
	FPE3	42	34.2					0.727	1.030	1.155	1.153	NO	NO	NO	NO
Five Star Fiber:	FF1	-270.5	-14.3	-92.3	-7.2	154.3	15.0	1.154	0.474	1.155	1.153	NO	NO	Yes	NO
	FF2	-6.5	-17.3					0.556	0.675	1.155	1.153	NO	NO	NO	NO
	FF3	0	10					0.598	1.149	1.155	1.153	NO	NO	NO	NO
Five Star Shear Key:	FS1	-9.5	-121.3	-65.7	-77.4	116.4	50.7	0.483	0.865	1.155	1.153	NO	NO	NO	NO
	FS2	-199.5	-21.9					1.150	1.095	1.155	1.153	NO	NO	NO	NO
	FS3	11.9	-89.1					0.667	0.230	1.155	1.153	NO	NO	NO	NO